IN VIVO EVALUATION OF THE CARDIOPROTECTIVE ACTIVITY OF VEGF-B

PhD Thesis

Scuola Normale Superiore di Pisa

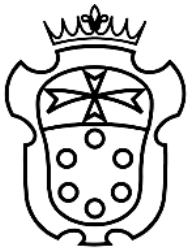

Uday Puligadda

Supervisor: Professor Mauro Giacca

“Live as if you were to die tomorrow. Learn as if you were to live forever.”

- Mahatma Gandhi

TABLE OF CONTENTS

Synopsis 1

1 Introduction 3

1.1 Myocardial ischemia (MI) 5

1.2 Peripheral artery disease 8

1.3 Mechanisms of blood vessel formation 9

1.3.1 The Vascular endothelial growth factor (VEGF) family and their receptors 11

1.3.1.1 VEGF-A 12

1.3.1.2 VEGF-B 17

1.3.1.3 VEGF Receptors (VEGFRs) 21

VEGFR-1 22

VEGFR-1 signaling 24

VEGFR-2 24

VEGFR-3 26

Neuropilins 27

Neuropilin1 (NP1) 28

1.4 Heart Failure (HF) 28

1.4.1 Morphological changes in the heart leading from myocardial infarction to HF 29

1.4.1.1 Compensatry and pathological hypertrophy 30

1.5 Gene therapy strategies for cardio vascular disorders 33

1.5.1 AAV 34

Structure 35

Preparation and purification of AAV 36

1.5.2 Gene therapy for the induction of therapeutic angiogenesis 37

1.5.3 Gene therapy strategies for the treatment of HF 42

2 Results I 46

2.1 Persistent expression of AAV-2-mediated VEGF-A and VEGF-B in normal rat myocardium 46

2.2 Angiogenic effect of VEGF factors in the normal rat myocardium 47

2.3 Prolonged expression of VEGF-B, a specific VEGFR-1 ligand preserves myocardial function: analysis of cardiac function after myocardial infarction by echocardiography 50

2.4 Analysis of cardiac tissues by histo-pathological studies: morphometric analyses of infarct samples 55

2.5 Analyses of vector genomes and their incorporated transgenes in the injected myocardium 56

2.6 Angiogenic effect of VEGF factors in infarcted hearts 58

2.7 Expression levels of VEGF receptors in vitro 59

2.8 Quantitative analyses of VEGF receptors in-vitro 61

2.9 In vivo expression of VEGF receptors in the heart 62

2.10 VEGF-A and VEGF-B protect cardiomyocytes from apoptosis 64

2.11 VEGF-A and VEGF-B activate expression of genes involved in myocardial metabolism and Contractility 66

2.12 VEGF-B overexpression counteracts induction of genes associated with pathological LV remodelling after MI 68

3 Results II 70

3.1 Localized hypertrophic response in cardiomyocytes 71

3.2 Protective role of VEGF-B against cardiomyocyte apoptosis 72

3.3 Activation state of Akt, GSK-3β and FoxO3a 76

4 Discussion 79

4.1 Cardiac gene transfer of VEGF-A and VEGF-B exerts beneficial activities after myocardial infarction in rats and in heart failure in dogs 79

4.2 Non angiogenic functions of VEGF family members 81

4.3 AAV vectors for cardiac gene transfer 83

4.4 Effects of VEGF-B on cardiomyocytes in vitro and in vivo 84

4.5 Conclusions 86

5 Materials and Methods 87

5.1 Production, purification and characterization of rAAV vectors 87

5.2 Preparation of neonatal cardiomyocytes 87

5.2.1 Preparation of cardiomyocyte cultures 87

5.2.2 Preparation of non-myocyte cultures 88

5.3 Isolation and treatment of neonatal rat ventricular cardiomyocytes 88

5.4 Quantification of mRNA by real-time PCR 89

5.5 Immunoprecipitation and Western blot analysis 91

5.6 Animal studies and echocardiography 92

5.6.1 Surgical procedure for MI 92

5.6.2 Echocardiography analysis 93

5.7 Histo-pathological studies 94

5.7.1 Morphometric analysis of infarct size 94

5.7.2 Masson's trichrome staining 94

5.7.3 Infarct size calculation 94

5.7.4 Immunoflorescence 94

5.7.5 TUNEL assay for apoptosis 95

5.8 Statistical analysis 95

6 Bibliography 96

7 Appendix 121

SYNOPSIS

Members of the vascular endothelial growth factor (VEGF) family and their receptors are important regulators of vasculogenesis, angiogenesis, and vessel maintenance in both embryos and adults. In particular, the 165-aa isoform of VEGF-A exerts its highly potent angiogenic and arteriogenic activity mainly through binding to VEGFR-2 in spite of its high affinity binding to VEGFR-1. However, the biological significance of VEGF interaction with VEGFR-1 remains elusive. One of our previous studies in dogs unveiled an unexpected cardioprotective activity of VEGF-A, which was already evident at 48 hours after the induction of a myocardial infarction and was even more marked at 4 weeks. Multiple recent evidences suggested that VEGF-B, a VEGFR-1 exclusive ligand, could be selectively active in the myocardium. However the available data did not define clearly the cardiac benefits of VEGF-B. Therefore, in the present study we wanted to investigate and compare the cardioprotective role of both VEGF-A (and in particular its 165 aminoacid isoform) and VEGF-B (167 aminoacid isoform) in a rat model of myocardial infarction through intracardiac injection of the respective genes. For the efficient and prolonged expression of these factors, we exploited viral vectors based on the Adeno-Associated Virus (AAV), as an efficient tool for in vivo gene transfer. By analyzing cardiac function by echocardiography, we observed that the prolonged expression of both VEGF factors induced a marked improvement in cardiac contractility, preserving viable cardiac tissue, and preventing left ventricular remodeling over time. In addition, we performed histopatho- logical studies on a subset of representative samples. Consistent with the functional outcome, we observed a more potent cardioprotection using the VEGFR-1 selective ligand, VEGF-B, despite its inability to induce angiogenesis. We then tried to dissect the molecular mechanisms by which VEGF-B might act on cardiomyocytes both in vitro and in vivo. We found that the action of VEGF-B was mainly mediated by the upregulation of VEGFR-1 and that stimulation of this receptor exerted positive inotropic and anti-apoptotic effects on cardiomyocytes. In addition, VEGF-B elicited a gene expression pattern reminiscent to the one observed in compensatory

heart hypertrophy, both in cultured cardiomyocytes and in infarcted hearts. We further expanded our investigation on the cardio protection conferred by VEGF-B_{167} in a pacing-induced hear failure model in canines. Interestingly, the findings obtained in this model were similar and totally in keeping with the observations done in the myocardial ischemic model in rats, again showing that VEGF-B_{167} exerted cardio protective effects in the absence of angiogenesis or pathological hypertrophy. Instead, it delayed the progression towards heart failure and prevented cardiomyocytes from apoptosis by controlling pro-apoptotic intracellular mediators, such as Akt and its downstream targets GSK-3β and FoxO3a.

INTRODUCTION

In the early periods of the 20th century, cardiovascular disorders (CVDs) were not the major cause of death, and accounted for less than 10% of deaths in the population globally. At the end of the century, however, according to the statistics of 2005, CVDs had become one of the major causes of mortality, being responsible for at least 30% of deaths in the general population. It is now estimated that CVDs cause 17 million deaths every year worldwide (World Health Report, 2006).

In Europe, CVDs account for 49% of all deaths (Rayner et al., 2003), corresponding to nearly 1.9 million people. In the United States, nearly 2400 individuals die of CVD every day, with an average of 1 death every 37 seconds. It is predicted that, by 2030, almost 23.6 million people will die from CVDs, which will then remain as the single leading causes of death (www.who.int/mediacentre/factsheets/fs317/en/index.html).

The incidence rate of CVDs is higher in Western countries than in developing countries, irrespective of industrialization, rapid progress in medical technologies, advancements in research and development of early prognostic methods or treatments. Current estimates indicate that CVDs incidence is about 50% in developed countries and about 28% in low and middle income countries (Mathers et al., 2006). However, in some developing countries, such as India, the burden of CVD is rising. The estimated prevalence of coronary heart disease is around 3–4% in rural areas and 8–10% in urban areas among adults older than 20 years, representing a twofold rise in rural areas and a six-fold rise in urban areas over the past four decades (Reddy et al., 2005).

Regarding the economic burden, the expenditure on CVD in the United States was nearly 350 billion USD, in 2003, comprising both direct and indirect costs (Hodgson et al., 2001).

The major common cause of CVD is atherosclerosis, which can affect various districts of the circulatory system and yields distinct clinical manifestations. The pathology of atherosclerosis initiates with the formation of early focal lesions (called as fatty streaks) in the intima of arteries,

essentially consisting of lipoproteins deposition, which bind to the extracellular matrix components, such as proteoglycans. At a later stage, chemical modifications such as lipoptotein oxidation and non enzymatic glycation occur. In lipoprotein oxidation, the lipoproteins undergo oxidative modifications and forms hydroperoxides, lysophospholipids, oxysterols and chlorotyrosyl moieties, whereas in non enzymatic glycation, which is especially relevant in diabetic patients with sustained hyperglycemia, apolipoproteins and other structural arterial proteins undergo glycation and lose their natural protective function. These events further accelerate atherogenesis. After accumulation of extracellular lipids, leukocytes such as lymphocytes and monocytes are recruited within fatty streaks. This is favored by the constituents of oxidatively modified LDL molecules, as well as by a few cytokines, like intereukin-1(IL-1) and tumor necrosis factor α (TNF-α), which stimulate expression of adhesion molecules and receptors on the surface of endothelial cells. Lymphocytes and monocytes penetrate the endothelial layer and take up residence in the intima. There, monocytes differentiate into macrophages and transform into lipid-laiden foam cells through the uptake of lipoprotein particles by receptor-mediated endocytosis. Some of the foam cells may die as result of apoptosis and result in the formation of a lipid rich center, called the *necrotic core*. Mononuclear phagocytes release a number of growth factors, such as platelet derived growth factor (PDGF), fibroblast growth factor (FGF) and other cytokines, which stimulate the proliferation of smooth muscle cells migrated from tunica media into the intima. This event in turn stimulates the additional deposition of extracellular matrix. The lesions with accumulation of macrophage-derived foam cells are transformed into fibro-fatty lesions with the accumulation of fibrous tissue and smooth muscle cells. These plaques also accumulate calcium, bound to bone-associated proteins, such as osteocalcin, osteopontin and bone morphogenic proteins. The process of atherosclerosis has been recently reviewed in detail by many reviewers (Insull 2009, Falk 2006, Virmani et al., 2002, Glass et al., 2001, Libby 2001, Lusis 2000).

Several risk factors contribute to plaque formation. These are classified into two categories: modifiable and unmodifiable. The modifiable risk factors can be modulated by life style (physical activity, healthy diet with high HDL intake, smoking cessation) or pharmacological

therapy for the predisposing conditions such as hypertension, hyper-cholestrolemia and diabetes mellitus. The unmodifiable factors include age, gender (men age ≥ 45years, women age ≥ 55years) and family history of premature coronary heart disease.

Given the social, economic, and sanitary burden of CVD, the identification of novel therapeutic strategies interfering with the molecular mechanisms of disease onset and progression is absolutely required. In this context, the appreciation of the potential value of gene therapy has been steadily growing over the last few years. The utilization of nucleic acids as therapeutic tools for CVD is currently envisaged in at least three main areas: i) treatment of cardiac and peripheral ischemic conditions by the induction of neoangiogenesis; ii) treatment of heart failure to preserve or improve cardiac function; iii) prevention of restenosis after percutaneous coronary intervention (PCI).

1.1 MYOCARDIAL ISCHEMIA (MI)

The term ischemia was first used by the German pathologist Rudolf Virchow. It derives from the Greek word “ischein” (to restrain) and “haima” (blood). Thus, "ischemia" refers to conditions of insufficient blood supply to a tissue (Bohuslav Ošťádal et al., 1999).

Myocardial ischemia specifically refers to a condition in which there is insufficient blood flow to the myocardium. Patients with myocardial ischemia fall into one of two large groups: patients with chronic coronary artery disease (CAD), with stable *angina pectoris.* These patients experience discomfort or pain in the chest or left arm, induced by physical activity or in stress, which can be relieved by rest and/or sublingual nitroglycerin. A second group consists of patients which present with acute coronary syndromes (ACSs), divided into patients with acute myocardial infarction (MI) with ST-segment elevation (STEMI) at their presenting electrocardiogram and patients with unstable angina or non-ST-segment elevation MI (UA/NSTEMI), accompanied by elevated levels of serum enzymes troponin T or I, and creatine phosphokinase. MI is an emergency condition treated by either percutaneous coronary angioplasty (with or without stent placement) or thrombolysis.

Myocardial ischemia is diagnosed by different tests, including: 1) electrocardiography (ECG), which records the electrical conduction activity of the heart; 2) exercise tolerance test, to evaluate the functional reserve of the heart; 3) echocardiography, to evaluate the condition of valves and chambers of the heart, and measure cardiac function; 4) contrast angiography (CT angiography/MR angiography), to assess the presence of atherosclerotic plaques in the coronary arteries; 5) nuclear ventriculography, to analyse the size of the heart chambers and their blood pumping ability using radioactive tracers (Hunt et al., 2005); 6) electron-beam computed tomography (EBCT), to detect coronary calcification observed in early stages of CAD (Haberl et al., 2001).

Patients with CAD are currently treated by pharmacological therapy to reduce morbidity and to prevent complications. The line of treatment consists of the use of drugs such as anti-platelet agents (aspirin, dipiridamole or clopidrogrel) to prevent thrombus formation, anti-anginal drugs (amlodipine or bepridil) to minimise the rate of occurrence as well as severity of angina attacks, inhibitors of angiotensinogen converting enzyme (ACE inhibitors, such as benazepril, captopril or ramipril) to lower blood pressure and protect the heart, beta-blockers (metoprolol or propranolol) to lower heart rate, blood pressure, and oxygen use by the heart, calcium channel antagonists (amlodipine, diltiazem or verapamil) to relax arteries, lowering blood pressure and reducing strain on the heart, diuretics to lower blood pressure and treat congestive heart failure, nitrates (nitroglycerin or isosorbide) to stop chest pain and improve blood supply to the heart; statins to lower blood cholesterol.

PCI is widely used in patients with symptomatic CAD and evidence of ischemia due to stenosis of one or two vessels, and even in selected patients with three-vessel disease. Coronary artery Bypass Grafting (CABG) is highly preferred in patients with stenosis of the left main coronary artery and in those with three-vessel CAD, especially with diabetes and/or impaired left ventricular function, who require revascularization.

Compared to pharmacological therapy, CABG shows better prognostic efficacy (increase in life expectancy) in only a selected group of patients with high risk atherosclerotic lesions, localized

in specific anatomical segments of the coronary arteries. However, CABG usually decreases symptoms and thus improves quality of life in most patients. PCI instead (defined as "elective" PCI to contrast it with "primary" PCI, performed in patients with acute MI) entails the use of an arterial catheter containing a deflated balloon at its extremity. The catheter is inserted through the femoral artery and the balloon is positioned, under angiographic guidance, at the level of the atherosclerotic plaque in the coronary artery. The balloon is then inflated to mechanically destroy the plaque and restore vessel perviousness. Concomitant with angioplasty, an endovascular tubular prosthesis (stent) is usually positioned in correspondence with the artery segment where the balloon was inflated in order to maintain patency of the vessel to prevent restenosis. When compared to pharmacological therapy, PCI does not seem to offer significant survival advantage. However, it significantly improves the patient's quality of life (episodes of angina, dyspnea and limitations of exercise capacity). PCI thus represents an extremely valuable alternative to CABG in the treatment of angina; as already reported above, CABG is only superior to PCI in a selected group of patients with high risk lesions.

In certain conditions, rupture of the atherosclerotic plaque causes acute MI through the sudden formation of a thrombus obstructing an atherosclerotic coronary artery. About 25-35% of patients with MI die before receiving medical assistance, usually due to ventricular fibrillation. For those who are rapidly hospitalized, prognosis has very significantly improved through the revascularization of the occluded artery. Revascularization can be obtained by mechanical of pharmacological treatment. The former consists in primary PCI, that is balloon angioplasty performed in emergency conditions, with or without stent placement. Primary PCI usually restores blood flow in more than 90% of patients. If this procedure is delayed more than 90 minutes from the initial medical contact, pharmacological thrombolysis can be attempted. This is achieved by using thrombolytic agents containing plasminogen activators (streptokinase or tissue plasminogen activator - tPA). These are enzymes that transform plasminogen into plasmin and thus degrade the fibrin network within the thrombus, eventually leading to dissolution of the thrombus. Collectively, patients with MI who are rapidly hospitalized and are

mechanically or pharmacologically revascularized have today a very high survival rate (90-95%).

1.2 PERIPHERAL ARTERY DISEASE

Peripheral artery disease (PAD) is caused by obstruction of large arteries in the arms and legs, in particular the iliac, femoral, popliteal and tibial arteries. The obstruction of large arteries can result from atherosclerosis, embolism or thrombus formation, or any other inflammatory process lead to stenosis. Patients may present with acute or chronic ischemia.

Similar to CAD, there are several predisposing factors to PAD, such as smoking, obesity, diabetes mellitus, dyslipidemia and hypertension. The disease is mostly observed in people over 50-55 years of age. The National Health and Nutrition Examination Surveys (NHANES) during the years 1999-2000 reported that approximately 5 million adults were affected by PAD and that the prevalence increased with age and disproportionately affected blacks (Selvin et al., 2004).

Fewer than 50% patients with PAD are asymptomatic, and diagnosis is only made after targeted investigation (typically, analysis of blood flow by echo-color-doppler). About 50% of cases have variable leg symptoms; of these, 10% of cases have classic symptoms of *intermittent claudication* (Hirsch et al., 2001, Crigui et al., 1985): patients, while walking, are forced to stop repeatedly due to leg pain, typically in the calves. Pain is due to the accumulation of lactic acid, which stimulates peripheral pain receptors - consequent to muscle activity in anaerobiosis, since the arterial stenosis does not allow proper supply of oxygenated blood. If the blood supply is diminished critically, patients may experience pain even at rest, in particular at night when legs are raised in bed. The pain initially develops in toes and in feet and then passes to calves. Ulcers may develop under feet and toes. In few cases, necrosis and then gangrene develops, which is irreparable. This is the end stage of PAD. In these cases, amputation of foot or leg or entire limb is unavoidable.

1.3 MECHANISMS OF BLOOD VESSEL FORMATION

The mechanism of blood vessel formation involves three processes: vasculogenesis, angiogenesis and arteriogenesis (Storkebaum et al., 2004). The term vasculogenesis traditionally refers to the de novo synthesis of blood vessels during embryonic development. In this process, a primitive capillary network is formed from angiogenic progenitor cells, called angioblasts, which differentiate into endothelial cells and coalesce to form an initial vascular plexus (Risau et al., 1995, Carmeliet 2003). Antigenic markers common to angioblasts and hematopoietic stem cells have been identified, consistent with the possibility that a common precursor (hemangioblast) might exist and be able to originate both hematopoietic and endothelial cells.

The budding of new capillary branches from existing blood vessels into new blood vessels is named angiogenesis. This process is usually observed during both embryonic development and in the adult life. The process is initiated by the metabolic activation, proliferation and migration of endothelial cells, concomitant with vast remodeling of the extracellular matrix. At subsequent times, the newly formed capillaries progressively mature by the addition of mural cells (pericytes and smooth muscle cells) allowing proper functionality, and a vascular network formed by larger vessels (arterioles and venules) is eventually formed.

Finally, in addition to vasculogenesis and angiogenesis, a third process of blood vessel formation exists, known as arteriogenesis. This process consists in the remodeling of existing arteries to increase their luminal diameter in response to physiological stimuli of vasoconstriction or vasodilatation. A classic example of arteriogenesis in the adult is the formation of a collateral network, visible upon angiography, in response to the progressive occlusion of an arterial vessel by an atherosclerotic plaque. In this process, vessels are generated to become medium and large arteries with properly developed tunica media (to control patency of vascular lumen), in order to functionally meet the demand of tissue perfusion (Heli et al., 2006).

If we observe the anatomy of blood vessels, capillaries are made up of a single layer of endothelial cells with supporting vascular pericytes, whereas arteries and veins consist of multiple layers (from inside to outside): tunica intima, the inner most layer surrounding the

lumen composed of endothelial cells, pericytes and basement membrane; tunica media, the middle layer composed of smooth muscle cells and extracellular matrix; tunica adventitia, which is particular prominent in large vessels, consisting of fibroblasts and their extracellular-matrix (Figure 1.1).

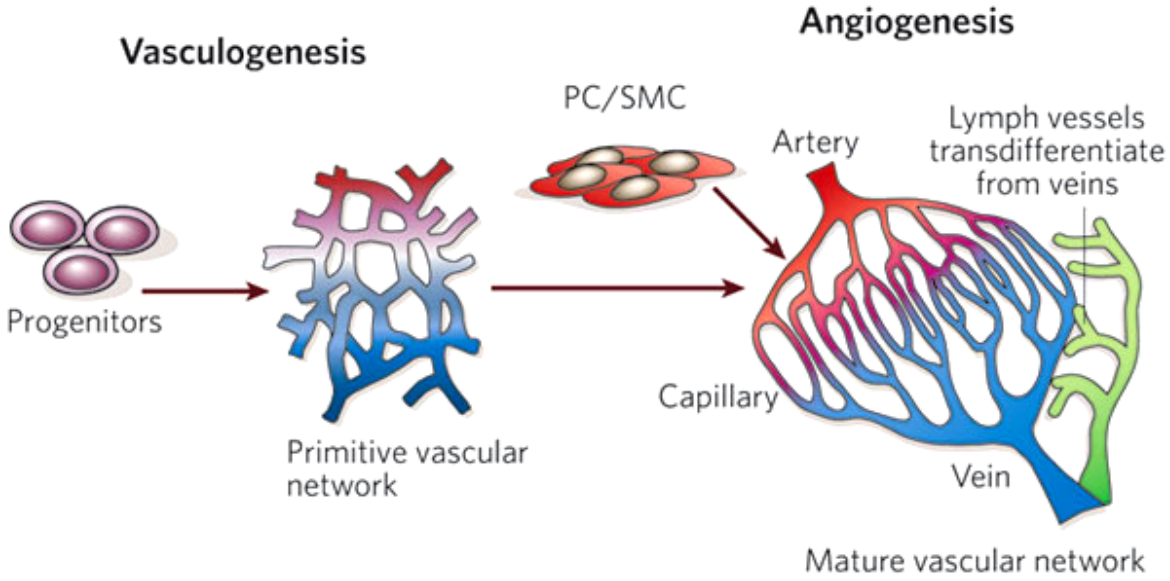

Figure 1.1 During vasculogenesis, endothelial progenitor cells develop into primitive vascular network, which expands further with the recruitment of SMC and pericytes and develops into fully functional vascular network. Lymphatic network emerges from transdifferentiation of veins (Carmeliet 2005).

In physiological conditions, the major stimulus for the process of angiogenesis is hypoxia. In hypoxic conditions, cells in the tissue start sensing the reduced O_2 concentration and initiate vascular responses to increase expression of genes encoding angiogenic growth factors. In this response pathway, the central element is HIF-1, a heterodimeric transcription factor able to activate expression of a series of genes. Among the induced genes are several angiogenic cytokines and their receptors. Among these, members of the vascular endothelial growth factor (VEGF) family and their receptors (VEGFR) are the most powerful, initial responsive elements in the angiogenic cascade, which are required in all phases of angiogenesis in the adult and vasculogenesis in the embryo (Wang et al., 1995, Carmeliet 2003, Ferrara et al., 2003).

1.3.1 The Vascular Endothelial Growth Factor (VEGF) family and their receptors

The mammalian family of the vascular endothelial growth factor (VEGF) includes 5 structurally related proteins: VEGF-A, VEGF-B, VEGF-C, VEGF-D and placental growth factor (PlGF). There are two additional VEGF family members of non mammalian origin: VEGF-E and VEGF-F. VEGF-E was identified in the Orf virus, which causes extensive vascular proliferation in human skin upon infection (Lyttle et al., 1994, Meyer et al., 1999, Ogawa et al., 1998). VEGF-F, instead, is a VEGF-like molecule isolated from the *Trimeresurus flavoviridis* Habu snake venom, which is able to induce vascular permeability preferentially through VEGFR-1 signaling (Takahashi et al., 2004).

The function of the different VEGF family members are mainly mediated by the cell surface tyrosine-kinase receptors VEGFR-1 (flt-1), VEGFR-2 (KDR/flk-1) and VEGFR-3 (flt-4), whose relative affinity and distribution mediate the biological effect (Carmeliet et al., 1999). More specifically, VEGF-A binds VEGFR-1 and -2; VEGF-B and PlGF selectively bind VEGFR-1, while VEGF-C and VEGF-D bind VEGFR-3. The last two factors mainly induce a lymphangiogenic response, leading to the formation of lymphatic rather than hematic vessels (Karkkainen et al., 2004, Stacker et al., 2001). The characteristics of VEGF-A and VEGF-B, which are the subject of research of this thesis, are reported in detail in the following sections (Figure 1.2).

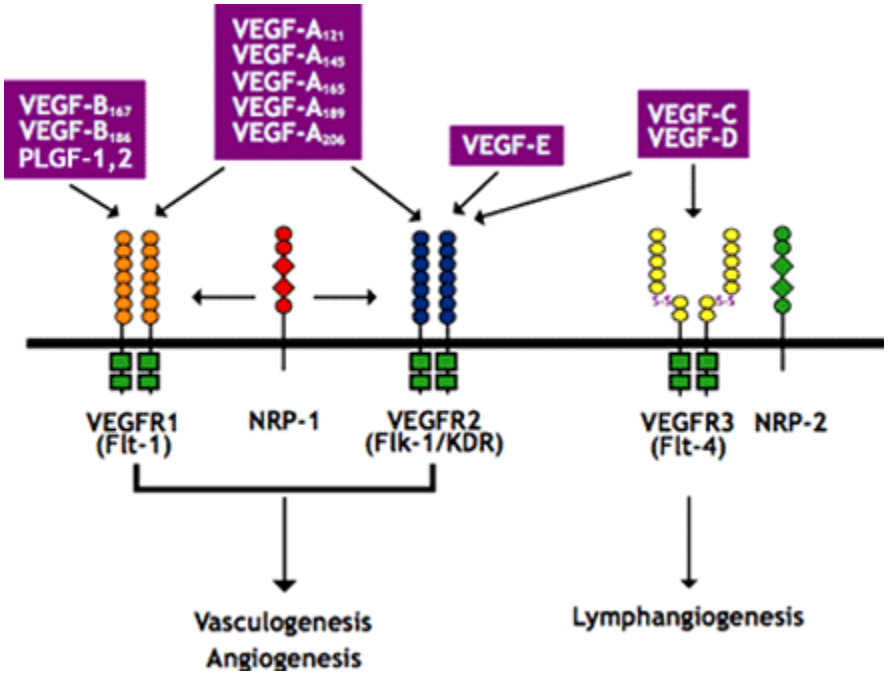

Figure 1.2 The multiple splicing isoforms of VEGF-A bind VEGFR-1 and VEGFR-2, whereas VEGF-B and PlGF only bind VEGFR-1. The Orf virus VEGF-E factor is a selective ligand for VEGFR-2. Of the other members of the VEGF family, VEGF-C and VEGF-D bind VEGFR-2 and VEGFR-3 and participate in the formation of the lymphatic network. Specific isoforms of VEGFs factors are also able to bind the co-receptor NP-1 and NP-2, which can heterodimerize with either VEGFR-1 or VEGFR-2 (Hicklin et al., 2005).

1.3.1.1 VEGF-A

VEGF-A is by far the best characterized member of VEGF family and the first one to be discovered. The need for timely and precisely regulated VEGF-A gene expression is highlighted by the remarkable observation that deletion of a single VEGF-A gene allele (Ferrara et al., 1996, Carmeliet et al., 1996) or modest gene overexpression (Miquerol et al., 2000) result in embryonic lethality.

VEGF-A has been originally described as Vascular Permeability Factor (VPF), due to its ability to increase vascular permeability and to disrupt vascular barrier integrity (Weis and Cheresh, 2005).

The purified protein molecule of the human VEGF-A gene, also referred to as VEGF, is 46-kDa in weight. It dissociates upon reduction into two apparently identical 23 kDa subunits (Ferrara

et al., 1989). The human gene is located on chromosome 6 (p12) and is composed by 8 exons and 7 introns, (Tischer et al., 1991), with a coding region of about 14 kb. The VEGF pre-mRNA undergoes alternative splicing to produce at least eight different protein isoforms, composed of 121, 165, 189 (Tischer et al., 1991), 145 (Poltorak et al., 1997), 162 (Lange et al., 2003), 165b (Bates et al., 2002), 183 (Jingjing et al., 1999) and 206 (Houck et al., 1991) amino acids, respectively. Among these isoforms: VEGF-A_{121}, VEGF-A_{145}, VEGF-A_{148}, VEGF-A_{165}, VEGF-A_{183}, VEGF-A_{189} and VEGF-A_{206}, are generated by alternative splicing of exons 6 and 7, whereas the, $VEGF_{165b}$ isoform is generated by exon 8 distal splice site selection, thus differing from the canonical $VEGF_{165}$ only in the carboxy-terminal six amino acids (resulting in change of the amino acid sequence form CDKPRR to SLTRKD) (Harper and Bates, 2008). Surprisingly, this isoform seems to bind VEGFR-2 with the same affinity as $VEGF_{165}$, but it lacks any angiogenic property, and is therefore defined as antiangiogenic (Woolard et al., 2004). In mice, all isoforms are one amino acid shorter than their human counterparts (Figure 1.3).

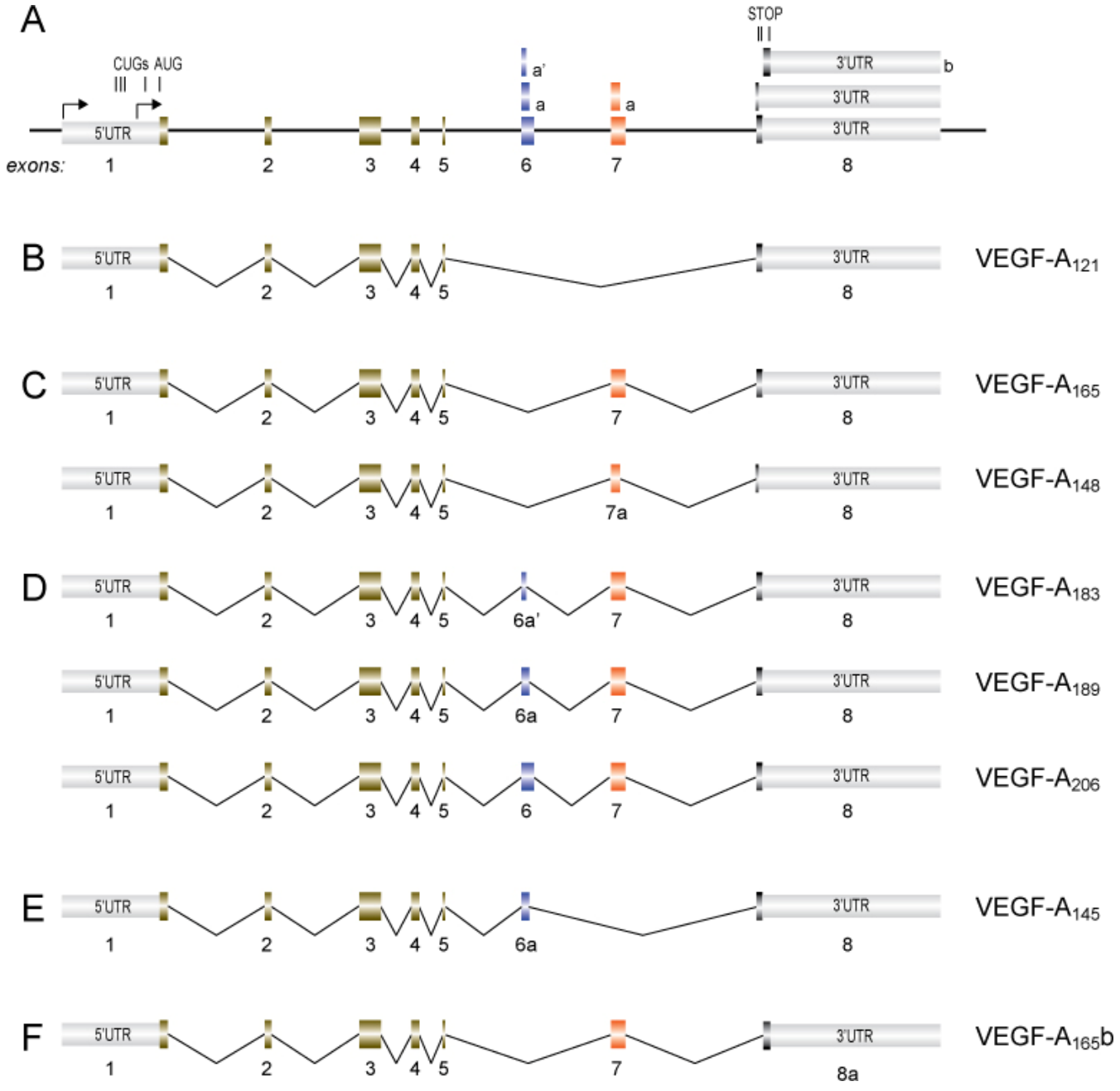

Figure 1.3 Comparitive mRNA structures of VEGF-A isoforms A) Schematic representation of the VEGF-A gene intron and exon organization. Arrows indicate transcriptional start site. The position of translation initiation and termination codons are shown B) mRNA with exon 5/8 junction c) mRNAs including exon 7 D) mRNAs including exon 6 and 7 E) mRNA including exon 6 F) mRNA contain alterative exon 8b.

VEGF-A binds with high affinity to two tyrosine kinase receptors: Flt-1(fms-related tyrosine kinase 1) or VEGFR-1 and Flk-1(Fetal liver kinase 1)/KDR(kinase insert domain receptor) or VEGFR-2, as well as to a non tyrosine kinase co-receptor: neuropilin-1 (NP-1) (Ferrara, 2004).

All the isoforms (with the exception of $VEGF_{121}$, which is acidic and freely soluble) are highly basic, poorly diffusible in nature. In particular, the longest isoforms, once released into the extracellular environment, bind to heparin sulfate proteoglycans (HSPGs) on the cell membrane and to the extracellular matrix at various degrees, with the only exception of $VEGF_{121}$, as it lacks the heparin binding domain. VEGF-A_{165}, which is the predominant isoform in vivo, has an intermediate capacity to bind HSPGs (Ferrara, 2004).

The regulation of VEGF-A production occurs at multiple levels, including transcription, splicing, mRNA stability, translation and subcellular localization of the various factor isoforms. At the transcriptional level, many stimuli, including growth factors, p53 mutation, nitric oxide (NO), hormones, cytokines and cellular stress control VEGF expression (Takahashi and Shibuya, 2005). In particular, hypoxia, via Hypoxia Inducible Factor 1 (HIF-1) is the major positive regulator of VEGF expression. Hypoxic conditions induce accumulation of the highly instable α subunit of HIF-1, leading to the formation of an active transcriptional activator that binds to the Hypoxia Responsive Elements (HRE) in the 5' flanking region of the VEGF promoter (Pages and Pouyssegur, 2005). Hypoxia is a key factor in stabilizing VEGF mRNA by binding of regulatory proteins to 3' untranslated region (UTR), and in translating VEGF mRNA via Internal Ribosomal Entry Site sequences present in the 5' UTR (Stein et al.,1998). VEGF is expressed in most of the cell types including vascular smooth muscle cells, chondrocytes, epithelial cells, neutrophils, macrophages, monocytes, mesenchymal cells, pituitary and pancreatic endocrine cells, hepatocytes and even many tumor cells types. The $VEGF_{165}$ isoform is the one preferentially expressed by most tissues (followed by $VEGF_{121}$ and $VEGF_{189}$), it is secreted as a homo-dimer with moderate affinity for heparin and is a powerful inducer of endothelial cell migration, proliferation, survival and vascular permeability (Leung et al., 1989; Senger et al., 1983). How the differential splicing of these isoforms is regulated in vivo is however largely unknown.

VEGF plays an important role in two major processes of vascular development: vasculogenesis and angiogenesis. The non redundant role of the different VEGF isoforms in vessel development is highlighted by the observation that $VEGF_{164}$ mice (which only express the $VEGF_{164}$ isoform) are normal and healthy, while $VEGF_{120}$ puppies (which only express the $VEGF_{121}$ isoform) exhibit serious vascular remodelling defects, including defective branching (Stalmans et al., 2002).

Even the quantity of VEGF-A is critical in order to obtain normal vessel development, since VEGF-A is haploinsufficient (Carmeliet et al., 1996; Ferrara et al., 1996). Recent data have pointed out the importance of VEGF also in vessel maintenance: VEGF produced by ECs is crucial for vascular homeostasis, through a cell-autonomous VEGF signaling mechanism (Lee et al., 2007); this observation confirms the fundamental and complex role of VEGF in vessel biology.

VEGF is considered as survival factor for endothelial cells, based on the experiments conducted both *in vitro* and *in vivo* (Gerber et al., 1998, Alon et al., 1995). In vitro, VEGF prevents endothelial cell apoptosis in serum starved conditions by binding selectively to its Flk-1 receptor but not to its Flt-1 receptor, followed by the activation of the phosphatidylinositol 3-kinase (PI3 kinase)/Akt pathway (Gerber et al., 1998). The major indications of the capacity of VEGF to act as a survival factor for endothelial cell in vivo come from experiments performed by exposing the retinal vasculature of newborn mice to hyperoxia in order to reduce VEGF levels. This results in a gradual regression of the retinal capillary vasculature, which can be prevented by the intraocular injection of VEGF, thus unequivocally identifying this protein as a potent pro-survival factor (Alon et al., 1995).

Beyond its peculiar activity on endothelial cells, recent evidence indicates VEGF as a pleiotropic molecule. For instance, VEGF has direct action on a variety of neural cells. Its neuronal protective function was observed in mice with reduced VEGF levels within the nervous system, as these mice developed motor neuron degeneration. Further studies revealed its important role in preventing neuronal death after acute spinal cord or cerebral ischemia (Storkebaum et al., 2004). In addition, VEGF also displayed a potent activity in promoting survival and

regeneration of skeletal muscle cells (Arsic et al., 2004; Germani et al., 2003) and seems to have a role in liver homeostasis as well (LeCouter et al., 2003).

As far as disease conditions are concerned, up-regulation of VEGF-A was implicated in the pathogenesis of tumors, age related-macular degeneration, proliferative retinopathy, rheumatoid arthritis, psoriasis, polycystic ovary syndrome, ascites and brain edema. In contrast, lower levels of VEGF-A associated with amyotrophic lateral sclerosis and pre-eclampsia (Ferrara 2004).

Finally, in our laboratory we observed an effect of VEGF-A_{165} on bone marrow (BM) derived $CD11b^+$ cells, as these cells expressed VEGF receptors. In particular we observed the induction of VEGF-dependent BM cells migration, proliferation and secretion of cytokines able to trigger smooth muscle cell recruitment (Zacchigna et al., 2008).

1.3.1.2 VEGF-B

VEGF-B was first cloned and characterized by Grimmond et al. (1996) and designated as VEGF related factor (VRF) from a human fetal brain library and from normal and tumor tissues. Two alternatively spliced isoforms, having 186 and 167 amino acids, have been identified. These isoforms differ at their carboxy-terminal ends, as a consequence of a shift in the open reading frame (ORF). Both have a high degree of homology at the amino terminus with VEGF-A, and the shorter form contains all the 16 cysteine residues present in VEGF-A_{165}. Since the VEGF-B gene also contains a signal peptide, it is considered a secreted factor. The gene presents a ~5 kb coding region, which comprises 8 exons. It is located at the D11S750 locus on Human chromosome 11q13. The alternative spliced forms arise from either the inclusion or exclusion of exon 6; the two transcripts appear to be ubiquitously expressed in both normal and malignant tissues.

The human VEGF-B_{167} mRNA is 1.4 kb in length and shares 88% sequence identity with mouse VEGF-B_{167}. It differs from VEGF-B_{186} in lacking exon 6 and its C-terminus contains a strongly basic cystein rich heparin binding domain, similar to VEGF-A and other related growth factors, which is absent in VEGF-B_{186}. VEGF-B_{186} is indeed less basic, more hydrophobic and highly

soluble in nature (Olofsson et al. 1996a). However, Northern blot analysis of human tissues showed that both isoforms are similarly abundant in heart, skeletal muscle, pancreas, and prostate (Olofsson et al. 1996b).

More recently, an additional spliced form, VEGF-B_{155}, was discovered. It contains 155 amino acids and has same C-terminal sequence of VEGF-B_{167}, but lacks exon 5 and 6 (Gollmer et al., 2000)(Figure 1.4).

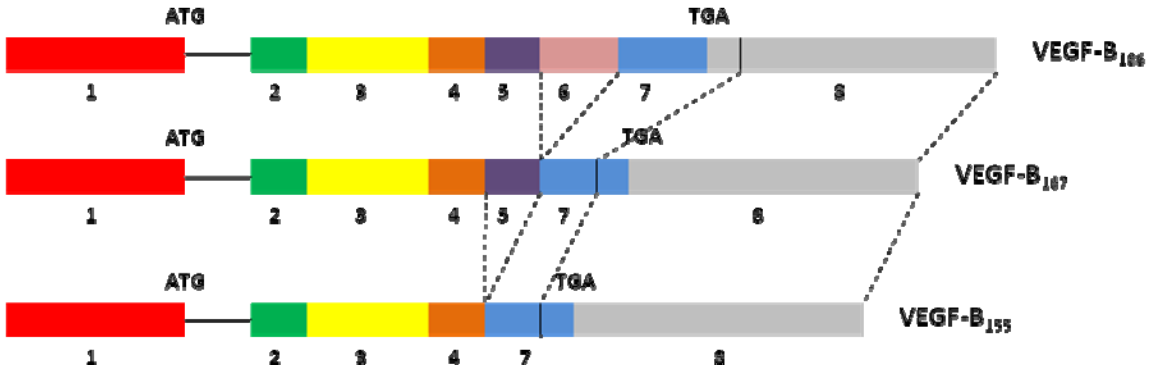

Figure 1.4 Comparative structures of VEGF-B isoforms. The number of each exon is given below for each gene structure. Splicing of exon 6 and 5 introduces a 1-base frameshift and a different reading frame in VEGF-B_{167} and VEGF-B_{155} respectively compared to longest isoform VEGF-B_{186}. The STOP codon of VEGF-B_{167} and VEGF-B_{155} are located 41 bases downstream of the STOP codon of VEGF-B_{186}

The different VEGF-B isoforms are secreted as disulfide-linked homodimers, but can form heterodimers with other VEGF members and still act as endothelial cell growth factors (Olofsson et al., 1996b).

VEGF-B has a wide range of tissue distribution. It is highly expressed in heart, brain, testis and kidney cells (Lagercrantz et al., 1996) and less in developing muscle, bone, pancreas, adrenal gland, and in the smooth muscle cell layer of several larger vessels (Olofsson 1996a).

From in vitro experiments, it was found that VEGF-B_{186} has a peculiar regulatory function in endothelial extracellular matrix degradation, adhesion and migration during the process of angiogenesis by binding selectively to VEGFR-1 (Olofsson et al., 1998). In vivo, VEGF-B plays an important role in pathologic vascular remodeling and synovial angiogenesis of arthritis. This

was studied in two different mice models of arthritis: antigen induced arthritis (AIA) and collagen induced arthritis (CIA). In both conditions, VEGF-B$^{-/-}$ mice displayed significant reduction in synovial inflammation with increase in vessel density and swollen knee joints after 7 days of intra-articular injection of the inflammatory stimulus (methylated bovine serum albumin (mBSA) in AIA and chick type II collagen (CII) in CIA) (Mould et al., 2003).

In addition to this phenotype, VEGF-B$^{-/-}$ mice displayed vascular dysfunction, reduction in heart size, thickened ventricular wall and impairment in recovery of energy metabolism after coronary occlusion even though they are healthy and fertile, thus indicating a specific role of VEGF-B in development or function of the coronary vasculature (Bellomo et al., 2000). When the heart function was analyzed by ECG, VEGF-B knockout mice had atrial conduction abnormalities with prolonged PQ interval. From these data, it was concluded that VEGF-B is important for normal cardiac function in adults and has no essential role during the development of the cardiovascular system. In these mice, there is no evidence of up-regulation of VEGF-A or PIGF mRNA levels to compensate the loss of VEGF-B (Aase et al., 2001).

Additional gene targeted experiments showed that VEGF-B stimulates angiogenesis in ischemic myocardium whereas it has a minor role in vessel growth in skin, retina, lung and ischemic limb (Li et al., 2008). Mice expressing cardiac specific VEGF-B$_{167}$ transgene showed cardiac hypertrophy with increase in size of blood vessels and have lower heart rate and blood pressure. However, this cardiac hypertrophy had no affect on normal cardiac function. Interestingly, these mice had alteration in lipid metabolism, indicating a role of VEGF-B on this function (Karpanen et al., 2008).

Louzier et al. (2003) assessed the effects of VEGF-B in chronic hypoxic pulmonary hypertension by investigating VEGF-B$^{-/-}$ mice and over-expressing both VEGF-B isoforms through adenoviral-mediated delivery of the genes to the rat lungs. No significant differences were found in the pulmonary hemodynamics, right ventricular hypertrophy, distal vessel muscularization, or vascular density after 3 weeks of hypoxia between VEGF-B$^{-/-}$ mice and control mice. The protective effects of both isoforms were similar to human VEGF A$_{165}$ except an

increase in eNOS expression and vascular permeability in the lungs after 5 days of VEGF-A overexpression.

Adenoviral mediated intra-myocardial gene transfer of VEGF-B_{186} isoform was reported to induce angiogenesis and arteriogenesis in ischemic myocardium of pigs and rabbits. These effects were reported to be mediated through G-protein signaling pathway via activation of neuropilin receptor-1. Cardiomyocytes were protected from apoptosis and had metabolic effects by inducing expression of fatty acid transport protein-4 and lipid and glycogen accumulation (Lahteenvuo et al., 2009). The results of these experiments, however, were potentially blurred by the pro-inflammatory response to first-generation adenoviral vectors, which were used to delivery the VEGF-B_{186} gene to the myocardium.

Again related to lipid metabolism, VEGF-B was reported to have a role in endothelial targeting of lipids to peripheral tissues. VEGF-B is highly expressed in heart and brown adipose tissue; both these tissues are enriched with mitochondria to metabolize fatty acids, a major energy source (Hagberg et al., 2010). In VEGF-$B^{-/-}$ mice, lipids are accumulated in these tissues instead of being transported into white adipose tissue, and the tissue lipid uptake appeared compromised. By comparing the expression pattern of VEGF-B with the distribution of mitochondrial proteins, there was strong correlation, different from VEGF-A and PIGF. However, a deeper analysis of this VEGF-$B^{-/-}$ phenotype indicated that VEGF-B does not regulate or influence mitochondrial gene expression, but its co-expression with mitochondrial proteins produced a novel regulatory mechanism with tight coordination between endothelial uptake and mitochondrial lipid utilization. In particular, these resulted supported the conclusion that VEGF-B affects the uptake of long chain fatty acids (LCFAs) by endothelial cells from the circulation and their further transport to the surrounding tissues for mitochondrial processing; this regulation would be mediated by interaction with VEGFR-1 and neuropilin-1 (Hagberg et al., 2010).

Similar to VEGF-A, also VEGF-B_{186} appears to have a direct protective effect on neurons, as observed in SOD1 (superoxide dismutase-1) mutant rats, which represent an accepted model of

ALS (amyotrophic lateral sclerosis). It also protected cultured primary motor neurons against degeneration and the magnitude of protection was remarkably higher when studied comparatively with VEGF-A and other classical neurotrophic factors, such as brain derived neurotrophic factor (BDNF), and ciliary neurotrophic factor (CNTF) (Poesen et al., 2008). In addition, VEGF-B regulates neurogenesis in the adult brain in both in vitro (Sun et al., 2004) and in vivo (Sun et al., 2006). Finally, VEGF-B isoforms are abundantly expressed in all grades of human astrocytomas, even more than $VEGF_{165}$ and $VEGF_{121}$; of notice, in cultured glioblastomas cells, the levels of expression of VEGF-B appear insensitive to conditions like hypoxia and glucocorticoid treatment (in contrast, dexamethasone is known to reduce VEGF-A expression) (Gollmer et al., 2000).

Li et al. (2008b) observed that VEGF-B is a potent apoptosis inhibitor by suppressing the expression of the BH3 (Bcl-2 homology domain 3)-only proteins (Bmf, Hrk, Bad, Bid, Bim) and other apoptotic related genes (TNF-α, Trp53inp1, Casp8, Bak, Bax), through the activation of VEGFR-1, both in the brain and in the retina, without inducing angiogenesis. Its antiapoptotic activity was tested in two conditions such as axotomy-induced neuronal apoptosis and NMDA (N-methyl-D-aspartic acid)-induced neuronal death of retina in which the neurons were rescued after intra-vitreal administration of $VEGF\text{-}B_{167}$.

1.3.1.3 VEGF Receptors (VEGFRs)

A key element in the complex regulation of VEGF activity is represented by the VEGF receptors (VEGFR): VEGFR-1 (Fms-related tyrosine kinase; Flt1), VEGFR-2 (Kinase insert Domain Receptor;KDR or Fetal liver kinase; Flk1) and VEGFR-3 (Flt4), expressed by several cell types (Figure 1.5). VEGFRs belong to the Receptor Tyrosine Kinase (RTK) super family. Members of this family consist of an extracellular domain composed by seven immuno globulin (Ig)-like domains, a short transmembrane and a juxtamembrane segment, and are characterized by a split intracellular tyrosine kinase domain interrupted by a 70 aa long kinase insert domain (Carmeliet, 2005b; Matsumoto and Claesson-Welsh, 2001; McTigue et al., 1999; Olsson et al., 2006; Roskoski, 2008; Shibuya and Claesson-Welsh, 2006).

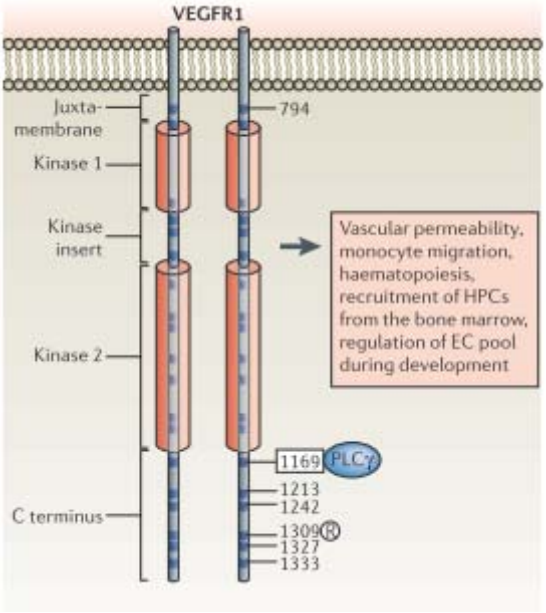

Figure 1.5 Intracellular domains of dimerized and activated VEGFR-1 is shown with tyrosine-phosphorylation sites, which are indicated by numbers. Circled R indicates use of the phosphorylation site. Dark blue square indicates the position of tyrosine residue. Binding of signaling molecule; PLCγ, phospholipase C-γ (dark blue oval) to certain phosphorylation site (boxed number), initiates the signaling cascade. Final biological outcome that is coupled to the respective receptor is indicated in pink box. (Olsson et al., 2006)

VEGFR-1

VEGFR-1(Flt-1) has high affinity towards VEGF-A, VEGF-B, PIGF and VEGF-F (De Vries et al., 1992, Olofsson et al., 1998, Park et al., 1994, Takahashi et al., 2004). Northern blot analysis showed that it is highly expressed in placenta and, at lower levels, in liver, muscle, kidney and choriocarcinoma cells. In rats, it is abundant in tissues and is expressed highly in lungs (Shibuya et al., 1990). Its expression was observed on the surface of different cell types such as endothelial cells (LeCouter et al., 2003), monocytes (Barleon et al., 1996), stem cells (Hattori et al., 2002), pericytes (Yamagishi et al., 1999), cancer cells (Wey et al., 2005), astrocytes (Krum et al., 2002) neurons (Sun et al., 2006), megakaryocytes, smooth muscle cells, osteoclasts (Casella et

al., 2003, Sawano et al., 2001) and microglia (Forstreuter et al., 2002); in several of these different cell types, the receptor plays an important role in their activation, proliferation and migration.

Even if VEGFR-1 and VEGFR-2 are structurally similar, the function of VEGFR-1 is rather different and multifaceted. VEGFR-1 has a 10-fold higher affinity for VEGF-A compared to VEGFR-2 (Waltenberger et al., 1994), however its activator function on endothelial cells is very limited or absent. For this reason, it was suggested that the receptor might act as a negative regulator of angiogenesis by acting as a decoy receptor, subtracting VEGF-A from binding to VEGFR-2. This function was supported by the early embryonic phenotype of VEGFR-1 knockout mice. These mice displayed abnormal vascular channels and died in utero at embryonic day 9.5, indicating that VEGFR-1 is essential for the organization of the embryonic vasculature, normal endothelial cell-cell or cell-matrix interactions, but not for endothelial cell differentiation (Fong et al., 1995). In contrast, VEGFR-2 null mutant mice exhibited impaired endothelial and hematopoietic cell development. Knocking out the tyrosine kinase domain of VEGFR-1 in mice had no affect on vascular development, further indicating that Flt-1 differs from Flk-1 in showing higher binding affinity to VEGF, but having lower kinase activity (Hiratsuka et al., 1998). Therefore, it has been assumed that VEGFR-1 acts as a VEGF-A trap, preventing excessive VEGFR-2 activation during embryonic development (Shibuya, 2001).

A physiological role of this endogenous VEGF-A trap was shown to be be physiologically present in adult life: a soluble VEGFR-1VEGFR-1, known as sFlt1 and expressed also by human placenta (Shibuya et al., 1990), is essential in order to preserve corneal avascularity (Ambati et al., 2006; Ambati et al., 2007).

Beside interacting with VEGFR-2, thus either synergising or inhibiting VEGF-A activity, VEGFR-1 can also interact with NP-1. This latter event plays an active role in the migration of monocytes and macrophages (Barleon et al., 1996; Zacchigna et al., 2008c) and mediates migration of haematopoietic bone marrow progenitors to initiate the pre-metastatic niche in mouse models of tumor metastasis (Kaplan et al., 2005).

VEGFR-1 signaling

Despite its ability to bind VEGF-A with more than 10-fold higher affinity than VEGFR-2, VEGFR-1 only undergoes weak phosphorylation, even if all kinase motifs are conserved (Waltenberger et al., 1994). Relevant to this issue, VEGFR-1 and VEGFR-2 share a 43% of overall homology, lower in the extracellular domain (33%) and higher in the kinase domains (70%). Nevertheless, the mechanism responsible for VEGFR-1 kinase-impaired activity is still debated. Several VEGFR-1 tyrosine residues were identified as potentially phosphorylated, together with their interacting partners (among others, SH2 domain containing protein, p38/PI3K, Growth Factor Receptor -bound protein 2 (Grb2) and Nkc) (Olsson et al., 2006; Shibuya, 2006).

Takahashi et al. (2003) reported that binding of VEGF to its receptor VEGFR-1stimuates signal transduction of both PI3K/Akt and ERK/mitogen-activated protein kinase (MAPK) in activated hepatic stellate cells in vitro. In another report, it was observed that activation of VEGFR-1 through VEGF-B has strong anti apoptotic action in rescuing neurons in the retina and brain of mouse models of ocular neurodegenerative disorders and stroke, respectively. This effect is predominantly mediated by intracellular singaling of ERK1/2 or Akt pathways and inhibition of proapoptotic BH3-only proteins and other apoptosis- and cell death–related proteins, including p53 and members of the caspase family via VEGFR-1(Li et al., 2008b). From these studies it is evident that VEGFR-1 is strongly associated with AKT and ERK/MAPK pathways in its regulation.

VEGFR-2

The gene for VEGFR-2 or KDR (kinase insert domain receptor) was cloned from a human endothelial cells cDNA library (Terman et al., 1991). Activation of VEGFR-2 induces endothelial cell proliferation, migration, angiogenesis, tube formation, vascular permeability and promotes their survival (Olsson et al., 2006). This receptor is also expressed, albeit at lower levels, in other cell types, such as various types of stem cells (Rafii et al., 2003), CD34/AC133-positive bone-marrow precursors, neuronal cells (Asahara et al., 1999), in which it mainly induces

proliferation, recruitment, growth and survival (Sondell et al., 2000, Jin et al., 2006). By acting as the main receptor for VEGF-A, it plays a major role in both angiogenesis and vasculogenesis (Millauer et al., 1993).

Extensive experimental evidence showed that VEGFR-2 signaling is required for cardio vascular development (Shalaby et al., 1995) and it plays a major role in neovasculari- zation in both physiological and pathological conditions. During development, VEGFR-2 expression is detectable from E7.5 in mesodermal cells, which then migrate and differentiate into primitive ECs (Shalaby et al., 1995). During adult life, VEGFR-2 is expressed mostly in vascular and lymphatic ECs, even if lower levels of VEGFR-2 are detected in haematopoietic stem cells, neurons, osteoblasts as well as megakaryocites (Matsumoto and Claesson-Welsh, 2001). Yamashita et al. (2000) observed that FLK positive cells derived from embryonic stem cells can act as vascular progenitors; these cells can differentiate into endothelial and mural cells and form mature vessels in three-dimensional cultures and in chick embryos

In several organs, the activities of this receptor extend beyond angiogenesis. For instance, the interaction between VEGF-A and KDR plays a pivot role for the normal development of the ocular vasculature at early developmental stages but also for nonvascular retinal developmental functions, such as coordination of neural retinal development (Gogat et al., 2004).

In contrast with the canonical pro-angiogenic role of VEGF-A/VEGFR-2 signaling, Greenberg et al. (2008) defined a role for VEGF-A mediated activation of VEGFR-2 as an inhibitor of neovascularization, on the basis of its capacity to disrupt vascular smooth muscle cell function. VEGF-A can indeed suppress the assembly of a receptor complex consisting of platelet derived growth factor receptor-B (PDGFRB) and VEGFR-2, thus decreasing pericyte coverage, preventing vessel maturation and promoting endothelial cell proliferation. Another report showed that a secreted form of VEGFR-2 (sVEGFR-2) can inhibit developmental and reparative lymphangiogenesis induced by VEGF-C. Tissue-specific loss of sVEGFR-2 in mice at birth induced spontaneous lymphatic invasion in a developed mouse model of alymphatic cornea and hyperplasia of skin lymphatics without affecting blood vasculature. In contrast,

administration of sVEGFR-2, inhibited the process of lymphangiogenesis but not hemangiogenesis when tested in different models such as mouse model of corneal transplantation, corneal allograft and suture-induced corneal neovascularization where lymphangiogenesis is the major process (Albuquerque et al., 2009).

VEGFR-3

VEGFR-3/Flt4 constitutes the receptor for the VEGF-C and VEGF-D family members. The observation that, in adults, VEGFR-3 expression is restricted to the lymphatic endothelium, together with the availability of genetic models, essentially linked this receptor to lymphatic development and maintenance (Kaipainen et al., 1995, Veikkola et al., 2001). In particular, VEGFR-3 signaling is required for lymphatic EC sprouting, as well as for lymphatic vessel maintenance through the inhibition of apoptosis (Alitalo et al., 2005). Nonetheless, VEGFR-3 gene knockout mice exhibit defects in arterial-venous remodelling of the primary vascular plexus, leading to embryonic lethality from day E9.5 (Dumont et al., 1998). Therefore, during embryonic development, VEGFR-3 activity is not restricted to lymphatics, but has an important function in blood vessel development as well. Recent data extended the role of VEGFR-3 in angiogenesis also during adult life; VEGFR-3 was found to be highly expressed in angiogenic sprouts, while targeting of VEGFR-3 signaling resulted in decreased sprouting, vascular density, vessel branching and EC proliferation in different mouse angiogenesis models (Tammela et al., 2008).

VEGFR-3 is also found to be up-regulated in the tumor microvasculature, thus opening the possibility to exploit VEGFR-3 targeting agents to inhibit tumor growth (Saharinen et al., 2004). The extension of the VEGFR-3 role not only to lymphatic biology, but also to pathological and embryonic development, warrants further studies to define the molecular mediators of these diverse activities, still incompletely explored.

As already mentioned in the case of VEGFR-1, VEGFR-3 signaling can be modulated by the interaction with VEGFR-2 and other co-receptors, such as NP2. The formation of these complexes is biologically relevant and, for example, VEGFR-2-VEGFR-3 heterodimers

might form in vivo both in lymphatic cells and subtypes of ECs, resulting in differential phosphorylation sites and eventually differential signaling (Dixelius et al., 2003).

All these observations suggest that VEGFR-3, besides its fundamental role in lymphatic vessel development and maintenance, also acts as a regulator of vascular network formation and therefore may constitute an additional target of anti-angiogenic therapies.

Neuropilins

Neuropilins (NP1 and NP2), initially identified as receptors for class 3 semaphorins, in association with plexin family receptors, mediate repulsive axon guidance in the developing nervous system (Fujisawa, 2004). Even if NP1 and NP2 share only 44% homology, they have similar structural features but different binding and signaling properties (Neufeld et al., 2002). In particular, Semaphorin3A (SEMA3A) only binds NP1, SEMA3F and SEMA3G interact only with NP2, while SEMA3B, SEMA3C and SEMA3D bind both receptors. Additionally, NP1 and NP2 also display specific and mutually selective binding to factors not belonging to the SEMA family, such as VEGF-A, VEGF-B, VEGF-C, PlGF, PDGF-bb, FGF2, TGF β, Hepatocyte Growth Factor (HGF) and galectin. Moreover, neuropilins differ in VEGF-A isoform binding, as NP2 binds to VEGF-A_{165} and VEGF-A_{145} , while NP1 mainly binds VEGF-A_{165} (Shraga-Heled et al., 2007, Pan et al., 2007).

The biological difference between NP1 and NP2 is enforced by their non-redundant role in development, as NP1 deficient mice die during mid-gestation with defects in the heart, vasculature, and nerve projection (Kawasaki et al., 1999), while NP2 knockout mice are viable and display only defects in nerve projection (Chen et al., 2000; Giger et al., 2000). Interestingly, the double NP1/NP2 knockout mouse had a more severe abnormal vascular phenotype than either NP1 or NP2 single knockouts, resembling the phenotypes of VEGF-A and VEGFR-2 knockouts (Takashima et al., 2002).

Neuropilin1 (NP1)

NP1 is a functional, transmembrane receptor, able to mediate signaling from structurally distinct ligands during nervous system, heart and vascular development. In particular, NP1 expression in EC is required for cardiovascular development (Gu et al., 2003), and is important for the formation of the primitive capillary plexus, partially independently from blood flow (Jones et al., 2008). It selectively binds the VEGF-A_{165} isoform and it is expressed at high levels in heart and placenta, moderately in lung, liver, skeletal muscle, kidney, and pancreas, and poorly in brain (Soker et al., 1998).

Due to its short and catalytically inactive intracellular tail, NP1 has been traditionally considered a dead receptor, only able to enhance VEGF-induced signal through VEGFR-2 interaction. On the contrary, recent evidence suggests that NP1 mediates HUVEC adhesion to extracellular matrix (Murga et al., 2005) as well as increases VEGF-A-induced EC survival (Wang et al., 2007), independently from VEGFR-2. Thus, NP1 seems to regulate EC functions by almost two different mechanisms: by enhancing VEGF binding to VEGFR-2 and by a VEGFR-2 independent signaling, but how these mechanisms are coordinated is still an unresolved question.

1.4 HEART FAILURE

The term *heart failure* (HF) refers to a clinical syndrome, in which an abnormality of cardiac structure or function is responsible for the inability of the heart to fill with or eject blood at a rate commensurate with the requirements of the metabolizing tissues. Clinically, the cardinal symptoms of HF are fatigue and dyspnea, associated with the presence of pulmonary and/or peripheral edema. In case of left ventricular failure, patients may have pulmonary edema, dyspnea even at rest. In case of right ventricular failure, patients may have ascites, edema of lower limbs and hepatomegaly. In case of biventricular failure, patients may have fluid accumulation between lungs and chest wall (pleural effusion).

HF and its complications are diagnosed by echocardiography (to measure left ventricular function) or electrocardiography (to identify arrhythmias), chest radiography (to diagnose

pulmonary edema), angiography (to evaluate the patency of coronary arteries in patients with history of coronary artery disease) and blood and urine tests (to analyze liver function and total blood count).

Current standard treatment for HF includes the use of ACE inhibitors, diuretics, calcium antagonists, digoxin, β-blockers or antiplatelet agents. If the patient couldn't respond to medication, surgical interventions are preferred to implant devices, such as pacemakers, defribrillators and left ventricular assist devices (LVADs). In most severe cases, heart transplantation can be considered.

The etiology of HF includes coronary artery disease (CAD) (in 65-70% of patients), inherited cardiomyopathy, hypertension, hyperthyroidism or valvular abnormalities (National Institute of Clinical Excellence 2003, Clinical Knowledge Summaries, 2006, British Heart Foundation 2004).

The incidence is increasing with age, being about 1:1000 after 65 years of age (Lloyd et al., 2002), resulting in a heavy socio-economical burden. The cost of expenditure for HF in United States was 34.8$ billion in 2008 (Rosamond et al., 2008) and nearly 2% of total sanitary budget in United Kingdom (Stewart et al., 2002).

1.4.1 Morphological changes in the heart leading from myocardial infarction to HF

HF is the final common pathway for several pathologies of the heart. Before reaching this stage, the heart undergoes several changes, collectively referred to as ventricular remodeling, essentially due to changes in loading condition. Among the most common etiologies of HF is ischemic heart disease. In this case, disease progression can be schematically divided in two phases: an early phase (within 3 days from the ischemic event) during which the infarct region expands and may lead to cardiac rupture, and a late phase (after the first 3 days), which involves dilatation of ventricle, distortion in shape and compensatory hypertrophy, paralleled by intense formation of scar tissue in the infarcted zone (Sutton et al., 2000). Due to these sudden changes, the chamber radius progressively increases while the thickness of the anterior wall gradually decreases (Litwin et al., 1994). As a consequence, the number of viable cardio-

myocytes in that area gradually reduces, which leads to loss of overall contractile function, particularly evident in the case of transmural infarcts (Pfeffer 1995). Additional changes, such as increase in end systolic and end diastolic volumes with decrease in ejection fraction and shortening fraction (Pennock et al., 1997) are frequently observed. All these changes can be predicted and measured by echocardiography.

1.4.1.1 Compensatory and pathological hypetrophy

Cardiac hypertrophy is the responsiveness of heart to various extrinsic stimuli such as arterial hypertension or valvular heart disease, or even to an intrinsic stimulus as in familial hypertrophic cardiomyopathy. Traditionally, it was believed that hypertrophy was an adaptive response required to preserve normal cardiac output, altered by stress conditions. However, recent evidences suggest that the hypertrophic process is mostly a maladaptive process (Vakili et al., 2001, Frey et al., 2003). When the hypertrophic stimulus is prolonged, it can either lead to sudden death or progress to heart failure. Two distinct forms of cardiac hypertrophy are known and characterized. Physiological hypertrophy is determined by physiological stimuli such as exercise, pregnancy and post natal growth, and consists in the proportional growth of cardiomyocyte number, cardiomyocyte size and vascular network, without any cardiac fibrosis. Pathological hypertrophy is mainly seen in patho-physiological stress conditions such as aortic stenosis, neurohormonal activation, cardiac injury or inflammation. The various cellular changes observed in pathological cardiac hypertrophy are increase in cell size, reduced cell:capillary ratio, increased fibrosis, increase in protein synthesis concomitant with increase in contractile protein content into sarcomeric units (sarcomere higher organization) (Aoki et al. 2000b, Frey et al., 2003) and induction of certain genes such as natriuretic peptides (ANF, BNP), skeletal α-actins, growth factors like endothelin-1, insulin-like growth factor-1, transforming growth factor -β1 (Takahashi et al., 1994), sarcomeric proteins βMHC in rodents, myosin light chains 1α and 2α (Sutton et al., 2000, Sadoshima et al., 1992).

One of the factors known to induce compensatory/physiological hypertrophy of cardiomyocytes is thyroid hormone (T3 or T4). It increases speed of systolic contraction and

diastolic relaxation, heart rate, while it decreases vascular tone and hypertrophy of cardiomyocytes. By binding to its receptors –α, (predominant isoform) and -β on cardiomyocytes, it induces calcium flux into the cell through activation of genes encoding SERCA2a and myofibrillar proteins, such as α MHC and through the downregulation of β MHC. T3 stimulates PI3 kinase dependent AKT phophorylation, which in turn induces a gene expression pattern compatible with physiological cardiac hypertrophy (Dillmann 2010). Recent evidence suggests that in pressure overload conditions, the receptor levels of thyroid hormone decreases, together with a simultaneous decrease in serum levels of T3 and T4: both these events represent negative prognostic indicators in the progression toward heart failure.

Pathological hypertrophy is caused by several factors. Among these, the α-adrenergic agonist phenylephrine (PE) constitute widely used agents to study the molecular mechanisms of pathological hypertrophy. PE blocks norepinephrine at α -adrenergic receptors (α -1 and -2), members of the 7-transmembrane spanning Gq protein-coupled receptor family and exerts positive inotropic and chronotropic effects on cardiomyocytes (Srivastava et al., 1977). In neonatal rat myocardial cells, α-adrenergic agonists or endothelin-1 activate hydrolysis of phosphatidylinositol and generates two potential intracellular signals, inositol phosphates and diacylglycerol (De Jonge et al., 1995) (Shubeita et al., 1990). Diacylglycerol in turn activates protein kinase C (Mochly-Rosen et al., 1990), calcineurin and MAP kinase signaling pathways (Dillmann 2010, Wakatsuki et al., 2004). All these changes cause accumulation and assembly of contractile proteins (myosin light chain-2(MLC-2)) into sarcomeric proteins, increase in cell size, alterations in cardiac metabolism, intracellular calcium changes, changes in myofibrillar protein contraction coupling, cardiac hypertrophy and activation of embryonic gene expression pattern, such as reduced expression levels of SERCA2a, αMHC and increased expression levels of β MHC (Dillmann 2010, Ross et al., 1990, Chien et al., 1991). Following is a description of a few key molecular players involved in pathologically hypertrophy, which were analyzed in the experiments reported in this thesis.

- Ryanodine receptors, present on the sarcoplasmic reticulum (SR), are key players in handling the calcium required for cardiac muscle excitation-contraction coupling. In myocardial cells, the RyR2 protein is activated by a relatively small increase in Ca^{+2} concentration within the cytoplasm, and triggers massive release of calcium from the SR depots into the cytosol. The expression levels of RyR2 are usually decreased in cardiac ischemia (Brillantes et al., 1992) and in dilated cardiomyopathy (Go et al., 1995).

- ANF and BNP are structurally related peptides. They are important in the regulation of renal and cardiovascular function. ANF is secreted by atria in response to pressure overload and, in most of the cases; it is an indicator of left ventricular dysfunction. Like ANF, BNP is secreted in response to pressure or volume overload by the ventricular myocardium. Both proteins are quite useful in diagnosis and prognosis of various cardiac abnormalities. The expression levels of ANF increase in both physiological and pathological hypertrophy, whereas up-regulation of BNP tends to be observed selectively in pathological conditions (Kong et al., 2005, Sakata et al., 2001).

- PGC1α (peroxisome proliferator activated receptor-γ co-activator) belongs to family of transcription co-activators involved in regulation of cellular energy metabolism. It is a co-activator of PPARα (peroxisome proliferator-activated receptor α). Both activators induce the expression of enzymes involved in fatty acid oxidation and of other proteins involved in mitochondrial energy transduction/production (mitochondrial biogenesis); the overall result of this shift in gene expression is the transformation of muscular tissue into fibrous tissue, which is more oxidative and less glycolytic in nature. In cardiac hypertrophy, the expression levels of PGC1α are markedly decreased and cause shift in the cardiac metabolism from fatty acid oxidation to glycolysis (Lehman 2002). In keeping with this concept, cultured cardiomyocytes respond to PE by down-regulating PGC1α, thereby suppressing fatty acid oxidation (Lehman 2002).

- Actins are ubiquitous structural proteins involved in several cellular functions, like cell adhesion, cell division, motility, cell shape maintenance and muscular contraction. They exist in

6 isoforms, 4 of which are predominantly expressed in skeletal, cardiac, vascular and enteric smooth muscles. They are α-skeletal actin, α-cardiac actin, α-smooth muscle actin and γ-smooth muscle actin. Among these, one of the isoforms of Skeletal α actin, Skeletal α actin 2- is the predominant isoform in cardiac muscle; its expression is induced by G protein coupled receptor signaling and is considered as a genetic marker for hypertrophy. In newborn rats, it is distributed uniformly in all myocardial fibrils, whereas in adults, it is limited to a small portion of cardiomyocytes. Under stimuli leading to cardiac hypertrophy, its concentration increases significantly to resist the physical forces (Chaponnier et al., 2004, Bishopric et al., 1987) both in vitro (Gosteli-Peter 1996) and in vivo (Black et al., 1991).

1.5 Gene therapy strategies for cardiovascular disorders

Our increasing understanding of the complex mechanisms controlling blood vessel formation led to the development of several approaches of gene therapy for the induction of therapeutic angiogenesis in ischemic tissues.

The first class of therapeutic genes considered in this context comprises those genes, which are naturally up-regulated during angiogenesis (VEGF-A, HIF-1). Activation or overexpression of these factors (which are sometimes referred as master regulatory factors) results in subsequent activation of their downstream effector pathways, and is therefore expected to recapitulate the whole angiogenic process. In addition, several molecules, known to be somehow involved in one of the multiple steps of angiogenesis (Fibroblast Growth Factor-1, Angiopoietin-1, Transforming Growth Factor-β and others) have been proposed as potential angiogenic factors for gene therapy and their efficacy has been so far proved in preclinical experimentation.

The success of heart-directed gene therapy has become more realistic thanks to the modern surgical approaches that allow to deliver genes efficiently into the coronary vessels or even directly into the myocardium. In particular, the approaches that have reached the clinics so far mainly entail the injection of the therapeutic genes into the coronary arteries by arterial catheterization or the direct administration to myocardium through a minimal thoracotomy

(for instance, during CABG surgery). Alternatively, experiments in large animal models have shown the feasibility of a retrograde delivery, by injecting the therapeutic vectors into coronary sinus, possibly associated to an increase in the venous pressure, in order to enhance the retrograde flow.

As in other fields, the success of a cardiovascular gene therapy application mainly depends on three major parameters, namely the choice of an appropriate therapeutic gene, the delivery of this gene to a sufficient number of cells and the achievement of appropriate levels of gene expression.

The most efficient viral vectors in the cardio vascular system are recombinant Adenovirus (Ad) or Adeno-Associated Virus (AAV) (Fisher et al., 1997, Guzman et al., 1993). Even though both vectors share a few similar features, such as the ability to transduce a variety of quiescent cell types after in vivo injection, for in vivo applications, adenoviral vectors are notably limited because of their strong immunogenicity and capacity to stimulate a potent inflammatory response (Yang et al. 1996). In addition, major safety concerns about a wider use of these vectors have been raised by the death of a young patient recruited in a gene therapy trial for the treatment of a rare metabolic disorder (OCT deficiency). This lethal event was most probably due to a systemic inflammatory response to the vector triggered by the expression of several wild type adenoviral genes by the transduced cells (Lehrman 1999).

For these reasons, AAV is becoming the vector of choice for a growing number of pre-clinical experimentations of cardiovascular gene therapy and has already progressed to the clinics in one case.

1.5.1 AAV

AAV is a small non-enveloped, single-stranded (ss) DNA virus with a diameter of 18–25 nm, belonging to the family Parvoviridae and the genus Dependovirus.

Members of this genus are widely diffuse in nature: well over 100 AAV variants have so far been isolated from primate sources, and new serotypes are continuously discovered. All

serotypes share a similar structure, genome size and genetic organization and have wide range of tissue tropism. Tissue specificity is determined by capsid serotype or pseudotypying of AAV. Among all the serotypes, serotype-2 is the most extensively studied so far. From the past several years, AAV has been much popularized as a safe viral vector in gene therapy applications because of its interesting favorable characteristics. It indeed transduces post mitotic tissues such as muscle, brain, heart and retina at high efficiency and maintains long term persistence transgene expression without any inflammatory or immune response (Favre et al., 2001).

Structure:- The wild type AAV genome is 4. 7kb in length with two open reading frames (ORFs) encoding for Cap and Rep genes for the synthesis of capsid and replicative proteins, respectively. It uses two different promoters and an alternative included exon to produce four protein isoforms (Rep 78, 68, 52 and 40) from its Rep gene and three different products (VP1, VP2, VP3) from its Cap gene. The coding sequence is flanked by two 145 bp inverted terminal repeats (ITRs), which have complementarity in their first 125 bp and form T-shaped hairpins at both ends of the genome. These palindromic sequences are the only *cis*-acting elements important for all major functions of AAV (viral DNA replication, assembly of the viral particles, integration/excision from the host genome) and is the only sequence of viral origin present in the vector DNA (Figure 1.6).

A

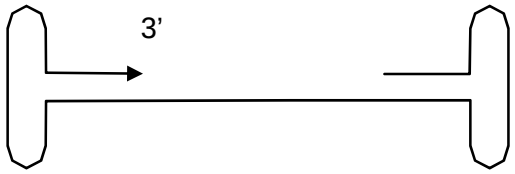

B

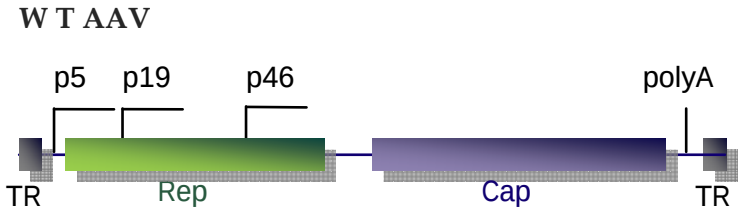

C

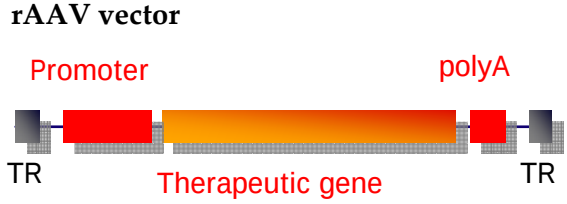

Figure 1.6 A) The replicative single stranded DNA of AAV B) Wild type AAV contains Cap and Rep genes to synthesize capsid and replicative proteins; the genome is flanked by two 145 bp inverted terminal repeats (ITRs) C) A recombinant AAV vector is constructed from its wild type counterpart by replacing the Cap and Rep genes with the therapeutic gene and a desirable promoter sequence.

The life cycle of wild type AAV strictly depends on the presence or absence of host cell co-infection with a helper virus. Under non-permissive conditions (i.e. without a helper virus), the AAV genome integrates at a specific site (AAVS1) on human chromosome 19q13.3 (Dutheil et al., 2000, Kotin et al., 1992, Linden et al., 1996), and establishes latent infection for indefinite periods of time. This peculiar characteristic might potentially open the gate for safe insertion of exogenous genes into the human genome, which is a highly desirable goal in the field of gene therapy. However, site specific integration entirely depends on the function of the AAV Rep proteins, this gene is removed from the vector DNA in order to control its unregulated expression, which is toxic to infected cells (Marcello et al., 2000). The current generation of AAV vectors persists inside non dividing cells mainly as extra chromosomal, concatemerized DNA (Schnepp et al., 2005).

Preparation and purification of AAV:- The capacity of AAV to persist in infected cells as a latent viral genome makes it an excellent tool for in-vivo gene transfer (Tratschin et al., 1984). When it is cloned into a plasmid, it is still infectious and produces viral particles. This virus can accommodate any transgene less than 4.5 kb in length within its 145 bp ITRs, to form a circular backbone suitable for vector production. The traditional method for rAAV production was based on co-transfection of vector plasmid together with a secondary plasmid, supplementing the Cap and Rep gene functions, into Adenovirus-infected cells (usually HEK 293 or HeLa cells). Recently, adenovirus co-infection was substituted by the use of a single plasmid assembling both the required AAV and adenoviral genes (providing helper functions), in order to reduce number of plasmids and to eliminate contaminants (Grimm et al., 1998).

AAV can be purified by different methods. The classical method of purification is density gradient (CsCl or ioxidanol) centrifugation. It is effective for small scale production, and yields highly pure viral preparations suitable for research studies. The viruses are centrifuged to

equilibrium in a CsCl salt, so that they are separated from the contaminants and collected in bands on the basis of their buoyant densities. The limitations in this process are cytotoxicity of CsCl, variable quality of vector preparations, significant loss of infectivity and aggregation during storage. More recently, iodixanol has been used as an alternative to CsCl to minimize toxicity. It prevents aggregation of rAAV particles and doesn't affect infectivity. For large scale production, chromatographic separation is widely used, including ion exchange, gel filtration and hydrophobic interaction. The purification by ion-exchange chromatography is based on the net charge of proteins on the exterior of the viral capsid and the net charge of the surface proteins which depends on pH of the exposed amino acid groups. Size-exclusion column chromatography or gel filtration chromatography is used to separate mature viral particles from partially assembled capsids, proteins and DNA fragments. It is the method of choice for the purification of viruses of different sizes. The main disadvantages in this method are the constraints with column sizes and the difficulty in separation of viruses from high molecular weight contaminants. The final mode of chromatographic separation is hydrophobic interaction chromatography. It is based on binding of viral capsid proteins to the column matrix through hydrophobic interaction in an aqueous solvent. However, purification of AAV by this method has not yet reached extensive application (Burova and Ioffe 2005).

1.5.2 Gene therapy for the induction of therapeutic angiogenesis

The main goal of this approach is to increase oxygen-rich blood supply through the development of new collateral blood vessels in ischemic areas. Traditionally, new blood vessel formation in the adult life occurs through capillary sprouting from pre-existing vessels. This process is initiated by the metabolic activation, proliferation and migration of endothelial cells, concomitant with vast remodelling of the extracellular matrix (Risau 1997).

Over the last 15 years, several cytokines and growth factors including VEGF, Hepatocyte growth factor (HGF), Fibroblast growth factor (FGF), PlGF, PDGF, Insulin like growth factor (IGF), Angiopoietins, nitric oxide synthase (NOS) and others are identified and used either as a single gene or in combinations to activate an angiogenic response. Following is a description of

the main genes so far considered for angiogenic gene therapy studies in different animal models.

In physiological conditions, the main regulator of angiogenesis is hypoxia. In conditions of low oxygen tension, the cellular transcription factor HIF-1 (Hypoxia Inducible Factor –1) is post-translationally stabilized and activates the expression of a vast series of genes, among which the vascular endothelial growth factor (VEGF) and its receptors are required in all phases of angiogenesis (Liu et al., 1995). In keeping with its prominent role in the formation of new blood vessels, VEGF is by far the most investigated molecule for the induction of therapeutic angiogenesis. Several experiments have been performed with the various VEGF isoforms in different animal models. Following is a short description of the results obtained by a few, selected, paradigmatic experiments. Tsurumi et al. (1996) observed that intramuscular (IM) injection of naked plasmid DNA encoding VEGF induced capillaries and collateral branching of existing vessels in a hind limb ischemia model of rabbits. Hao et al. (2007) compared the angiogenic efficacy of human VEGF-A_{165} delivered either as a plasmid (P) or by an adenoviral vector (Ad) in a rat myocardial infarction model and observed that in both cases, the biological effects, such as maintenance of increased arteriolar density and improved left ventricular function, were similar. In another experiment, adenoviral-mediated VEGF gene transfer induced the formation of a vast vascular network, initiated with sprouting of capillaries, arterioles, transformation of capillaries into arterioles and enlargement of large arteries and veins in a hind limb ischemia model in rabbits (Rissanen et al., 2005). Gowdak et al. (2000) demonstrated that intramuscular injection of AdVEGF-A_{121} resulted in a significant lengthening of arterioles and capillaries of non-ischemic limbs both in the rat and in the rabbit. Moreover, tissue perfusion was preserved in these animals when the vector was injected 2 weeks prior to the induction of hind limb ischemia. Tafuro et al., (2009) studied the process of neoangiogenesis of AAV-VEGF-A_{165} using tetracycline-inducible transactivator system in the hind limb ischemia model of mice. Long term expression of AAV-VEGF-A_{165} induced massive cellular infiltration with the formation of a large set of new vessels in the tibialis anterior muscle of rats (Arsic et al., 2003). Parsons-Wingerter et al. (2006) observed that treatment of Quail chorioallantoic

membranes with recombinant human VEGF-A_{165} can induce maximum vessel density at a low concentration after 24 hours; however, at higher concentrations, it promotes increase in vessel diameter as well as in the eNOS production, which is known to interact with downstream and upstream targets of VEGF and stimulate vasodilatation and vascular permeability during physiological angiogenesis. Intracardiac injection of AAV-VEGF-A_{165} induced angiogenesis in ischemic heart without any angioma formation (Su et al., 2000, Ferrarini et al., 2006). Lazarous et al., (1999) investigated the effect of VEGF when delivered pericardially and found that it maximized collateral perfusion and myocardial collateral development in canine model of progressive coronary occlusion in addition to angiogenesis. Schwarz et al., (2000) evaluated direct intracardial injection of plasmid encoding VEGF in the border zone of infarct tissue in ischemic rat hearts, and showed significant angiogenesis with improved regional blood flow without any angioma formation at the site of delivery. Later, VEGF was tested in several phase I clinical trials, essentially using adenoviral vectors in patients with coronary artery disease. Intracardiac administration of VEGF-A_{121} into the ischemic region showed an improvement in symptoms of angina without any adverse effects (Rosengart et al., 1999).

An alternative possibility is to use gene combinations, by mixing genes that should provide complementary activities. For instance, the VEGF gene has been extensively used in combination with other angiogenic genes. Examples of these combinations include VEGF/FGF (Kondoh et al., 2004), VEGF/PIGF (Zheng et al., 2006), VEGF/angiopoietin (Niagara et al., 2004, Arsic et al., 2003) or multiple isoforms of VEGF (Whitlock et al., 2004). The rational of using gene combinations is to provide functions that operate in subsequent steps of the angiogenic process, therefore resulting in a 'more complete' vessel maturation, similar to the concept of using master regulatory genes, described above.

Beside VEGF, another gene extensively considered for the induction of therapeutic angiogenesis is FGF. This name actually includes 22 related proteins, several of which have been implied in small and large blood vessel formation. For instance, FGF-2, FGF-4 and FGF-5 are believed to have peculiar angiogenic properties. Safi et al. (1999) reported that intracardiac delivery of adenovirus–expressed FGF gene induced neovascularization (resulting in a 2-fold increase in

intramural coronary arteriolar density and in a 17% increase in capillary network density) and reduced the size of myocardial infarction in rabbits. Intracoronary delivery of recombinant Ad-human FGF-5 in an ischemic porcine model showed significant improvement in myocardial blood flow with evidence of angiogenesis already evident at 2 weeks after the treatment and lasting until 12 weeks (Giordano et al., 1996).

HGF is a paracrine cellular growth factor secreted by mesenchymal cells. It regulates cell growth, motility, morphogenesis of epithelial, endothelial and haematopoietic progenitor cells. It is important for the development of multiple organs in embryos and plays an essential role in organ regeneration and wound healing in adults (Gallagher et al., 2000). The up-regulation HGF is partly mediated by VEGF (Dong et al., 2001). Aoki et al. (2000a) investigated the angiogenic potential of HGF by delivering its gene to rat myocardium both in ischemic and non ischemic conditions by HVJ-liposome transfection and found a significant increase in the number of Proliferating Cell Nuclear Antigen (PCNA) positive endothelial cells, particularly evident in ischemic conditions, indicating extensive endothelial cell proliferation in response to HGF.

PIGF is a dimeric glycoprotein belonging to the VEGF family. It shows high sequence similarity with VEGF and seems important in adult neovascularisation. Alternative splicing of a primary transcript produces 2 isoforms: PIGF-1 and -2. In-vivo, PIGF-1 gene transfer determined a potent neo-vascularisation in two models of neoangiogenesis, namely the rabbit cornea and the chicken chorioallantoic membranes, yet its angiogenic effect was less significant compared to VEGF or FGF (Ziche et al., 1997).

PDGF is a cationic glycoprotein existing in 5 different isoforms: PDGF-AA, PDGF-AB, PDGF-BB, PDGF-CC and PDGF-DD (Colciago et al. 2009). They all bind to the tyrosine kinase (RTK) cell surface receptors PDGFR-α and β. They are expressed widely in human tissues (Tallquist and Kazlauskas 2004), promote proliferation, migration and survival of several derived cells of mesenchymal origin, such as SMCs and fibroblasts. In particular, they support the growth of existing blood vessels by pericyte recruitment (Lindahl et al., 1997). An investigation disclosed that the combination of recombinant PDGF-B with VEGF (Richardson et al., 2001) or FGF-2 (Cao

et al., 2003) produced mature stable blood vessels even after their withdrawal in the rat cornea (Cao et al., 2003). Another isoform, PDGF-CC, delivered through an osmotic minipump enhanced post-ischemic revascularization in the heart and limb of mice, possibly by promoting the differentiation of bone marrow cells into endothelial and smooth muscle cells and stimulated their growth during vessel sprouting (Li et al., 2005).

IGF is also known as somatomedin C or mechano growth factor, and exists in 2 isoforms: IGF-1 and IGF-2. IGF-1 is the main mediator of the growth promoting effects of the growth hormone (GH). Hellstrom et al. (2001) investigated the angiogenic properties of IGF-1 using a retinopathy of prematurity (ROP) model in IGF-1 knockout mice. The authors reported that, in the absence of IGF-1, vessels ceased to grow and mature in the avascular retina even in the presence of sufficient VEGF levels; on the other side, when IGF-1 levels were up-regulated to a critical level, retinal neovascularization was triggered again. In addition, IGF-1regulates cell proliferation, differentiation and apoptosis of many cell types (Froesch et al., 1985, Barres et al., 1992). Buerke et al., (1995) described that transduction of recombinant human IGF-1 protected cardiomyocytes from apoptosis in a murine model of myocardial ischemia reperfusion. However the signaling pathway underlying the protective activity of IGF-1 is still under investigation.

Besides endothelial cell sprouting, functional new blood vessel formation also requires several factors (such as angiopoietins ad others), which act at later time points to promote vessel maturation. Angiopoietins exist in 2 isoforms: angiopoietin-1 (Ang1) and angiopoietin-2 (Ang-2). Ang-1 interacts with the Tie-2 receptor on the endothelial cell surface and reduces the permeability of the newly formed vasculature (Arsic et al., 2003, Asahara et al., 1998, Davis and Yancopoulos 1999, Thurston et al., 2000). The two ligands for Tie2, (Ang1 and Ang2) were originally described in tissue culture experiments as pro-angiogenic (Suri et al., 1996) and anti-angiogenic (Maisonpierre et al., 1997), respectively. The corneal pocket assay has shown that both Ang1 and Ang2 similarly act synergistically with VEGF-A to promote vessel growth (Asahara et al., 1998). In particular, transcorneal injection of recombinant human Ang-2 in the context of the transient ocular microvessel network of the papillary membrane (which

represents a unique in vivo model to study the effects of vascular regulators) promoted proliferation, migration of endothelial cells, rapid increase in capillary diameter, remodelling of the basal lamina and sprouting of new blood vessels in the presence of endogenous VEGF-A; in contrast, it promoted endothelial cell death and vessel regression in the absence of endogenous VEGF-A (Lobov et al., 2002). However, the data available over these factors in describing their function is largely controversial.

NO is synthesized from L-arginine in endothelial cells by the enzyme nitric oxide synthase (NOS3). NOS3 regulates vasomotor tone and blood flow by inhibiting smooth muscle contraction and platelet aggregation. It is responsible for the maintenance of systemic blood pressure, vascular remodelling and angiogenesis (Fulton et al., 1999). Adenoviral delivery of the NOS gene enhanced tissue perfusion and vasodilatation in a hind limb ischemia model in rats (Brevetti et al., 2003). However, direct evidence of its effect on endothelial cell proliferation and maintenance of vascular stability is poor (Cooney et al., 2006).

Beside all the above mentioned genes, other candidate therapeutic genes, currently under investigation to induce therapeutic angiogenesis, include Del-1 (developmentally regulated endothelial locus 1) (Zhong et al., 2003), early growth response-1 (Abdel-Malak et al., 2009), adrenomedullin (Tokunaga et al., 2004), sonic hedge-hog (Kusano et al., 2005), PR39 (Li et al., 2000), stromal cell derived factor-1α (Hiasa et al., 2004), Ets-1(Sato et al., 2001), Id-1(Nishiyama et al., 2005), endocrine gland-derived VEGF, a few cytokines such as monocyte chemoattractant protein-1 (Ito et al., 1997), granulocyte colony stimulating factor (Okazaki et al., 2006) and various transcription factors like zinc finger transcription factor (Dai et al., 2004). Further studies are clearly needed to prove the therapeutic potential of these molecules in vivo.

1.5.3 Gene therapy strategies for the treatment of HF

The goal of the HF therapy is to preserve or to correct alterations in basic key molecular mechanisms of cardiac function, mainly β-adrenergic receptor cascade or Ca^{+2} homeostasis.

Based on these mechanisms, some important molecules under study are SERCA2a, Phospholamban (PLN), Parvalbumin (PV), Protein phosphatise 1 inhibitor-1(PP-1-H-1), S100A1, Adenyl cyclase(AC)6 and GRK2.

In the failing myocardium, a critical observation is that the loss of activity of serum Ca^{+2} ATPases causes functional loss of calcium reuptake (Hasenfuss et al., 1994). In keeping with this finding, intracoronary delivery of Adv-SERCA2a in a rat heart failure model showed improvement in left ventricular function and survival rate 28 days after treatment (Del Monte et al., 2001). Similar results were obtained by AAV1-SERCA2a administration through epicardial coronary artery infusion in a HF model in pigs with mitral valve impairment (Kawase et al., 2008). Based on these results a clinical trial based on AAV-SERCA2a gene delivery to the myocardium of HF patients is currently undergoing at the Mount Sinai Hospital in New York, USA.

An alternative approach to activate serum Ca^{+2} ATPases for HF gene therapy is targeting PLN. Indeed, lowering the levels of PLN (as in KO mice) increases cardiac performance and decreases contractile defect in response to ß-adrenergic stimulation (Luo et al., 1994). In a therapeutic perspective, a dominant negative mutant PLN (PL-S16) was generated by introducing a mutation at serine-16 (S16E), where the target for PKA is located. This dominant negative PLN mutant was used to enhance SERCA2a activity. AAV-mediated overexpression of PL-S16E in HF models in both hamsters and mice prevented cardiomyocyte dysfunction (Hoshijima et al., 2002, Iwanaga et al., 2004). The mutant was also tested in sheep, using an adenoviral vector, administered through an intracoronary route (Kaye et al., 2007).

Decrease in intracellular Ca^{+2} sequestration causes prolonged relaxation, which is characteristic of disastolic dysfunction in HF patients. Correcting the diastolic dysfunction is an alternative approach. Wahr et al. (1999) hypothesized that expression of the Ca^{+2} binding protein parvalbumin in cardiac myocytes would lead to increased rates of Ca^{+2} sequestration and mechanical relaxation. Parvalbumin (PV) is a high affinity calcium binding protein belongs to the EF-hand Ca^{+2} binding motif super family. It is related to Calmodulin and Troponon C in structure and function. PV was tested in Dahl salt-sensitive (DS) rats as an experimental model

for diastolic dysfunction. The isolated cardiomyocytes from DS rats were transduced with an Ad vector containing an β-parvalbumin isoform. It was observed that the transduced cells showed faster relaxation than control cells (Rodenbaugh et al., 2007). In another study, it was revealed that Adv-mediated parvalbumin transduction in cardiomyocytes isolated from dogs with thoracic aorta constriction (TAC) showed improvement in relaxation kinetics along with depressed sarcomere shortening (Hirsch et al., 2004).

S100A1 is another protein abundantly expressed by cardiomyocyets and playing multiple roles in Ca^{+2} cycle. It belongs to S100 protein family, which includes several EF-hand Ca^{+2} binding proteins. It regulates RyR and SERCA2a. In diastole, S100A1 stabilises RyR (to minimise frequency of Ca^{+2} levels) and increases release of Ca^{+2} during systole. In addition, it augments SERCA2a activity during relaxation. It was observed that $S100A1^{-/-}$ mice and heterozygotes $S100A1^{-/+}$ have normal cardiac function under baseline conditions, but the contraction rate and relaxation rate were significantly reduced in response to ß-adrenergic stimulation. Induction of pressure overload by TAC for a period of 3 weeks in these mice caused deterioration of left-ventricular contractility indicating that the levels of S100A1 are essential for cardiac reserve to acute and chronic hemodynamic stress (Du et al., 2002). Intra-coronary AAV-mediated S100A1 delivery showed an enhancement in cardiac function and reversal of left ventricular remodelling after MI in rats (Pleger et al., 2007).

An additional process playing a relevant role in HF is receptor desensitization, which is essentially mediated by GRK2. This is a cytosolic protein, but when the GPCR β-AR receptor is stimulated, GRK2 moves to plasma membrane and binds the β and γ subunits of the G-protein, causing desensitisation. To inhibit this process, a peptide called βARKct, which consists in part of the carboxy terminus of GRK2, was used to prevent the binding of GRK2 to G-protein β and γ subunits at the plasma membrane (Iaccarino et al., 2004). The delivery of AdV-βARKct peptide via percutaneous intracoronay catheterization in post MI-rabbits rescued heart from HF and improved its contractile function (Shah et al., 2001). Similarly, Adenylyl cyclase-6 (AC6) is an enzyme that catalyzes the transformation of ATP into cyclic AMP, and is important in cardiac cycle in response to adrenergic stimulation. In humans, Adenylyl cyclase exists in 9

isoforms, of which isoform 5 and 6 are predominant in the heart. The concentrations of ßAR/Gαs/AC complex in cardiac myocytes are 1:200:3, indicating that ßAR and AC represent the limiting components in ßAR-mediated transmembrane signaling (Gao et al., 1999). In earlier studies, it was demonstrated that overexpression of AC6 did not activate cAMP generation chronically. But its overexpression in transgenic mice with Gαq overexpression showed improvement in LV function, generation of cyclic AMP levels, dysfunction of ßAR signaling, abolishment of cardiac hypertrophy and a better survival (Roth et al., 2002). The effect of overexpression of AC6 was also tested in other animal models, such as pigs, by intracoronary delivery of AdV-AC6; this approach again conferred protection against HF (Lai et al., 2004). Of notice, AC5 knockout mice appeared resistant to cardiac stress and hypertrophy, and exhibited a longer medial life span. They were also protected from hypertrophy, apoptosis, fibrosis, reduced cardiac function and aging-induced cardiomyopathy (Yan et al., 2007). However, whether AC isoform 5 and 6 have a specific or redundant role in the heart is not resolved yet.

RESULTS I

2.1 Persistent expression of AAV-2-mediated VEGF-A and VEGF-B in normal rat myocardium

AAV2 has the potential to drive persistent gene expression in post-mitotic tissues, such as skeletal, cardiac and neuronal tissues. In order to validate the persistence of the expression of the two transgenes VEGF-A and VEGF-B upon AAV serotype 2-mediated gene transfer, we generated two AAV2 vectors containing the VEGF-A and VEGF-B cDNAs under the control of the CMV IE promoter and delivered them into the left ventricular free wall of normal rat myocardium at the dose of 5×10^{10} AAV viral genomes (vg) per animal. Control animals were injected with either saline or AAV2-LacZ (n=6 per group). As the animals treated with either saline or AAV2-LacZ did not show any significant difference in any of the parameters analyzed in our study (not shown), we pooled the results from both groups and represented them as a single control group.

The expression levels of both transgenes were quantified by real-time PCR using VEGF-A and VEGF-B specific primers. We found persistent expression after 30 days (data not shown) and 90 days after viral inoculation (Figure 3.1.A, B). These results were consistent with our previous observations (Ferrarini et al., 2006, Mueller et al., 2008, Arsic et al., 2004), indicating that no major immune or inflammatory response exits against the vector at either time points.

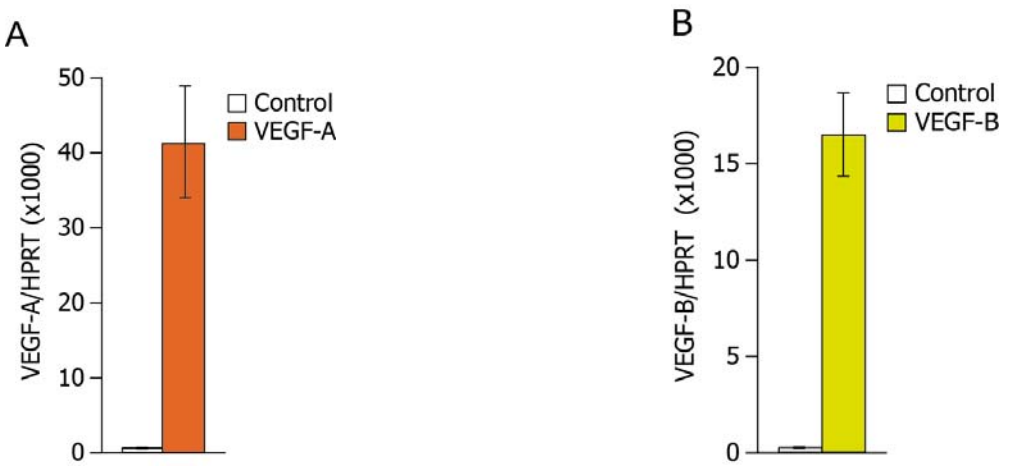

Figure 3.1 Effects of AAV-mediated VEGF-A and VEGF-B expression in normal rat myocardium. A, B) Levels of VEGF-A and VEGF-B transgene transcripts were evaluated by real-time PCR analysis over total ventricular RNA extracted 90 days after vector injection. Transgene expression levels (n=8) are normalized by the respective levels of endogenous HPRT gene.

2.2 Angiogenic effect of VEGF factors in the normal rat myocardium

In our previous studies, we observed that the prolonged expression of VEGF-A produces angiogenesis in the skeletal muscle (Arsic et al., 2003, Zacchigna et al., 2008). Similarly, we wanted to investigate the effect of VEGF-A and VEGF-B on normal rat myocardium after 30 days from vector delivery. The heart samples were analyzed by immunofluorescence using anti CD-31 and anti α-SMA antibodies to detect endothelial and smooth muscle cells (SMC), respectively. (Figure 3.2) In the case of samples treated with VEGF-A, there was a marked increase in the number of both capillaries and arterioles (Figure 3.3 A, B and C), having a diameter ranging from 20 to 250 μm, whereas in the case of samples treated with VEGF-B, there was a very modest angiogenic response with the exception of sporadic formation of enlarged vessels devoid of α-SMA and NG-2 positive mural cells (arrows in Figure 3.4).

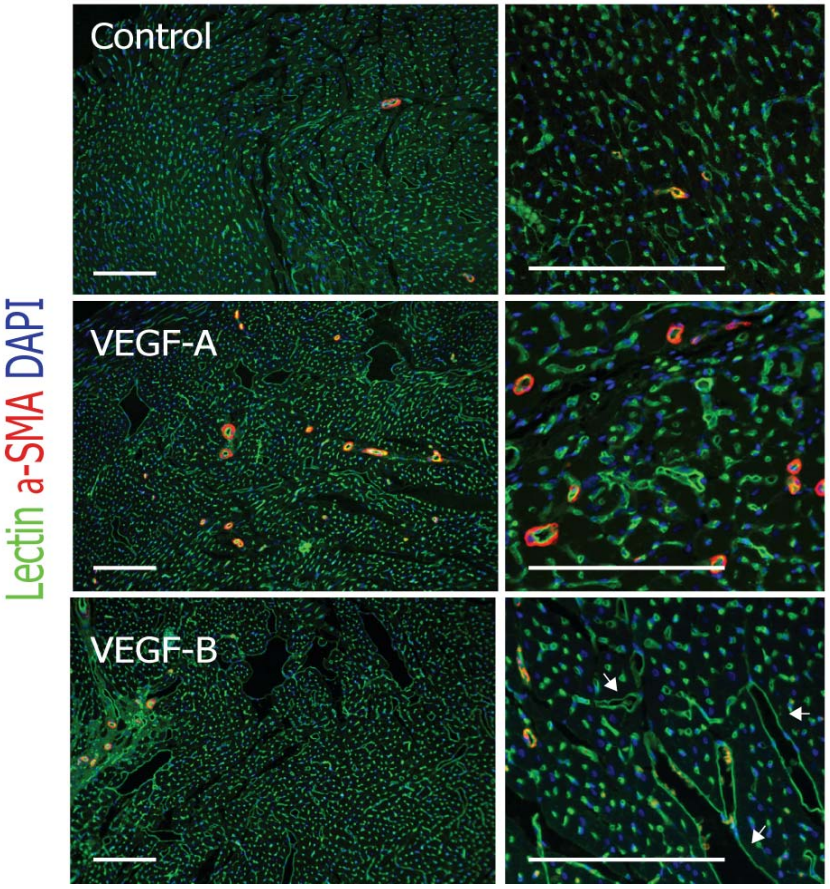

Figure 3.2 Left panels: representative immunostainings of the vasculature in rat myocardium injected with AAV-LacZ (control), AAV-VEGF-A, and AAV-VEGF-B, as indicated. Right panels: enlarged views. Capillaries were detected using FITC-conjugated *L. esculentum* lectin (Vector Laboratories), staining endothelial cells, and VSMCs using a Cy3-conjugated anti-αSMA mouse monoclonal antibody; nuclei were stained in blue with DAPI. Scale bars = 500 μm.

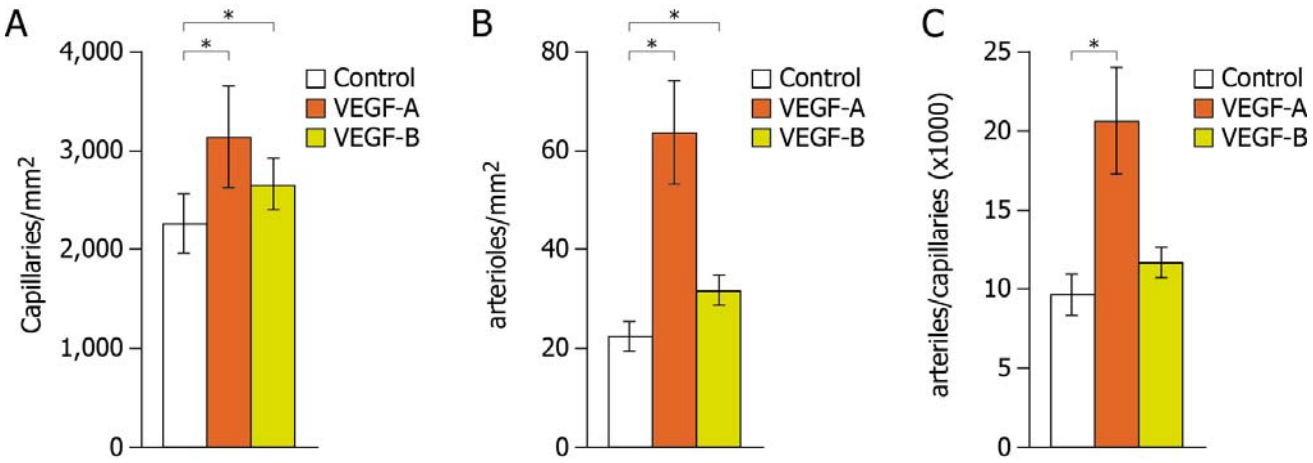

Figure 3.3 Quantification of capillary and arteriole density (A, B). Ratio between number of arteries and capillaries(C). Values are expressed as means ± SE. *P<0.05.

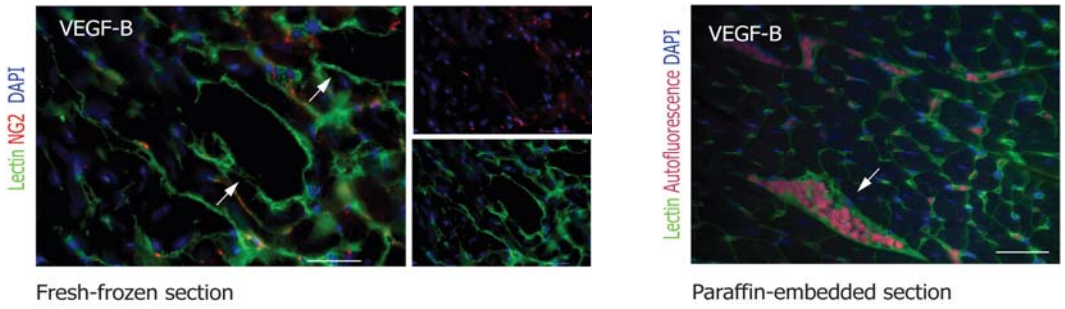

Figure 3.4 A very modest angiogenic response was triggered by VEGF-B in healthy rat myocardium. Left panel: frozen section showing endothelial cells stained with lectin in green and mural cells with anti-NG2 antibodies in red. Right panel: paraffin sections showing endothelial cells stained with lectin (in green) with no traces of αSMA-positive cells (the arrow indicates autofluorescent red blood cells).

2.3 Prolonged expression of VEGF-B, a specific VEGR-1 ligand, preserves myocardial function: analysis of cardiac function after myocardial infarction by echocardiography

Echocardiography is widely used to assess cardiac function in patients with cardiac disease. In our study, we assessed the in vivo effect of the two vectors on cardiac function after myocardial infarction by echocardiography. Rats (n=10/group) underwent myocardial infarction by permanent ligation of the left coronary descending artery and vectors (AAV-VEGF-A, AAV-VEGF-B, AAV-LacZ or saline) were delivered immediately after the ligation at the dose of 5×10^{10} viral particles in the peri-infarct area. Cardiac function was analysed by echocardiography at 1 month and 3 months after infarction. Representative M-mode echocardiography at the latter time points is shown in Figure 3.5.

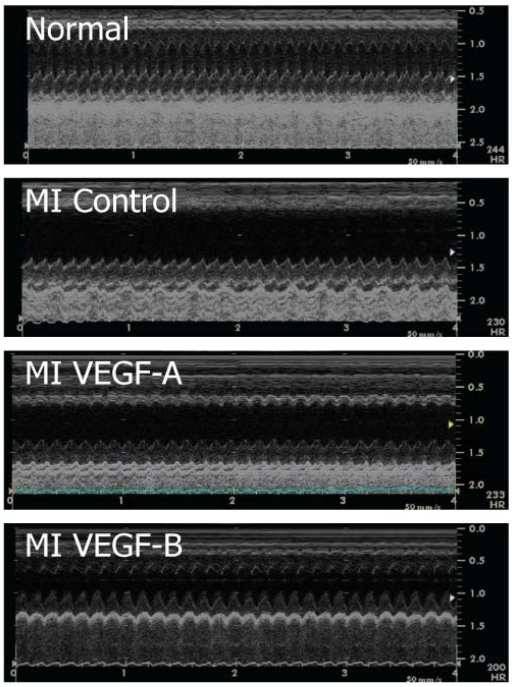

Figure 3.5 Representative trans-thoracic M-mode echographic profiles of different groups of animals, as indicated. The profile of an infracted heart injected with VEGF-B was similar to a normal profile, indicating significant recovery in functional contractility.

Global cardiac performance was assessed by measuring left ventricular (LV) ejection fraction (LVEF) and LV fraction shortening (LVFS). Both parameters were significantly preserved in both AAV-VEGF-B and AAV-VEGF-A treated infarct rats, as compared to the control group, in the absence of significant changes in heart rate ($P<0.05$) for both treatments at 1 and 3 months (Figure 3.6 A, B), respectively.

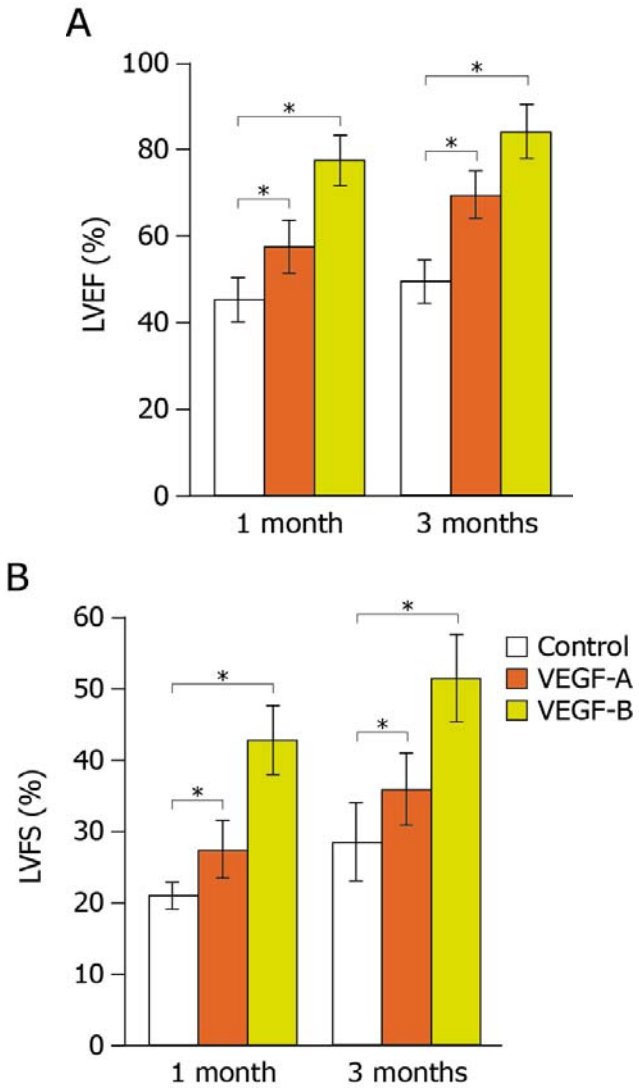

Figure 3.6 Echocardiographic analysis of AAV-injected and control mice at 1 and 3 months after MI showing LV ejection fraction (LVEF) and LV fractional shortening (LVFS). Values are expressed as means ±SE. *P<0.05.

These parameters were significantly preserved in infarct hearts treated with VEGF-B at 1 month and, in particular, at 3 months after treatment (LVEF: 48±8 vs. 85±9%; LVFS: 29±8 vs. 52±7% in control and VEGF-B animals, respectively; P<0.05 in all cases). Additional parameters, such as LV end-diastolic diameter (LVEDD) and LV end-systolic diameter (LVESD) were also significantly reduced in rats that had received AAV-VEFG-B at both time points (EDD: 7.9±1.2 and 6.8±0.8 mm; ESD: 5.9±0.7 and 3.8±0.9 mm in control and VEGF-B animals at 3 months of treatment; P<0.05 in all cases; Figure 3.7 A, B respectively).

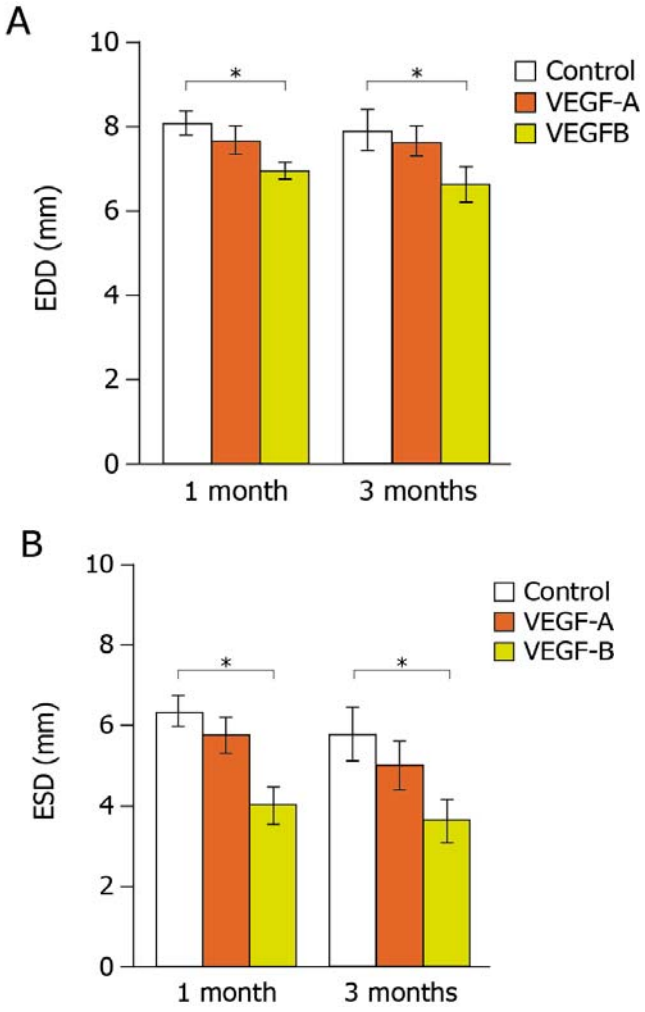

Figure 3.7 Echocardiographic analysis in AAV-injected and control mice at 1 and 3 months after MI, showing LV end-diastolic diameter (EDD) and LV end-systolic diameter (ESD). Values are expressed as means ±SE. *P<0.05.

The regional contractile response of LV was assessed by measuring anterior wall thickening (AWTK) and posterior wall thickening (PWTK) (Figure 3.8 A, B). In case of infarct hearts treated with VEGF-B, at both 1 and 3 months after cardiac gene transfer, the LV end-systolic wall thickening (AWTK) in the border zone of the infarct hearts was markedly improved compared to control rats (18.5 ± 3.0 vs. 32.2 ± 2.9% for control and VEGF-B at 3 months; P<0.05)

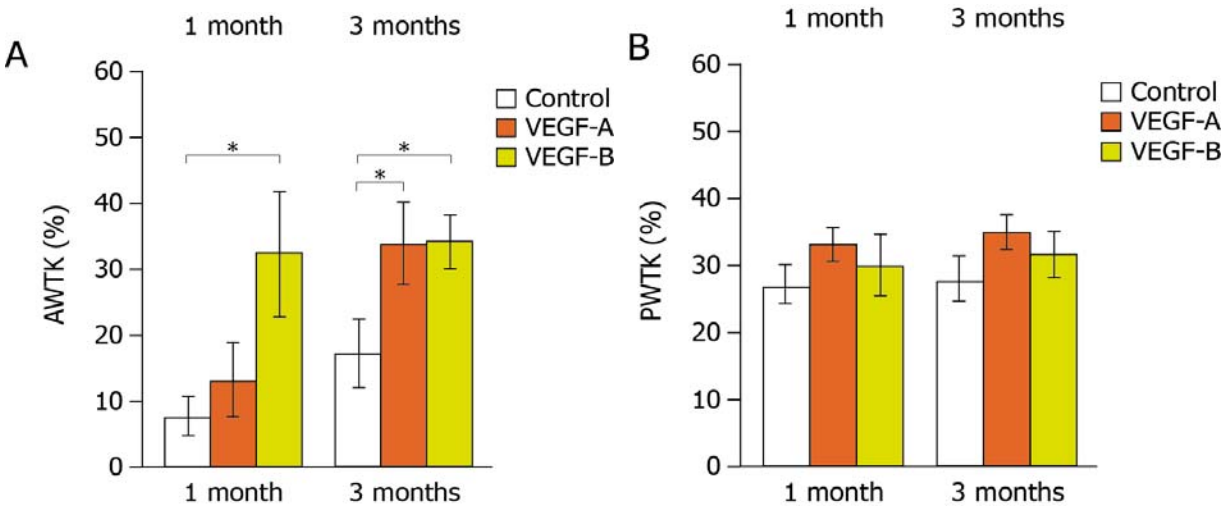

Figure 3.8 Echocardiographic analysis of AAV2-injected and control mice at 1 and 3 months after MI, showing LV end-systolic anterior wall thickening (AWTK) and LV end-systolic posterior wall thickening (PWTK). Values are expressed as means ±SE. *P<0.05.

Similarly, the LV anterior wall end-diastolic and end-systolic thickness (AWTd and AWTs, respectively) of the border zone, which are indices of regional mass, were selectively preserved in VEGF-B treated animals (P<0.05 in both cases; Figure 3.9 A, B). Whereas LV posterior wall end-diastolic and end-systolic thickness (PWTd and PWTs) for the corresponding left ventricle (Figure 3.9 C, D) did not show any significant difference**.** Throughout the analysis, we did not find any changes in the structure and function of the LV remote regions of the infarct hearts in any experimental group.

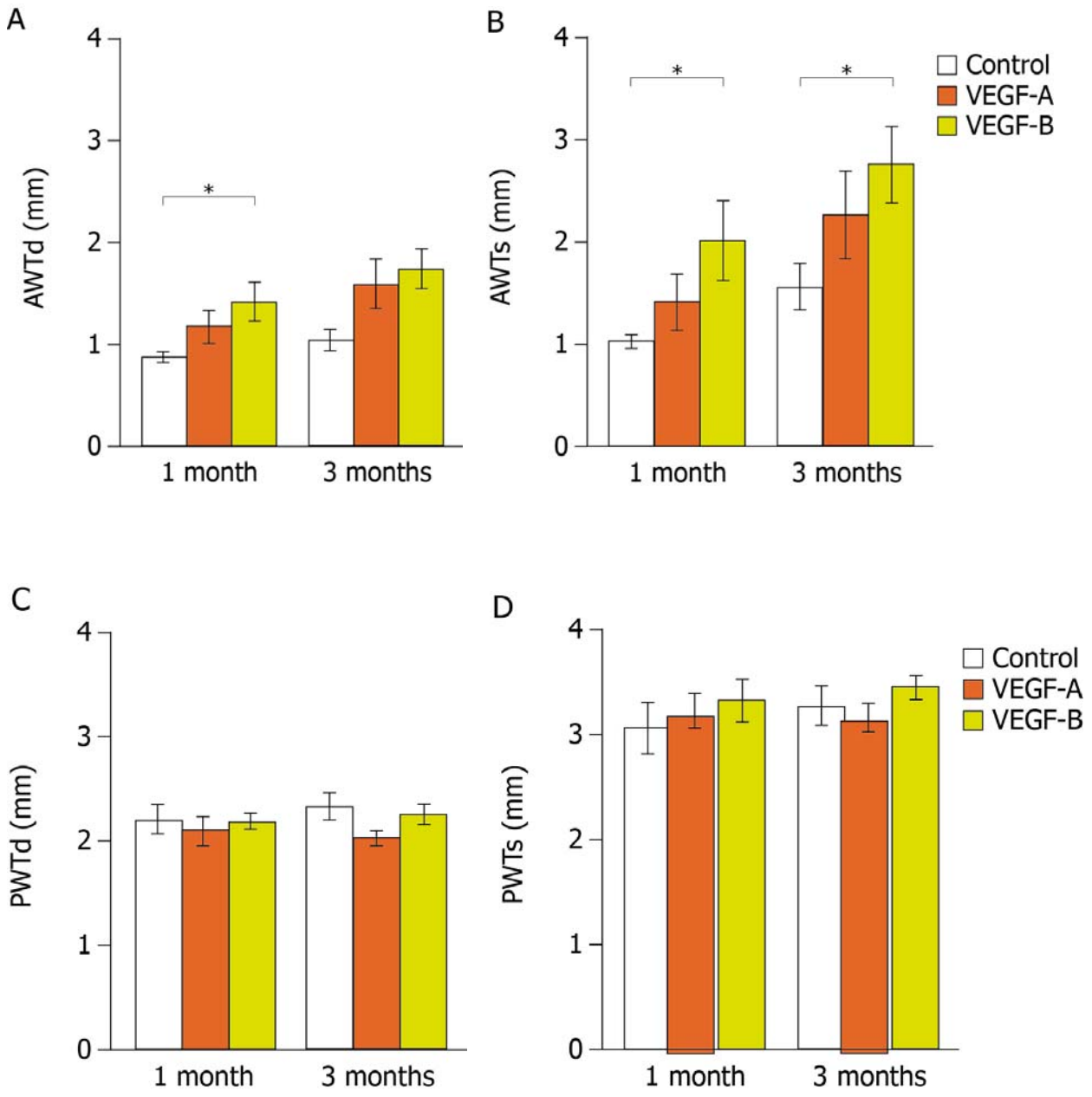

Figure 3.9 Echocardiographic analysis in AAV2-injected and control mice at 1 and 3 months after MI. LV anterior wall end-diastolic thickness (AWTd), and end-systolic thickness (AWTs) (A, B), Posterior wall end-diastolic thickness (PWTd), and end-systolic thickness (PWTs) (C, D). Values are expressed as means ±SE. *P<0.05.

Taken together, these data unanimously indicated that prolonged expression of both VEGF-A and VEGF-B markedly improved recovery of LV performance after infarction.

2.4 Analysis of cardiac tissues by histo-pathological studies: morphometric analyses of infarct samples

From echocardiographic analyses, we observed that the improvement in LV function upon VEGF-B gene transfer was due to preservation of LV mass. To confirm this result, we examined heart samples collected after sacrificing the animals at 3 months post-infarction to morphologically analyse cardiac fibrosis and chamber remodelling. The size of the infarct was estimated in the LV sections by trichrome staining. This analysis showed that the anterior wall of control samples underwent considerable thinning, which was minor in case of AAV-VEGF-A-, and even less evident in case of AAVVEGF-B-treated samples. Moreover, the preservation of contractile tissue was paralleled by a reduction in the fibrotic area (Figure 3.10 A for representative cross sections and Figure 3.10 C for high magnification view of the extent of fibrotic substitution). The infarct size was determined as 36.2± 6.0% of the LV in control animals vs. 21.5 ± 2.5 and 17.2 ± 3.5% in the VEGF-A and VEGF-B-expressing animals respectively ($P<0.05$ in both cases; Figure 3.10 B).

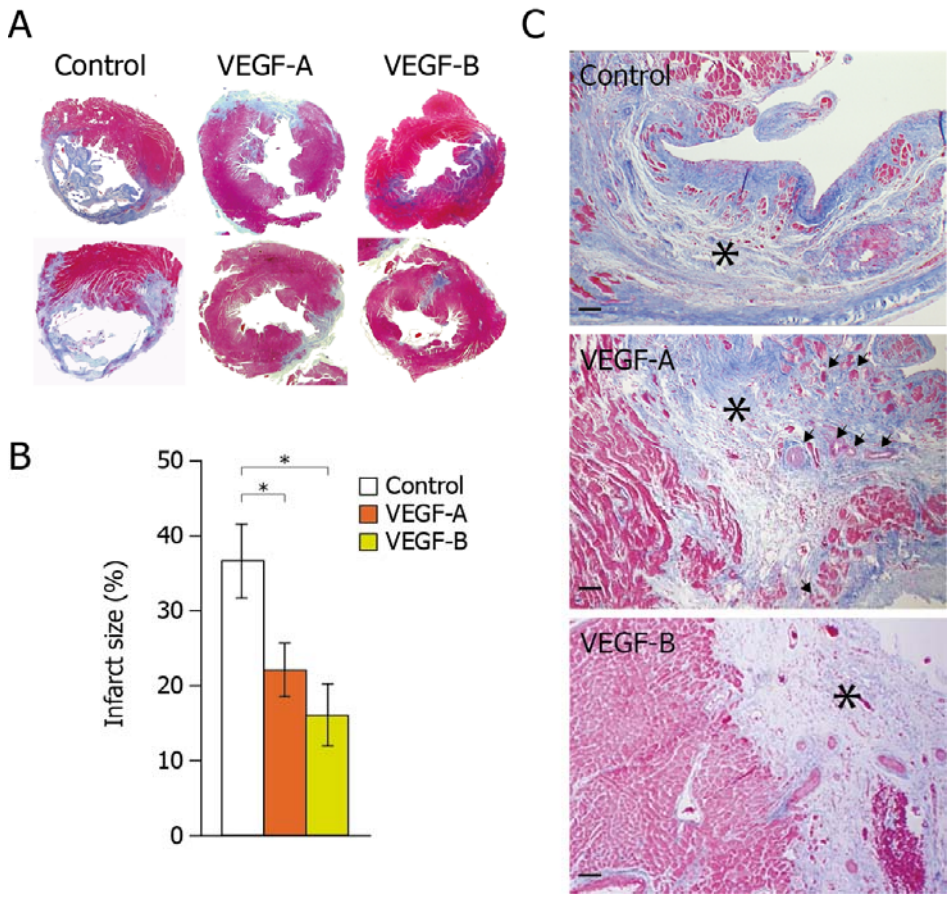

Figure 3.10 Morphometric and histological analysis of infarcted hearts 3 months after gene transfer A) Representative Azan trichrome staining of LV transverse sections of control, AAV-VEGF-A and AAV-VEGF-B-injected hearts. B) Quantification of infarct size (% of LV). C) High-magnification (×200) microphotographs of trichrome-stained sections showing the extent of fibrotic substitution of the infarcted scars (asterisks); arrows indicate new vessels in the VEGF-A expressing hearts. Values are expressed as means ± SE. *P< 0.05. Scale bars = 200 μm.

2.5 Analyses of vector genomes and their incorporated transgenes in the injected myocardium

The heart samples were analysed to confirm the persistence of vector genomes in the injected myocardium at the end of the experimental period (Figure 3.11A). Likewise, transgene (VEGF-A, VEGF-B) expression was also maintained, as quantified by real-time PCR by using transgene-specific primers (Figure 3.11B). The local expression of VEGF transgenes did not induce significant variation in the levels of VEGF receptors mRNA (Figure 3.11C).

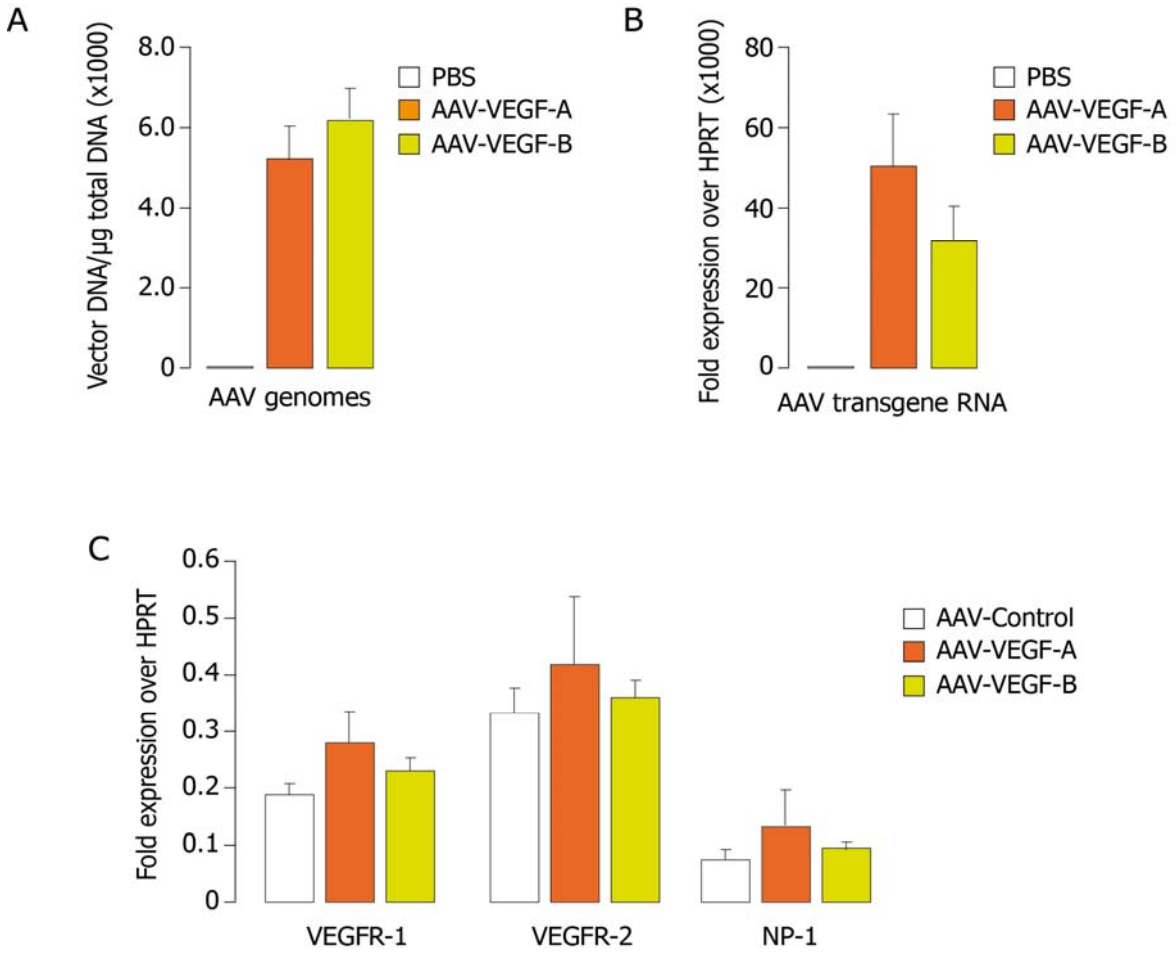

Figure 3.11 Assessment of the presence of vector genomes and of transgene expression in the injected heart samples A) Quantification of vector DNA from the total DNA B) The levels of transgene mRNAs, VEGF-A and VEGF-B C) Expression levels of VEGF receptor mRNAs, VEGFR-1, VEGFR-2 and NP-1. Values are expressed as means ± SE, after normalization over endogenous HPRT gene expression. *P<0.05 *vs* PBS control.

2.6 Angiogenic effect of VEGF factors in infarcted hearts

The heart samples were analysed by immunoflorescence and compared to non-infarcted samples to find any angiogenic response produced by either VEGF-A or VEGF-B. A representative picture of the vasculature of non infarct hearts (Figure 3.2) is shown in Figure 3.12 A and the quantification of number of capillaries and arterioles in Figure 3.12 B and 3.12 C, respectively.

Compared to non-infarct hearts (Figure 3.2), the animals treated with AAV-VEGF-A showed a significant increment in the number of capillaries and arterioles, which was not evident in those injected with AAV-VEGF-B.

From these observations, we concluded that the marked recovery of LV performance after MI, in particular observed after VEGF-B gene delivery, occurred in the absence of significant angiogenesis.

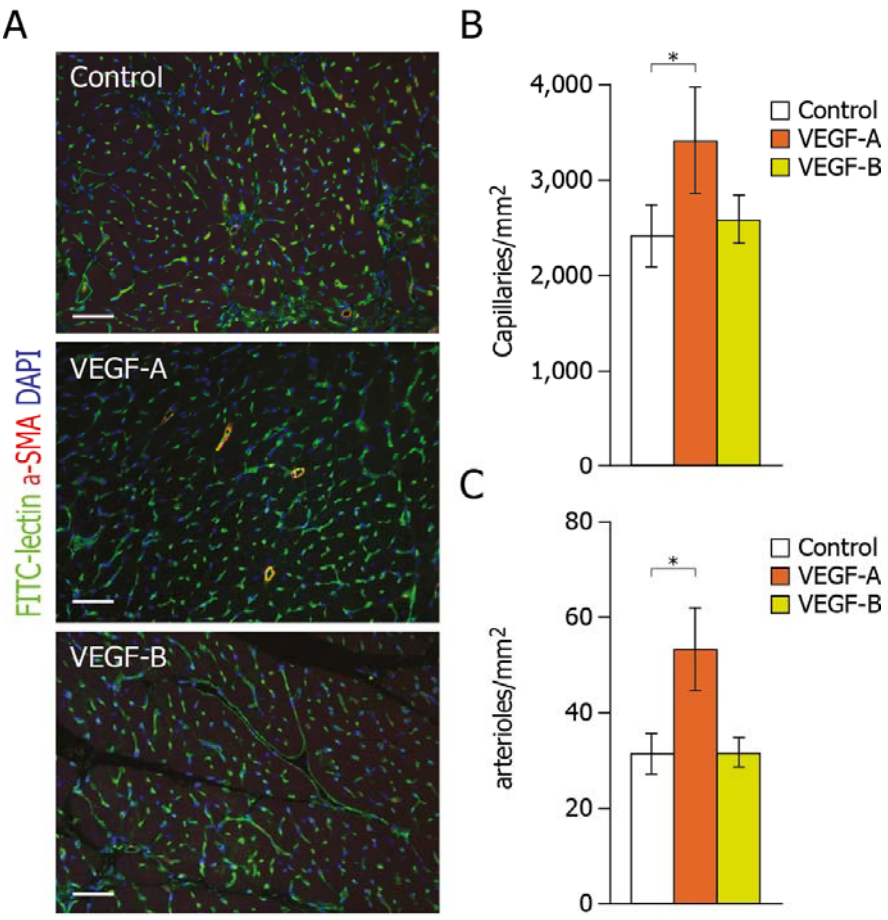

Figure 3.12 Histological analysis of infarcted hearts 3 months after gene transfer. A) Visualization of vessels by immunofluorescence in the peri-infarcted area (green, endothelial cells; red, α-SMA⁺ cells; blue, cell nuclei). B) Quantification of capillary density (FITC-lectin⁺ vessels). C) Quantification of α-SMA⁺ arterioles. Values are expressed as means ± SE. *P< 0.05. Scale bars = 200 μm.

2.7 Expression levels of VEGF receptors in vitro

After having analyzed the functional properties of VEGF-A and VEGF-B by echocardiographic and histopathological studies, we wanted to explore the possibility that these factors might have any direct effect on cardiomyocytes. Initially, we examined the expression levels of the different VEGF receptors in both cardiomyocytes and stromal cells of myocardium.

Total RNA was extracted from primary cultures highly enriched in α-actinin positive cardiomyocytes (>90% purity) by three subsequent sub-plating steps (explained in detail in Material and Methods and in Collesi et al., 2008) and from complementary cultures of α-actinin-negative stromal cells (<1% α-actinin positivity), maintained in culture for 7-14 days. We found that VEGFR-1, VEGFR-2 and NP-1 were expressed by cultured cardiomyocytes, albeit at levels that were 3 order of magnitude lower than those of human umbilical vein endothelial cells (HUVECs). In the stromal cells, we could detect the expression of VEGFR-1 and NP-1 but not of VEGFR-2 (Figure 3.13).

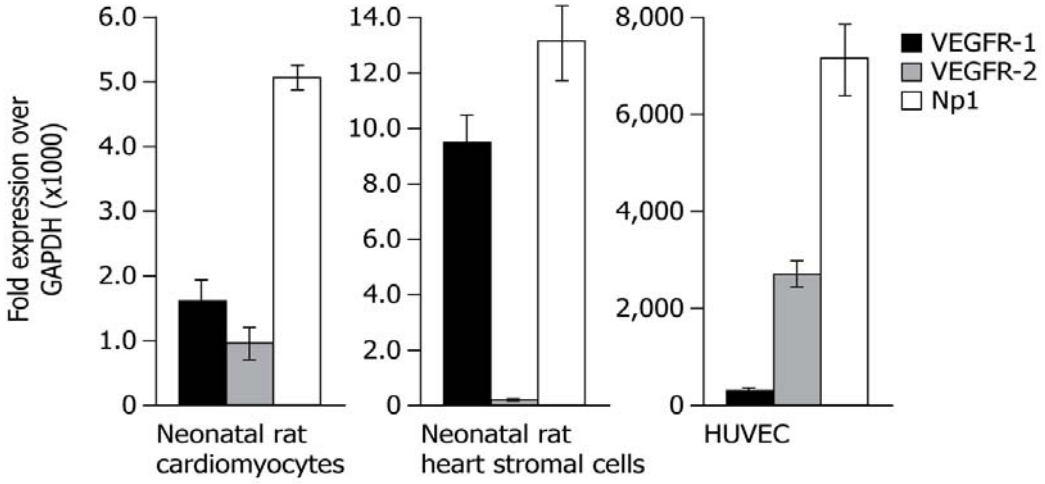

Figure 3.13 Cardiomyocytes express functional VEGF receptors. The levels of expression of VEGFR-1, VEGFR-2 and Np1 by real-time PCR in rat *α*-actinin positive neonatal cardiomyocytes, *α*-actinin-negative cardiac stromal cells, and HUVECs.

The expression levels of the three receptors were also analysed by placing cardiomyocytes in two different conditions, such as hypoxic environment (2%O_2) and oxidative stress (H_2O_2 100 μM). In both these conditions, the levels of expression of VEGFR-1 were more than 5-fold (hypoxic environment) and 3-fold (oxidative stress) increased over basal culture conditions. No significant changes were observed for the other two receptors (Figure 3.14).

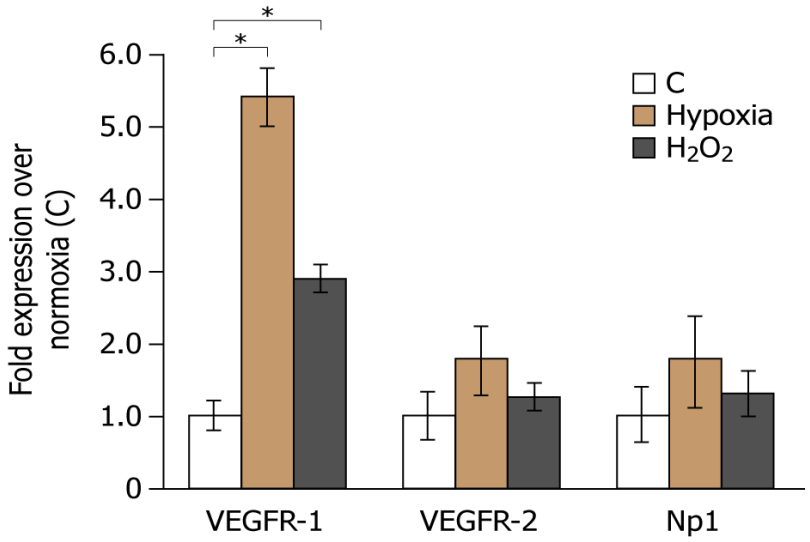

Figure 3.14 Cardiomyocytes express functional VEGF receptors. The levels of expression of VEGF receptors in cardiomyocytes in response to hypoxic (2% O_2) or oxidative stress (H_2O_2 100 μM).

2.8 Quantitative analyses of VEGF receptors in-vitro

The expression patterns of VEGF receptors (VEGFR-1, VEGFR-2, NP-1) were analysed quantitatively by western blot in neonatal cardiomyocyte lysates (Figure 3.15, top panel).

Most notably, these receptors appeared to be functional, from the immunoprecipitation with specific anti-VEGFR-1 and anti-VEGFR-2 antibodies and then from Western blot analysis with anti-phosphotyrosine antibodies, capable to detect specific phosphorylation of both VEGFR-1 and VEGFR-2 in response to recombinant VEGF-A and of VEGFR-1 in response to recombinant VEGF-B (Figure 3.15, bottom panel).

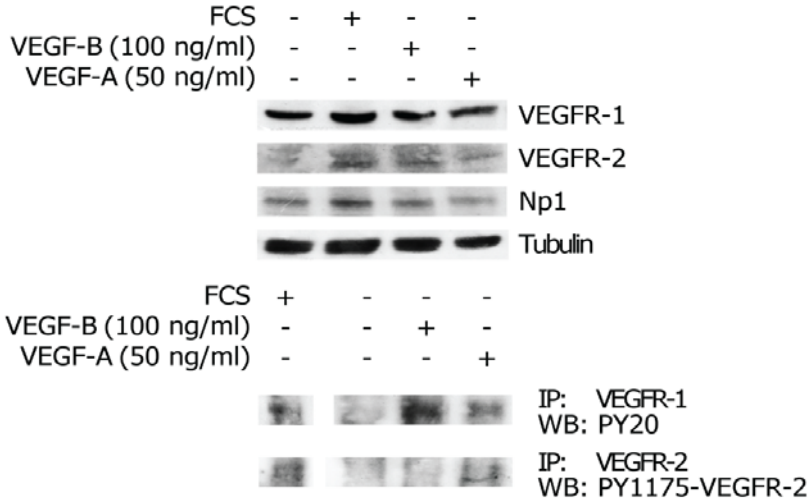

Figure 3.15 Cardiomyocytes express functional VEGF receptors C) Top panel: Western blotting showing specific detection of VEGFR-1, VEGFR-2, and Np1 in cell lysates of neonatal cardiomyocytes, with or without stimulation with fetal calf serum (FCS), recombinant VEGF-A, or VEGF-B, as indicated. Bottom panel: immunodetection of VEGF receptor phosphory- lation after stimulation. VEGFR-1 or VEGFR-2 specific immunocomplexes were probed with the indicated anti-phosphotyrosine specific antibodies.

2.9 In vivo expression of VEGF receptors in the heart

Later, we were interested to analyze receptor expression in samples of adult rat myocardium. Frozen sections were taken and stained with receptor-specific antibodies by immunofluorescence (Figure 3.16). In these sections, VEGFR-2 and NP-1 were localized between cardiomyocytes, where vascular endothelial cells are more abundant, whereas VEGFR-1 appeared to cluster over the intercalated disks between adjacent cardiomyocytes.

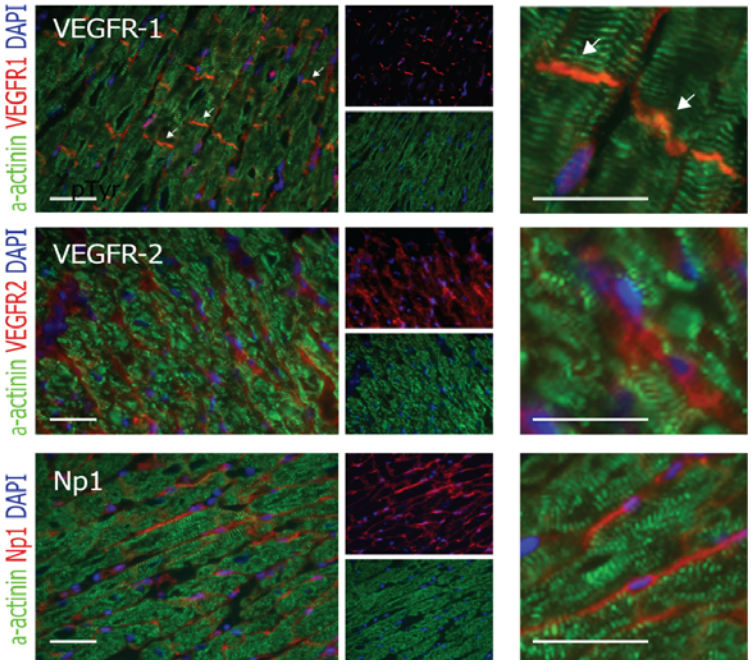

Figure 3.16 Immunofluorescence staining of VEGFR-1, VEGFR-2, and Np1 on histological sections of frozen adult rat heart tissue. Larger pictures on the left and magnifications on the right show fluorescence in all three channels (red, receptors; green, sarcomeric α-actinin; blue, cell nuclei); smaller pictures show 2-channel fluorescence (top: blue/red; bottom: blue/green). Arrows indicate VEGFR-1 clusters at the intercalated disks between cardiomyocytes. Scale bars = 200 μm. Values are expressed as means SE. *P < 0.05

2.10 VEGF-A and VEGF-B protect cardiomyocytes from apoptosis

The preservation of LV myocyte mass and the reduction in the infarct size in animals treated with VEGF-A and VEGF-B suggested that these factors might have either stimulated cardiomyocyte proliferation or prevented their death.

To start assessing the first hypothesis, we investigated the effect of VEGF-A and VEGF-B on rat neonatal cardiomyocytes. Under standard culture conditions (Collesi et al., 2008), 0.2% of neonatal cardiomyocytes incorporate BrdU at day 1 after isolation. The percentage of BrdU incorporated cardiomyocytes was unchanged upon addition of either recombinant VEGF-A or VEGF-B (Figure 3.17).

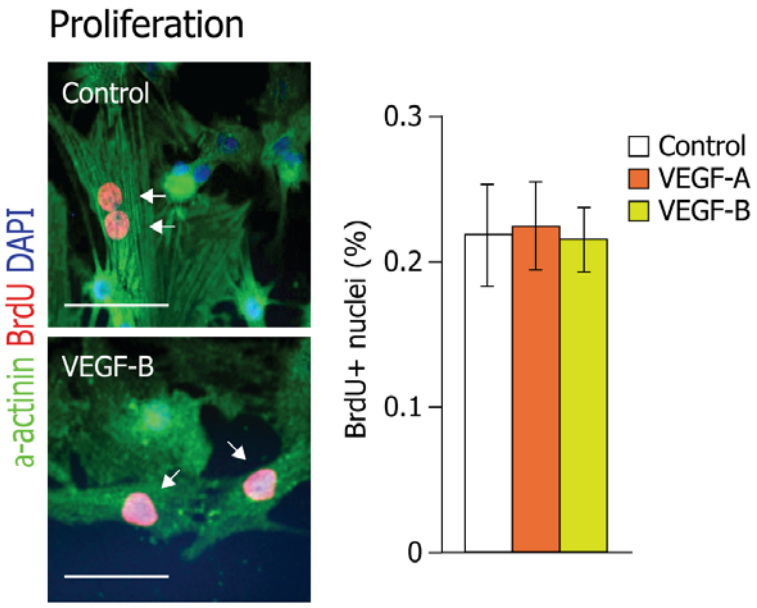

Figure 3.17 Recombinant VEGFs do not induce neonatal rat cardiomyocyte proliferation. Left panels: representative images of α-actinin-positive cardiac myocytes showing positivity to BrdU immunostaining (red; arrows) with or without exposure to recombinant VEGF-B. Right panel: quantification of BrdU-positive nuclei.

We also explored the possibility that expression of two factors after AAV-mediated gene delivery in the infarct hearts in vivo might promote regeneration of the damaged cardiac tissue through stimulation of cardiomyocyte replication or cardiac stem cell recruitment. For

this purpose, we injected a subset of infracted animals with BrdU. However, in keeping with the in vitro data, we failed to detect any increase in number of BrdU-positive proliferating cells within the infarct border zone in treated animals compared to controls (data not shown).

The alternative possibility was that VEGFs exerted protective role against ischemic death of cardiomyocytes. To test this hypothesis, we exposed cardiomyocytes to hypoxia for 48 h followed by 24 h reoxygenation either in the absence or presence of recombinant VEGF-B or VEGF-A. By TUNEL assay, we observed that the percentage of apoptotic cells dropped from ~17.2± 3.3% in controls to 7.6 ± 1.2 and 8.0± 1.0% in VEGF-A and VEGF-B treated cultures, respectively (*P<0.05 in both cases; Figure 3.18).

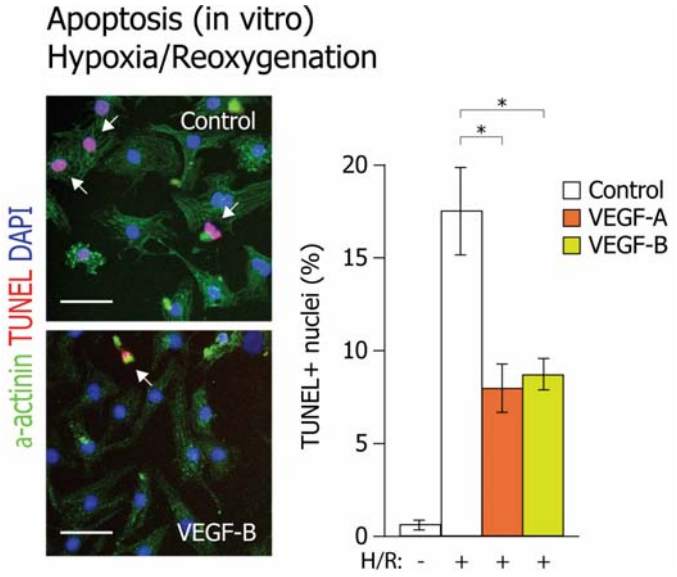

Figure 3.18 VEGFs protect cardiomyocytes from apoptosis *in vitro*. Left panels: representative images of TUNEL⁺ cardiomyocytes (arrows) exposed to hypoxia for 48 h followed by 24 h reoxygenation, either in the presence or absence of VEGF-B. Right panel: quantification of TUNEL⁺ nuclei.

A similar protective effect was also evident when cardiomyocytes were exposed for 90 min to the cardiotoxic drug epirubicin. Under these conditions, the number of dead cells in the cultures treated with either recombinant VEGF decreased from 61.8± 8.5% in controls to 13.8± 6.0 and 11.2 ± 4.2% in the VEGF-A and VEGF-B-treated cultures, respectively (P<0.05 in both cases; Figure 3.18).

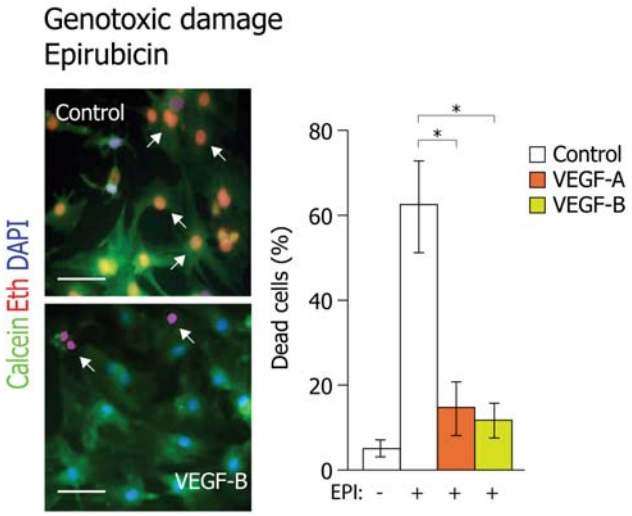

Figure 3.19 Left panels: representative images of a cell viability assay based on the simultaneous determination of live (green, calcein) and dead (red, ethidium homodimer-1, Eth; arrow) cardiomyocytes after *in vitro* exposure to epirubicin in the presence or absence of VEGF-B. Right panel: quantification of dead cells.

In congruence with our observations in vitro, we observed that both VEGFs exert a protective role against apoptosis, as assessed by counting TUNEL-positive nuclei in the infarct border zone at 48 hr after infarction. The number of TUNEL positive cells were significantly lower in animals injected with either AAV-VEGF-A or AAV-VEGF-B compared to controls (from 17.2±8.0 to 4.5±1.4 and 5.5± 1.5%, respectively; n=4/group; P <0.05 vs. control in both cases; Figure 3.20).

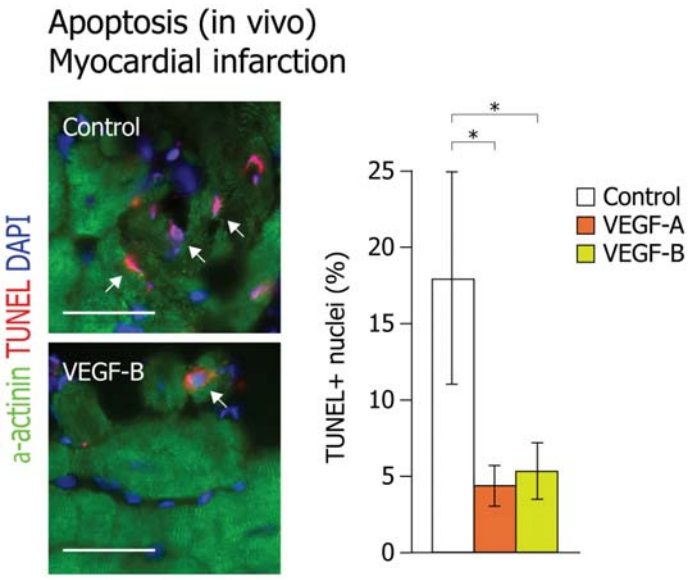

Figure 3.20 Detection of apoptotic nuclei *in vivo* at day 3 after MI. Right panels: representative images of TUNEL⁺ nuclei (arrows) in infarcted hearts from a control and a VEGF-B-injected mouse; cardiomyocytes are stained with anti-α-actinin antibodies (green). Right: quantification of TUNEL⁺ nuclei. Values are expressed as means ± SE. *P < 0.05. Scale bars =20 μm (3.17, 3.20); 50 μm (3.9.2, 3.9.3).

2.11 VEGF-A and VEGF-B activate expression of genes involved in myocardial metabolism and contractility

Besides protection from apoptosis, we observed important changes in regional contractility in the infarcted rats treated with VEGF-A and VEGF-B. These changes suggested that these factors might have direct influenced cardiomyocyte activity. To explore this assumption, we selected a series of genes involved in cardiac contractile function in cells treated for 24 hr with recombinant VEGF-A and VEGF-B in-vitro.

The selected genes were: αMHC, βMHC to analyze the composition of the contractile apparatus, SERCA2a, RYR to analyze calcium handling pathways, PGC1α to analyze mitochondrial energetics and skeletal α-actin and cardiac natriuretic peptides (ANF and BNP) as typical markers of hypertrophic response. The expression profiles of these genes in cardiomyocytes treated with recombinant factors was determined in two experimental conditions: response to α-adrenergic agonist phenylephrine and response to thyroid hormone

tri-iodo L- thyronine (T3). These compounds are known to induce characteristic myocyte hypertrophy responses, essentially consisting in the up-regulation of fetal genes (increase in βMHC, sk α-actin, ANF, and BNP) in case of PE (Eble et al., 1998, Simpson et al., 1994), mimicking pathological hypertrophy, and in an increase in αMHC and SERCA2a, paralleled by a decrease in αMHC transcripts in case of T3, mimicking physiological hypertrophy (Brent 1994, Dillmann 2010).

Both VEGF-A and VEGF-B were found to increase the expression of αMHC (which is the predominant contractile protein in adult rodents; Tardiff et al., 2000) and to repress expression of βMHC, similar to T3, but different from PE ($P<0.05$ between VEGF-treated and control cardiomyocytes). VEGF-B also inhibited the expression of sk α-actin. Both factors promoted elevation of the ANF and BNP transcripts and, most notably, elevation of the SERCA2a, RYR and PGC1α mRNAs, similar to T3 ($P<0.05$) (Figure 3.21).

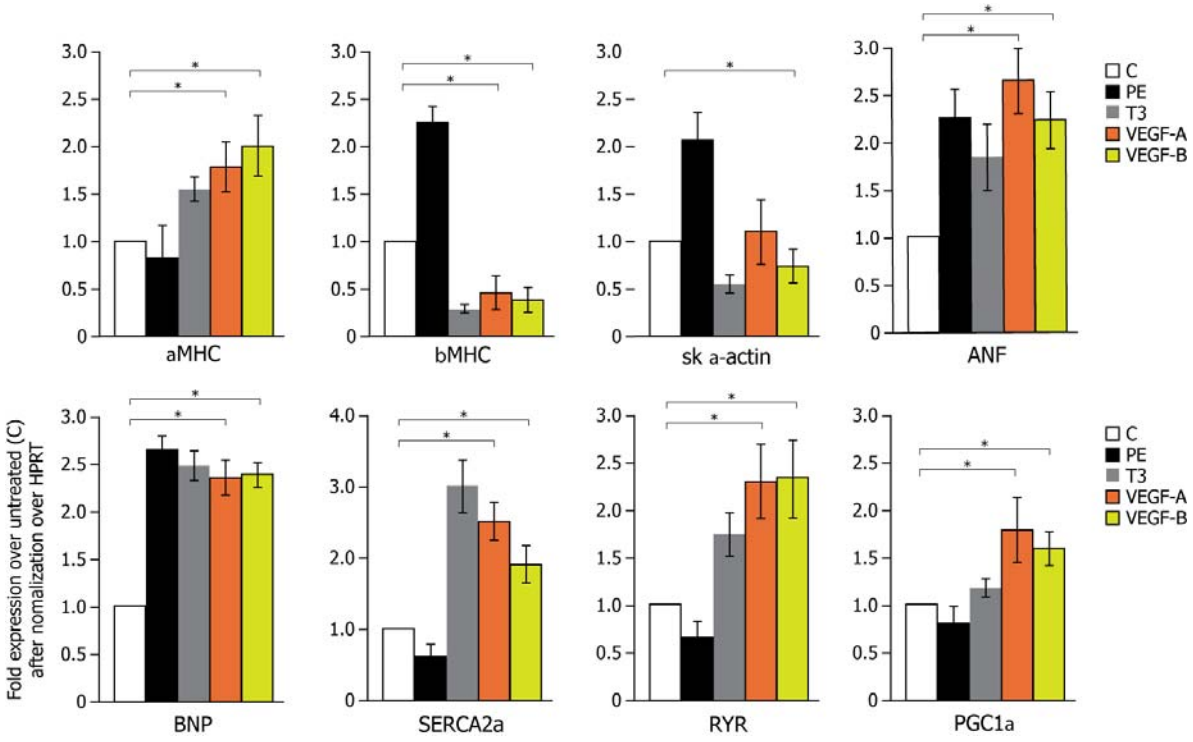

Figure 3.21 Cardiomyocyte treatment with both VEGF-A and VEGF-B induces a gene expression pattern proper of compensatory hypertrophic response. Results of real-time PCR quantification of the levels of expression of the indicated genes in neonatal rat

cardiomyocytes after exposure to recombinant VEGF-A, VEGF-B, phenylephrine (PE), or thyroid hormone (T3). Values are expressed as means ± SE, after normalization with HPRT expression. *P < 0.05 *vs*. untreated control cells (C).

From these observations, it is clear that both VEGF-A and VEGF-B evoke a gene expression programme of compensatory hypertrophy in isolated cardiomyocytes, which is similar to that induced by the thyroid hormone. Interestingly, this whole response can be initiated by the sole treatment with VEGF-B, a selective VEGFR-1 ligand.

2.12 VEGF-B overexpression counteracts induction of genes associated with pathological LV remodelling after MI

To further explore whether a similar hypertrophic response also occurred in vivo, we analyzed the expression profile of the same set of genes in LV tissues from a subset of AAV-transduced, infarcted animals (n=6/group) by real time PCR. Consistent with the echocardiography results, control animals at 3 months after infarction showed a characteristic pattern of gene expression commonly associated with pathological LV remodelling, involving significant ($P<0.05$) higher expression of βMHC and sk α-actin contractile proteins, an increase in levels of cardiac natriuretic peptides, and a decrease in levels of SERCA2a, RYR, and PGC1α mRNAs as compared to normal rats (Figure 3.22).

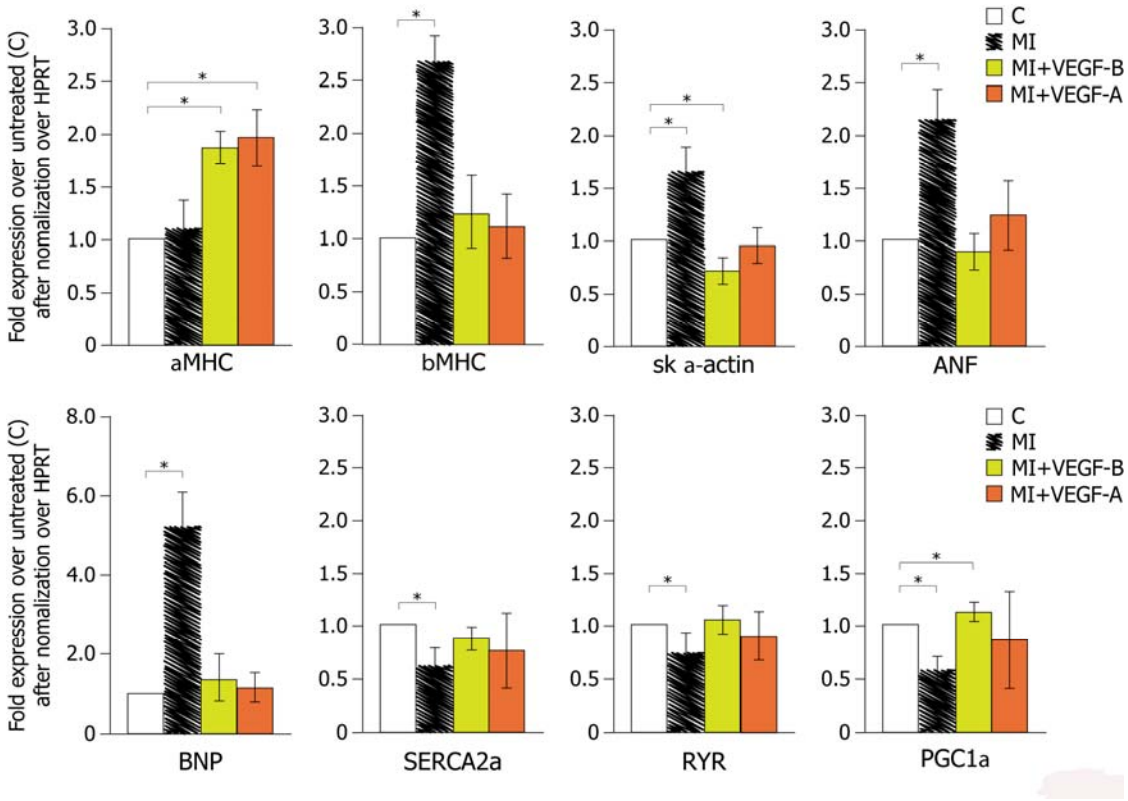

Figure 3.22 AAV2-mediated VEGF-B and VEGF-A expression prevents pathological hypertrophy gene expression in the myocardium of infarcted rats. RNA was extracted from the left ventricle of control and AAV2-VEGF-B- and AAV2-VEGF-A injected rats at 3 months after MI. Real-time PCR quantifications of the levels of expression of the indicated factors, after normalization for HPRT. Values are expressed as means ± SE. *P< 0.05 *vs.* uninfarcted control hearts (C).

Remarkably, these modifications were all significantly counteracted by both VEGFs and more evident upon VEGF-B overexpression. In the VEGF-A and VEGF-B-treated hearts, the expression levels of gens such as βMHC, ANF, BNP, SERCA2a, and RYR were unchanged when compared to normal animals. In addition, expression of αMHC and PGC1α was significantly increased, and that of sk α-actin was decreased relative to controls (P<0.05 in all cases). Collectively, these observations further support the conclusion that VEGFR-1 stimulation exerts a beneficial effect on the myocardial tissue.

RESULTS II

Based on our results on the rat model of myocardial infarction, in collaboration with the group of F. Recchia at the New York Medical College, Valhalla, New York, USA, we explored the hypothesis that VEGF-B might exert non angiogenesis-related cardioprotective effects in non-ischemic dilated cardiomyopathy. For this purpose, an AAV-9 vector expressing the VEGF-B_{167} cDNA ($1x10^{10}$ genome copies) was injected into the myocardium of chronically instrumented dogs developing tachypacing-induced dilated cardiomyopathy (Pepe et al., 2010) . After 4 weeks of pacing, GFP-transduced dogs (AAV-Control, n=8) were in overt congestive heart failure, while the VEGF-B-transduced (AAV-VEGF-B, n=8) were still in a well-compensated state, with physiological levels of arterial pPO_2. By echocardiographic analyses, LV end-diastolic pressure in AAV-VEGF-B and AAV-Control was, respectively, 15.0±1.5 vs 26.7±1.8 mmHg and LV regional fractional shortening was 9.4±1.6% vs 3.0±0.6% (all $P<0.05$) (Pepe et al., 2010).

Further studies were carried out at ICGEB Trieste to better define the mechanisms of these effects by histo-pathological analysis. To investigate whether the protective action was mediated by a process of angiogenesis, the LV samples were stained with immunoflorescent lectin and anti-α-SMA antibodies, in order to detect endothelial and vascular smooth muscle cells, respectively. We found that the capillary density was reduced by 15% in AAV-Control-injected hearts compared to either normal or AAV-VEGF-B treated animals (Figure 3.1 A, B). The density of microvessels with α-SMA positive wall was not significantly different among the three groups (Figure 3.1 A, C).

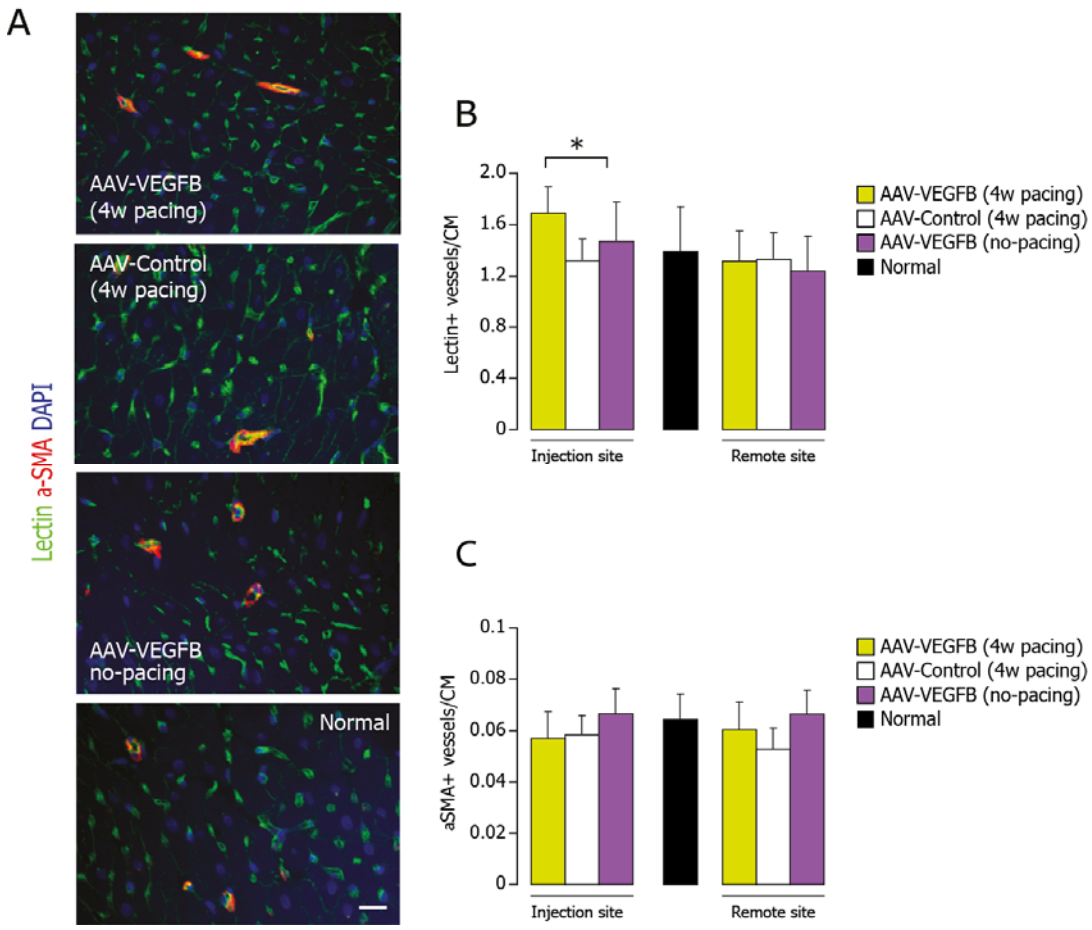

Figure 3.1 A) Representative photomicrographs of myocardial tissue showing double immunoflorescence staining for endothelial (lectin$^+$, green) and vascular smooth muscle (α-SMA$^+$, red) cells, whereas nuclei were stained with DAPI (blue). B and C) Microvessel density was normalized by the number of cardiomyocyte fibers.

3.1 Localized hypertrophic response in cardiomyocytes

Cardiomyocytes cross sectional area from the dog hearts was measured to detect any hypertrophic response. The cross-sectional area was significantly increased in both paced and non paced, AAV-VEGF-B-treated compared to normal hearts (Figure 3.2 A and B). However, this effect was local, essentially limited to the site of injection, and therefore insufficient to induce detectable LV hypertrophic response caused by AAV-VEGF-B by echocardiography.

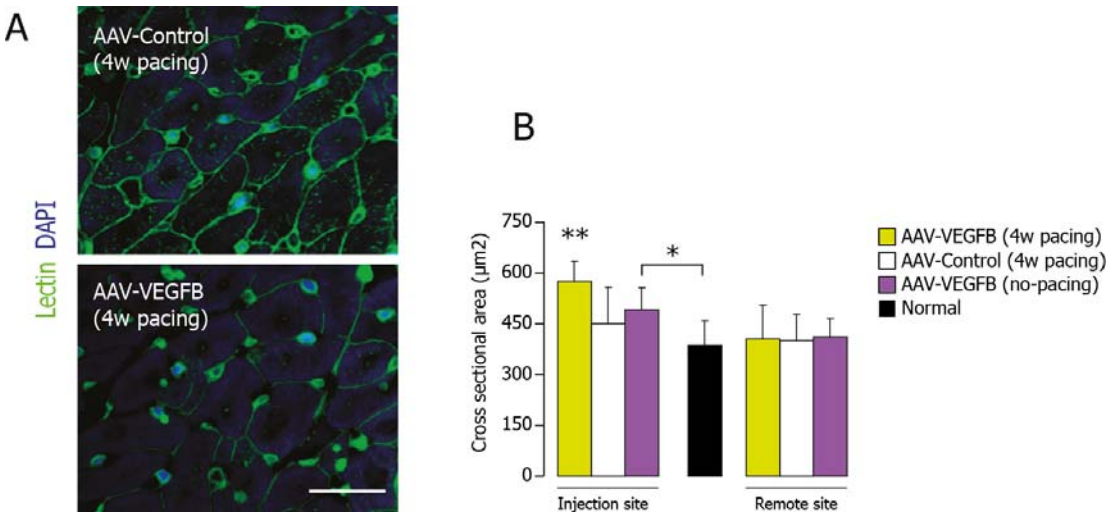

Figure 3.2 FITC-conjugated lectin (green) was used to quantify cardiomyocyte cross sectional area. *P<0.05 *vs* normal; n=6 per group.

3.2 Protective role of VEGF-B against cardiomyocyte apoptosis

The observed preservation of LV contractility gave rise to the assumption that AAV-VEGF-B might have inhibited cardiomyocyte loss, which usually occurs during dilated cardiomyopathy. To analyze the extent of apoptosis in our experimental samples, we used both TUNEL and Caspase activity assays. The amount of TUNEL-positive nuclei was approximately 8-fold increased in AAV-control relative to normal hearts; whereas it was half in the hearts injected with AAV-VEGF-B (these values were still higher than normal, as shown in Figure 3.3 A, B). Similarly, activation of caspases, as detected by Western Blotting against activated Caspase 3 and by caspase 9 activity assay, was clearly detectable only in the AAV control group (Figure 3.4 A, B).

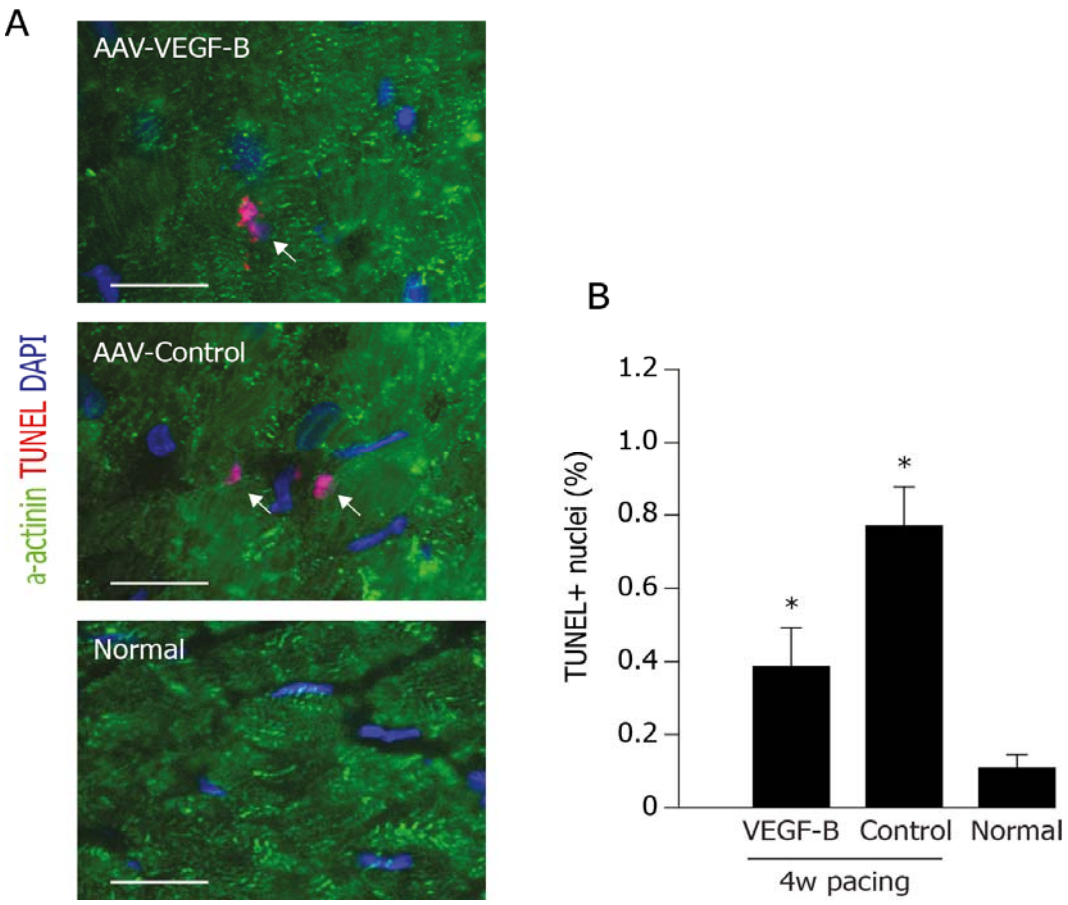

Figure 3.3 Cardiomyocyte apoptotic nuclei (white arrows) by TUNEL (red) analysis. Cardiomyocytes are stained with α-actinin (green). Bars: *P<0.05 *vs* AAV-control; n=4 per group.

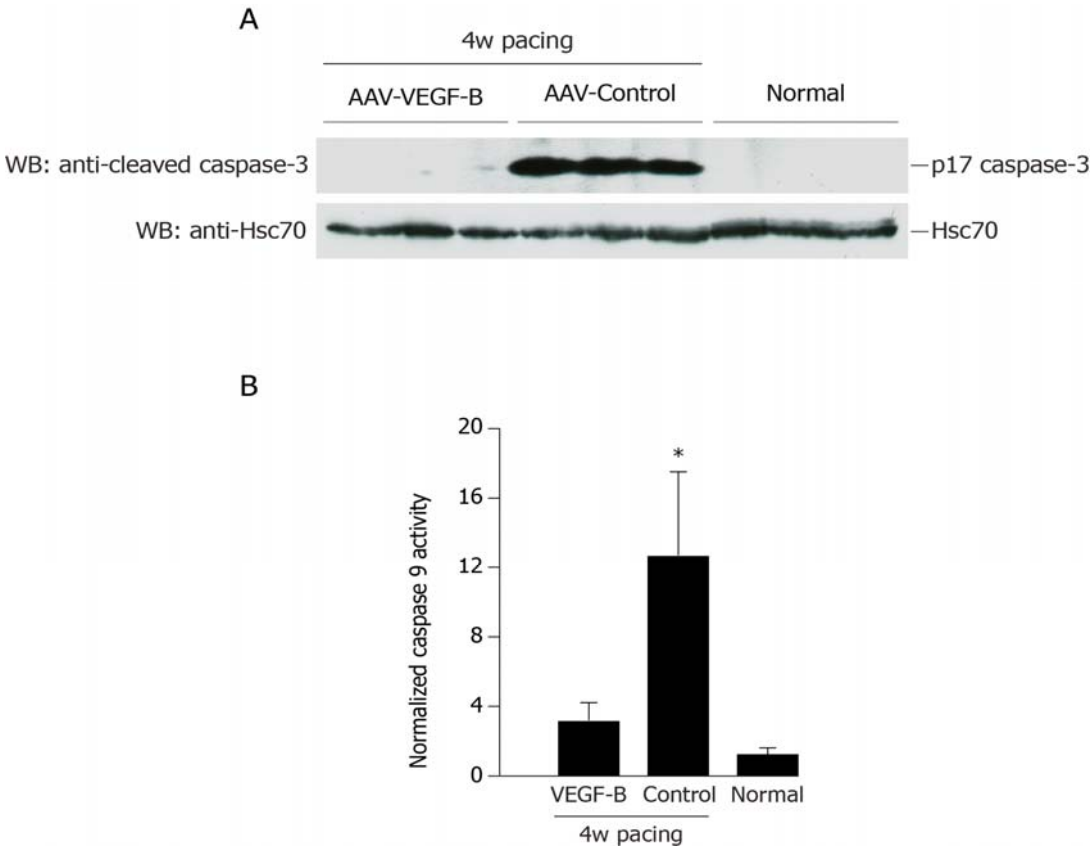

Figure 3.4 Representative Western blotting analysis of activated/cleaved caspase-3 (17 kDa). The bands were not detectable in normal and AAV-VEGF-B-injected animals, indicating virtually no cleavage.

We also wanted to ascertain the extent of AAV-mediated VEGF-B$_{167}$ transduction in the hearts of the treated animals, by analyzing the levels of both AAV DNA and transgene transcripts in by real-time PCR in the hearts of untreated, AAV-Control- and AAV-VEGFB-injected animals. The levels of AAV DNA were not significantly different between the two AAV-injected groups, indicating similar transduction efficiency and persistence of AAV vectors in both groups (Figure 3.5, left panel). In contrast, VEGF-B expression was undetectable in both uninjected and AAV-Control-injected (not shown) animals, while it was readily detectable at the site of AAV-VEGF-B inoculation and, at a lesser extent, at a remote site in the heart of the same animals, indicative of diffusion of the AAV9 vector (Figure 3.5, right panel).

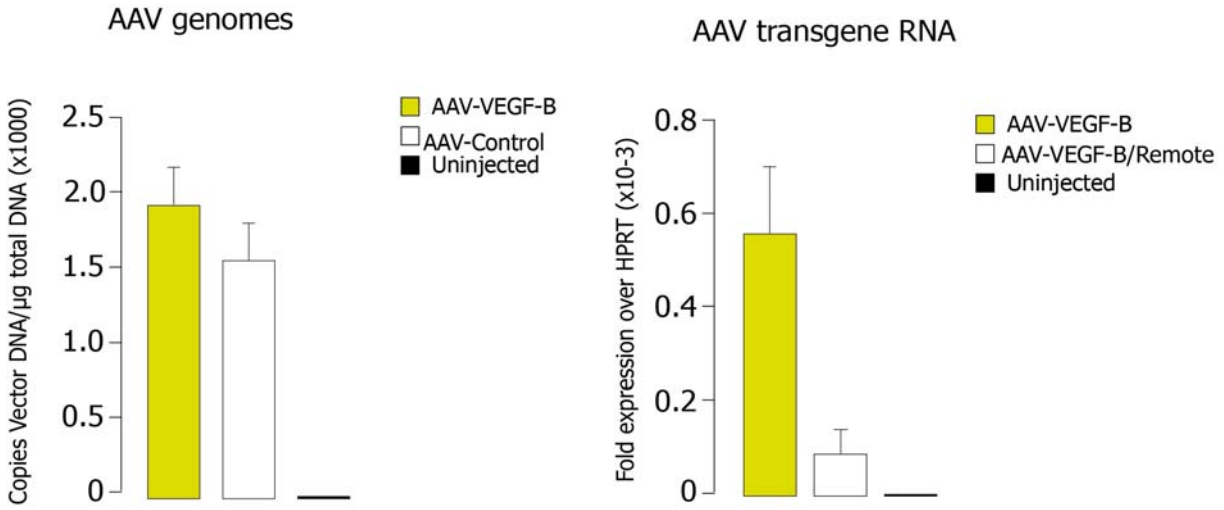

Figure 3.5 Levels of AAV genomes and AAV-mediated transgene expression in the myocardium of transduced animals. Left panel: the amount of AAV genomes was not significantly different between AAV-VEGF-B and AAV-Control LV myocardium at the injection site (n= 5/ group). Right panel: The murine VEGF-B$_{167}$ transgene transcript was clearly expressed at the injection site and detectable also in the LV remote site, although the level were approximately 85% lower (n= 5/group).

We also quantified the endogenous expression levels of VEGF-B$_{167}$ and VEGF$_{165}$ by real time PCR, since it is known that decreased endogenous expression of VEGF-A$_{165}$ may cause downregulation of VEGFR-1 (Abraham et al., 2000). In the case of VEGF-B$_{167}$, there was no significant difference among the groups, whereas in the case of VEGF$_{165}$ the expression was 0.87±0.4 in AAV-VEGF-B, 0.63±0.1 in AAV-Control (normalized to Hprt gene values, $P<0.05$ versus normal) and 1.05±0.1 in normal (data not shown). We further quantified the expression levels of the VEGF receptors VEGFR-1, VEGFR-2 and neuropilin-1, in the heart samples of the different groups. The expression of VEGFR-1 was reduced approximately 4-fold in AAV-Control and AAV-VEGF-B relative to normal hearts, and neuropilin-1 was also down-regulated to 50% and 30% in AAV-control and AAV-VEGF-B, respectively (Figure 3.6). On the other hand, there was no significant difference in the levels of VEGFR-2. From these results, we concluded that decreased gene expression of VEGF-A, but not VEGF-B $_{167}$, was associated with VEGFR-1 and neuropilin-1 downregulation, even in the AAV-VEGF-B group, but not in expression levels of VEGFR-2 and the reduced levels of VEGFR-1 and neuropilin-1 were compensated by supplementary, exogenous VEGF-B.

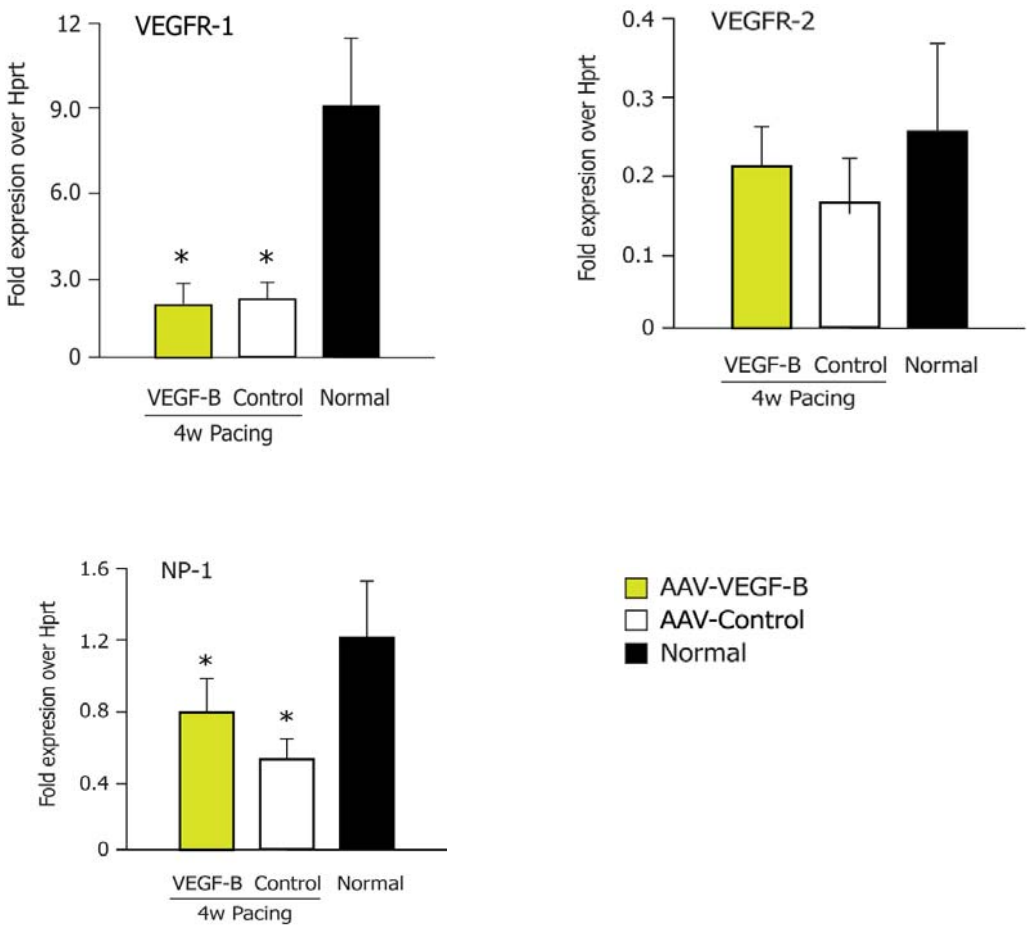

Figure 3.6 Real-time PCR quantification of VEGFR-1, VEGFR-2 and neuropilin-1 (NP-1) gene expression. *P<0.05 *vs* normal; n=6 per group.

3.3 Activation state of Akt, GSK-3β and FoxO3a

From both Caspase and TUNEL assays, it was evident that VEGF-B counteracts loss of both cardiomyocytes and capillary endothelial cells in the failing myocardium. To further confirm the anti-apoptotic role of VEGF-B, we analyzed the phosphorylation pattern of Akt, which is known to exert an antiapoptotic activity in cardiac failure conditions, as well as of its two downstream targets (cytosolic target GSK-3β and nuclear target FoxO3a). Akt hyper-phosphorylation was detected in both AAV-Control and AAV-VEGF-B-treated failing hearts. Quite interestingly, when analyzing its targets, the levels of protein expression were not significantly different among groups, but their phosphorylation was significantly reduced in AAV-Control compared to normal, indicating insufficient Akt activation. In the case of AAV-

VEGF-B, physiological levels of phospho-GSK-3β were re-established, and the levels of phopho-FoxO3a were even super-physiological (Figure 3.7).

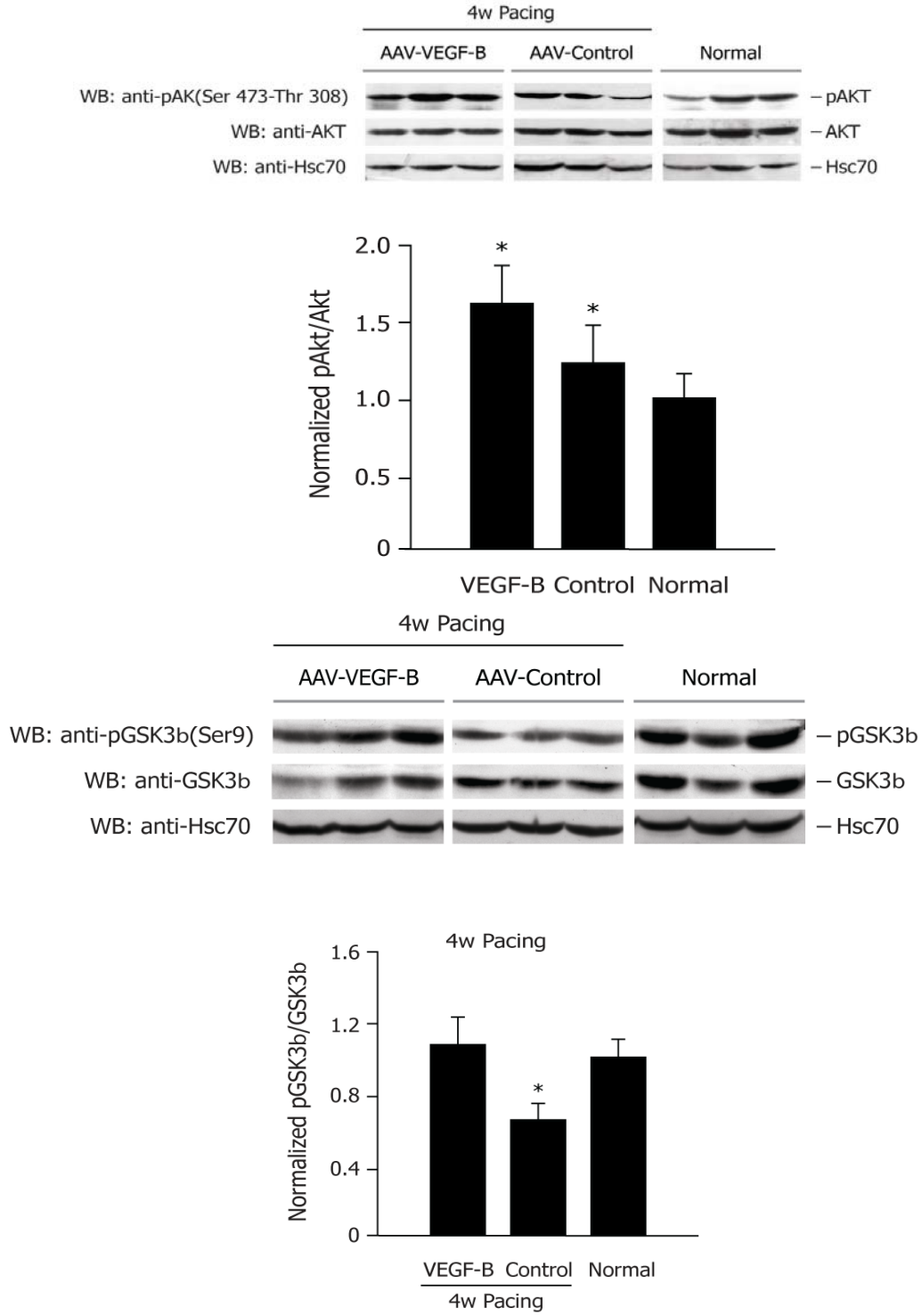

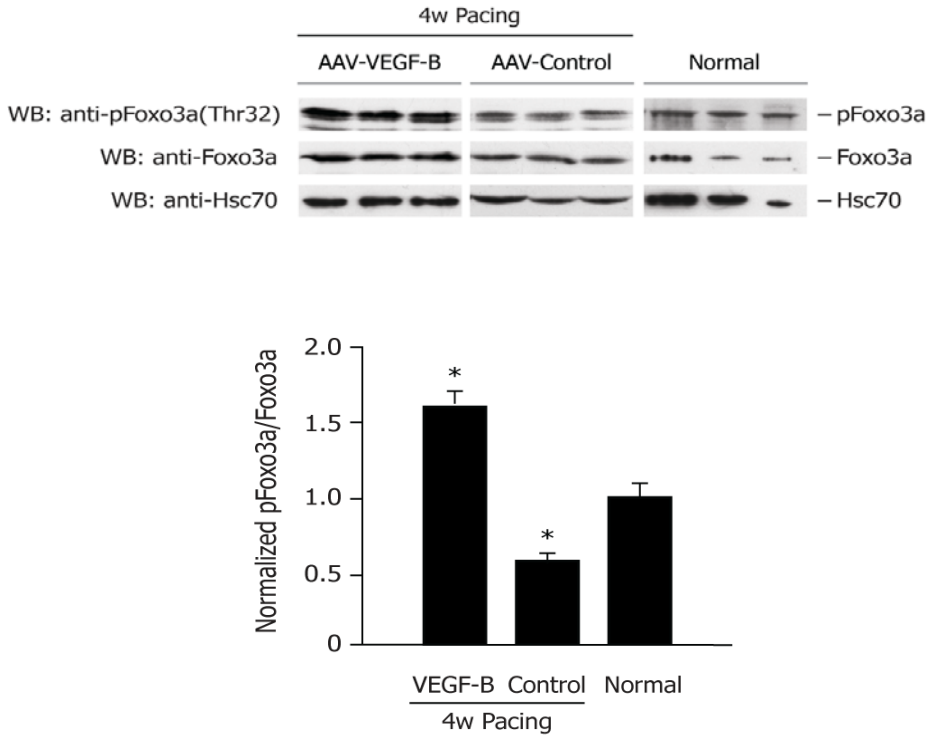

Figure 3.7 Western blotting analysis of activating phosphorylation of Akt and inactivating phosphorylation of its downstream targets GSK-3β and FoxO3a. *P<0.05 *vs* normal; (n=6/ group).

DISCUSSION

4.1 Cardiac gene transfer of VEGF-A and VEGF-B exerts beneficial activities after myocardial infarction in rats and in heart failure in dogs

The major conclusion that can be drown from the studies presented in this thesis is that a persistent expression of VEGF after myocardial infarction exerts prolonged beneficial effects in terms of contractility, prevention of pathological LV remodelling, and preservation of viable cardiac tissue. All our findings are consistent with the notion that VEGF exerts these effects through the activation of VEGFR-1 expressed by cardiomyocytes. In particular, we have observed that: 1) isolated rat cardiomyocytes express VEGFR-1; 2) VEGFR tyrosine kinases become activated on binding to the recombinant VEGFR-1 ligands PlGF and VEGF-B; 3) the levels of expression VEGFR-1 are selectively up-regulated in pathological conditions, such as hypoxia and oxidative stress; 4) most notably, cardiomyocyte treatment with VEGF-B activates a peculiar gene expression program, reminiscent of that observed during compensatory hypertrophy. In this context, the localization of VEGFR-1 in the intercalated disks between adjacent cardiomyocytes appears very interesting, since these structures also act as mechanical stress sensors during muscle contraction, and support synchronized cardiomyocyte contraction (Hoshijima, 2006). However, the functional significance of VEGFR-1 localization at these structures remains an outstanding question, which will require additional investigation.

In addition to these supporting evidences, obtained by using an experimental model of myocardial infarction in rats, the cardioprotective role of VEGF-B was also proven in another model, namely pacing induced dilated cardiomyopathy in dogs. Pacing-induced dilated cardiomyopathy is one the well studied and widely used experimental model to understand the pathophysiology of congestive heart failure (CHF). Earlier, different techniques were used to study CHF, such as the generation of pressure load by aortic or pulmonary stenosis, the production of volume overload by aortic insufficiency, arteriovenous shunt, the induction of MI by coronary ligation or embolism, or use of myocardial toxic drugs (adriamycin,

catecholamines). However, none of these techniques are as effective as pacing induced cardiomyopathy in mimicking the entire pathophysiology of human CHF (Moe et al., 1999). The advantages of this method are: 1) It avoids surgical trauma associated to procedures such as thoracotomy and pericardectomy, which significantly interfere with heart physiology and function 2) Continuation of pacing for a prolonged period of time helps to understand sequential changes 3) The magnitude of the stimulus can be controlled precisely by a programmed pacemaker 4) It produces several clinical symptoms of human CHF, such as cardiomegaly, pulmonary congestion, hypoperfusion, ascites and cachexia with biventricular failure. Cessation of pacing may reverse the condition of CHF.

Whipple et al. (1962) first reported the experimentation of this method in dogs and revealed that rapid atrial pacing of above 330 beats\min can induce symptoms and physical signs of CHF. Over the past decade, canines have been used widely to study the pathophysiology of HF and they are considered the model of choice, better than other species such as sheep, pig, rabbit and rat, because they closely recapitulate the sequential changes of human HF in a reproducible manner. In the canine model, the major changes observed from the early phase of pacing to the progression of CHF, are impairment of left and/or right ventricular systolic pump function, which leada to progressive cardiac enlargement and hypertrophy. These changes persist until the onset of typical symptoms of CHF. Of notice, chronic rapid pacing causes a marked dilation of cardiac chambers without or with little hypertrophic response. Morphometric analyses reveals a severe loss in cardiomyocyte number and an increased volume of the remaining cardiomyocytes (reactive hypertrophy), with significant increase in their length to diameter ratio. The cardiac fibrillar collagen network is altered and associated to the appearance of interstitial edema and disintegration of collagen fibres (Moe et al., 1997). Hemodynamic changes occur within minutes after inception of pacing, mainly consisting in a drop in cardiac output, with a slower decrease in mean arterial pressure. These parameters are maintained almost unchanged until progression into CHF (Elsner et al., 1995). From echocardiographic analyses, the most common observations are a continuous increase in LV volume and decrease in ejection fraction (Howard et al., 1991), thinning of ventricular wall and decrease in LV

shortening due to decrease in posterior wall thickening and posterior and septal wall thickness (Wilson et al., 1987). In addition, increase in end diastolic diameter (preload) and end systolic wall stress (after load) are often observed (Moe et al., 1992).

In our experiments, transduction of failing dog hearts with VEGF-B_{167} exerted a remarkably beneficial effect. In particular: 1) after 4 weeks of tachypacing, hearts transduced with VEGF-B_{167} maintained a LV end-diastolic pressure compatible with physiological pulmonary blood oxygenation, and LV wall thickness and both global and regional contractile function were either not significantly changed or preserved compared to baseline; 2) there was no alteration in the density of LV microvessels endowed with smooth muscle wall upon VEGF-B_{167} gene transfer and only a modest prevention of the capillary rarefaction found in control-paced dogs, thus ruling out a major angiogenic activity of this factor; 3) the low rate of apoptosis and the normalized levels of active capsase-9 and -3 in myocardial tissue upon VEGF-B_{167} gene transfer indicate a potent antiapoptotic and pro-trophic action of VEGF-B_{167}, which likely averted both cardiomyocyte and endothelial cell loss; 4) the antiapoptotic kinase Akt was more active in the failing heart, as previously found in human and tachypacing-induced heart failure (Haq et al., 2001, Sasaki et al., 2009); of notice, phosphorylation/inactivation of its 2 major targets in cytosolic and nuclear compartments, ie, GSK-3β and FoxO3a, (Pap et al., 1998, Shiraishi et al., 2004, Webster 2004) was significantly reduced by AAV- VEGF-B_{167} compared to normal hearts, thus reestablishing normal levels of GSK-3β and FoxO3a phosphorylation.

Regarding the direct role of members of the VEGF family on cardiomyocytes, it might be worth noting that, both in zebrafish and in cultured rat cardiomyocytes, VEGF-A has been reported to exert a positive inotropic effect by increasing calcium transients through its interaction with VEGFR-1 and downstream PLCγ-1 activation (Rottbauer et al., 2005).

4.2 Non angiogenic functions of VEGF family members

One of our previous studies on the effect of VEGF-A_{165} gene transfer to infarcted dog hearts, revealed a marked functional improvement within 48 hours after VEGF-A_{165} gene delivery, a temporal frame which is not compatible with the formation of new blood vessels, overall

suggestive of a direct protective effect on cardiomyocytes (Ferrarini et al., 2006, Laguens et al., 2002). Hence, the observation that VEGFs might directly act on cardiomyocytes is not surprising. A large body of evidence indeed indicates that expression of VEGF receptors and their ligands are widespread and that their signalling might transmit a variety of fundamental non angiogenic functions, largely independent from endothelial cell proliferation. For instance, among the biological activities recently ascribed to VEGFs are the capability to prevent neuronal cell death from ischemia and to promote neurogenesis (Jin et al., 2002, Lambrechts et al., 2003), the capacity to stimulate hepatocyte regeneration after liver damage (LeCouter et al., 2003), the ability to promote osteoblast migration and differentiation (Deckers et al., 2000, Mayr-Wohlfart et al., 2002). In the skeletal muscle, it was shown that VEGF-A exerts a powerful regenerative effect after ischemic and nonischemic muscle damage by promoting satellite cell differentiation (Arsic et al., 2004, Messina et al., 2007). Along with these, several groups have described the effective role of VEGF-A on various cells of hematopoietic origin and its importance in mediating monocyte chemotaxis (Barleon et al., 1996), hematopoietic stem cell survival (Gerber et al., 2002), mobilization of endothelial progenitor cells (Lyden et al., 2001), and the selective recruitment of a population of bone marrow-derived, $CD11b^{+}$ mononuclear cells which is essential for vessel maturation at the sites of adult neoangiogenesis (Zacchigna et al., 2008). In keeping with these findings, in our experimental models, the prolonged expression of VEGF-B in the heart elicited only a modest angiogenic response compared to VEGF-A, essentially consisting in the generation of enlarged vessels devoid of α-SMA-positive cells.

A lack of angiogenesis and presence of abnormally enlarged capillaries was recently reported in a VEGF-B transgenic mouse (Karpanen et al., 2008). An apparent controversy exists among the possible angiogenic role of VEGF-B when delivered exogenously in vivo, as shown by the promotion of unrestricted angiogenesis (Silvestre et al., 2003), the ability to potentiate rather than induce angiogenesis when transgenically expressed in endothelial cells (Mould et al., 2005), the induction of selective revascularization of the ischemic myocardium but not of other organs (Li et al., 2008a) and the non-angiogenic effect in several tissues after adenoviral gene delivery (Rissanen et al., 2003, Bhardwaj et al., 2003). Recent work has indicated that delivery

VEGF-B to the infarcted myocardium in rabbits and pigs using an adenoviral vector promoted angiogenesis and arteriogenesis by acting on endothelial cells (Lahteenvuo et al., 2009).

All these apparent discrepancies might be attributable to the differences in genetic background, phenotyping methodology, use of different VEGF-B isoforms or, most importantly, use of different strategies for VEGF-B overproduction (recombinant proteins, naked plasmid DNA, or adenoviral vectors).

4.3 AAV vectors for cardiac gene transfer

AAV vectors currently represent the only available system to deliver genes to the adult myocardium and to obtain a prolonged expression over time. Other vector systems, such as the first generation adenoviruses used in other studies, are fraught with the induction of potent inflammatory and immune reactions (Liu et al., 2003), which, besides blurring the biological response, restrict the observations to a few days after vector administration.

More in general, AAV vectors represent an outstanding tool for in vivo gene transfer into post-mitotic cells (i.e. cells that are permenentaly out of the cell cycle), for a series of reasons, which are summarized as follows. i) AAV vectors do not express any viral protein; therefore, they are not immunogenic and do not cause inflammation (in contrast to first and second generation adenoviral vectors); as a consequence, therapeutic gene expression usually lasts for month- or year-long periods. In this respect, it is however worth mentioning that, while this conclusion certainly holds true in mouse, pig and dog, which are not the natural hosts of human AAVs, from which most of the vectors are currently derived, it might be different in humans and non-human primates, where the pre-existing immunity against the virus in some cases might determine the elimination of the transduced cells over the first weeks post-inoculation. ii) AAV vectors do not integrate into the host cell genome, however persist in an episomal form, probably in as head-to-tail or head-to-head extrachromosomal concatamers, in non-replicating cells; therefore, they avoid the problem of insertional mutagenesis (in contrast to retroviral vectors). Of notice, the property of the wild type virus to integrate site-specifically into the AAVS1 region of human chromosome 19q13.4 strictly requires the AAV Rep protein (Weitzman

et al., 1994; Dutheil et al., 2000); since the gene coding for this protein is not present in the vectors, site-specific integration does not occur. iii) Possibly as a consequence of the lack of integration into the transduced cells chromosomes, therapeutic gene expression is not subject to significant methylation and silencing (in contrast to retroviral vectors) (Snyder et al., 1997, Challita et al., 1994); iv) AAV vectors can be generated at high titers, thus allowing the simultaneous expression of different genes from the same cells or tissues. This property could be of great importance in light of the possibility to deliver multiple growth factor coding genes, for example for gene therapy to induce functional therapeutic angiogenesis or to improve cardiac function during heart failure, or for the administration of multiple shRNAs to inhibit different proteins acting along a same metabolic pathway (see Introduction). v) AAV vectors do not experience the problem of transcriptional interference from different promoters. The therapeutic gene can thus be controlled by any promoter of choice, provided that its length is suitable for cloning into AAV.

Taken together, these properties have encouraged, over the last 5 years, the use of these vectors in over 50 clinical trials, which have enrolled several hundred patients. These are Phase I/II trials for various hereditary (in particular, hemophilia B, deficit of α1-antitripsin, cystic fibrosis, muscular dystrophies, retinal degeneration) and acquired (rheumatoid arthritis, Parkinson's disease, Alzheimer's disease) disorders. As reported in the Introduction, a single trial exploiting AAV vectors for cardiovascular disorders was initiated in 2008 at the Mount Sinai Hospital in New York, entailing intracoronary injection of AAV1-SERCA2a in patients with heart failure (Brian et al., 2009).

4.4 Effects of VEGF-B on cardiomyocytes in vitro and in vivo

With the possible direct modulation of cardiac contractility, the main consequences of VEGF expression are protection of cardiomyocytes from apoptosis and induction of a gene expression program of compensatory hypertrophy. Cardiomyocytes thus join the list of the numerous cell types in which different VEGF family members exert a powerful antiapoptotic effect, including endothelial cells (Neufeld et al., 1999), neurons (Storkebaum et al., 2004), embryonic stem cells,

(Brusselmans et al., 2005) and skeletal muscle cells (Arsic et al., 2004, Germani et al., 2003). Protection from apoptosis was clearly evident when VEGF-B was administered, in both cultured cardiomyocytes and after myocardial infarction in vivo, suggesting that a relevant receptor mediating the antiapoptotic effect was VEGFR-1. The experiments in dogs further confirmed the antiapoptotic and protrophic actions of VEGF-B_{167} by maintaining a low rate of apoptosis and by normalizing the levels of active capsase-9 and -3 in myocardial tissue. The recent observations that VEGF-B rescues retinal and motor neurons from apoptosis (Li et al., 2008, Poesen et al., 2008) and inhibits the expression of a number of proapoptotic genes in noncardiomyocyte cells (Li et al., 2008) are fully consistent with our conclusion.

In addition to protection from apoptosis, VEGF-B transduction in the heart elicited a peculiar gene expression profile, consisting of the activation of αMHC and the repression of βMHC and skeletal α-actin, and the increase in SERCA2a, RYR, and PGC1α gene expression, together with the increase in the levels of the cardiac natriuretic peptide mRNAs. This pattern of gene expression resembles the gene expression induced by the thyroid hormone T3, which is usually considered a marker of benign, compensatory hypertrophic response to cardiac stimulation (Trivieri et al., 2006, Schaub et al., 1997). In our pacing induced heart failure model, local administration of VEGF-B_{167} induced a local increase in the cardiomyocyte cross sectional area, but not as high to determine superphysiological or even untoward structural changes, such as neoangiogenesis and cardiac hypertrophy. These findings appear to be in full agreement with the recent observations that a transgenic mouse overexpressing VEGF-B showed clear signs of cardiac hypertrophy even without compromising cardiac function (Karpanen et al., 2008); always in keeping with these concepts, VEGF-B-knockout mice had smaller hearts (Bellomo et al., 2000) and the injection of the VEGF-B after infarction led to myocardial hypertrophy (Tirziu et al., 2007). Our results extend these findings further, and show that these effects of VEGF-B are exerted through a direct activity of the growth factor on cardiomyocytes.

Of note, in our experiments, VEGF-A and VEGF-B equally protected cardiomyocytes from apoptosis and induced a beneficial gene expression profile; however, VEGF-B scored superior to VEGF-A in preserving LV function after myocardial infarction. These observations might

indicate that the two factors activate VEGFR-1 differently either by exploiting different co-receptors or by prolonging the activation of VEGFR-2 by VEGF-A, which might be somehow detrimental for the infarcted myocardium through inducing a leaky vasculature. Further experiments will be required to distinguish these possibilities.

4.5 Conclusions

In conclusion, our findings show that VEGF-B exerts a marked beneficial effect on both infarcted myocardium and pacing induced heart failure condition by preventing loss of cardiac mass, by promoting cardiac contractility and by delaying the progression of pacing-induced dilated cardiomyopathy toward congestive failure. These results have major, obvious therapeutic implications in terms of both direct utilization of VEGF-B for therapeutic purposes and the identification of alternative synthetic activators of VEGFR-1.

MATERIALS AND METHODS

5.1 Production, purification and characterization of rAAV vectors

The rAAV vectors used in this study were based on the pTR-UF5 construct, provided by N. Muzyczka (University of Florida, Gainesville,FL). The coding sequences of the VEGF165 and VEGF-B cDNAs were obtained by RT-PCR amplification from HL60 and 293 cell RNA respectively and cloned in the vector under the control of CMV promoter to substitute GFP gene. Cloning and propagation of AAV plasmids was carried out in the JC 8111 E. coli strain. Infectious AAV2 vector particles were generated in 293 cells, cultured in 150-mm-diameter Petri dishes, and then co-transfected each plate containing 15 μg of each vector plasmid together with 45 μg of the packaging/helper plasmid, pDG (provided by J.A. Kleinschmidt, Heidelberg, Germany), which can express AAV and adenovirus helper functions. Viral stocks were obtained by CsCl gradient centrifugation (Arsic et al., 2003, Zacchigna et al., 2008). rAAV titers were determined by measuring the copy number of viral genomes in pooled, dialyzed gradient fractions by competitive PCR procedure. In this, the primers and the competitors were mapped in the CMV promoter region which was common for all vectors. Viral preparations used in this work for animal transduction had titers ranged between $1 X 10^{13}$ and $1 X 10^{14}$ viral genome copies per ml.

5.2 PREPARATION OF NEONATAL CARDIOMYOCYTES

5.2.1 Preparation of cardiomyocyte Culture

Primary cultures of cardiac myocytes were prepared by following the variation from the original method described by Simpson et al., (1982), Orlowski et al., (1990). Hearts were removed from 1-day-old Wistar rats anaesthetized by ether under aseptic conditions. The ventricles were minced into 2-3-mm^3 fragments.

The fragments were digested approximately 10 to 15 times for 5 min each with slow stirring preceded by 10 times up and down gentle pipetting of tissue pieces with CBFHH with 1.5-2

mg/ml trypsin and 20μg/ml DNase. At the end of each cycle, the supernatant was collected into solution containing calf serum (10% v/v) to neutralize action of trypsin.

The dissociated cells were collected by centrifugation and resuspended in growth media (MEM/PB12 with 5% calf serum). To enrich myocytes selectively, dissociated cells were preplated for 45min at 37°C. During this process, non-myocytes are attached readily to the bottom of the culture dish.

The resultant suspension of cardiomyocytes was plated onto the collagen-coated silicone sheet at a concentration of 1.6 X $l0^5$ cells/ml. Bromodeoxyuridine (BrdU) (0.1 mM) was added during the first 24-36 h to prevent proliferation of non-cardiomyocytes. The culture medium (DMEM with 10μg/mlgentimicin and 10% FBS) was changed 24-36 h after seeding to a defined serum-free MEM (MEM with 10μg/ml insulin, 10μg/ml transferrin and 0.1 w/v% BSA).

5.2.2 Preparation of Non-myocyte Culture

Highly enriched cultures of non-myocytes were prepared by two passages of cells adhered to the culture dish during the preplating procedure. Until the second passage, cells were maintained in the same culture medium (DMEM with 10μg/ml gentamicin) but with 10% fetal bovine serum. Then second passage was done in the same serum free medium (Sadoshima et al., 1992).

5.3 Isolation and treatment of neonatal rat ventricular cardiomyocytes

Ventricular myocytes from 1-2-days-old rats of ≥90% purity (Pfeffer et al., 1979) were collected and plated at a density of 500 cells/mm^2 into 100-mm dishes (for RNA, and protein analysis), or multiwell slides coated with 0.2% gelatin (for immunofluorescence staining). The cells were treated with rhVEGF-A (100 ng/ml), rhVEGF-B (100 ng/ml), rmuPlGF (100 ng/ml) (R&D Systems), thyroid hormone (100 nM; Sigma) and phenylephrine (20 μM; Sigma). To detect VEGF receptors, growth factor stimulation was performed at 37°C for 7 min in serum-free medium containing 4.5g/l glucose, 0.1% w/v BSA, 4μg/ml B12, 10 μg/ml insulin, 10μg/ml transferrin.

Apoptosis was induced by culturing serum-starved cells for 48 h at 37°C in 5% O_2/95% N_2 atmosphere using hypoxia incubator (Billups-Rothenberg, San Diego, CA) and then the conditions were changed to 20% O_2 for additional 24 h. Cells were fixed in 3% PFA and 2% sucrose in PBS. Apoptotic cells were visualized by TUNEL (TdT-mediated dUTP nick end labeling) assay, using in situ cell death detection kit, TMR red (Roche Diagnostics) according to the manufacturer's instructions. In case of rat samples, at least 10 high-magnification fields were counted for each experimental condition. Analysis of cardiomyocyte survival was performed using the Live and Dead assay (Molecular Probes) after treatment with 200 nM epirubicin for 90 min in serum free medium.

5.4 Quantification of mRNA by real-time PCR

Total RNA was extracted from isolated cardiomyocytes, fibroblasts, Human Umbilical Vein Endothelial Cells (HUVEC) and from left ventricular myocardium of rats and dogs using TRIzol reagent (Invitrogen,Carlsbad, CA, USA) according to manufacturer's instructions. It was digested by DNAse I and then reverse transcribed by using random hexameric primers (Invitrogen). Then cDNA was used as template to quantity expression levels of rat VEGF receptors (VEGFR-1, VEGFR-2, NP-1), canine VEGF receptors (VEGFR-1, VEGFR-2, NP-1), canine's specific VEGF-B^{167} and VEGF-A^{165}, vector transgenes VEGF-A, VEGF-B as well as α-MHC, β-MHC, skACT, ANF, BNP, SERCA2a, RYR2 and PGC1α. The housekeeping genes GAPDH or rat's specific and canine's specific HPRT were used individually for normalization of the results. All the amplifications were performed on BIO-RAD (CFX96 real time system), using pre-developed and custom-designed assays (Applied Biosystems Foster City, CA, USA) or SYBRGreen (Bio-Rad Laboratories, Hercules, CA, USA).

For the detection of vector specific DNA in heart samples, total DNA were purified by Proteinase K/phenol-chloroform extraction method, and then subjected to real-time PCR amplification using TaqMan probe and primers that have specificity for the sequence in the CMV promoter, which is common to all AAV vectors in the study.

Sequences of the primers and probes:

Primers

Rat PGC-1	F 5'-TGCAGCCAAGACTCTGTATGG-3',
	R 5'-GGCAAAGAGGCTGGTCCTC-3';
rat BNP:	F 5'-CAGCTCTCAAAGGACCAAGG-3',
	R 5'-GCCCAAAGCAGCTTGAACTA-3';
rat HPRT:	F 5'-GCCCTTGACTATAATGAGCACTCAG-3',
	R 5'-GTAGATTCAACTTGCCGCTGTTT-3';
mouse iVEGF-B:	F 5'-TTGCACTGCTGCAGCTGGCTC-3',
	R 5'-GCTGGGCACTAGTTGTTTGA-3';
CMV promoter:	F 5'-TGGGCGGTAGGCGTGTA-3',
	R 5'-CGATCTGACGGTTCACTAAACG-3'

Taqman probes (assay)

Rat β-MHC:	(FAM)-Rn00568328_m1;
rat α-MHC:	(FAM)-Rn00568304_m1;
rat RYR2:	(FAM)-Rn01470303_m1;
rat SERCA2a:	(FAM)-Rn00568762_m1;
rat ANP:	(FAM)-Rn00561661_n1;
rat sk α-actin:	(FAM)-Rn00570060_g1;
rat Flk1:	(FAM)-Rn 00564986_m1;
rat Flt1:	(FAM)-Rn 01409523_g1;
rat NP1:	(FAM)-Rn 00435380_m1;
human VEGF-A165:	(FAM)-Hs00173626_m1;
rat GAPDH:	(VIC)-TaqMan Endogenous control (4352338E);
CMV:	(FAM) - TGGGAGGTCTATATAAGC.
CMV DNA:	F: 5′-TGGGCGGTAGGCGTGTA -3′,
	R: 5′-GATCTGACGGTTCACTAAACGAG-3′
Mouse VEGF-B167:	F: 5′-TTGCACTGCTGCAGCTGGCTC-3′,
	R: 5′-GCTGGGCACTAGTTGTTTGA-3′
Canine VEGF-B167:	F: 5′-AGAAGAAAGTGGTGCCATGG-3′,
	R: 5′-GCTGGGCACTAGTTGTTTGA-3′
Canine VEGF-A165:	F: 5′- AACCCTGGAGCGTTCCCTGT -3′,

	R: 5′- ACCGCCTGGGCTTGTCACAT-3′
Canine VEGFR-1:	F: 5'- AAATCTGCCTGTGGAAGGAATG -3'
	R: 5'- GCCTGAGCCATGTTCAAGGT -3'
	Probe: FAM-AACAGTTCTGCAGTA
Canine VEGFR-2:	F: 5'- GGAACCGGAACCTCACCAT -3'
	R: 5'- GGCAGGTGTAGAGGCCTTCA -3'
	Probe: FAM- CGTAGGGTGAGGAAG
Canine neuropilin-1:	F: 5'- GTCAGAGATTATCCTGGAATTTGAAAG-3'
	R: 5'- GGCAGGTGTAGAGGCCTTCA -3'
	Probe: FAM- CGTAGGGTGAGGAAG
Canine Hprt:	F: 5'- TCATTACGCTGAGGATTTGG -3'
	R: 5'- AGAGGGCTACGATGTGATGG -3'

5.5 Immunoprecipitation and Western blot analysis

For the detection of VEGF receptors, freshly isolated cardiomyocytes were allowed to attach in 100-mm dishes and then left overnight in serum-free medium. Stimulation was performed by incubating the cell cultures at 37°C for 7 min in 2 ml of serum or 2 ml of serum-free medium containing 50 ng/ml recombinant hu-VEGF-A165 and 100 ng/ml huVEGF-B. After washing with PBS on ice, samples were lysed in RIPA buffer (20 mM Tris-HCl, pH 7.4; 150 mM NaCl; 5 mM EDTA; 1% NaDoc; 1% Triton X-100; and 0.1% SDS) containing 90 μg/ml PMSF, 100 μM NaVO4, 50 mM NaF, 20 μg/ml aprotinin, and 20 μg/ml leupeptin (Sigma-Aldrich). Protein concentration was determined by the Bradford method (Bio-Rad Laboratories); 200 μg of proteins was resolved on 6% SDS-PAGE and transferred to nitrocellulose membranes (GE Healthcare, New York, NY, USA). Immunoblots were blocked in 5% bovine serum albumin in TBS-Tween (50 mM Tris-HCl, pH 7.4; 200 mM NaCl; and 0.1% Tween 20). Membranes were incubated with the following primary antibodies (dilution 1:1000) overnight at 4°C: rabbit poly-clonal anti-Flk-1 (C-1158; Santa Cruz Biotechnology, Santa Cruz, CA, USA), rabbit polyclonal anti-Flt-1 (C-17; Santa Cruz Biotechnology), mouse monoclonal anti-phospho-Tyrosine (PY20; Biolegend, San Diego, CA, USA), goat polyclonal anti-rat neuropilin-1 (AF566; R&D Systems), and mouse monoclonal tubulin (B-5–1-2; Sigma). The membranes were washed

in Tris-buffered saline and 0.1% Tween 20 in blocking buffer and incubated with the appropriate HPR-conjugated secondary antibodies for 45 min at room temperature. Proteins were detected by enhanced chemiluminescence (GE Healthcare). In vivo VEGF receptor tyrosine phosphorylation was evaluated by Western blot analysis with anti-phosphotyrosine antibodies on immunoprecipitates. Two milligrams of cell lysates was incubated with either rabbit polyclonal anti-Flk-1 (C-1158; Santa Cruz Biotechnology) or rabbit polyclonal anti-Flt-1 (C-17; Santa Cruz Biotechnology) antisera coupled to Sepharose-Protein A (20 ml packed beads/ml lysate) overnight at 4°C in agitation. Sepharose-protein A bound proteins were washed 4 times with RIPA buffer and separated on 6% SDS–polyacrylamide gels followed by immunoblotting with either mouse monoclonal anti-phosphotyrosine antibodies (PY20; Biolegend) or with anti-Flk-1 specific phosphotyrosine antibodies (VEGF-Receptor2-Y1175; Cell Signaling, Beverly, MA, USA).

In dog samples, activation of the apoptotic pathway was detected by quantifying cleaved caspase-3. Through western blot analyses, activated/cleaved caspase-3 and activation state of Akt, and of its two targets GSK-3β and FoxO3a was determined. The constitutive form of heat shock protein of 70 kDa (HSC70) was used for loading control. Eighty μg of proteins were resolved on SDS-PAGE minigels and transferred to nitrocellulose membranes (GE Healthcare). They were incubated with the following primary antibodies (dilution 1:1000) overnight at 4°C: rat monoclonal HSC70 (SPA-815' StressGen Assay Designs), rabbit polyclonal anti-Akt, rabbit polyclonal anti-pAkt (Thr 308), rabbit polyclonal anti-pGSK-3β (Ser 9), rabbit polyclonal anti cleaved-caspase 3, rabbit polyclonal anti-pFoxO3a (Thr32), rabbit polyclonal anti-Foxo3a (all from Cell Signaling) and rabbit polyclonal anti-GSK-3β (Calbiochem).

5.6 Animal studies and echocardiography

5.6.1 Surgical procedure for MI:

Male wistar rats of 250-275 gr were anesthetized with zolizepam (vial zoletil 100(Virbac S.r.l, Italy) 100 g per 5ml distilled water) mixed with 1 ml of 0.5% atropine sulphate (ATI S.r.l, Italy)

at 5mg/kg b.wt intra-peritoneally. The site of incision was shaved and sterilized with povidine iodine.

The animal was intubated with 16-guage i/v catheter intra-tracheally and connected to ventilator (Model 131, Nemi scientific inc.) through PE tubing at the rate of 60 to 65 breaths/min and a tidal volume of 3-3.5 ml. Tidal volume and ventilation rate are calculated by formulas provided by the company:

$$Vt = 0.0062 \times Mb\ 1.01$$

An oblique skin incision was made over pectoral region; fascia and muscles were separated by blunt dissection. The region of left IInd vertebral space was dissected carefully without damaging the lung lobes. The IInd intercostals space was opened widely. The pericardium was severed and heart was exposed. Left anterior descending artery was ligated close to left atrium with 7/0 mono filament nylon (ref-1647G, Ethicon Inc, USA). Ten µl of recombinant AAV vectors were administered in three separate injections into the viable myocardium bordering the infarct using tuberculin syringe (30G) (Accu-fine-ref-03543307001, Roche). The chest was closed, followed by muscle layer and then skin with 4/0 braided silk (Medacta International S.A. ref-S2019).

Animal care and treatment were conducted in conformity with institutional guidelines in compliance with national and international laws and policies (EEC Council Directive 86/ 609, OJL 358, December 12th 1987). Wistar rats were obtained from Harlan and maintained under controlled environmental conditions.

5.6.2 Echocardiography analysis

The animals were sedated with 50% of the anaesthetic dose used during MI. Transthoracic echocardiography was performed at one and three months after MI with echocardiography system (MyLab® 30, Esaote, Genoa, Italy) equipped with a 12-MHz linear transducer, as previously described by Ventura et al., (2007) and Sahn et al., (1978). Analysis was done as recommended by the American Society of Echocardiography and all measurements were

performed by an experienced cardiologist and an echocardiography expert blinded to treatment groups.

5.7 Histo-Pathological studies

5.7.1 Morphometric analysis of infarct size

After echocardiography analysis, the animals were sacrificed after 3 mo, hearts were collected immediately and washed in PBS. The left ventricle including interventricular septum was dissected out carefully from atria and right ventricle and then cut into 3- 4 pieces of equal thickness from apex to base transversely fixed in 4% PFA embedded in paraffin and finally made into 5μm thick sections.

5.7.2 Masson's Trichrome staining

It was performed on paraffin sections according to manufacturer's protocol from Bio-optica (Masson tricromica, 04-010802, Italy).

5.7.3 Infarct size calculation

The infarct size was calculated as percentage of (endocardial+epicardial circumference of infarct area)/(endocardial+epicardial circumference of LV) for each piece at three equally different levels using image J(NIH) software.

5.7.4 Immunoflorescence

For detection of VEGF receptors, immunofluorescence was performed on frozen heart tissue sections (5μm thick), fixed in IHC Zinc Fixative (Pharmingen, BD Biosciences, San Jose, CA, USA) and blocked for 30 min with 5% goat or 5% horse serum in PBS containing 2% triton X 100, depending on the secondary antibody. The following primary antibodies were used: goat anti-mouse Flk-1 (AF644, R&D Systems) 1:100, goat polyclonal anti-mouse Flt-1 (AF471, R&D Systems) 1:20, goat polyclonal anti-rat neuropilin-1 (AF566, R&D Systems), 1:50, mouse anti-α-sarcomeric actinin monoclonal antibody (EA-53, Abcam, Cambridge MA, USA), 1:100. Alexa

Fluor 594 donkey anti-goat, Alexa Fluor 594 donkey anti-rabbit, and Alexa Fluor 488 donkey anti-mouse were used as secondary antibodies (Molecular Probes, Eugene, OR, USA). Finally nuclei were counter stained with DAPI.

5.7.5 TUNEL Assay for apoptosis

TUNEL assay was performed on frozen sections (5μm thick) of infarct left ventricles collected in 3 days after MI. The sections were permeabilised with 2% triton X 100 in PBS followed by blocking in with 5% FBS in PBS contain 2% triton X 100 for 1hr. The primary antibody: sarcomeric α actinin (EA-53, Abcam, Cambridge MA, USA) was used and diluted 1:100 in blocking buffer, then followed by labelling as per manufacturer guidelines (in situ cell death detection kit, TMR red, Roche Diagnostics). The nuclei were counter stained with DAPI (H-1200, Vector laboratories, CA).

In case of dog samples, the number of apoptotic cardiomyocytes was calculated as the percentage of the TUNEL positive per 1000 total cardiomyocyte nuclei. All Images were acquired at room temperature with a DMLB upright fluorescence microscope (Leica Microsystems, Wetzlar, Germany) equipped with charge coupled device camera (CoolSNAP CF; Roper Scientific, Trenton, NJ, USA) using MetaView 4.6 quantitative analysis software (MDS Analytical Technologies, Toronto, Canada).

The cardiomyocyte cross-sectional area in canine's samples was quantified from photomicrograph of FITC-conjugated *Lycopersicum esculentum* lectin stained paraffin histological sections, using ImageJ software (NIH).

5.8 Statistical analysis

One-way ANOVA and Benferroni/Dunn's post-hoc test was used to compare multiple groups. Pairwise comparison between groups was performed using the Student's t-test. Dose-response effect was assessed by regression analysis. $P<0.05$ was considered statistically significant.

BIBLIOGRAPHY

Aase K, Euler GV, et al. (2001) Vascular Endothelial Growth Factor-B-Deficient Mice Display an Atrial Conduction Defect. Circulation 104: 358-364.

Abdel-Malak NA, Mofarrahi M, et al. (2009) Early Growth Response-1 Regulates Angiopoietin-1-Induced Endothelial Cell Proliferation, Migration, and Differentiation. Arteriosclerosis, Thrombosis, and Vascular Biology. 29:209-216.

Abraham D, Hofbauer R, et al. (2000) Selective downregulation of VEGF-A(165), VEGF-R(1), and decreased capillary density in patients with dilative but not ischemic cardiomyopathy. Circ Res 87:644–647.

Albuquerque RJC, Hayashi T, et al. (2009) Alternatively spliced vascular endothelial growth factor receptor-2 is an essential endogenous inhibitor of lymphatic vessel growth. Nature Med. 15: 1023-1030.

Alitalo K, Tammela T, et al. (2005) Lymphangiogenesis in development and human disease. Nature 438: 946-953.

Alon T, Hemo I, et al. (1995) Vascular endothelial growth factor acts as a survival factor for newly formed retinal vessels and has implications for retinopathy of prematurity. Nat Med 1:1024–1028.

Ambati BK, Nozaki M, et al. (2006) Corneal avascularity is due to soluble VEGF receptor-1. Nature 443: 993-997.

Ambati, BK, Patterson E, et al. (2007) Soluble vascular endothelial growth factor receptor-1 contributes to the corneal antiangiogenic barrier. Br J Ophthalmol 91: 505-508.

Aoki M, Morishita R, et al.. (2000a) Angiogenesis induced by hepatocyte growth factor in non-infarcted myocardium and infarcted myocardium: up-regulation of essential transcription factor for angiogenesis, ets. Gene Ther 7: 417-427.

Aoki H, Sadoshima J et al. (2000b) Myosin light chain kinase mediates sarcomere organization during cardiac hypertrophy in vitro. Nature Medicine 6:183-88.

Arsic N, Zacchigna S, et al. (2004) Vascular endothelial growth factor stimulates skeletal muscle regeneration in vivo. Mol. Ther. 10: 844 – 854.

Arsic N, Zentilin L, et al. (2003) Induction of functional neovascularization by combined VEGF and angiopoietin-1 gene transfer using AAV vectors. Mol. Ther 7: 450-459.

Asahara T, Chen D, et al. (1998) Tie2 receptor ligands, angiopoietin-1 and angiopoietin-2, modulate VEGF- induced postnatal neovascularization. Circ Res 83: 233-240.

Asahara T, Takahashi T, et al. (1999) VEGF contributes to postnatal neovascularization by mobilizing bone marrow-derived endothelial progenitor cells. Embo J 18: 3964-3972.

Barleon B, Sozzani S, et al. (1996) Migration of human monocytes in response to vascular endothelial growth factor (VEGF) is mediated via the VEGF receptor flt-1. Blood 87: 3336-3343.

Barres B A, Hart I K, et al. (1992) Cell death and control of cell survival in the oligodendrocyte lineage. Cell 70: 31-46.

Bates D O, Cui T G, et al. (2002) VEGF165b, an inhibitory splice variant of vascular endothelial growth factor, is down-regulated in renal cell carcinoma. Cancer Res 62: 4123-4131.

Bellomo D, Headrick J P, et al. (2000) Mice lacking the vascular endothelial growth factor-B gene (Vegfb) have smaller hearts, dysfunctional coronary vasculature, and impaired recovery from cardiac ischemia. Circ Res 86: E29-E35.

Bishopric NH, Simpson PC, et al. (1987) Induction of the skeletal alpha-actin gene in alpha 1-adrenoceptor-mediated hypertrophy of rat cardiac myocytes. J Clin Invest 80: 1194-1199.

Bhardwaj S, Roy H, et al. (2003) Angiogenic responses of vascular endothelial growth factors in periadventitial tissue. Hum. Gene Ther. 14, 1451–1462.

Black FM, Packer SE, et al. (1991) The vascular smooth muscle alpha-actin gene is reactivated during cardiac hypertrophy provoked by load. J Clin Invest 88: 1581-1588.

Bohuslav Ošťádal and František Kolář (1999) Cardiac ischemia: from injury to protection.

Brent GA (1994) The molecular basis of thyroid hormone action. N Engl J Med 331 : 847 –853.

Brevetti LS, Chang DS, et al. (2003) Overexpression of endothelial nitric oxide synthase increases skeletal muscle blood flow and oxygenation in severe rat hind limb ischemia. J Vasc Surg 38: 820-826.

Brillantes AM, Allen P, et al. (1992) Differences in cardiac calcium release channel (ryanodine receptor) expression in myocardium from patients with end-stage heart failure caused by ischemic versus dilated cardiomyopathy. Circ Res 71: 18-26.

BRITISH HEART FOUNDATION (2004) Living with heart failure. In: Foundation LBH (ed),

Brian JE, Zsebo KM (2009) SERCA2a Gene Transfer Therapy for Heart Failure.US Cardiology 6(1):46-9.

Brusselmans K, Bono F, et al. (2005) A novel role for vascular endothelial growth factor as an autocrine survival factor for embryonic stem cells during hypoxia. J. Biol. Chem. 280: 3493–3499.

Buerke M, Murohara T, et al. (1995) Cardioprotective effect of insulin-like growth factor I in myocardial ischemia followed by reperfusion. Proc Natl Acad Sci U S A 92: 8031-8035.

Burova E and Ioffe E (2005) Chromatographic purification of recombinant adenoviral and adeno-associated viral vectors: methods and implications. Gene Therapy 12: S5–S17.

Cao R, Brakenhielm E, et al. (2003) Angiogenic synergism, vascular stability and improvement of hind-limb ischemia by a combination of PDGF-BB and FGF-2. Nat Med 9: 604-613.

Carmeliet P, Ferreira V, et al. (1996) Abnormal blood vessel development and lethality in embryos lacking a single VEGF allele. Nature 380: 435-439.

Carmeliet P (2003) Angiogenesis in health and disease. Nat Med 9:653-660.

Carmeliet P (2005a) Angiogenesis in life, disease and medicine.Nature 438: 932–936.

Carmeliet, P (2005b) VEGF as a key mediator of angiogenesis in cancer. Oncology 69 Suppl 3, 4-10.

Carmeliet P, Ng YS, et al. (1999) Impaired myocardial angiogenesis and ischemic cardiomyopathy in mice lacking the vascular endothelial growth factor isoforms VEGF164 and VEGF188. Nat Med 5: 495-502.

Casella I, Feccia T, et al. (2003) Autocrine-paracrine VEGF loops potentiate the maturation of megakaryocytic precursors through Flt1 receptor. Blood 101: 1316-1323.

Challita PM and Kohn DB (1994) Lack of expression from a retroviral vector after transduction of murine hematopoietic stem cells is associated with methylation in vivo. Proc Natl Acad Sci USA 91: 2567-2571.

Chaponnier C and Gabbiani G (2004) Pathological situations characterized by altered actin isoform expression. J Pathol 204: 386-395.

Chen H, Bagri A, et al. (2000) Neuropilin-2 regulates the development of selective cranial and sensory nerves and hippocampal mossy fiber projections. Neuron 25: 43-56.

Chien KR, Knowlton KU, et al. (1991) Regulation of cardiac gene expression during myocardial growth and hypertrophy: molecular studies of an adaptive physiologic response. FASEB J. 5(15):3037-46.

CLINICAL KNOWLEDGE SUMMARIES (2006) Heart failure. Clinical Knowledge Summaries.

Colciago A, Celotti F, et al. (2009)In Vitro Effects of PDGF Isoforms (AA, BB, AB and CC) on Migration and Proliferation of SaOS-2 Osteoblasts and on Migration of Human Osteoblasts. International Journal of Biomedical Science 5(4): 380-389.

Collesi C, Zentilin L, et al. (2008) Notch1 signaling stimulates proliferation of immature cardiomyocytes. J. Cell Biol. 183: 117–128.

Cooney R, Hynes SO, et al. (2006) Adenoviral-mediated gene transfer of nitric oxide synthase isoforms and vascular cell proliferation. J Vasc Res 43: 462-472.

Criqui MH, Fronek A, et al. (1985) The sensitivity, specificity and predictive value of traditional clinical evaluation of Peripheral arterial disease. Circulation 71: 516-522.

Dai Q, Huang J, et al. (2004) Engineered zinc finger-activating vascular endothelial growth factor transcription factor plasmd DiNA induces therapeutic angiogenesis in rabbits with hindlimb ischemia. Circulation 110: 2467-2475.

Davis S and Yancopoulos GD (1999) The angiopoietins: Yin and Yang in angiogenesis. Curr Top Microbiol Immunol, 237: 173-185.

Deckers MM, Karperien M, et al. (2000) Expression of vascular endothelial growth factors and their receptors during osteoblast differentiation. Endocrinology 141: 1667–1674.

De Jonge HW, Atsma DE, et al. (1995) Alpha-adrenergic agonist and endothelin-1 induced intracellular Ca^{2+} response in the presence of a Ca^{2+} entry blocker in cultured rat ventricular myocytes. Cell Calcium 18:(6) 515-525.

Del Monte F, Williams E, et al. (2001) Improvement in survival and cardiac metabolism after gene transfer of sarcoplasmic reticulum $Ca^{(2+)}$-ATPase in a rat model of heart failure. Circulation 104: 1424-1429.

De Vries C, Escobedo JA, et al. (1992) The fms-like tyrosine kinase, a receptor for vascular endothelial growth factor. Science 255: 989-991.

Dillmann W (2010) Cardiac hypertrophy and thyroid hormone signaling. Heart Fail Rev 15: 125-132.

Dixelius J, Makinen T, et al. (2003) Ligand-induced vascular endothelial growth factor receptor-3 (VEGFR-3) hetero-dimerization with VEGFR-2 in primary lymphatic ECs regulates tyrosine phosphorylation sites. J Biol Chem 278: 40973-40979.

Dong G, Chen Z, et al. (2001) Hepatocyte growth factor/scatter factor-induced activation of MEK and PI3K signal pathways contributes to expression of proangiogenic cytokines interleukin-8 and vascular endothelial growth factor in head and neck squamous cell carcinoma. Cancer Res 61: 5911-5918.

Du XJ, Cole TJ, et al. (2002) Impaired cardiac contractility response to hemodynamic stress in S100A1-deficient mice. Mol Cell Biol 22: 2821-2829.

Dumont DJ, Jussila L, et al. (1998) Cardiovascular failure in mouse embryos deficient in VEGF receptor-3. Science 282: 946-949.

Dutheil N, Shi F, et al. (2000) Adeno-associated virus site-specifically integrates into a muscle-specific DNA region. Proc Natl Acad Sci U S A 97: 4862-4866.

Eble, DM, Qi M, et al. (1998) Contractile activity is required for sarcomeric assembly in phenylephrine-induced cardiac myocyte hypertrophy. Am. J. Physiol. 274: C1226 –C1237.

Elsner D, Riegger GA (1995) Experimental heart failure produced by rapid ventricular pacing in the dog. J Card Fail 1(3):229-47.

Falk E. (2006) Pathogenesis of Atherosclerosis. J Am Coll Cardiol 47:7-1.

Favre D, Provost N, et al. (2001) Immediate and long term safety of recombinant Adeno Associated Virus (rAAV) injection into the Nonhuman primate muscle. Mol Ther 4:559-566.

Ferrara N, Henzel WJ (1989) Pituitary follicular cells secrete a novel heparin-binding growth factor specific for vascular endothelial cells. Biochem. Biophys. Res. Commun. 161: 851-858.

Ferrara N, Carver-Moore K, et al. (1996) Heterozygous embryonic lethality induced by targeted inactivation of the VEGF gene. Nature 380: 439-442.

Ferrara N, Gerber HP et al. (2003) The biology of VEGF and its receptors. Nature Medicine 9: 669 - 676.

Ferrara N (2004) Vascular endothelial growth factor: basic science and clinical progress. Endocr Rev 25: 581-611.

Ferrarini M, Arsic N, et al. (2006) Adeno-associated virus-mediated transduction of VEGF165 improves cardiac tissue viability and functional recovery after permanent coronary occlusion in conscious dogs. Circ Res 98: 954-961.

Fisher KJ, Jooss K, et al. (1997) Recombinant adeno-associated virus for muscle directed gene therapy. Nat Med 3: 306-312.

Fong GH, Rossant J, et al. (1995) Role of the Flt-1 receptor tyrosine kinase in regulating the assembly of vascular endothelium. Nature 376: 66-70.

Forstreuter F, Lucius R, et al. (2002) Vascular endothelial growth factor induces chemotaxis and proliferation of microglial cells. J Neuroimmunol 132: 93-98.

Frey N and Olson EN (2003) Cardiac hypertrophy: The Good, the Bad, and the Ugly. Annu. Rev. Physiol 65: 45-79.

Froesch ER, Schmid C, et al. (1985) Insulin-like growth factor I/somatomedin C: A potent inducer of oligodendrocyte development. Annu.Rev. Physiol 47: 443-467.

Fujisawa H (2004) Discovery of semaphorin receptors, neuropilin and plexin, and their functions in neural development. J Neurobiol 59: 24-33.

Fulton D, Gratton, JP, et al. (1999) Regulation of endothelium-derived nitric oxide production by the protein kinase Akt. Nature 399: 597-601.

Gallagher JT, Lyon M (2000) "Molecular structure of Heparan Sulfate and interactions with growth factors and morphogens". in Iozzo, M, V.. Proteoglycans: structure, biology and molecular interactions. Marcel Dekker Inc. New York, New York. pp. 27–59.

Gao MH, Lai NC, et al. (1999) Adenylylcyclase increases responsiveness to catecholamine stimulation in transgenic mice. Circulation 99: 1618-1622.

Gerber HP, Malik AK, et al. (2002) VEGF regulates haematopoietic stem cell survival by an internal autocrine loop mechanism. Nature 417: 954 –958.

Gerber HP, McMurtrey A, et al. (1998) VEGF regulates endothelial cell survival by the PI3-kinase/Akt signal transduction pathway. Requirement for Flk-1/KDR activation. J Biol Chem 273:30336–30343.

Germani A, Di Carlo A, et al. (2003) Vascular endothelial growth factor modulates skeletal myoblast function.Am. J. Pathol. 163: 1417–1428.

Giger RJ, Cloutier JF, et al. (2000) Neuropilin-2 is required in vivo for selective axon guidance responses to secreted semaphorins. Neuron 25: 29-41.

Giordano F, Ping P, et al. (1996) Intracoronary gene transfer of fibroblast growth factor-5 increases blood flow and contractile function in an ischemic region of the heart. Nat Med 2: 534-539.

Glass CK and Witztum JL (2001) Atherosclerosis. the road ahead. Cell 104(4):503-16.

Go LO, Moschella MC, et al. (1995) Differential regulation of two types of intracellular calcium release channels during end-stage heart failure. J Clin Invest 95: 888-894.

Gollmer JC, Ladoux A, et al. (2000) Expression of vascular endothelial growthfactor-b in human astrocytoma Neuro-Oncology 2: 80-86.

Gogat K, Le Gat L, et al. (2004) VEGF and KDR gene expression during human embryonic and fetal eye development. Invest Ophthal Vis Sci 45: 7-14.

Gosteli-Peter MA, Harder BA, et al. (1996) Triiodothyronine Induces Over-Expression of α-Smooth Muscle Actin, Restricts Myofibrillar Expansion and Is Permissive for the Action of Basic Fibroblast Growth Factor and Insulin-like Growth Factor I in Adult Rat Cardiomyocytes. J. Clin. Invest 98: 1737-1744.

Gowdak LH, Poliakova L, et al. (2000) Adenovirus mediated VEGF $_{121}$ gene transfer stimulates angiogenesis in normoperfused skeletal muscle and preserves tissue perfusion after induction of ischemia.Circulation 102(5):565–571.

Greenberg JI, Shields DJ, et al. (2008) A role for VEGF as a negative regulator of pericyte function and vessel maturation. Nature 456: 809-813.

Grimm D, Kern A, et al. (1998) Novel tools for production and purification of recombinant adeno associated virus vectors. Hum Gene Ther 9: 2745-2760.

Grimmond S, Lagercrantz J, et al. (1996) Cloning and characterization of a novel human gene related to vascular endothelial growth factor. Genome Res 6: 124-131.

Gu C, Rodriguez ER, et al. (2003) Neuropilin-1 conveys semaphorin and VEGF signaling during neural and cardiovascular development. Dev Cell 5: 45-57.

Guzman RJ, Lemarchand P, Crystal RG, et al. (1993) Efficient gene transfer into myocardium by direct injection of adenovirus vectors. Circ Res 73: 1202-1207.

Haberl R, Becker A, et al. (2001) Correlation of coronary calcification and angiographically documented stenoses in patients with suspected coronary artery disease: results of 1,764 patients. J Am Coll Cardiol 37(2):451-7.

Hagberg CE, Falkevall A, et al. (2010) Vascular endothelial growth factor B controls endothelial fatty acid uptake. Nature 464:917–921.

Haq S, Choukroun G, et al. (2001) Differential activation of signal transduction pathways in human hearts with hypertrophy versus advanced heart failure. Circulation 103: 670-677.

Harper SJ and Bates DO (2008) VEGF-A splicing: the key to anti angiogenic therapeutics? Nat Rev Cancer 8: 880-887.

Hasenfuss G H, Reinecke R, et al. (1994) Relation between myocardial function and expression of sarcoplasmic reticulum $Ca^{(2+)}$-ATPase in failing and nonfailing human myocardium. Circulation Research 75: 434-442.

Hao, X, Mansson-Broberg A, et al. (2007) Myocardial angiogenesis after plasmid or adenoviral VEGF-A(165) gene transfer in rat myocardial infarction model. Cardiovasc Res 73: 481–487.

Hattori K, Heissig B, et al. (2002) Placental growth factor reconstitutes hematopoiesis by recruiting $VEGFR1^{(+)}$ stem cells from bone-marrow microenvironment. Nat Med 8: 841-849.

Heli M, Eitenmuller I, et al. (2006) Arteriogenesis versus angiogenesis: Similarities and differences. J Cell Mol Med 10:45-55.

Hellstrom A, Perruzzi C, et al. (2001) Low IGF-I suppresses VEGF-survival signaling in retinal endothelial cells: direct correlation with clinical retinopathy of prematurity. Proc Nat Acad Sci 98: 5804-5808.

Herttuala SY, Rissanen TT, et al. (2006). Vascular endothelial growth factors: biology and current status of clinical applications in cardiovascular medicine. J Am Coll Cardiol 49: 1015–1026.

Hiasa K, Ishibashi M, et al. (2004) Gene transfer of stromal cell-derived factor-1α enhances ischemic vasculogenesis and angiogenesis via vascular endothelial growth factor/endothelial nitric oxide synthase-related pathway: next-generation chemokine therapy for therapeutic neovascularization. Circulation 109: 2454-2461.

Hicklin DJ and Ellis LM (2005) Role of the Vascular Endothelial Growth Factor Pathway in Tumor Growth and Angiogenesis. Journal of Clinical Oncology 23: 1011-1027.

Hiratsuka S, Minowa O, et al. (1998) Flt-1 lacking the tyrosine kinase domain is sufficient for normal development and angiogenesis in mice. Proc Natl Acad Sci USA 95: 9349-9354.

Hirsch AT, Criqui MH, et al. (2001) Peripheral arterial disease, detection, awareness, and treatment in primary care. JAMA 286: 1317-1324.

Hirsch JC, Borton AR, et al. (2004) Comparative analysis of parvalbumin and SERCA2a cardiac myocyte gene transfer in a large animal model of diastolic dysfunction. Am J Physiol Heart Circ Physiol 286: H2314-H2321.

Hodgson TA and Cai L (2001) Medical care expenditures for Hypertwnsion, its Complications, and its Comorbities. Medical care 39 599-615.

Hoshijima M (2006) Mechanical stress-strain sensors embedded in cardiac cytoskeleton: Z disk, titin, and associated structures. Am. J. Physiol. Heart. Circ. Physiol. 290: H1313–H1325.

Hoshijima M, Ikeda Y, et al. (2002) Chronic suppression of heart-failure progression by a pseudophosphorylated mutant of phospholamban via in vivo cardiac rAAV gene delivery. Nat Med 8: 864-871.

Houck KA, Ferrara N, et al. (1991) The vascular endothelial growth factor family: identification of a fourth molecular species and characterization of alternative splicing of RNA. Mol Endocrinol 5: 1806-1814.

Howard RJ, Moe GW, et al. (1991) Sequential echocardiographic-Doppler assessment of left ventricular remodeling and mitral regurgitation during evolving experimental heart failure. Cardiovasc Res 25: 468-74.

Hunt SA, AbrahamWT, et al. (2005) ACC/AHA 2005 Guideline Update for the Diagnosis and Management of Chronic Heart Failure in the Adult . Circulation 112:e154-e235.

Iaccarino G and Koch WJ (2004) in vivo adenoviral-mediated gene transfer of the beta arkct to study the role of g beta gamma in arterial restenosis. Methods Mol Biol 237: 181-192.

Insull W (2009) The Pathology of Atherosclerosis: Plaque Development and Plaque Responses to Medical Treatment The American Journal of Medicine 122: (1), S3-S14.

Ito WD, Arras, M, et al. (1997) Monocyte chemotactic protein-1 increases collateral and peripheral conductance after femoral artery occlusion. Circ Res 80: 829-837.

Iwanaga Y, Hoshijima M, et al. (2004) Chronic phospholamban inhibition prevents progressive cardiac dysfunction and pathological remodeling after infarction in rats. J Clin Invest 113: 727-736.

Jin K, Mao XO, et al. (2006) Vascular endothelial growth factor stimulates neurite outgrowth from cerebral cortical neurons via Rho kinase signaling. J Neurobiol 66: 236-242.

Jin K, Zhu Y, et al. (2002) Vascular endothelial growth factor (VEGF) stimulates neurogenesis in vitro and in vivo. Proc. Natl. Acad. Sci. USA 99: 11946 –11950.

Jingjing L, Xue Y, et al. (1999) Human Muller cells express VEGF183, a novel spliced variant of vascular endothelial growth factor. Invest Ophthalmol Vis Sci 40: 752-759.

Jones EA, Yuan L, et al. (2008) Separating genetic and hemodynamic defects in neuropilin 1 knockout embryos. Development 135: 2479-2488.

Kaipainen A, Korhonen J, et al. (1995) Expression of the fms-like tyrosine kinase 4 gene becomes restricted to lymphatic endothelium during development. Proc Natl Acad Sci U S A 92: 3566-3570.

Kaplan RN, Riba RD, et al. (2005) VEGFR1-positive haematopoietic bone marrow progenitors initiate the pre-metastatic niche. Nature 438: 820-827.

Karpanen T, Bry M, et al. (2008) Overexpression of Vascular Endothelial Growth Factor-B in Mouse Heart Alters Cardiac Lipid Metabolism and Induces Myocardial Hypertrophy. Circulation Research 103: 1018 –1026.

Kawase Y, Ly HQ, et al. (2008) Reversal of cardiac dysfunction after long-term expression of SERCA2a by gene transfer in a pre-clinical model of heart failure. J Am Coll Cardiol 51: 1112-1119.

Kawasaki T, Kitsukawa, T, et al. (1999) A requirement for neuropilin-1 in embryonic vessel formation. Development 126: 4895-4902.

Kaye DM, Preovolos A, et al. (2007) Percutaneous cardiac recirculation-mediated gene transfer of an inhibitory phospholamban peptide reverses advanced heart failure in large animals. J Am Coll Cardiol 50: 253-260.

Karkkainen MJ, Haiko P, et al. (2004) Vascular endothelial growth factor C is required for sprouting of the first lymphatic vessels from embryonic veins. Nat Immunol 5: 74-80.

Kondoh K, Koyama H, et al. (2004) Conduction performance of collateral vessels induced by

vascular endothelial growth factor or basic fibroblast growth factor. Cardiovasc Res 61: 132-142.

Kong SW, Bodyak N, et al. (2005) Genetic expression profiles during physiological and pathological cardiac hypertrophy and heart failure in rats. Physiol Genomics 21: 34-42.

Kotin RM, Linden, et al. (1992) Characterization of a preferred site on human chromosome 19q for integration of adeno-associated virus DNA by non-homologous recombination. Embo J 11: 5071-5078.

Krum JM, Mani N, et al. (2002) Angiogenic and astroglial responses to vascular endothelial growth factor administration in adult rat brain. Neuroscience 110: 589-604.

Kusano KF, Pola, R, et al. (2005) Sonic hedgehog myocardial gene therapy: tissue repair through transient reconstitution of embryonic signaling. Nat Med 11: 1197-1204.

Laguens R, Meckert CP, et al. (2002) Entrance in mitosis of adult cardiomyocytes in ischemic pig hearts after plasmid-mediated rhVEGF165 gene transfer. Gene Ther 9: 1676-1681.

Lai NC, Roth DM, et al. (2004) Intracoronary adenovirus encoding adenylyl cyclase VI increases left ventricular function in heart failure. Circulation 110: 330 -336.

Lambrechts D, Storkebaum E, et al. (2003) VEGF is a modifier of amyotrophic lateral sclerosis in mice and humans and protects motoneurons against ischemic death. Nat. Genet. 34: 383–394.

Lagercrantz J, Larsson C, et al. (1996) Expression of the VEGF-related factor gene in pre- and postnatal mouse. Biochem Biophys Res Commun. 220**:**147–152.

Lahteenvuo JE, Lahteenvuo MT, et al. (2009) Vascular Endothelial Growth Factor-B Induces Myocardium-Specific Angiogenesis and Arteriogenesis via Vascular Endothelial Growth Factor Receptor-1- and Neuropilin Receptor-1-Dependent Mechanisms. Circulation 119: 845 - 856.

Lange T, Guttmann-Raviv N, et al. (2003) VEGF162, a new heparin-binding vascular endothelial growth factor splice form that is expressed in transformed human cells. J Biol Chem 278: 17164-17169.

Lazarous DF, Shou M, et al. (1999) Adenoviral-mediated gene transfer induces sustained pericardial VEGF expression in dogs: effect on myocardial angiogenesis. Cardiovasc Res 44: 294-302.

LeCouter J, Moritz DR, et al. (2003) Angiogenesis-independent endothelial protection of liver: role of VEGFR-1. Science 299: 890-893.

Lee KK and Workman JL (2007) Histone acetyltransferase complexes: one size doesn't fit all. Nat Rev Mol Cell Biol 8: 284-295.

Lehman JJ and Kelly DP (2002) Transcriptional activation of energy metabolic switches in the developing and hypertrophied heart. Clinical and Experimental Pharmacology and Physiology 29: 339-345.

Lehrman S, (1999) Virus treatment questioned after gene therapy death. Nature, 401: 517-518.

Leung DW, Cachianes G, et al. (1989) Vascular endothelial growth factor is a secreted angiogenic mitogen. Science 246: 1306-1309.

Li X, Tjwa M, et al. (2008a) Reevaluation of the role of VEGF-B suggests a restricted role in the revascularization of the ischemic myocardium. Arterioscler Thromb Vasc Biol. 28,1614 –1620.

Li Y, Zhang F, et al. (2008b) VEGF-B inhibits apoptosis via VEGFR-1-mediated suppression of the expression of BH3-only protein genes in mice and rats. J. Clin. Invest. 118: 913–923.

Li J, Post M, et al. (2000) PR39, a peptide regulator of angiogenesis. Nat Med 6: 49-55.

Li Q, Bolli R, et al. (1998) Gene therapy with extracellular superoxide dismutase attenuates myocardial stunning in conscious rabbits. Circulation 98: 1438-1448.

Li X, Tjwa M, et al. (2005) Revascularization of ischemic tissues by PDGF-CC via effects on endothelial cells and their progenitors. J Clin Invest 115:118-127.

Libby P (2001) Current Concepts of the Pathogenesis of the Acute Coronary Syndromes. *Circulation*. 104:365.

Lindahl P, Johansson, BR, et al. (1997) Pericyte loss and microaneurysm formation in PDGF-B-deficient mice. Science 277: 242-245.

Linden RM, Ward P, et al. (1996) Site-specific integration by adeno-associated virus. Proc Natl Acad Sci U S A 93: 11288-11294.

Litwin SE, Katz SE, et al. (1994) Serial echocardiographic assessment of left ventricular geometry and function after large myocardial infarction in the rat. Circulation 89: 345-354.

Litwin SE, Zhang D, et al. (2000) Dyssynchronous Ca^{2+} sparks in myocytes from infarcted hearts. Circ. Res 87: 1040-1047.

Liu Q and Muruve DA (2003) Molecular basis of the inflammatory response to adenovirus vectors. Gene Ther. 10: 935–940.

Liu Y, Cox SR, et al. (1995) Hypoxia regulates vascular endothelial growth factor gene expression in endothelial cells. Identification of a 5' enhancer. Circ Res 77: 638-643.

Lloyd-Jones DM, Larson MG, et al. (2002) Lifetime risk for developing congestive heart failure: the Framingham Heart Study. Circulation 106: 3068-3072.

Lobov IB, Brooks PC, et al. (2002) Angiopoietin-2 displays VEGF-dependent modulation of capillary structure and endothelial cell survival in vivo. Proc Natl Acad Sci USA 99: 11205-11210.

Louzier V, Raffestin B, et al. (2003) Role of VEGF-B in the lung during development of chronic hypoxic pulmonary hypertension. Am J Physiol Lung Cell Mol Physiol 284: L926–L937.

Lusis AJ (2000) Atherosclerosis. Nature 407:233.

Luo W, Grupp IL, et al. (1994) Targeted ablation of the phospholamban gene is associated with markedly enhanced myocardial contractility and loss of beta-agonist stimulation. Circ Res 75: 401-409.

Lyden D, Hattori K, et al. (2001) Impaired recruitment of bone-marrow-derived endothelial and hematopoietic precursor cells blocks tumor angiogenesis and growth. Nat. Med. 7: 1194 –1201.

Lyttle DJ, Fraser KM, et al. (1994) Homologs of vascular endothelial growth factor are encoded by the poxvirus orf virus. J Viol 68: 84-92.

Maisonpierre PC, Suri C, et al. (1997) Angiopoietin-2, a natural antagonist for Tie2 that disrupts in vivo angiogenesis. Science 277(5322):55-60.

Marcello A, Massimi P, et al. (2000) Adeno-associated virus type 2 Rep protein inhibits human papillomavirus type 16 E2 recruitment of the transcriptional coactivator p300. J Virol 74: 9090-9098.

Marx SO, Gaburjakova J, et al. (2001) Coupled gating between cardiac calcium release channels (ryanodine receptors. Circ. Res 88: 1151-1158.

Mathers CD, Lopez AD et al. (2006) The Burden of Disease and Mortality by Condition: Data Methods, and Results for 2001. In *Global Burden of Disease and Risk Factors*, eds.. Lopez AD, Mathers CD, Ezzati M, Jamison D T and Murray C J L. New York: Oxford University Press.

Matsumoto T and Claesson-Welsh L (2001) VEGF receptor signal transduction. Sci STKE RE21.

Mayr-Wohlfart U, Waltenberger J, et al. (2002) Vascular endothelial growth factor stimulates chemotactic migration of primary human osteoblasts. Bone 30: 472– 477.

McTigue MA, Wickersham JA, et al. (1999) Crystal structure of the kinase domain of human vascular endothelial growth factor receptor 2: a key enzyme in angiogenesis. Structure 7: 319-330.

Messina S, Mazzeo A, et al. (2007) VEGF overexpression via adeno-associated virus gene transfer promotes skeletal muscle regeneration and enhances muscle function in mdx mice. FASEB J. 21: 3737–3746.

Meyer M, Clauss M, et al. (1999) A novel vascular endothelial growth facot encoded by Orf virus, VEGF-E, mediates angiogenesis via signalling through VEGFR-2(KDR) but not VEGFR-1(Flt-1) receptor tyrosine kinases. Embo J 18: 363-374.

Millauer B, Wizigmann-Voos S, et al. (1993) A High affinity VEGF binding and developmental expression suggest Flk-1 as a major regulator of vasculogenesis and angiogenesis. Cell 72: 835-846.

Miquerol L, Langille BL, et al. (2000) Embryonic Development is Disrupted by Modest Increases in Vascular Endothelial Growth Factor Gene Expression. Development 127(18): 3941-3946.

Mochly-Rosen D, Henrich C J, et al. (1990) A protein kinase C isozyme is translocated to cytoskeletal elements on activation. Cell Regul 1(9):693-706.

Moe GW and Armstrong P (1999) Pacing-induced heart failure: a model to study the mechanism of disease progression and novel therapy in heart failure. Cardiovascular Research 42: 591–599.

Moe G, Konig A, et al. (1997) Early activation of programmed induced heart failure in rabbits. Beneficial effects on left ventricular cell death may contribute to heart failure progression. Can J Cardiol and myocyte function. Circulation 95:1918–1929.

Moe GW, Angus C, et al. (1992) Evaluation of indices of left ventricular contractility and relaxation in evolving canine experimental heart failure. Cardiovasc Res 26:362-6.

Mould AW, Sonia AG, et al. (2005) Transgenic overexpression of vascular endothelial growth factor-B isoforms by endothelial cells potentiates postnatal vessel growth in vivo and in vitro. Circ. Res. 97:e60–e70.

Mould A W, Tonks ID, et al. (2003) Vegfb gene knockout mice display reduced pathology and synovial angiogenesis in both antigen-induced and collagen-induced models of arthritis. Arthritis Rheum. 48: 2660-2669.

Mueller C and Flotte T R (2008) Clinical gene therapy using recombinant adeno-associated virus vectors. Gene Ther. 15, 858 –863.

Murga M, Fernandez-Capetillo O, et al. (2005) Neuropilin-1 regulates attachment in human ECs independently of vascular endothelial growth factor receptor-2. Blood 105: 1992-1999.

NATIONAL INSTITUTE OF CLINICAL EXCELLENCE London (2003) Chronic heart failure - management of chronic heart failure in adults in primary and secondary care. National Institute of Clinical Excellence.

Neufeld G, Kessler O, et al. (2002) The interaction of Neuropilin-1 and Neuropilin-2 with tyrosine-kinase receptors for VEGF. Adv Exp Med Biol 515: 81-90.

Neufeld G, Cohen T, et al. (1999) Vascular endothelial growth factor (VEGF) and its receptors. FASEB J. 13: 9 –22.

Niagara MI, Haider H, et al. (2004) Autologous skeletal myoblasts transduced with a new adenoviral bicistronic vector for treatment of hind limb ischemia. J Vasc Surg 40: 774-785.

Nicolaou P, Rodriguez P, et al. (2009a) Inducible Expression of Active Protein Phosphatase-1 Inhibitor-1 Enhances Basal Cardiac Function and Protects Against Ischemia/Reperfusion Injury. Circ. Res 104: 1012-1020.

Nishiyama K, Takaji K, et al. (2005) Id1 gene transfer confers angiogenic property on fully differentiated endothelial cells and contributes to therapeutic angiogenesis. Circulation 112: 2840-2850.

Ogawa S, Oku A, et al. (1998) A novel type of vascular endothelial growth factor, VEGF-E (NZ-7 VEGF), preferentially utilizes KDR/Flk-1 receptor and carries a potent mitotic activity without heparin-binding domain J Biol Chem 273: 31273-31282.

Okazaki T, Ebihara S, et al. (2006) Granulocyte colony-stimulating factor promotes tumor angiogenesis via increasing circulating endothelial progenitor cells and $Gr1^{+}CD11b^{+}$ cells in cancer animal models. . International Immunology 18: 1-9.

Olofsson B, Korpelainen E, et al. (1998) Vascular endothelial growth factor B (VEGF-B) binds to VEGF receptor-1 and regulates plasminogen activator activity in endothelial cells Proc Natl Acad Sci USA 95: 11709-11714.

Olofsson B, Pajusola K, et al. (1996b) Genomic organization of the mouse and human genes for vascular endothelial growth factor B (VEGF-B) and characterization of a second splice isoform. J Biol Chem 271: 19310-19317.

Olofsson B, Pajusola K, et al. (1996a) Vascular endothelial growth factor B, a novel growth factor for endothelial cells. Proc Natl Acad Sci USA 93: 2576-2581.

Olson EN (2004) A decade of discoveries in cardiac biology. Nature Medicine 10: 467 – 474.

Olsson AK, Dimberg A, et al. (2006) VEGF receptor signalling ? in control of vascular function Nature Reviews Molecular Cell Biology 7: 359-371.

Ono MYK, Ohkusa T, et al. (2000) Altered stoichiometry of FKBP12.6 versus ryanodine receptor as a cause of abnormal Ca^{2+} leak through ryanodine receptor in heart failure. Circulation 102: 2131-2136.

Orlowski J and Lingrel J B (1990) Thyroid and glucocorticoid hormones regulate the expression of multiple Na,K-ATPase genes in cultured neonatal rat cardiac myocytes. J. Biol. Chem 266 3462-3470.

Pages G and Pouyssegur J (2005) Transcriptional regulation of the Vascular Endothelial Growth Factor gene--a concert of activating factors. Cardiovasc Res 65: 564-573.

Pan Q, Chathery Y, et al. (2007) Neuropilin-1 binds to VEGF121 and regulates EC migration and sprouting. J Biol Chem 282: 24049-24056.

Pap M and Cooper G (1998) Role of glycogen synthase kinase-3 in the phosphatidylinositol 3-kinase/Akt cell survival pathway. J Biol Chem 273: 19929-19932.

Park JE, Chen HH, et al. (1994) Placenta growth factor. Potentiation of vascular endothelial growth factor bioactivity, in vitro and in vivo, and high affinity binding to Flt-1 but not to Flk-1/KDR. J Biol Chem 269: 25646-25654.

Parsons-Wingerter P, Chandrasekharan UM, et al. (2006) A VEGF165-induced phenotypic switch from increased vessel density to increased vessel diameter and increased endothelial NOS activity. Microvasc Res 72: 91–100.

Pennock GD, Yun DD, et al. (1997) Echocardiographic changes after myocardial infarction in a model of left ventricular diastolic dysfunction. Am J Physiol Cell Physiol 273: H2018-2029.

Pepe M, Mamdani M, et al. (2010) Intramyocardial VEGF-B167 gene delivery delays the progression towards congestive failure in dogs with pacing-induced dilated cardiomyopathy. Circ Res 106(12):1893-903.

Pfeffer MA (1995) Left ventricular remodeling after acute myocardial infarction. Annu Rev Med 46: 455-466.

Pfeffer MA, Pfeffer JM, et al. (1979) Myocardial infarct size and ventricular function in rats. Circ. Res. 44: 503–512.

Pleger ST, Most P, et al. (2007) Stable myocardial-specific AAV6-S100A1 gene therapy results in chronic functional heart failure rescue. Circulation 115: 2506-2515.

Poesen K, Lambrechts D, et al. (2008) Novel role for vascular endothelial growth factor (VEGF) receptor-1 and its ligand VEGF-B in motor neuron degeneration. J. Neurosci. 28: 10451–10459.

Poltorak Z, Cohen T, et al. (1997) VEGF145, a secreted vascular endothelial growth factor isoform that binds to extracellular matrix. J Biol Chem 272: 7151-7158.

Rafii S and Lyden D (2003) Therapeutic stem and progenitor cell transplantation for organ vascularization and regeneration. Nat Med 9: 702-712.

Rayner M and Petersen S (2003) European cardiovascular disease statistics. British Heart Foundation: London. from: http://www.heartstats.org/homepage.asp

Reddy SK, Shah B, et al. (2005) Responding to the threat of chronic diseases in India. Lancet 366:1744-1749.

Richardson TP, Peters MC, et al. (2001) Polymeric system for dual growth factor delivery. Nat Biotechnol 19: 1029-1034.

Risau, W (1997) Mechanisms of angiogenesis. Nature 386: 671-674.

Risau W and Flamme I (1995) Vasculogenesis. Annu Rev Cell Dev Biol 11:73-91.

Rissanen TT and Ylä-Herttuala S (2007) Current Status of Cardiovascular Gene Therapy. Molecular Therapy 15: 1233-1247.

Rissanen TT, Korpisalo P, et al. (2005) Blood flow remodels growing vasculature during vascular endothelial growth factor gene therapy and determines between capillary arterialization and sprouting angiogenesis. Circulation 112: 3937–3946.

Rissanen TT, Markkanen JE, et al. (2003) VEGF-D is the strongest angiogenic and lymphangiogenic effector among VEGFs delivered into skeletal muscle via adenoviruses. Circ. Res. 92:1098 –1106.

Rodenbaugh DW, Wang W, et al. (2007) Parvalbumin isoforms differentially accelerate cardiac myocyte relaxation kinetics in an animal model of diastolic dysfunction. Am J Physiol Heart Circ Physiol 293: H1705-H1713.

Rosamond W F, Katherine F, et al. (2008) Heart disease and stroke statistics--2008 update: a report from the American Heart Association Statistics Committee and Stroke Statistics Subcommittee. Circulation 117: e25-146.

Rosengart TK, Lee LY, et al. (1999) Angiogenesis gene therapy: phase I assessment of direct intramyocardial administration of an adenovirus vector expressing VEGF121 cDNA to individuals with clinically significant severe coronary artery disease. Circulation 100: 468-474.

Roskoski R, Jr. (2008) VEGF receptor protein-tyrosine kinases: structure and regulation. Biochem Biophys Res Commun 375: 287-291.

Ross RS, Rockman HA, et al. (1990) In vivo hypertrophy in transgenic mice segregates inducible from tissue specific expression of the ANF gene. Clin Res 39: 296A.

Roth DM, Bayat H, et al. (2002) Adenylyl cyclase increases survival in cardiomyopathy. Circulation 105: 1989-1994.

Rottbauer W, Just S, et al. (2005) VEGF-PLC1γ pathway controls cardiac contractility in the embryonic heart. Genes Dev. 19: 1624 –1634.

Rouis M, Adamy C, et al. (1999) Adenovirus mediated overexpression of tissue inhibitor of metalloproteinase-1 reduces atherosclerotic lesions in apolipoprotein E-deficient mice. Circulation 100: 533-540.

Sadoshima J, Jahn L, et al. (1992) Molecular characterization of the stretch-induced adaptation of cultured cardiac cells. An in vitro model of load-induced cardiac hypertrophy. J Biol Chem. 267: 10551-10560.

Safi J, DiPaula AF, et al. (1999) Adenovirus-mediated acidic fibroblast growth factor gene transfer induces angiogenesis in the nonischemic rabbit heart. Microvasc Res 58: 238-249.

Sah R, Ramirez RJ, et al. (2002) Modulation of Ca^{2+} release in cardiac myocytes by changes in repolarization rate: role of phase-1 action potential repolarization in excitation-contraction coupling. Circ. Res 90: 165-173.

Sahn DJ, DeMaria A, et al. (1978) Recommendations regarding quantitation in M-mode echocardiography: results of a survey of echocardiographic measurements. Circulation 58: 1072–1083.

Saharinen P, Tammela T, et al. (2004) Lymphatic vasculature: development, molecular regulation and role in tumor metastasis and inflammation. Trends Immunol 25, 387-395.

SakataY,Yamamoto K, et al. (2001) Ventricular production of natriuretic peptides and ventricular structural remodeling in hypertensive heart failure. J Hypertens 19: 1905-1912.

Sasaki H, Asanuma H, et al. (2009) Metformin prevents progression of heart failure in dogs: role of AMP-activated protein kinase. Circulation 119: 2568-2577.

Sato Y, Teruyama K, et al. (2001) Role of transcription factors in angiogenesis: Ets-1 promotes angiogenesis as well as endothelial apoptosis. .Ann N Y Acad Sci 947: 117-123.

Sawano A, Iwai S, et al. (2001) Flt-1, vascular endothelial growth factor receptor 1, is a novel cell surface marker for the lineage of monocyte-macrophages in humans. Blood 97: 785–791.

Schnepp, BC, Jensen RL, et al. (2005) Characterization of adeno-associated virus genomes isolated from human tissues. J Virol 79: 14793-14803.

Schwartz SM, DeBlois D, et al. (1995) The intima: Soil for atherosclerosis and restenosis. Circ Res 77: 445-65.

Schaub MC, Hefti MA, et al. (1997) Various hypertrophic stimuli induce distinct phenotypes in cardiomyocytes. J. Mol. Med. 75: 901–920.

Schwartz ER, Speakman MT, et al. (2000) Evaluation of the effects of intramyocardial injection of DNA expressing vascular endothelial growth factor (VEGF) in a myocardial infarction model in the rat - angiogenesis and angioma formation. J Am Coll Cardiol 35: 1323-1330.

Selvin E and Erlinger TP (2004) Prevalence of and risk factors for Peripheral arterial disease in the United States: results from the NHANES 1999-2000. Circulation 110: 738-743.

Senger DR, Galli SJ, et al. (1983) Tumor cells secrete a vascular permeability factor that promotes accumulation of ascites fluid. Science 219, 983-985.

Shah AS, White DC, et al. (2001) In vivo ventricular gene delivery of a β-adrenergic receptor kinase inhibitor to the failing heart reverses cardiac dysfunction. Circulation 103: 1311-1316.

Shalaby F, Rossant J, et al. (1995) Failure of blood-island formation and vasculogenesis in Flk-1-deficient mice. Nature 376: 62-66.

Shibuya M and Welsh CL (2006) Signal transduction by VEGF receptors in regulation of angiogenesis and lymphangiogenesis. Exp Cell Res 312: 549-560.

Shibuya, M. (2001) Structure and dual function of vascular endothelial growth factor receptor-1 (Flt-1). Int J Biochem Cell Biol 33: 409-420.

Shibuya M, Yamaguchi, S, et al. (1990) Nucleotide sequence and expression of a novel human receptor-type tyrosine-kinase gene (flt) closely related to the fms family. Oncogene 5: 519-524.

Shiraishi I, Melendez J, et al. (2004) Nuclear targeting of Akt enhances kinase activity and survival of cardiomyocytes. Circ Res 94: 884-891.

Shraga-Heled N, Kessler O, et al. (2007) Neuropilin-1 and neuropilin-2 enhance VEGF121 stimulated signal transduction by the VEGFR-2 receptor. Faseb J 21: 915-926.

Shubeita H E, McDonough PM, et al. (1990) Endothelin induction of sarcomere assembly and cardiac gene expression in ventricular myocytes: a paracrine mechanism for myocardial cell hypertrophy. J Biol Chein 265: 20555-20562.

Silvestre JS, Tamarat R, et al. (2003) Vascular endothelial growth factor-Bpromotes in vivo angiogenesis. Circ. Res. 93: 114 –123.

Simpson PC, Kariya K, et al. (1994) The molecular basis of thyroid hormone action. N. Engl. J. Med. 331: 847– 853.

Simpson P, McGrath A, et al. (1982) Myocyte hypertrophy in neonatal rat heart cultures and its regulation by serum and by catecholamines. Circ Res 51: 787-801.

Sjaastad I, Wasserstrom JA, et al. (2003) Heart failure - a challenge to our current concepts of excitation-contraction coupling. J. Physiol 54: 33-47.

Snyder RO, Spratt SK et al. (1997) Efficient and stable adeno-associated virus-mediated transduction in the skeletal muscle of adult immunocompetent mice. Hum Gene Ther 8: 1891-1900.

Soker S, Takashima S, et al. (1998) Neuropilin-1 is expressed by endothelial and tumor cells as an isoform-specific receptor for vascular endothelial growth factor. Cell 92: 735-745.

Sondell M, Sundler F, et al. (2000) Vascular endothelial growth factor is a neurotrophic factor

which stimulates axonal outgrowth through the flk-1 receptor. Eur J Neurosci 12: 4243-4254.

Srivastava RD, Kalitha M, et al. (1977) A mechanism of action of phenylephrine on heart. Indian J Physiol Pharmacol. 21(3):167-74.

Stacker SA, Caesar C, et al. (2001) VEGF-D promotes the metastatic spread of tumor cells via the lymphatics. Nat Med 7, 186-191.

Stalmans I, Ng YS, et al. (2002) Arteriolar and venular patterning in retinas of mice selectively expressing VEGF isoforms. J Clin Invest 109: 327-336.

Stein I, Itin A, et al. (1998) Translation of vascular endothelial growth factor mRNA by internal ribosome entry: implications for translation under hypoxia. Mol Cell Biol 18: 3112-3119.

Stewart S, Jenkins. A, et al. (2002) The current cost of heart failure to the National Health Service in the UK. Eur J Heart Fail 4: 361-371.

Storkebaum E, Lambrechts D, et al. (2004) VEGF: once regarded as a specific angiogenic factor, now implicated in neuroprotection.BioEssays 26: 943 – 954.

Storkebaum E and Carmeliet, P (2004) VEGF: a critical player in neurodegeneration. J. Clin. Invest. 113: 14 –18.

Su H, Lu R, et al. (2000) Adeno-associated viral vectormediated vascular endothelial growth factor gene transfer induces neovascular formation in ischemic heart. Proc Natl Acad Sci USA 97: 13801-13806.

Sun Y, Jin K, et al. (2006) Vascular endothelial growth factor-B (VEGFB) stimulates neurogenesis: evidence from knockout mice and growth factor administration. Dev Biol 289: 329-335.

Sun Y K, Jin JT, et al. (2004) Increased severity of cerebral ischemic injury in vascular endothelial growth factor-B (VegfB)-deficient mice. J Cereb Blood Flow Metab 24: 1146-1152.

Suri C, Jones PF, et al. (1996) Requisite role of angiopoietin-1, a ligand for the TIE2 receptor, during embryonic angiogenesis. Cell 87:1171-1180.

Sutton MG and Sharpe N (2000) Left ventricular remodeling after myocardial infarction: pathophysiology and therapy. Circulation 101: 2981-2988.

Tafuro S, Ayuso E, et al. (2009) Inducible adeno-associated virus vectors promote functional angiogenesis in adult organisms via regulated vascular endothelial growth factor expression. Cardiovasc Res. 83(4):663-71.

Takahashi N, Calderone A, et al. (1994) Hypertrophic stimuli induce transforming growth factor-beta 1 expression in rat ventricular myocytes. J Clin Invest 94: 1470-1476.

Takahashi H, and Shibuya M (2005) The vascular endothelial growth factor (VEGF)/VEGF receptor system and its role under physiological and pathological conditions. Clin Sci (Lond) 109: 227-241.

Takahashi H, Hattori S, et al. (2004) A Novel Snake Venom Vascular Endothelial Growth Factor (VEGF) Predominantly Induces Vascular Permeability through Preferential Signaling via VEGF Receptor-1. The Journal of Biological Chemistry 279: 46304-46314.

Takahashi M, Matsui A, et al. (2003)ERK/MAPK-dependent PI3K/Akt phosphorylation through VEGFR-1 after VEGF stimulation in activated hepatic stellate cells. Hepatol Res. 26(3):232-236.

Takashima S, Kitakaze M, et al. (2002) Targeting of both mouse neuropilin-1 and neuropilin-2 genes severely impairs developmental yolk sac and embryonic angiogenesis. Proc Natl Acad Sci U S A 99: 3657-3662.

Tallquist M and Kazlauskas A (2004) PDGF signaling in cells and mice. Cytokine Growth Factor Rev 15: 205-213.

Tammela T, Zarkada G, et al. (2008) Blocking VEGFR-3 suppresses angiogenic sprouting and vascular network formation. Nature 454, 656-660.

Tardiff JC, Hewett TE, et al. (2000) Expression of the beta (slow)-isoform of MHC in the adult mouse heart causes dominant-negative functional effects. Am J Physiol Heart Circ Physiol 278: H412–H419.

Terman BI, Carrion ME, et al. (1991) Identification of a new endothelial cell growth factor receptor tyrosine kinase. Oncogene 6: 1677-1683.

Thurston G, Rudge JS, et al. (2000) Angiopoietin-1 protects the adult vasculature against plasma leakage. Nat Med, 6: 460-463.

Tirziu, D, Chorianopoulos E, et al. (2007) Myocardial hypertrophy in the absence of external stimuli is induced by angiogenesis in mice. J. Clin. Invest. 117: 3188–3197.

Tischer E, Mitchell R, et al. (1991) The human gene for vascular endothelial growth factor.

Multiple protein forms are encoded through alternative exon splicing. J Biol Chem 266.

Tokunaga N, Nagaya N, et al. (2004) Adrenomedullin gene transfer induces therapeutic angiogenesis in a rabbit model of chronic hind limb ischemia: benefits of a novel nonviral vector, gelatin. Circulation 109: 526-531.

Tratschin JD, West MH, et al. (1984) A human parvovirus, adeno-associated virus, as a eucaryotic vector: transient expression and encapsidation of the procaryotic gene for chloramphenicol acetyltransferase. Mol Cell Biol, 4: 2072-2081.

Trivieri MG, Oudit GY, et al. (2006) Cardiac-specific elevations in thyroid hormone enhance contractility and prevent pressure overload-induced cardiac dysfunction. Proc. Natl. Acad. Sci. U S A 103: 6043–6048.

Tsurumi Y, Takeshita S, et al. (1996) Direct intramuscular gene transfer of naked DNA encoding vascular endothelial growth factor augments collateral development and tissue perfusion. Circulation 94: 3281-3290.

Vakili BA, Okin PM, et al. (2001) Prognostic implications of left ventricular hypertrophy. Am Heart J 141: 334-341.

Veikkola T, Jussila, L, et al. (2001) Signalling via vascular endothelial growth factor receptor-3 is sufficient for lymphangiogenesis in transgenic mice. Embo J 20: 1223-1231.

Ventura C, Cantoni S, et al. (2007) Hyaluronan mixed esters of butyric and retinoic acid drive cardiac and endothelial fate in term placenta human mesenchymal stem cells and enhance cardiac repair in infracted rat hearts. J. Biol. Chem. 282: 14243–14252.

Virmani R, Burke AP, et al. (2002) Pathology of the unstable plaque. Prog Cardiovasc Dis 44(5):349-56.

Wahr, PA, Michele D E, et al. (1999) Parvalbumin gene transfer corrects diastolic dysfunction in diseased cardiac myocytes. Proc. Nat. Acad. Sci. 96: 11982-11985.

Wakatsuki T, Schlessinger J, et al. (2004) The biochemical response of the heart to hypertension and exercise. Trends Biochem Sci 29(11):609–617.

Waltenberger J, Claesson-Welsh L, et al. (1994) Different signal transduction properties of KDR and Flt1, two receptors for vascular endothelial growth factor. J Biol Chem 269: 26988-26995.

Wang GL and Semenza GL (1995) Purification and characterization of hypoxia-inducible factor 1. J Biol Chem 270:1230-1237.

Wang L, Dutta S.K, et al. (2007) Neuropilin-1 modulates p53/caspases axis to promote EC survival. PLoS One 2: e1161.

Webster KA (2004) Aktion in the nucleus. Circ Res 94: 856-859.

Weitzman MD, Kyostio SR, et al. (1994) Adeno-associated virus (AAV) Rep proteins mediate complex formation between AAV DNA and its integration site in human DNA. Proc Natl Acad Sci USA 91: 5808-5812

Wey JS, Fan F, et al. (2005) Vascular endothelial growth factor receptor-1 promotes migration and invasion in pancreatic carcinoma cell lines. Cancer 104: 427-438.

Whipple GH, Sheffield LT, et al. (1962) Reversible congestive heart failure due to chronic rapid stimulation of the normal heart. In: Proc New Engl Cardiovasc Soc. 20:39–40.

Whitlock PR, Hackett NR, et al. (2004) Adenovirus-mediated transfer of a minigene expressing multiple isoforms of VEGF is more effective at inducing angiogenesis than comparable vectors expressing individual VEGF cDNAs. Mol Ther 9: 67-75.

Weis SM and Cheresh DA (2005) Patho-physiological consequences of VEGF-induced vascular permeability. Nature 437: 497-504.

Wilson JR, Douglas P, et al. (1987) Experimental congestive heart failure produced by rapid ventricular pacing in the dog: cardiac effects. Circulation 75:857-67.

Winslow RD, Sharma SK, et al. (2005) Restenosis and drug-eluting stents. Mt Sinai J Med 72: 81-89.

Woolard J, Wang WY, et al. (2004) VEGF165b, an inhibitory vascular endothelial growth factor splice variant: mechanism of action, in vivo effect on angiogenesis and endogenous protein expression. Cancer Res 64: 7822-7835.

Yamagishi S, Yonekura H, et al. (1999) Vascular endothelial growth factor acts as a pericyte mitogen under hypoxic conditions. Lab Invest 79: 501-509.

Yamashita J, Itoh H, et al. (2000) Flk1-positive cells derived from embryonic stem cells serve as vascular progenitors. Nature 408: 92-96.

Yamamoto T, Yano M, et al. (1999) Abnormal Ca^{2+} release from cardiac sarcoplasmic reticulum in tachycardia-induced heart failure. Cardiovasc Res 44: 146-155.

Yan L, Vatner DE, et al. (2007) Type 5 adenylyl cyclase disruption increases longevity and protects against stress. Cell 130: 247-258

Yang Y, Haecker SE, et al. (1996) Immunology of gene therapy with adenoviral vectors in mouse skeletal muscle. Hum Mol Genet, 5: 1703-1712.

Yano KOM, Ohkusa T, et al. (2000) Altered interaction of FKBP12.6 with ryanodine receptor as a cause of abnormal Ca2+ release in heart failure. Cardiovasc Res 48: 323-331.

Zacchigna S, Pattarini L, et al. (2008) Bone marrow cells recruited through the Neuropilin-1 receptor promote arterial formation at the sites of adult neoangiogenesis. J Clin Invest 118: 2062-2075.

Zheng SY, Murakami M, et al. (2006) Chimeric VEGF-E (NZ7)/PlGF promotes angiogenesis via VEGFR-2 without significant enhancement of vascular permeability and inflammation. Arterioscler Thromb Vasc Biol 26: 2019-2026.

Zhong J, Eliceiri B, et al. (2003) Neovascularization of ischemic tissues by gene delivery of the extracellular matrix protein Del-1. J Clin Invest 112: 30-41.

Ziche M, Maglione D, et al. (1997) Placenta growth factor-1 is chemotactic, mitogenic, and angiogenic. Lab Invest 76: 517-531.

APPENDIX

Publications related to the thesis:

1. Zentilin L*, **Puligadda U*,** Lionetti V*, Zacchigna S, Collesi C, Pattarini L, Ruozi G, Camporesi S, Sinagra G, Pepe M, Recchia FA, Giacca M. (2010) Cardiomyocyte VEGFR-1 activation by VEGF-B induces compensatory hypertrophy and preserves cardiac function after myocardial infarction. *The FASEB Journal* 24(5):1467-78. (* These authors contributed equally to this work)

2. Pepe M, Mamdani M, Zentilin L, Csiszar A, Qanud K, Zacchigna S, Ungvari Z, **Puligadda U**, Moimas S, Xu X, Edwards JG, Hintze TH, Giacca M, Recchia FA. (2010) Intramyocardial VEGF-B167 Gene Delivery Delays the Progression Towards Congestive Failure in Dogs With Pacing-Induced Dilated Cardiomyopathy. *Circulation Research*. 106(12):1893-903.

Other publications:

1. Manasseri B, Cuccia G, Moimas S, D'Alcontres FS, Polito F, Bitto A, Altavilla D, Squadrito F, Geuna S, Pattarini L, Zentilin L, Collesi C, **Puligadda U**, Giacca M, Colonna MR (2007) Microsurgical arterovenous loops and biological templates: A novel in vivo chamber for tissue engineering. *Microsurgery*. 27(7):623-9.

2. Carrer A, Zacchigna S, Moimas S, Pattarini L, Zentilin L, Ruozi G, Mano M, **Puligadda U**, Sinigaglia M, Maione F, Serini G, Giraudo E, Bussolino F and Giacca M. Neuropilin-1-expressing mononuclear cells (NEMs), recruited by Semaphorin-3A,contribute to vessel normalization and inhibit tumor growth. (Submitted to *Journal of Clinical Investigation*).

The FASEB Journal article fj.09-143180. Published online December 17, 2009.

Cardiomyocyte VEGFR-1 activation by VEGF-B induces compensatory hypertrophy and preserves cardiac function after myocardial infarction

Lorena Zentilin,[*,1] Uday Puligadda,[*,1] Vincenzo Lionetti,[†,1] Serena Zacchigna,[*] Chiara Collesi,[*] Lucia Pattarini,[*] Giulia Ruozi,[*] Silvia Camporesi,[*] Gianfranco Sinagra,[‡] Martino Pepe,[§] Fabio A. Recchia,[†,§] and Mauro Giacca[*,‖,2]

[*]Molecular Medicine Laboratory, International Centre for Genetic Engineering and Biotechnology (ICGEB), Trieste, Italy; [†]Scuola Superiore Sant'Anna, Sector of Medicine, Pisa, Italy; [‡]SC Cardiologia, Azienda Ospedaliera-Universitaria "Ospedali Riuniti di Trieste," Ospedale di Cattinara, Trieste, Italy; [§]New York Medical College, Valhalla, New York, USA; and [‖]Department of Biomedicine, Faculty of Medicine, University of Trieste, Trieste, Italy

ABSTRACT **Mounting evidence indicates that the function of members of the vascular endothelial growth factor (VEGF) family extends beyond blood vessel formation. Here, we show that the prolonged intramyocardial expression of VEGF-A_{165} and VEGF-B_{167} on adeno-associated virus-mediated gene delivery determined a marked improvement in cardiac function after myocardial infarction in rats, by promoting cardiac contractility, preserving viable cardiac tissue, and preventing remodeling of the left ventricle (LV) over time. Consistent with this functional outcome, animals treated with both factors showed diminished fibrosis and increased contractile myocardium, which were more pronounced after expression of the selective VEGF receptor-1 (VEGFR-1) ligand VEGF-B, in the absence of significant induction of angiogenesis. We found that cardiomyocytes expressed VEGFR-1, VEGFR-2, and neuropilin-1 and that, in particular, VEGFR-1 was specifically up-regulated in hypoxia and on exposure to oxidative stress. VEGF-B exerted powerful antiapoptotic effect in both cultured cardiomyocytes and after myocardial infarction *in vivo*. Finally, VEGFR-1 activation by VEGF-B was found to elicit a peculiar gene expression profile proper of the compensatory, hypertrophic response, consisting in activation of αMHC and repression of βMHC and skeletal α-actin, and an increase in SERCA2a, RYR, PGC1α, and cardiac natriuretic peptide transcripts, both in cultured cardiomyocytes and in infarcted hearts. The finding that VEGFR-1 activation by VEGF-B prevents loss of cardiac mass and promotes maintenance of cardiac contractility over time has obvious therapeutic implications.—Zentilin, L., Puligadda, U., Lionetti, V., Zacchigna, S., Collesi, C., Pattarini, L., Ruozi, G., Camporesi, S., Sinagra, G., Pepe, M., Recchia, F. A., Giacca, M. Cardiomyocyte VEGFR-1 activation by VEGF-B induces compensatory hypertrophy and preserves cardiac function after myocardial infarction. *FASEB J.* 24, 000–000 (2010). www.fasebj.org**

Key Words: apoptosis · adeno-associated virus, angiogenesis · gene therapy · gene expression

MEMBERS OF THE VASCULAR ENDOTHELIAL growth factor (VEGF) family and their receptors are essential regulators of vasculogenesis, angiogenesis, and vessel maintenance in both embryo and adults (for reviews, see refs. 1–4). In particular, the 165-aa isoform of VEGF-A (VEGF-A herein for brevity) possesses full angiogenic and arteriogenic activity, mainly through binding to VEGFR-2, which stimulates pathways important for mitogenesis, migration, and survival of endothelial cells (4, 5).

VEGF-A also binds VEGFR-1 with an affinity that is ≥10 times higher than that of VEGFR-2 (6); however, the significance of this interaction remains elusive, especially since this receptor appears unable to transduce an angiogenic signal in endothelial cells (7). Multiple evidence suggests that VEGF-B, a VEGFR-1-exclusive ligand that is produced in a heparin-binding isoform of 167 aa (VEGF-B_{167}) and a diffusible isoform of 186 aa (VEGF-B_{186}) (7, 8) might selectively be active in the myocardium. Indeed, the VEGF-B gene, shows prominent expression in the heart during embryonic development (9), and mice with knockouts for this factor display a mild cardiac phenotype, characterized, at least in one strain, by decreased heart size (10). In addition, recent evidence indicates that transgenic mice specifically expressing VEGF-B_{167} in the myocardium undergo massive myocardial hypertrophy, in the absence of a significant increase of cardiac angiogenesis (11).

A few studies have also explored the effects of VEGF-A and VEGF-B in the heart after myocardial infarction. In particular, VEGF-B_{167} was described to significantly increase revascularization of the infarcted myocardium; however, it failed to enhance vascular growth in the skin or ischemic limb (12). The reasons

[1] These authors contributed equally to this work.

[2] Correspondence: CGEB Trieste, Molecular Medicine Laboratory, Padriciano, 99, 34012 Trieste (Italy). E-mail: giacca@icgeb.org

doi: 10.1096/fj.09-143180

for the selective cardiac benefit of VEGF-B delivery remained unexplained. Another recent study, entailing the delivery of VEGF-B_{186} after infarction in pigs and rabbits using adenoviral vectors, indicated that the factor induced myocardial-specific angiogenesis and arteriogenesis and, most notably, improved myocardial function a few days after vector injection (13). As far as VEGF-A is concerned, in a previous study of acute myocardial infarction in dogs, we observed that the sustained expression of this factor, delivered to the heart using an adeno-associated virus (AAV)-based vector determined remarkable recovery of the regional myocardial contractility, up to 4 wk after injury (14). Surprisingly, the improvement in myocardial function started to be significant as early as 48 h after vector injection, a temporal frame not compatible with the formation of new blood vessels and suggestive of a direct effect of VEGF on resident cardiomyocytes, additional to angiogenesis (14).

Taken together, this variegated information leaves a series of essential questions outstanding, including to what extent the cardiac effects of the VEGFs are secondary to the induction of angiogenesis or directly exerted onto myocardial cells, which is the receptor involved, and how long the beneficial effect exerted by the factors lasts after cardiac injury. To provide answers to these questions, we took advantage of the possibility of delivering *in vivo* VEGF-A and VEGF-B_{167} (herein VEGF-B for brevity) to the heart using vectors based on the AAV, and to assess their effects for prolonged periods of time both in normal conditions and after myocardial infarction. Over the past few years, these vectors have gained increasing popularity due to several favorable characteristics, in particular, their ability to transduce postmitotic cells, including cardiomyocytes, at high efficiency and to drive gene expression for very prolonged periods of time in the absence of noticeable inflammation (15, 16).

Here, we show that the AAV-mediated, intramyocardial expression of VEGF-A and, most notably, of VEGF-B determines a marked improvement in cardiac function after permanent coronary artery occlusion in rats, ensuing from the direct protection of cardiomyocytes from apoptosis and up-regulation of genes driving compensatory, hypertrophic response. These results clearly indicate that the role of VEGFs in the heart extends beyond their angiogenic properties, and point toward VEGFR-1 signaling as an important mediator of cardiomyocyte function, with clear therapeutic implications.

MATERIALS AND METHODS

Production, purification, and characterization of rAAV vectors

rAAV vectors were prepared by the AAV Vector Unit at ICGEB Trieste (http://www.icgeb.org/avu-core-facility.html), as described previously (17, 18). AAV titers were in the range of 1×10^{12} to 1×10^{13} genome copies (gc)/ml.

Animal studies and echocardiography

Animal care and treatment were conducted in conformity with institutional guidelines in compliance with national and international laws and policies (European Economic Community Council Directive 86/609, OJL 358, December 12, 1987), after institutional review board approval. Myocardial infarction (MI) was produced in male Wistar rats at 2 mo of age, by permanent left anterior descending coronary artery ligation, as described previously (19). After ligation, they were immediately injected into the LV with 10 μl of recombinant AAV vectors, corresponding to 5×10^{10} gc, with 3 separate injections into the viable myocardium bordering the infarct using a tubercoline syringe with a 30-gauge needle. Four groups of animals were studied (n=10/group), receiving AAV2-VEGF-A, AAV2-VEGF-B, AAV2-LacZ, or saline.

To evaluate global and regional LV function, transthoracic echocardiography was performed before thoracotomy, 28 d and 3 mo after MI in sedated rats with a commercially available echocardiography system (MyLab 30; Esaote, Genoa, Italy) equipped with a 12-MHz linear transducer, as described previously (20). Analysis was as recommended by the American Society of Echocardiography (21); all measurements were performed by an experienced cardiologist and an echocardiography expert blinded to treatment groups.

At the end of the echocardiography study, hearts were collected, and the LV, including the interventricular septum, was carefully dissected. After washing in PBS, each specimen was cut into 4 or 5 pieces of equal thickness from base to apex, fixed in 4% paraformaldeyde, and embedded in paraffin for histological analysis. Infarct size was measured on 5-μm-thick sections as the percentage of (endocardial+epicardial circumference of infarct area)/(endocardial+epicardial circumference of LV).

For the detection of apoptosis *in vivo*, infarcted hearts were collected and snap-frozen 3 d after MI. Frozen sections from each sample were fixed in 4% buffered paraformaldehyde (PFA) and then treated as described above for immunostaining and TUNEL.

Isolation and treatment of neonatal rat ventricular cardiomyocytes

Ventricular myocytes from 1- to 2-d-old rats were prepared according to a previously detailed protocol, yielding ≥90% purity (22). Cells were collected and plated at a density of 500 cells/mm^2 into 100-mm dishes (for RNA and protein analysis), or multiwell slides coated with 0.2% gelatin (for immunofluorescence staining). When indicated, cells were treated with rhVEGF-A (100 ng/ml; R&D Systems, Minneapolis, MN, USA), rhVEGF-B (100 ng/ml; R&D Systems), thyroid hormone (100 nM; Sigma, St. Louis, MO, USA) and phenylephrine (20 μM; Sigma). For the detection of VEGF receptors, growth-factor stimulation was performed at 37°C for 7 min in serum-free medium containing 4.5 g/L glucose, 0.1% w/v BSA, 4 μg/ml B12, 10 μg/ml insulin, and 10 μg/ml transferrin.

Apoptosis was induced by culturing serum-starved cells for 48 h at 37°C in a 5% O_2-95% N_2 atmosphere using a hypoxia incubator chamber (Billups-Rothenberg, San Diego, CA, USA) and then switching to 20% O_2 for an additional 24 h. Cells were then fixed in 3% PFA and 2% sucrose in PBS. Apoptotic cells were visualized by the TUNEL (TdT-mediated dUTP nick-end labeling) assay, using the *in situ* cell death detection kit, TMR red (Roche Diagnostics, Mannheim, Germany), according to the manufacturer's instructions. At least 10 high-magnification fields were counted for each experimental condition. Analysis of cardiomyocyte survival was

performed using the Live&Dead assay (Molecular Probes, Eugene, OR, USA) after treatment with 200 nM epirubicin for 90 m in serum free medium.

Quantification of nucleic acids by real-time PCR

Total RNA from isolated cardiomyocytes or dissected LV heart tissue samples was extracted using TRIzol reagent (Invitrogen, Carlsbad, CA, USA) according to the manufacturer's instructions, and reverse-transcribed using hexameric random primers.

Quantification of gene expression was performed by real-time PCR, using predeveloped and custom-designed assays (Applied Biosystems, Foster City, CA, USA) or SYBRGreen (Bio-Rad Laboratories, Hercules, CA, USA). Total RNA from isolated cardiomyocytes or dissected LV heart tissue samples was extracted using TRIzol reagent (Invitrogen) according to manufacturer's instructions and reverse transcribed using hexameric random primers. The cDNA was used as a template for real-time PCR amplification to detect the expression levels of the rat VEGF receptors (*VEGFR-1*, *VEGFR-2*, *NP-1*), as well as of α-*MHC*, β-*MHC*, *sk* α-*actin*, *ANF*, *BNP*, *SERCA2a*, *RYR2*, and *PGC1*α. The housekeeping genes *GAPDH* and *HPRT* were used to normalize the results.

For the detection of vector specific DNA in heart samples, total DNA, purified by Proteinase K/phenol-chloroform extraction method, was subjected to real-time PCR amplification using a TaqMan probe and primers that specifically match sequences in the CMV promoter, common to all AAV vectors used in this study.

Sequences of primers and probes used

Primers

Rat *PGC-1* F 5′-TGCAGCCAAGACTCTGTATGG-3′, R 5′-GGCAAAGAGGCTGGTCCTC-3′; rat *BNP*: F 5′-CAGCTCTCAAAGGACCAAGG-3′, R 5′-GCCCAAAGCAGCTTGAACTA-3′; rat *HPRT*: F 5′-GCCCTTGACTATAATGAGCACTCAG-3′, R 5′-GTAGATTCAACTTGCCGCTGTTT-3′; mouse *iVEGF-B*: F 5′-TTGCACTGCTGCAGCTGGCTC-3′, R 5′-GCTGGGCACTAGTTGTTTGA-3′; CMV promoter: F 5′-TGGGCGGTAGGCGTGTA-3′, R 5′-CGATCTGACGGTTCACTAAACG-3′.

Taqman probes (assay)

Rat β-*MHC*: (FAM)-Rn00568328_m1; rat α-*MHC*: (FAM)-Rn00568304_m1; rat *RYR2*: (FAM)-Rn01470303_m1; rat *SERCA2a*: (FAM)-Rn00568762_m1; rat *ANP*: (FAM)-Rn00561661_n1; rat *sk* α-*actin*: (FAM)-Rn00570060_g1; rat *Flk1*: (FAM)-Rn 00564986_m1; rat *Flt1*: (FAM)-Rn 01409523_g1; rat *NP1*: (FAM)-Rn 00435380_m1; human *VEGF-A*$_{165}$: (FAM)-Hs00173626_m1; rat *GAPDH*: (VIC)-TaqMan Endogenous control (4352338E); CMV: (FAM)-TGGGAGGTCTATATAAGC.

Histology and immunofluorescence

Vasculature staining was performed on paraffin-embedded sections, blocked for 1 h with 2% BSA in PBS; endothelial cells were detected using FITC-conjugated *Lycopersicum esculentum* lectin (Vector Laboratories) and vascular smooth muscle cells (VSMCs) using a Cy3-conjugated anti-α-SMA mouse monoclonal antibody (clone 1A4, Sigma). Pericytes were detected using a rabbit polyclonal anti-NG2 antibody (Chemicon, Temecula, CA, USA) on 4% paraformaldehyde-fixed frozen sections after overnight blocking with 5% horse serum. The detection of VEGF receptors by immunofluorescence was performed on frozen sections (5 μm thick), fixed in IHC Zinc Fixative (Pharmingen, BD Biosciences, San Jose, CA, USA), and blocked for 30 m with 5% goat or 5% horse serum in PBS, depending on the secondary antibody.

The following primary antibodies were used for immunofluorescence studies in cardiomyocytes: goat anti-mouse Flk-1 (AF644; R&D Systems), 1:100; goat polyclonal anti-mouse Flt-1 (AF471; R&D Systems), 1:20; goat polyclonal anti-rat neuropilin-1 (AF566; R&D Systems), 1:50; and mouse anti-α-sarcomeric actinin monoclonal antibody (EA-53; Abcam, Cambridge MA, USA), 1:100. Alexa Fluor 594 donkey anti-goat, Alexa Fluor 594 donkey anti-rabbit, and Alexa Fluor 488 donkey anti-mouse were used as secondary antibodies (Molecular Probes). Nuclei were counterstained with DAPI.

Images were acquired at room temperature with a DMLB upright fluorescence microscope (Leica Microsystems, Wetzlar, Germany) equipped with a charge-coupled device camera (CoolSNAP CF; Roper Scientific, Trenton, NJ, USA) using MetaView 4.6 quantitative analysis software (MDS Analytical Technologies, Toronto, ON, Canada).

Immunoprecipitation and Western blot analysis

For the detection of VEGF receptors, freshly isolated cardiomyocytes were allowed to attach in 100-mm dishes and then left overnight in serum-free medium. Stimulation was performed by incubating the cell cultures at 37°C for 7 min in 2 ml of serum or 2 ml of serum-free medium containing 50 ng/ml recombinant huVEGF-A$_{165}$ and 100 ng/ml huVEGF-B. After washing with PBS on ice, samples were lysed in RIPA buffer (20 mM Tris-HCl, pH 7.4; 150 mM NaCl; 5 mM EDTA; 1% NaDoc; 1% Triton X-100; and 0.1% SDS) containing 90 μg/ml PMSF, 100 μM $NaVO_4$, 50 mM NaF, 20 μg/ml aprotinin, and 20 μg/ml leupeptin (Sigma-Aldrich). Protein concentration was determined by the Bradford method (Bio-Rad Laboratories); 200 μg of proteins was resolved on 6% SDS-PAGE and transferred to nitrocellulose membranes (GE Healthcare, New York, NY, USA). Immunoblots were blocked in 5% bovine serum albumin in TBS-Tween (50 mM Tris-HCl, pH 7.4; 200 mM NaCl; and 0.1% Tween 20). Membranes were incubated with the following primary antibodies (dilution 1:1000) overnight at 4°C: rabbit polyclonal anti-Flk-1 (C-1158; Santa Cruz Biotechnology, Santa Cruz, CA, USA), rabbit polyclonal anti-Flt-1 (C-17; Santa Cruz Biotechnology), mouse monoclonal anti-phospho-Tyrosine (PY20; Biolegend, San Diego, CA, USA), goat polyclonal anti-rat neuropilin-1 (AF566; R&D Systems), and mouse monoclonal tubulin (B-5–1-2; Sigma). Membranes were then washed in Tris-buffered saline and 0.1% Tween 20 in blocking buffer and incubated with the appropriate HPR-conjugated secondary antibodies for 45 m at room temperature. Proteins were detected by enhanced chemiluminescence (GE Healthcare).

In vivo VEGF receptor tyrosine phosphorylation was evaluated by Western blot analysis with anti-phosphotyrosine antibodies on immunoprecipitates. Two milligrams of cell lysates was incubated with either rabbit polyclonal anti-Flk-1 (C-1158; Santa Cruz Biotechnology) or rabbit polyclonal anti-Flt-1 (C-17; Santa Cruz Biotechnology) antisera coupled to Sepharose-Protein A (20 ml packed beads/ml lysate) overnight at 4°C with agitation. Sepharose-protein A-bound proteins were washed 4 times with RIPA buffer and separated on 6% SDS–polyacrylamide gels, followed by immunoblotting with either mouse monoclonal anti-phosphotyrosine antibodies (PY20; Biolegend) or with anti-Flk-1 specific phosphotyrosine antibodies (VEGF-Receptor2-Y1175; Cell Signaling, Beverly, MA, USA).

Statistical analysis

One-way ANOVA and Bonferroni/Dunn's *post hoc* test were used to compare multiple groups. Pairwise comparison between groups was performed using the Student's *t* test. Dose-response effect was assessed by regression analysis. $P < 0.05$ was set as a threshold for statistical significance.

RESULTS

Long-term effects of AAV-mediated VEGF-B and VEGF-A expression in normal rat myocardium

To comparatively assess the effects of VEGF-A and VEGF-B, we generated two AAV vectors, based on AAV serotype 2 (AAV2), expressing the respective cDNAs in a constitutive manner from the CMV IE gene promoter. The efficiency of transduction and expression of these vectors were first assessed by injecting 5×10^{10} AAV particles into the LV free wall of normal rats; control animals were injected with either saline or AAV2-LacZ (n=6/group). As detected by real-time PCR quantification, the levels of expression of the two transgenes was persistent at both 30 d (not shown) and 90 d postinjection (**Fig. 1*A, B***). Consistent with our previous observations (14, 17, 23), no inflammatory response was detected in the animals injected with either saline or AAV2-LacZ at either time point (data not shown). No differences were detected between AAV2-LacZ- or saline-injected animals in none of the parameters considered throughout this work, neither in normal nor in infarcted animals. The results obtained in the two groups were therefore pooled and collectively labeled as control in all figures.

Representative images of the vasculature in the AAV-injected and control hearts at 30 d after injection are shown in Fig. 1*C* after staining with anti-CD31 and anti-αSMA antibodies to detect endothelial and smooth muscle cells (SMCs), respectively. Consistent with our previous findings in the normoperfused skeletal muscle (17, 18), we observed that the prolonged expression of VEGF-A in the heart determined a marked angiogenic response, characterized by a significant increase in the number of capillaries (Fig. 1D) and, most notably, of small arteries in the 20- to 250-μm-diameter range (Fig. 1*E*), with a consequent increase in the arteriole/capillary ratio (Fig. 1*F*). In contrast, AAV2-VEGF-B had a very modest angiogenic effect, with the exception of the sporadic formation of enlarged vascular structures, connected to the circulation, apparently devoid of αSMA- and NG2-positive mural cells (arrows in Fig. 1*C* and Supplemental Fig. 1).

VEGF-B, a specific VEGFR-1 ligand, preserves myocardial function after infarction

Next, we assessed the effects of the two vectors on cardiac function after myocardial infarction. Rats (n=10/group) underwent permanent left descendent coronary artery ligation and immediate injection into the LV peri-infarcted area of 5×10^{10} viral particles of AAV2-VEGFA, AAV2-VEGFB, AAV2-LacZ, or saline (pooled control group). Global and regional LV function was analyzed by echocardiography at 1 and 3 mo after infarction; representative M-mode echocardiograms at the latter time point are shown in **Fig. 2*A***. The LV ejection fraction (LVEF) and LV fractional shortening (LVFS) were significantly preserved in infarcted rats injected with both AAV2-VEGF-B and AAV-VEGF-A, compared to untreated animals, in the absence of significant changes in heart rate (P<0.05 for both treatments at either time point; Fig. 2*B*, *C*, respectively). Preservation of LV performance was significantly more pronounced in the infarcted hearts treated with

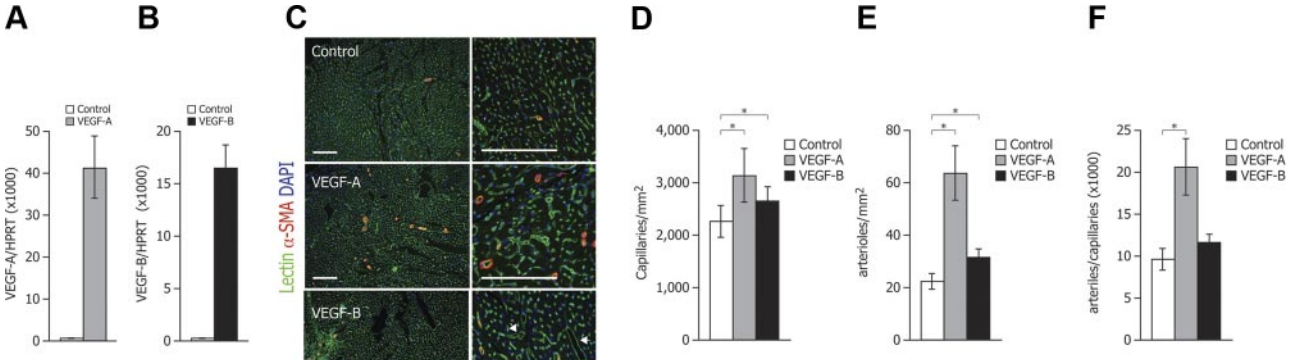

Figure 1. Effects of AAV-mediated VEGF-B and VEGF-A expression in normal rat myocardium. *A*, *B*) Levels of VEGF-A (*A*) and VEGF-B (*B*) transgene transcripts evaluated by real-time PCR analysis on total ventricular RNA extracted 90 d after vector injection. Transgene expression levels (n=8) are normalized for those of the endogenous HPRT gene. *C*) Left panels: representative immunostainings of the vasculature in rat myocardium injected with AAV-LacZ (control), AAV-VEGF-A, and AAV-VEGF-B, as indicated. Right panels: enlarged views. Capillaries were detected using FITC-conjugated *L. esculentum* lectin (Vector Laboratories), staining endothelial cells, and VSMCs using a Cy3-conjugated anti-αSMA mouse monoclonal antibody; nuclei were stained in blue with DAPI. Scale bars = 500 μm. *D*, *E*) Quantification of capillary and arteriole density. *F*) Ratio between number of arteries and capillaries. Values are expressed as means ± SE. *$P < 0.05$.

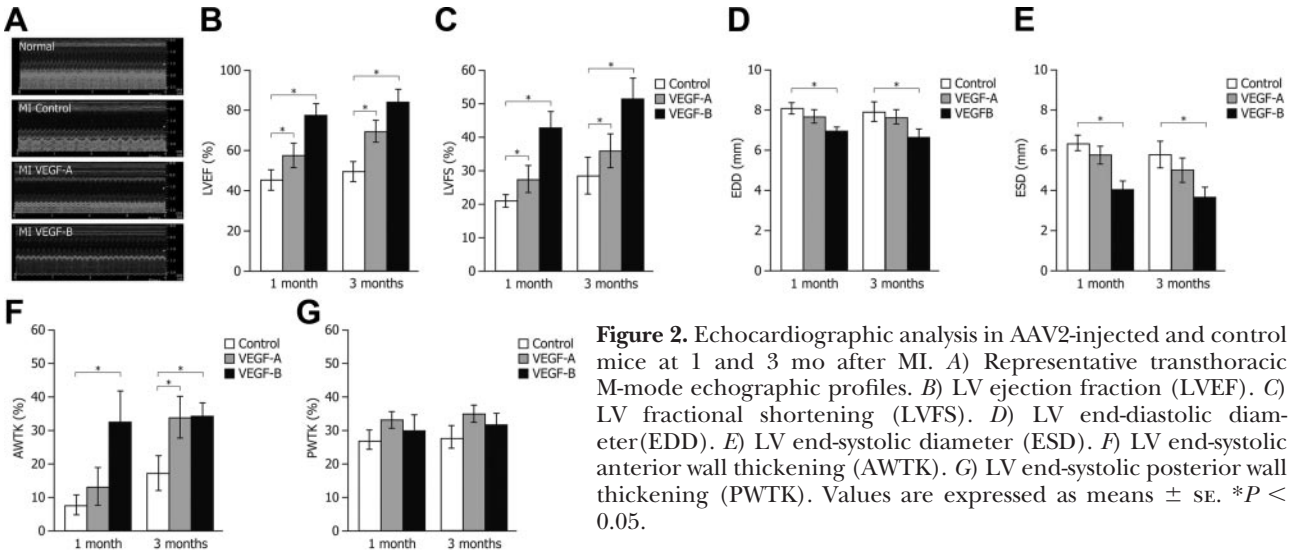

Figure 2. Echocardiographic analysis in AAV2-injected and control mice at 1 and 3 mo after MI. *A*) Representative transthoracic M-mode echographic profiles. *B*) LV ejection fraction (LVEF). *C*) LV fractional shortening (LVFS). *D*) LV end-diastolic diameter(EDD). *E*) LV end-systolic diameter (ESD). *F*) LV end-systolic anterior wall thickening (AWTK). *G*) LV end-systolic posterior wall thickening (PWTK). Values are expressed as means ± SE. $*P <$ 0.05.

VEGF-B at 1 mo and, in particular, at 3 mo of treatment (LVEF: 48±8 *vs.* 85±9%; LVFS: 29±8 *vs.* 52±7% in control and VEGF-B animals, respectively; $P<0.05$ in all cases). At both time points, the LV end-diastolic diameter (EDD) and LV end-systolic diameter (ESD) were also significantly reduced in rats that had received AAV2-VEGF-B (EDD: 7.9±1.2 and 6.8±0.8 mm; ESD: 5.9±0.7 and 3.8±0.9 mm in control and VEGF-B animals at 3 mo of treatment; $P<0.05$ in all cases; Figs. 2*D, E,* respectively).

The changes of regional cardiac contractility are shown in Fig. 2*F, G*. At both 1 and 3 mo after cardiac gene transfer, the LV end-systolic wall thickening (AWTK) in the border zone of the infarcted hearts injected with AAV2-VEGF-B was markedly improved compared to control rats (18.5±3.0 *vs.* 32.2±2.9% for control and VEGF-B at 3 mo; $P<0.05$). Similarly, the LV anterior wall end-diastolic and end-systolic thickness (AWTd and AWTs, respectively) of the border zone, two indexes of regional mass, were selectively preserved in the infarcted hearts expressing VEGF-B ($P<0.05$ in both cases; Supplemental Fig. 2*A, C*). No changes in the function and structure of the LV remote regions of the infarcted hearts were observed in any experimental group.

With the caveat that echocardiography in small animals might not provide sufficient sensitivity to detect differences in thickening of the border zone of a small MI, these data unanimously indicated that the prolonged expression of both VEGF-A and VEGF-B markedly improved recovery of LV performance after infarction.

Animals were sacrificed at 3 mo by induction of ischemia, and the hearts were examined for postinfarction fibrosis and chamber remodeling. Morphometric analysis of trichromic-stained LV sections showed that the anterior wall of infarcted control animals underwent considerable thinning, consistent with the echocardiographic results. In contrast, the AAV2-VEGFA- and, more remarkably, the AAV2-VEGFB-treated hearts showed significant preservation of contractile tissue and reduction of the fibrotic area (see **Fig. 3*A*** for representative cross-sections and Fig. 3*C* for high-magnification view of the extent of fibrotic substitution); the infarct size was determined as 36.2 ± 6.0% of the LV in control animals *vs.* 21.5 ± 2.5 and 17.2 ± 3.5% in the VEGF-A- and VEGF-B-expressing animals, respectively ($P<0.05$ in both cases; Fig. 3*B*).

Molecular characterization of heart samples on animal sacrifice confirmed the persistence of the vector genomes in the injected myocardium (Supplemental Fig. 3*A*). Consistently, AAV-mediated expression of both VEGF-A and VEGF-B was detected by real-time PCR using transgene specific primers (Supplemental Fig. 3*B*). The local expression of the transgenes did not induce significant variation of the levels of VEGF receptors mRNA (Supplemental Fig. 3*C*).

Similar to noninfarcted hearts (Fig. 1), the animals treated with VEGF-A showed a significant increment in the number of capillaries and arterioles, which was not evident in those injected with AAV2-VEGF-B (see Fig. 3*D* for representative images and Fig. 3*E, F* for quantification of the number of capillaries and arterioles, respectively).

Thus, the marked recovery of LV ventricular performance after myocardial infarction, in particular, observed on VEGF-B gene delivery occurred in the absence of significant induction of angiogenesis.

Cardiomyocytes express functional VEGF receptors *in vitro* and *in vivo*

To explore whether VEGF exerted a direct effect on cardiomyocytes, we first assessed the levels of expression of the VEGF receptors in these cells. A first set of experiments was performed using total RNA extracted from primary cultures highly enriched in α-actinin-positive cardiomyocytes by three subsequent subplating steps (>90% purity; see Materials and Methods and ref. 22); these cultures were established along complementary cultures of α-actinin-negative stromal cells (<1% α-actinin positivity). Both cultures were maintained for

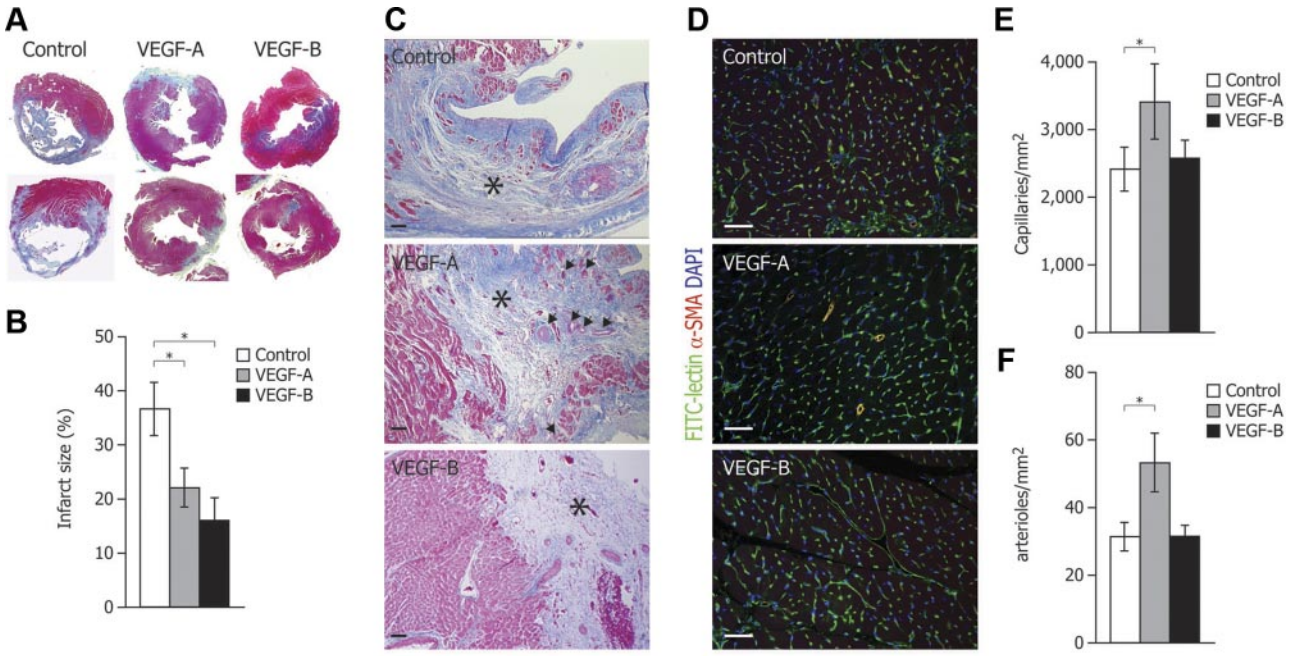

Figure 3. Morphometric and histological analysis of infarcted hearts 3 mo after gene transfer. *A*) Representative Azan trichrome stainings of LV transverse sections of control and AAV2-VEGF-A- and AAV2-VEGF-B-injected hearts. *B*) Quantification of infarct size (% of LV). *C*) High-magnification (×200) microphotographs of trichrome-stained sections showing the extent of fibrotic substitution of the infarcted scars (asterisks); arrows indicate new vessels in the VEGF-A expressing hearts. *D*) Visualization of vessels by immunofluorescence in the peri-infarcted area (green, endothelial cells; red, α-SMA$^+$ cells; blue, cell nuclei). *E*) Quantification of capillary density (FITC-lectin$^+$ vessels). *F*) Quantification of α-SMA$^+$ arterioles. Values are expressed as means ± SE. *$P < 0.05$. Scale bars = 200 μm.

7–14 d. We found that *VEGFR-1*, *VEGFR-2*, and *Np1* were all expressed in neonatal rat cardiomyocytes, albeit at levels that were 3 orders of magnitude lower than those of human umbilical vein endothelial cells (HUVECs); stromal cells only expressed *VEGFR-1* and *Np1*, not *VEGFR-2* (**Fig. 4*A***). Of potential interest, expression of *VEGFR-1* selectively increased when cardiomyocytes were placed in a hypoxic environment (2% O_2) or exposed to oxidative stress (H_2O_2 100 μM); >5 fold and ~3-fold induction, respectively; Fig. 4*B*).

Expression of VEGFR-1, VEGFR-2, and Np1 was also detected by Western blot analysis in neonatal cardiomyocyte cell lysates (Fig. 4*C*, top panel). Most notably, these receptors appeared to be functional, since immmunoprecipitation using specific anti-VEGFR-1 and anti-VEGFR-2 antibodies followed by Western blot analysis with anti-phosphotyrosine antibodies revealed specific phosphorylation of both VEGFR-1 and VEGFR-2 in response to recombinant VEGF-A and of VEGFR-1 in response to recombinant VEGF-B (Fig. 4*C*, bottom panel).

Finally, expression of VEGF receptors was also detected by immunofluorescence on histological sections of frozen adult rat heart tissue (Fig. 4*D*). Of interest, while the localization of VEGFR-2 and Np1 fluorescence was consistent with the prominent expression of these receptors on vascular endothelial cells, VEGFR-1 appeared to cluster at the intercalated disks between cardiomyocytes.

VEGF-A and VEGF-B inhibit cardiomyocyte apoptosis

The reduction in infarct size and preservation of muscle mass in animals treated with VEGF-A and VEGF-B suggested that these factors either stimulated the limited cardiomyocyte proliferation that is normally observed in the infarct border zone (24) or prevented delayed cardiomyocyte loss after infarction. The former possibility was tested by evaluating the effects of the two factors on cardiomyocyte proliferation. Under standard culture conditions (22), ~0.2% of neonatal cardiomyocytes incorporate BrdU at d 1 after isolation; this percentage was unchanged on addition of either recombinant VEGF-A or VEGF-B (**Fig. 5*A***). We also explored the possibility that the expression of the two factors after AAV-mediated gene delivery in the infarcted hearts *in vivo* might promote regeneration of the damaged cardiac tissue through stimulation of cardiomyocyte replication or cardiac stem cell recruitment. However, we failed to detect any increase in the number of BrdU-positive, proliferating cells in infarct border zone in any of the treated animals compared to controls (data not shown).

An alternative possibility is that the VEGFs might induce protection of cardiomyocytes against ischemic death. To test this hypothesis, we exposed cardiomyocytes to hypoxia for 48 h followed by 24 h reoxygenation either in the absence, or presence, of recombinant VEGF-B or VEGF-A. As revealed by a TUNEL assay, the percentage of apoptotic cells dropped from

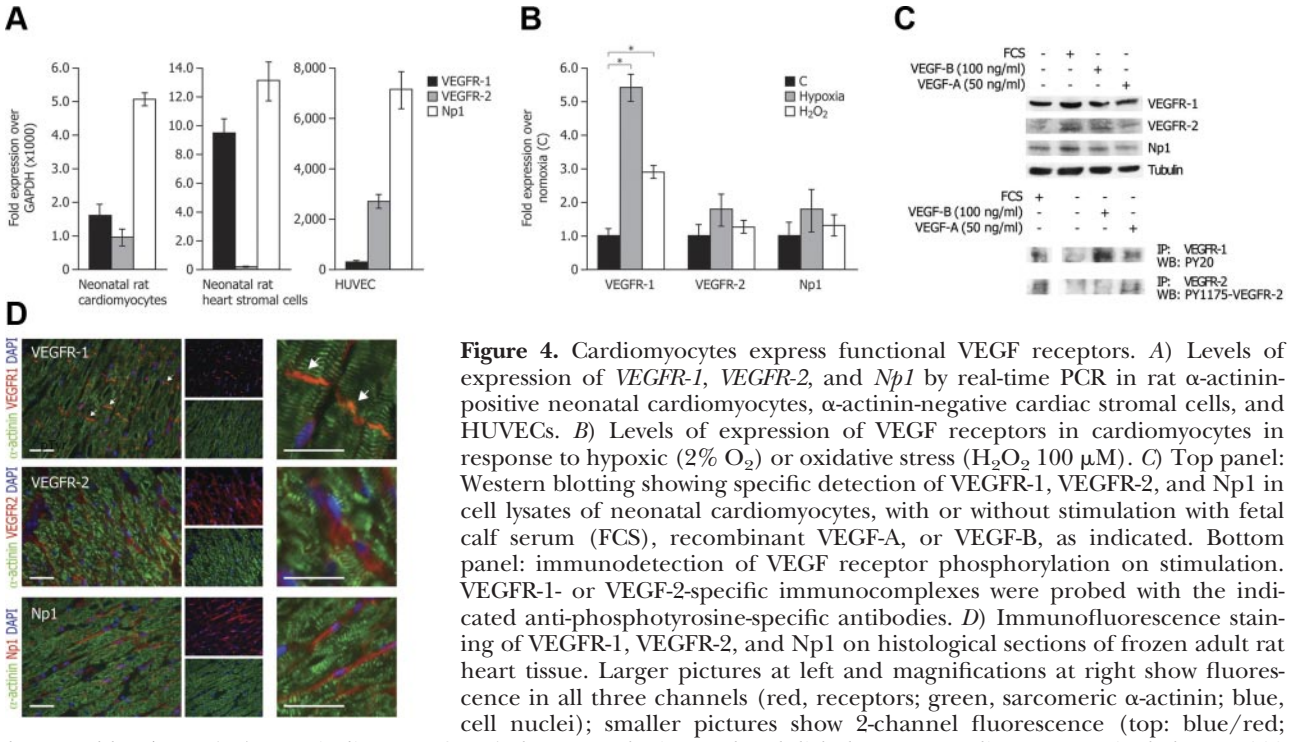

Figure 4. Cardiomyocytes express functional VEGF receptors. *A*) Levels of expression of *VEGFR-1*, *VEGFR-2*, and *Np1* by real-time PCR in rat α-actinin-positive neonatal cardiomyocytes, α-actinin-negative cardiac stromal cells, and HUVECs. *B*) Levels of expression of VEGF receptors in cardiomyocytes in response to hypoxic (2% O_2) or oxidative stress (H_2O_2 100 μM). *C*) Top panel: Western blotting showing specific detection of VEGFR-1, VEGFR-2, and Np1 in cell lysates of neonatal cardiomyocytes, with or without stimulation with fetal calf serum (FCS), recombinant VEGF-A, or VEGF-B, as indicated. Bottom panel: immunodetection of VEGF receptor phosphorylation on stimulation. VEGFR-1- or VEGF-2-specific immunocomplexes were probed with the indicated anti-phosphotyrosine-specific antibodies. *D*) Immunofluorescence staining of VEGFR-1, VEGFR-2, and Np1 on histological sections of frozen adult rat heart tissue. Larger pictures at left and magnifications at right show fluorescence in all three channels (red, receptors; green, sarcomeric α-actinin; blue, cell nuclei); smaller pictures show 2-channel fluorescence (top: blue/red; bottom: blue/green). Arrows indicate VEGFR-1 clusters at the intercalated disks between cardiomyocytes. Scale bars = 200 μm. Values are expressed as means ± SE. *$P < 0.05$.

~17.2 ± 3.3% of controls to 7.6 ± 1.2 and 8.0 ± 1.0% in the VEGF-A and VEGF-B-treated cultures, respectively ($P<0.05$ in both cases; Fig. 5*B*). The protection from death was also evident when cardiomyocytes were exposed for 90 min to the cardiotoxic drug epirubicin. Under these conditions, the number of dead cells in the cultures added with either recombinant VEGF decreased from 61.8 ± 8.5% in controls to 13.8 ± 6.0 and 11.2 ± 4.2% in the VEGF-A and VEGF-B-treated cultures, respectively ($P<0.05$ in both cases; Fig. 5*C*).

Consistent with the conclusion that VEGF exerts an antiapoptotic effect, we also observed that the number of TUNEL-positive cells in the infarct border zone at 48 h after infarction was significantly lower in the animals injected with either AAV2-VEGF-A or AAV2-VEGF-B compared to controls (from 17.2±8.0 to 4.5±1.4 and 5.5±1.5%, respectively; $n=4$/group; $P < 0.05$ *vs.* control in both cases; Fig. 5*D*).

VEGF-A and VEGF-B activate expression of genes involved in the regulation of myocardial contractility and metabolism

Besides protection from apoptosis, the changes in regional contractility observed in the infarcted animals treated with VEGF-A and VEGF-B also suggested that these factors might directly affect cardiomyocyte activity. To further explore this issue, we analyzed the levels of expression of a series of genes involved in cardiomyocyte function in cells treated for 24 h with recombinant VEGF-A or VEGF-B. In particular, we evaluated the expression profile of genes specifically involved in cardiac contractility (α*MHC*, β*MHC*), intracellular calcium handling (*SERCA2a*, *RYR2*), mitochondrial energetics (*PGC1*α), and of some typical genetic markers of hypertrophy, such as skeletal α-actin (sk α-act) and cardiac natriuretic peptides (*ANF* and *BNP*). The modifications in the levels of expression of these genes were compared to those found in response to the α-adrenergic agonist phenylephrine (PE) or to the thyroid hormone triiodo-L-thyronine (T3). These compounds are known to induce characteristic myocyte hypertrophy responses, consisting in the up-regulation of fetal genes of pathological hypertrophy (including β*MHC*, *sk* α*-act*, *ANF*, and *BNP*) in the case of PE (25, 26), while reproducing physiological hypertrophy (increase of α*MHC* and *SERCA2a*, and repression of β*MHC* transcripts) in the case of T3 (27, 28).

Both VEGFs were found to increase expression of α*MHC* (which is the predominant contractile protein in adult rodents; ref. 29) and repress that of β*MHC*, similar to T3, and different from PE ($P<0.05$ between VEGF-treated and control cardiomyocytes). VEGF-B also inhibited expression of *sk* α*-act*. Both factors promoted elevation of the *ANF* and *BNP* transcripts and, most notably, they also determined elevation of the *SERCA2a*, *RYR*, and *PGC1*α mRNAs, similar to T3 ($P<0.05$) (**Fig. 6**).

Taken together, these data indicate that both VEGF-A and VEGF-B evoke, in isolated cardiomyocytes, a gene expression program proper of compensatory hypertrophy similar to that induced by the thyroid hormone. Of note, this response can be initiated by the sole treatment with VEGF-B, a selective VEGFR-1 ligand.

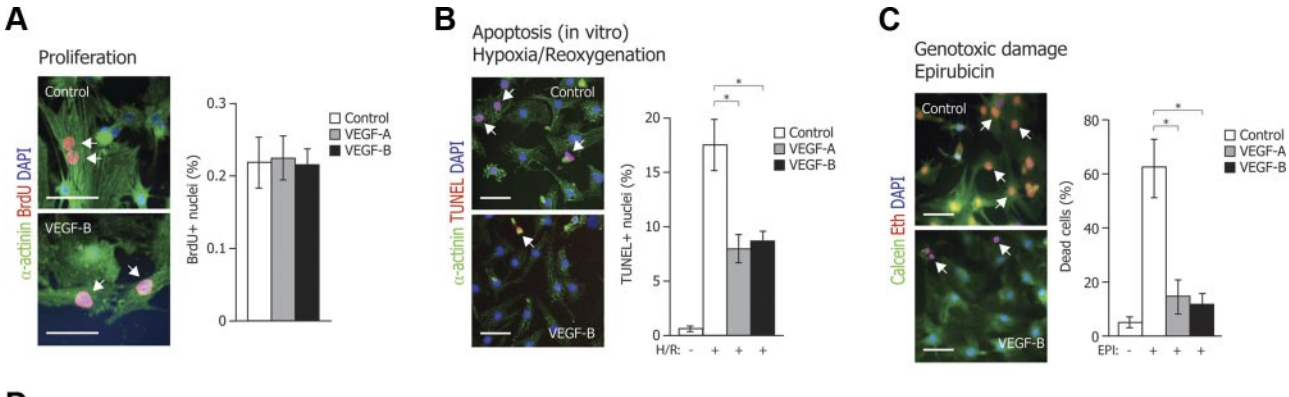

Figure 5. VEGFs protect cardiomyocytes from apoptosis *in vitro* and *in vivo*. *A*) Recombinant VEGFs do not induce neonatal rat cardiomyocyte proliferation. Left panels: representative images of α-actinin-positive cardiac myocytes showing positivity to BrdU immunostaining (red; arrows) with or without exposure to recombinant VEGF-B. Right panel: quantification of BrdU-positive nuclei. *B*) VEGFs protect cardiomyocytes from apoptosis *in vitro*. Left panels: representative images of TUNEL$^+$ cardiomyocytes (arrows) exposed to hypoxia for 48 h followed by 24 h with or without VEGF-B. Right panel: quantification of TUNEL$^+$ nuclei. *C*) Left panels: representative images of a cell viability assay based on the simultaneous determination of live (green, calcein) and dead (red, ethidium homodimer-1, Eth; arrow) cardiomyocytes after *in vitro* exposure to epirubicin in the presence or absence VEGF-B. Right panel: quantification of dead cells. *D*) Detection of apoptotic nuclei *in vivo* at d 3 after MI. Right panels: representative images of TUNEL$^+$ nuclei (arrows) in infarcted hearts from a control and a VEGF-B-injected mouse; cardiomyocytes are stained by positivity to α-actinin (green). Right: quantification of TUNEL$^+$ nuclei. Values are expressed as means ± SE. *$P < 0.05$. Scale bars = 20 μm (*A*, *D*); 50 μm (*B*, *C*).

VEGF-B overexpression counteracts the induction of genes involved in pathological LV remodeling after myocardial infarction

To further explore the effects of VEGF receptor stimulation *in vivo*, we also analyzed the expression profile of LV tissue from a subset of AAV-transduced, infarcted animals (n=6/group) by real-time PCR. Consistent with the echocardiography results, control animals at 3 mo after infarction showed the characteristic pattern of gene expression commonly associated with pathological LV remodeling, involving significant (P<0.05) overexpression of βMHC and sk α-act contractile proteins, an increase in the cardiac natriuretic peptides, and a decrease in the levels of *SERCA2a*, *RYR*, and *PGC1*α mRNAs as compared to normal rats (**Fig. 7**). Remarkably, these modifications were all significantly counteracted by both VEGF-A and, most notably, VEGF-B overexpression. In the VEGF-A and VEGF-B-treated hearts, the levels of β*MHC*, *ANF*, *BNP*, *SERCA2a*, and *RYR* were unchanged compared to normal animals; those of α*MHC* and *PGC1*α were even significantly

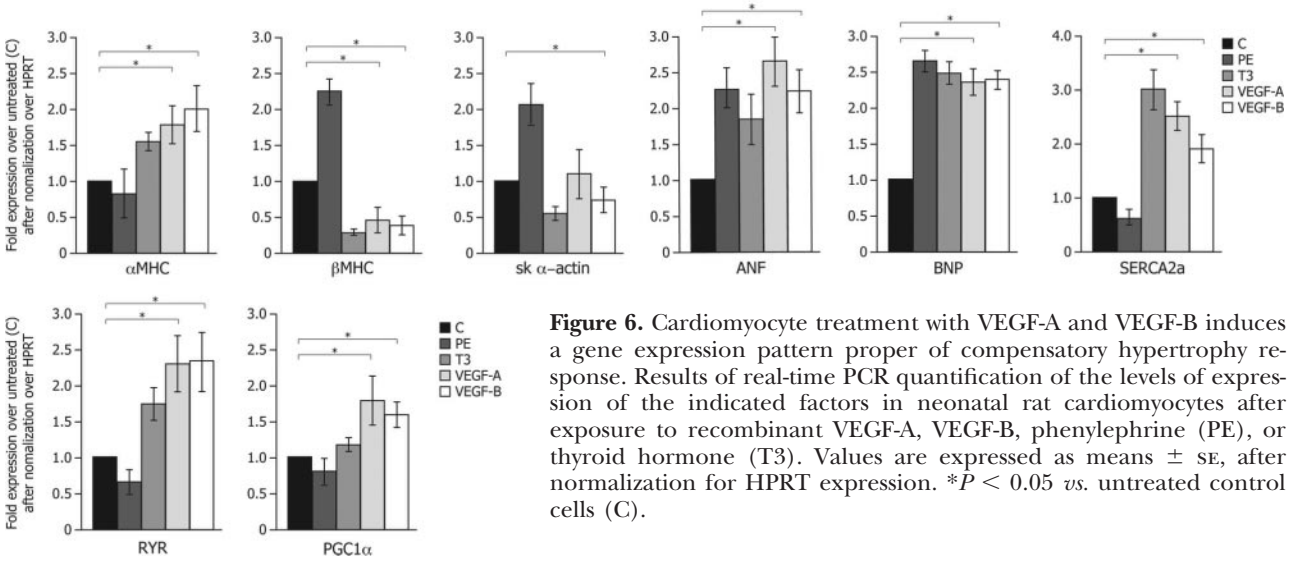

Figure 6. Cardiomyocyte treatment with VEGF-A and VEGF-B induces a gene expression pattern proper of compensatory hypertrophy response. Results of real-time PCR quantification of the levels of expression of the indicated factors in neonatal rat cardiomyocytes after exposure to recombinant VEGF-A, VEGF-B, phenylephrine (PE), or thyroid hormone (T3). Values are expressed as means ± SE, after normalization for HPRT expression. *$P < 0.05$ *vs.* untreated control cells (C).

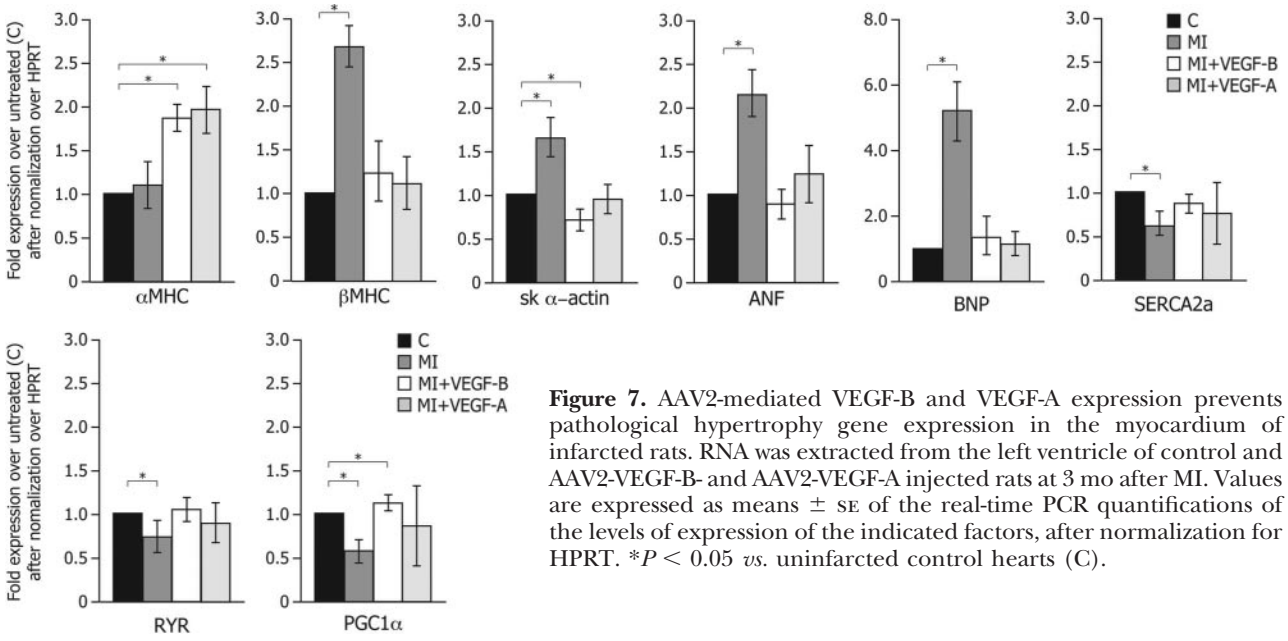

Figure 7. AAV2-mediated VEGF-B and VEGF-A expression prevents pathological hypertrophy gene expression in the myocardium of infarcted rats. RNA was extracted from the left ventricle of control and AAV2-VEGF-B- and AAV2-VEGF-A injected rats at 3 mo after MI. Values are expressed as means ± SE of the real-time PCR quantifications of the levels of expression of the indicated factors, after normalization for HPRT. $*P < 0.05$ *vs.* uninfarcted control hearts (C).

increased, and that of sk α-act was decreased ($P<0.05$ in all cases).

Collectively, these observations further support the conclusion that VEGFR-1 stimulation by specific ligands exerts a beneficial effect on the myocardial tissue.

DISCUSSION

A relevant conclusion of this study is that the continuous expression of VEGF after myocardial infarction exerts prolonged beneficial effects in terms of increase in contractility, prevention of pathological LV remodeling, and preservation of viable cardiac tissue. All our findings are consistent with the notion that VEGF exerts these effects through the activation of VEGFR-1 expressed in cardiomyocytes: *1*) isolated rat cardiomyocytes express VEGFR-1; *2*) VEGFR tyrosine kinases becomes activated on binding to the recombinant VEGFR-1 ligands PlGF and VEGF-B; *3*) the levels of expression VEGFR-1 are selectively up-regulated in hypoxia and on oxidative stress; and *4*) most notably, cardiomyocyte treatment with VEGF-B activates a peculiar gene expression program, reminiscent of that observed during compensatory hypertrophy. In this context, the localization of VEGFR-1 in the intercalated disks between cardiomyocytes appears intriguing, since these structures also act as mechanical stress sensors during muscle contraction, besides supporting synchronized cardiomyocyte contraction (30). Further studies are clearly required to understand the functional significance of VEGFR-1 localization at these structures. In this respect, it might be worth noting that, both in zebrafish and in cultured rat cardiomyocytes, VEGF-A has been reported to exert a positive inotropic effect by increasing calcium transients through its interaction with VEGFR-1 and downstream PLCγ-1 activation (31).

The observation that VEGFs exert a direct activity on cardiomyocytes is indeed not surprising. A large body of evidence now indicates that expression of the VEGF receptors is not restricted to endothelial cells and that their ligands exert a variety of fundamental functions in other cell types. These nonangiogenic functions of VEGFs include, among others, the potential to prevent neuronal cell death from ischemia and promote neurogenesis (32, 33), the capacity to stimulate hepatocyte regeneration after liver damage (34), and the ability to promote osteoblast migration and differentiation (35, 36). In the skeletal muscle, we showed that VEGF-A exerts a powerful regenerative effect after ischemic and nonischemic muscle damage by promoting satellite cell differentiation (23, 37). Finally, several groups have described an effect of VEGF-A on various cells of hematopoietic origin, showing that this factor is able to mediate monocyte chemotaxis (38), hematopoietic stem cell survival (39), mobilization of endothelial progenitor cells (40), and the selective recruitment of a population of bone marrow-derived, $CD11b^+$ mononuclear cells, which are essential for vessel maturation at the sites of adult neoangiogenesis (18).

The different VEGF receptors appear variably involved in mediating these nonangiogenic functions of their ligands. For example, skeletal muscle regeneration appears to selectively require VEGFR-2, since PlGF is ineffective at stimulating this process compared to VEGF-A (23); in contrast, the effects on monocytes require VEGFR-1 (38), those on hematopoietic progenitors are mediated by both VEGFR-1 and VEGFR-2 (39–41), and those determining the recruitment of bone marrow-derived $CD11b^+$ cells require the presence of Np1 (18).

The prolonged expression of VEGF-B in the heart elicits only a modest angiogenic response compared to VEGF-A, essentially consisting in the generation of enlarged vessels devoid of α-SMA-positive cells. A lack

of angiogenesis and presence of abnormally enlarged capillaries was also recently reported in a VEGF-B-transgenic mouse (11). An apparent controversy exists concerning the possible angiogenic role of VEGF-B exogenously delivered *in vivo*, ranging from promotion of unrestricted angiogenesis (42), ability to potentiate, rather than induce, angiogenesis when transgenically expressed in endothelial cells (43), induction of selective revascularization of the ischemic myocardium but not of other organs (12), or no angiogenic effect at all in several tissues after adenoviral gene delivery (44, 45). Recent work has also indicated that the delivery VEGF-B to the infarcted myocardium in rabbits and pigs using an adenoviral vector promoted angiogenesis and arteriogenesis by acting on endothelial cells (13). All these apparent discrepancies might be attributable to differences in genetic background, phenotyping methodology, use of different VEGF-B isoforms, or, most important, use of different strategies for VEGF-B overproduction (recombinant proteins, naked plasmid DNA, or adenoviral vectors). In this respect, AAV vectors currently represent the only available system to deliver genes to the adult myocardium and allow their prolonged expression over time. Other vector systems, such as the first generation adenoviruses used in other studies, are fraught with the induction of a potent inflammatory and immune reaction (46), which, besides blurring the biological response, restricts observation to a few days after vector inoculation.

Besides the possible direct modulation of cardiac contractility, the main consequences of VEGF expression are, on one hand, the protection of cardiomyocytes from apoptosis while, on the other hand, the induction of a gene expression program of compensatory hypertrophy. Cardiomyocytes thus join the list of the numerous cell types in which different VEGF family members exert a powerful antiapoptotic effect, including endothelial cells (5), neurons (47), embryonic stem cells, (48) and skeletal muscle cells (23, 49). Protection from apoptosis was clearly evident when VEGF-B was administered, in both cultured cardiomyocytes and after myocardial infarction *in vivo*, again suggesting that a relevant receptor mediating the antiapoptotic effect was VEGFR-1. The recent observations that VEGF-B rescues retinal and motor neurons from apoptosis (50, 51) and inhibits the expression of a number of proapoptotic genes in noncardiomyocyte cells (50) is fully consistent with this conclusion.

In addition to protection from apoptosis, VEGF-B transduction in the heart elicited a peculiar gene expression profile, consisting of the activation of αMHC and the repression of βMHC and skeletal α-actin, and the increase in SERCA2a, RYR, and PGC1α gene expression, together with the increase in the levels of the cardiac natriuretic peptide mRNAs. This pattern of gene expression resembles that induced by the thyroid hormone T3, which is usually considered a marker of benign, compensatory hypertropic response to cardiac stimulation (52, 53). These findings appear to be in full agreement with the recent observation that a transgenic mouse overexpressing VEGF-B showed clear signs of cardiac hypertrophy, but without compromising cardiac function (11); with the report that VEGF-B-knockout mice have smaller hearts (10); and with the observation that the injection of the VEGF-B protein after infarction leads to myocardial hypertrophy (54). Our results extend these findings further, and show that these effects of VEGF-B are exerted through direct activity on cardiomyocytes. Of note, in our experiments, VEGF-A and VEGF-B equally protected cardiomyocytes from apoptosis and induced a beneficial gene expression profile; however, VEGF-B scored superior to VEGF-A in preserving LV function after myocardial infarction. This observation might either indicate that the two factors activate VEGFR-1 differently, for example, exploiting different coreceptors, or that the prolonged activation of VEGFR-2 by VEGF-A might be somehow detrimental for the infarcted myocardium, for example, by inducing a leaky vasculature. Further experiments will obviously be required to distinguish between these possibilities.

In conclusion, the finding that VEGF-B exerts a marked beneficial effect on the infarcted myocardium by preventing loss of cardiac mass and promoting cardiac contractility has obvious therapeutic implications, in terms of both direct utilization of VEGF-B (or PlGF) for therapeutic purposes and the identification of alternative, synthetic activators of VEGFR-1. FJ

The authors are grateful to Marina Dapas and Michela Zotti for superb technical support in AAV production, to Mauro Sturnega for help in animal experimentation, and to Suzanne Kerbavcic for editorial assistance. This work was supported by a grant from the Fondazione CR Trieste, Trieste, Italy; by grants from the Regione Friuli Venezia Giulia, Italy; and by a grant from the World Anti-Doping Agency (WADA), Montreal, Canada. F.A.R. is an Established Investigator of the American Heart Association.

REFERENCES

1. Ferrara, N., Gerber, H. P., and LeCouter, J. (2003) The biology of VEGF and its receptors. *Nat. Med.* **9,** 669–676
2. Carmeliet, P. (2005) Angiogenesis in life, disease and medicine. *Nature* **438,** 932–936
3. Adams, R. H., and Alitalo, K. (2007) Molecular regulation of angiogenesis and lymphangiogenesis. *Nat. Rev. Mol. Cell. Biol.* **8,** 464–478
4. Olsson, A. K., Dimberg, A., Kreuger, J., and Claesson-Welsh, L. (2006) VEGF receptor signalling - in control of vascular function. *Nat. Rev. Mol. Cell. Biol.* **7,** 359–371
5. Neufeld, G., Cohen, T., Gengrinovitch, S., and Poltorak, Z. (1999) Vascular endothelial growth factor (VEGF) and its receptors. *FASEB J.* **13,** 9–22
6. Sawano, A., Iwai, S., Sakurai, Y., Ito, M., Shitara, K., Nakahata, T., and Shibuya, M. (2001) Flt-1, vascular endothelial growth factor receptor 1, is a novel cell surface marker for the lineage of monocyte-macrophages in humans. *Blood* **97,** 785–791
7. Park, J. E., Chen, H. H., Winer, J., Houck, K. A., and Ferrara, N. (1994) Placenta growth factor. Potentiation of vascular endothelial growth factor bioactivity, in vitro and in vivo, and high affinity binding to Flt-1 but not to Flk-1/KDR. *J. Biol. Chem.* **269,** 25646–25654
8. Olofsson, B., Pajusola, K., Kaipainen, A., von Euler, G., Joukov, V., Saksela, O., Orpana, A., Pettersson, R. F., Alitalo, K., and Eriksson, U. (1996) Vascular endothelial growth factor B, a

novel growth factor for endothelial cells. *Proc. Natl. Acad. Sci. U. S. A.* **93,** 2576–2581
9. Lagercrantz, J., Farnebo, F., Larsson, C., Tvrdik, T., Weber, G., and Piehl, F. (1998) A comparative study of the expression patterns for vegf, vegf-b/vrf and vegf-c in the developing and adult mouse. *Biochim. Biophys. Acta* **1398,** 157–163
10. Bellomo, D., Headrick, J. P., Silins, G. U., Paterson, C. A., Thomas, P. S., Gartside, M., Mould, A., Cahill, M. M., Tonks, I. D., Grimmond, S. M., Townson, S., Wells, C., Little, M., Cummings, M. C., Hayward, N. K., and Kay, G. F. (2000) Mice lacking the vascular endothelial growth factor-B gene (VEGFB) have smaller hearts, dysfunctional coronary vasculature, and impaired recovery from cardiac ischemia. *Circ. Res.* **86,** E29–E35
11. Karpanen, T., Bry, M., Ollila, H. M., Seppanen-Laakso, T., Liimatta, E., Leskinen, H., Kivela, R., Helkamaa, T., Merentie, M., Jeltsch, M., Paavonen, K., Andersson, L. C., Mervaala, E., Hassinen, I. E., Yla-Herttuala, S., Oresic, M., and Alitalo, K. (2008) Overexpression of vascular endothelial growth factor-B in mouse heart alters cardiac lipid metabolism and induces myocardial hypertrophy. *Circ. Res.* **103,** 1018–1026
12. Li, X., Tjwa, M., Van Hove, I., Enholm, B., Neven, E., Paavonen, K., Jeltsch, M., Juan, T. D., Sievers, R. E., Chorianopoulos, E., Wada, H., Vanwildemeersch, M., Noel, A., Foidart, J. M., Springer, M. L., von Degenfeld, G., Dewerchin, M., Blau, H. M., Alitalo, K., Eriksson, U., Carmeliet, P., and Moons, L. (2008) Reevaluation of the role of VEGF-B suggests a restricted role in the revascularization of the ischemic myocardium. *Arterioscler. Thromb. Vasc. Biol.* **28,** 1614–1620
13. Lahteenvuo, J. E., Lahteenvuo, M. T., Kivela, A., Rosenlew, C., Falkevall, A., Klar, J., Heikura, T., Rissanen, T. T., Vahakangas, E., Korpisalo, P., Enholm, B., Carmeliet, P., Alitalo, K., Eriksson, U., and Yla-Herttuala, S. (2009) Vascular endothelial growth factor-B induces myocardium-specific angiogenesis and arteriogenesis via vascular endothelial growth factor receptor-1- and neuropilin receptor-1-dependent mechanisms. *Circulation* **119,** 845–856
14. Ferrarini, M., Arsic, N., Recchia, F. A., Zentilin, L., Zacchigna, S., Xu, X., Linke, A., Giacca, M., and Hintze, T. H. (2006) Adeno-Associated Virus-mediated transduction of VEGF165 improves cardiac tissue viability and functional recovery after permanent coronary occlusion in conscious dogs. *Circ. Res.* **98,** 954–961
15. Favre, D., Provost, N., Blouin, V., Blancho, G., Cherel, Y., Salvetti, A., and Moullier, P. (2001) Immediate and long-term safety of recombinant adeno-associated virus injection into the nonhuman primate muscle. *Mol. Ther.* **4,** 559–566
16. Mueller, C., and Flotte, T. R. (2008) Clinical gene therapy using recombinant adeno-associated virus vectors. *Gene Ther.* **15,** 858–863
17. Arsic, N., Zentilin, L., Zacchigna, S., Santoro, D., Stanta, G., Salvi, S., Sinagra, G., and Giacca, M. (2003) Induction of functional neovascularization by combined VEGF and angiopoietin-1 gene transfer using AAV vectors. *Mol. Ther.* **7,** 450–459
18. Zacchigna, S., Pattarini, L., Zentilin, L., Moimas, S., Carrer, A., Sinigaglia, M., Arsic, N., Tafuro, S., Sinagra, G., and Giacca, M. (2008) Bone marrow cells recruited through the Neuropilin-1 receptor promote arterial formation at the sites of adult neoangiogenesis. *J. Clin. Invest.* **118,** 2062–2075
19. Pfeffer, M. A., Pfeffer, J. M., Fishbein, M. C., Fletcher, P. J., Spadaro, J., Kloner, R. A., and Braunwald, E. (1979) Myocardial infarct size and ventricular function in rats. *Circ. Res.* **44,** 503–512
20. Ventura, C., Cantoni, S., Bianchi, F., Lionetti, V., Cavallini, C., Scarlata, I., Foroni, L., Maioli, M., Bonsi, L., Alviano, F., Fossati, V., Bagnara, G. P., Pasquinelli, G., Recchia, F. A., and Perbellini, A. (2007) Hyaluronan mixed esters of butyric and retinoic acid drive cardiac and endothelial fate in term placenta human mesenchymal stem cells and enhance cardiac repair in infarcted rat hearts. *J. Biol. Chem.* **282,** 14243–14252
21. Sahn, D. J., DeMaria, A., Kisslo, J., and Weyman, A. (1978) Recommendations regarding quantitation in M-mode echocardiography: results of a survey of echocardiographic measurements. *Circulation* **58,** 1072–1083
22. Collesi, C., Zentilin, L., Sinagra, G., and Giacca, M. (2008) Notch1 signaling stimulates proliferation of immature cardiomyocytes. *J. Cell Biol.* **183,** 117–128
23. Arsic, N., Zacchigna, S., Zentilin, L., Ramirez-Correa, G., Pattarini, L., Salvi, A., Sinagra, G., and Giacca, M. (2004) Vascular endothelial growth factor stimulates skeletal muscle regeneration in vivo. *Mol. Ther.* **10,** 844–854
24. Beltrami, A. P., Urbanek, K., Kajstura, J., Yan, S. M., Finato, N., Bussani, R., Nadal-Ginard, B., Silvestri, F., Leri, A., Beltrami, C. A., and Anversa, P. (2001) Evidence that human cardiac myocytes divide after myocardial infarction. *N. Engl. J. Med.* **344,** 1750–1757
25. Eble, D. M., Qi, M., Waldschmidt, S., Lucchesi, P. A., Byron, K. L., and Samarel, A. M. (1998) Contractile activity is required for sarcomeric assembly in phenylephrine-induced cardiac myocyte hypertrophy. *Am. J. Physiol.* **274,** C1226–C1237
26. Simpson, P. C., Kariya, K., Karns, L. R., Long, C. S., and Karliner, J. S. (1991) Adrenergic hormones and control of cardiac myocyte growth. *Mol. Cell. Biochem.* **104,** 35–43
27. Brent, G. A. (1994) The molecular basis of thyroid hormone action. *N. Engl. J. Med.* **331,** 847–853
28. Dillmann, W. (2009) Cardiac hypertrophy and thyroid hormone signaling. [E-pub ahead of print] *Heart Fail. Rev.* PMID: 19125327
29. Tardiff, J. C., Hewett, T. E., Factor, S. M., Vikstrom, K. L., Robbins, J., and Leinwand, L. A. (2000) Expression of the beta (slow)-isoform of MHC in the adult mouse heart causes dominant-negative functional effects. *Am. J. Physiol. Heart. Circ. Physiol.* **278,** H412–H419
30. Hoshijima, M. (2006) Mechanical stress-strain sensors embedded in cardiac cytoskeleton: Z disk, titin, and associated structures. *Am. J. Physiol. Heart. Circ. Physiol.* **290,** H1313–H1325
31. Rottbauer, W., Just, S., Wessels, G., Trano, N., Most, P., Katus, H. A., and Fishman, M. C. (2005) VEGF-PLCγ1 pathway controls cardiac contractility in the embryonic heart. *Genes Dev.* **19,** 1624–1634
32. Jin, K., Zhu, Y., Sun, Y., Mao, X. O., Xie, L., and Greenberg, D. A. (2002) Vascular endothelial growth factor (VEGF) stimulates neurogenesis in vitro and in vivo. *Proc. Natl. Acad. Sci. U. S. A.* **99,** 11946–11950
33. Lambrechts, D., Storkebaum, E., Morimoto, M., Del-Favero, J., Desmet, F., Marklund, S. L., Wyns, S., Thijs, V., Andersson, J., van Marion, I., Al-Chalabi, A., Bornes, S., Musson, R., Hansen, V., Beckman, L., Adolfsson, R., Pall, H. S., Prats, H., Vermeire, S., Rutgeerts, P., Katayama, S., Awata, T., Leigh, N., Lang-Lazdunski, L., Dewerchin, M., Shaw, C., Moons, L., Vlietinck, R., Morrison, K. E., Robberecht, W., Van Broeckhoven, C., Collen, D., Andersen, P. M., and Carmeliet, P. (2003) VEGF is a modifier of amyotrophic lateral sclerosis in mice and humans and protects motoneurons against ischemic death. *Nat. Genet.* **34,** 383–394
34. LeCouter, J., Moritz, D. R., Li, B., Phillips, G. L., Liang, X. H., Gerber, H. P., Hillan, K. J., and Ferrara, N. (2003) Angiogenesis-independent endothelial protection of liver: role of VEGFR-1. *Science* **299,** 890–893
35. Deckers, M. M., Karperien, M., van der Bent, C., Yamashita, T., Papapoulos, S. E., and Lowik, C. W. (2000) Expression of vascular endothelial growth factors and their receptors during osteoblast differentiation. *Endocrinology* **141,** 1667–1674
36. Mayr-Wohlfart, U., Waltenberger, J., Hausser, H., Kessler, S., Gunther, K. P., Dehio, C., Puhl, W., and Brenner, R. E. (2002) Vascular endothelial growth factor stimulates chemotactic migration of primary human osteoblasts. *Bone* **30,** 472–477
37. Messina, S., Mazzeo, A., Bitto, A., Aguennouz, M., Migliorato, A., De Pasquale, M. G., Minutoli, L., Altavilla, D., Zentilin, L., Giacca, M., Squadrito, F., and Vita, G. (2007) VEGF overexpression via adeno-associated virus gene transfer promotes skeletal muscle regeneration and enhances muscle function in mdx mice. *FASEB J.* **21,** 3737–3746
38. Barleon, B., Sozzani, S., Zhou, D., Weich, H. A., Mantovani, A., and Marme, D. (1996) Migration of human monocytes in response to vascular endothelial growth factor (VEGF) is mediated via the VEGF receptor flt-1. *Blood* **87,** 3336–33343
39. Gerber, H. P., Malik, A. K., Solar, G. P., Sherman, D., Liang, X. H., Meng, G., Hong, K., Marsters, J. C., and Ferrara, N. (2002) VEGF regulates haematopoietic stem cell survival by an internal autocrine loop mechanism. *Nature* **417,** 954–958
40. Lyden, D., Hattori, K., Dias, S., Costa, C., Blaikie, P., Butros, L., Chadburn, A., Heissig, B., Marks, W., Witte, L., Wu, Y., Hicklin, D., Zhu, Z., Hackett, N. R., Crystal, R. G., Moore, M. A., Hajjar,

K. A., Manova, K., Benezra, R., and Rafii, S. (2001) Impaired recruitment of bone-marrow-derived endothelial and hematopoietic precursor cells blocks tumor angiogenesis and growth. *Nat. Med.* **7,** 1194–1201
41. Ziegler, B. L., Valtieri, M., Porada, G. A., De Maria, R., Muller, R., Masella, B., Gabbianelli, M., Casella, I., Pelosi, E., Bock, T., Zanjani, E. D., and Peschle, C. (1999) KDR receptor: a key marker defining hematopoietic stem cells. *Science* **285,** 1553–1558
42. Silvestre, J. S., Tamarat, R., Ebrahimian, T. G., Le-Roux, A., Clergue, M., Emmanuel, F., Duriez, M., Schwartz, B., Branellec, D., and Levy, B. I. (2003) Vascular endothelial growth factor-B promotes in vivo angiogenesis. *Circ. Res.* **93,** 114–123
43. Mould, A. W., Greco, S. A., Cahill, M. M., Tonks, I. D., Bellomo, D., Patterson, C., Zournazi, A., Nash, A., Scotney, P., Hayward, N. K., and Kay, G. F. (2005) Transgenic overexpression of vascular endothelial growth factor-B isoforms by endothelial cells potentiates postnatal vessel growth in vivo and in vitro. *Circ. Res.* **97,** e60–70
44. Rissanen, T. T., Markkanen, J. E., Gruchala, M., Heikura, T., Puranen, A., Kettunen, M. I., Kholova, I., Kauppinen, R. A., Achen, M. G., Stacker, S. A., Alitalo, K., and Yla-Herttuala, S. (2003) VEGF-D is the strongest angiogenic and lymphangiogenic effector among VEGFs delivered into skeletal muscle via adenoviruses. *Circ. Res.* **92,** 1098–1106
45. Bhardwaj, S., Roy, H., Gruchala, M., Viita, H., Kholova, I., Kokina, I., Achen, M. G., Stacker, S. A., Hedman, M., Alitalo, K., and Yla-Herttuala, S. (2003) Angiogenic responses of vascular endothelial growth factors in periadventitial tissue. *Hum. Gene Ther.* **14,** 1451–1462
46. Liu, Q., and Muruve, D. A. (2003) Molecular basis of the inflammatory response to adenovirus vectors. *Gene Ther.* **10,** 935–940
47. Storkebaum, E., and Carmeliet, P. (2004) VEGF: a critical player in neurodegeneration. *J. Clin. Invest.* **113,** 14–18
48. Brusselmans, K., Bono, F., Collen, D., Herbert, J. M., Carmeliet, P., and Dewerchin, M. (2005) A novel role for vascular endothelial growth factor as an autocrine survival factor for embryonic stem cells during hypoxia. *J. Biol. Chem.* **280,** 3493–3499
49. Germani, A., Di Carlo, A., Mangoni, A., Straino, S., Giacinti, C., Turrini, P., Biglioli, P., and Capogrossi, M. C. (2003) Vascular endothelial growth factor modulates skeletal myoblast function. *Am. J. Pathol.* **163,** 1417–1428
50. Li, Y., Zhang, F., Nagai, N., Tang, Z., Zhang, S., Scotney, P., Lennartsson, J., Zhu, C., Qu, Y., Fang, C., Hua, J., Matsuo, O., Fong, G. H., Ding, H., Cao, Y., Becker, K. G., Nash, A., Heldin, C. H., and Li, X. (2008) VEGF-B inhibits apoptosis via VEGFR-1-mediated suppression of the expression of BH3-only protein genes in mice and rats. *J. Clin. Invest.* **118,** 913–923
51. Poesen, K., Lambrechts, D., Van Damme, P., Dhondt, J., Bender, F., Frank, N., Bogaert, E., Claes, B., Heylen, L., Verheyen, A., Raes, K., Tjwa, M., Eriksson, U., Shibuya, M., Nuydens, R., Van Den Bosch, L., Meert, T., D'Hooge, R., Sendtner, M., Robberecht, W., and Carmeliet, P. (2008) Novel role for vascular endothelial growth factor (VEGF) receptor-1 and its ligand VEGF-B in motor neuron degeneration. *J. Neurosci.* **28,** 10451–10459
52. Trivieri, M. G., Oudit, G. Y., Sah, R., Kerfant, B. G., Sun, H., Gramolini, A. O., Pan, Y., Wickenden, A. D., Croteau, W., Morreale de Escobar, G., Pekhletski, R., St Germain, D., Maclennan, D. H., and Backx, P. H. (2006) Cardiac-specific elevations in thyroid hormone enhance contractility and prevent pressure overload-induced cardiac dysfunction. *Proc. Natl. Acad. Sci. U. S. A.* **103,** 6043–6048
53. Schaub, M. C., Hefti, M. A., Harder, B. A., and Eppenberger, H. M. (1997) Various hypertrophic stimuli induce distinct phenotypes in cardiomyocytes. *J. Mol. Med.* **75,** 901–920
54. Tirziu, D., Chorianopoulos, E., Moodie, K. L., Palac, R. T., Zhuang, Z. W., Tjwa, M., Roncal, C., Eriksson, U., Fu, Q., Elfenbein, A., Hall, A. E., Carmeliet, P., Moons, L., and Simons, M. (2007) Myocardial hypertrophy in the absence of external stimuli is induced by angiogenesis in mice. *J. Clin. Invest.* **117,** 3188–3197

Received for publication August 10, 2009.
Accepted for publication November 25, 2009.

Circulation Research
JOURNAL OF THE AMERICAN HEART ASSOCIATION

Intramyocardial VEGF-B167 Gene Delivery Delays the Progression Towards Congestive Failure in Dogs With Pacing-Induced Dilated Cardiomyopathy

Martino Pepe, Mohammed Mamdani, Lorena Zentilin, Anna Csiszar, Khaled Qanud, Serena Zacchigna, Zoltan Ungvari, Uday Puligadda, Silvia Moimas, Xiaobin Xu, John G. Edwards, Thomas H. Hintze, Mauro Giacca and Fabio A. Recchia

Circ. Res. published online Apr 29, 2010;
DOI: 10.1161/CIRCRESAHA.110.220855
Circulation Research is published by the American Heart Association. 7272 Greenville Avenue, Dallas, TX 72514
 Print ISSN: 0009-7330. Online ISSN: 1524-4571

Intramyocardial VEGF-B_{167} Gene Delivery Delays the Progression Towards Congestive Failure in Dogs With Pacing-Induced Dilated Cardiomyopathy

Martino Pepe,* Mohammed Mamdani,* Lorena Zentilin,* Anna Csiszar, Khaled Qanud, Serena Zacchigna, Zoltan Ungvari, Uday Puligadda, Silvia Moimas, Xiaobin Xu, John G. Edwards, Thomas H. Hintze, Mauro Giacca, Fabio A. Recchia

Rationale: Vascular endothelial growth factor (VEGF)-B selectively binds VEGF receptor (VEGFR)-1, a receptor that does not mediate angiogenesis, and is emerging as a major cytoprotective factor.

Objective: To test the hypothesis that VEGF-B exerts non–angiogenesis-related cardioprotective effects in nonischemic dilated cardiomyopathy.

Methods and Results: AAV-9–carried VEGF-B_{167} cDNA (10^{12} genome copies) was injected into the myocardium of chronically instrumented dogs developing tachypacing-induced dilated cardiomyopathy. After 4 weeks of pacing, green fluorescent protein–transduced dogs (AAV-control, n=8) were in overt congestive heart failure, whereas the VEGF-B–transduced (AAV-VEGF-B, n=8) were still in a well-compensated state, with physiological arterial P_{O_2}. Left ventricular (LV) end-diastolic pressure in AAV-VEGF-B and AAV-control was, respectively, 15.0±1.5 versus 26.7±1.8 mm Hg and LV regional fractional shortening was 9.4±1.6% versus 3.0±0.6% (all $P<0.05$). VEGF-B prevented LV wall thinning but did not induce cardiac hypertrophy and did not affect the density of α-smooth muscle actin–positive microvessels, whereas it normalized TUNEL-positive cardiomyocytes and caspase-9 and -3 activation. Consistently, activated Akt, a major negative regulator of apoptosis, was superphysiological in AAV-VEGF-B, whereas the proapoptotic intracellular mediators glycogen synthase kinase (GSK)-3β and FoxO3a (Akt targets) were activated in AAV-control, but not in AAV-VEGF-B. Cardiac VEGFR-1 expression was reduced 4-fold in all paced dogs, suggesting that exogenous VEGF-B_{167} exerted a compensatory receptor stimulation. The cytoprotective effects of VEGF-B_{167} were further elucidated in cultured rat neonatal cardiomyocytes exposed to 10^{-8} mol/L angiotensin II: VEGF-B_{167} prevented oxidative stress, loss of mitochondrial membrane potential, and, consequently, apoptosis.

Conclusions: We determined a novel, angiogenesis-unrelated cardioprotective effect of VEGF-B_{167} in nonischemic dilated cardiomyopathy, which limits apoptotic cell loss and delays the progression toward failure. (*Circ Res*. 2010;106:00-00.)

Key Words: Heart Failure ■ Vascular Endothelial Growth Factors ■ Gene Therapy

Vascular endothelial growth factor (VEGF)-B, 1 of the 5 members of the VEGF family,[1] is relatively understudied compared to VEGF-A, yet is emerging as a major cytoprotective factor.[2,3] Expressed in tissues with elevated metabolism, including myocardium,[4] the VEGF-B gene encodes for 2 isoforms, VEGF-B_{167} and VEGF-B_{186}, which selectively bind the receptors VEGFR-1 and neuropilin-1.[4,5] Based on data from knockout and transgenic animals, this growth factor is minimally angiogenic and its absence is compatible with birth and growth, although it seems important for physiological cardiac development.[6–8] Li et al have recently elucidated mechanisms responsible for VEGF-B–induced cytoprotection: VEGF-B_{167}, via VEGFR-1, downregulates genes of the apoptosis/cell death-related pathways, in vitro, and can rescue neurons from apoptosis in mouse models of retinal and brain damage.[2] The same authors found that, under pathological conditions, VEGF-B_{167}, albeit unable to induce blood vessel growth, is critically required for the survival of newly formed vascular cells.[3] We have later shown that VEGF-B_{167} gene transfer in infarcted rat hearts

Original received November 23, 2009; resubmission received March 23, 2010; revised resubmission received April 14, 2010; accepted April 15, 2010.

From the Department of Physiology (M.P., M.M., K.Q., X.X., J.G.E., T.H.H., F.A.R.), New York Medical College, Valhalla, NY; International Centre for Genetic Engineering and Biotechnology (L.Z., S.Z., U.P., M.G.), Trieste, Italy; Reynolds Oklahoma Center on Aging (A.C., Z.U.), Department of Geriatric Medicine, University of Oklahoma Health Science Center, Oklahoma City; and Sector of Medicine (F.A.R.), Scuola Superiore Sant'Anna, Pisa, Italy.

*These authors contributed equally to this work.

Correspondence to Fabio A. Recchia, MD, PhD, Department of Physiology, New York Medical College, Valhalla, NY 10595. E-mail fabio_recchia@nymc.edu

Circulation Research **is available at http://circres.ahajournals.org** **DOI: 10.1161/CIRCRESAHA.110.220855**

Non-standard Abbreviations and Acronyms	
AAV-control	paced dogs transduced with green fluorescent protein
AAV-VEGF-B	paced dogs transduced with VEGF-B_{167}
Ang II	angiotensin II
GFP	green fluorescent protein
GSK	glycogen synthase kinase
LV	left ventricular
MVO_2	myocardial oxygen consumption per minute
VEGF	vascular endothelial growth factor
VEGFR	vascular endothelial growth factor receptor

attenuates remodeling and preserves viable cardiac tissue and contractility in the absence of significant induction of angiogenesis.[9] This is suggestive of an angiogenesis-unrelated, direct prosurvival effect of VEGF-B_{167} on cardiomyocytes; however, no studies, to date, have tested a similar protective role in cardiac diseases, such as dilated cardiomyopathy, not associated with major vasculopathic/ischemic events. Although it is not the principal cause of heart failure, dilated cardiomyopathy is particularly malignant, accounting for the majority of cardiac transplants in the US,[10] and its underlying etiology remains in most cases undetermined. By definition, dilated cardiomyopathy is not caused by large necrotic tissue loss consequent to coronary artery disease; hence, it would not benefit from neoangiogenesis, whereas it is characterized by modest and widespread myocardial fibrosis and increased apoptosis.[11,12] Interestingly, a clinical study found that in dilated, but not in ischemic cardiomyopathy, a higher rate of apoptosis was associated with a more rapidly deteriorating clinical course.[13] Moreover, experimental studies have shown that a few hundred apoptotic cells per million are sufficient to cause dilated cardiomyopathy, which can be prevented by halting the mechanisms of cell death.[14,15] It is also noteworthy that cardiac VEGRF-1 expression is downregulated in patients with dilated, but not ischemic cardiomyopathy.[16] Based on these observations, we tested the hypothesis that VEGF-B_{167} overexpression can attenuate the structural and functional derangement of cardiac muscle in dilated cardiomyopathy. Our study was conducted in canine pacing-induced heart failure, which remains to date one of the best available preclinical models of human dilated cardiomyopathy. The prevalence of apoptosis in dog hearts subjected to sustained tachypacing is similar to that found in patients,[17] and the time course of failure is very predictable; therefore, this model is well-suited to test potential cytoprotective and protrophic effects of VEGF-B_{167} delivery. To obtain sustained expression over time, VEGF-B_{167} gene transfer was performed by using recombinant adeno-associated virus of serotype 9 (AAV9), a vector with marked cardiotropism.[18] Mechanisms of cell protection were further tested in cultured cardiomyocytes.

Methods

An expanded Methods section is available in the Online Data Supplement at http://circres.ahajournals.org.

Surgical Instrumentation and AAV Delivery

Twenty-two adult, male, mongrel dogs (25 to 27 kg) were chronically instrumented as previously described.[19,20] In addition, 2 pairs of piezoelectric crystals were implanted in the midmyocardium of the left ventricular (LV) free wall, orthogonal to the ventricular long axis, 10 to 15 mm apart, to assess regional circumferential shortening. During surgery and following a random order, in 14 dogs the heart was transduced with VEGF-B_{167} and in 8 dogs with the green fluorescent protein (GFP) transgene by 10 intramyocardial injections of 0.1 mL of AAV9 vectors (0.5×10^{11} genome copies per injection) into the LV free wall, according to a predefined map (Online Figure I). Some of the points of injection were previously tagged with epicardial thick silk stitches to allow postmortem identification of the spots. One injection was performed in between each of the 2 pairs of piezoelectric crystals.

Experimental Protocol

Ten to 12 days after surgery and AAV delivery, baseline hemodynamics, regional shortening, echocardiographic measurements were taken and paired arterial and coronary sinus blood samples collected in conscious, nonsedated animals, trained to lie down quietly and unrestrained on the laboratory table. Data were taken at spontaneous heart rate and after 10 minutes pacing at 210 bpm. Absolute myocardial flow was measured by injecting stable isotope-labeled microspheres, both at spontaneous heart rate and during pacing.[21] After these baseline measurements, 8 of the 14 VEGF-B_{167}–transduced (AAV-VEGF-B group) and the 8 GFP-transduced dogs (AAV-control group) were subjected to chronic LV pacing at 210 bpm for 3 weeks; then the rate was increases to 240 bpm for an additional week. The same measurements performed at baseline (0 weeks pacing) were repeated at 3 and 4 weeks of pacing, except for the microsphere injection and paired arterial and coronary sinus blood sampling, which were repeated only at 4 weeks, when the protocol was completed. Based on our previous studies in dogs undergoing this pacing protocol, at 3 weeks dogs are still in compensated failure,[19,20] whereas at 4 weeks, they reach end-stage heart failure, characterized by a LV end-diastolic pressure of $\geq$25 mm Hg, drop in arterial Po_2, and dyspnea. The remaining 6 VEGF-B_{167}-transduced dogs were monitored for 4 weeks but not paced and used to assess potential functional and morphological changes attributable to long-term VEGF-B_{167} overexpression in a normal heart (AAV-VEGF-B nonpaced group).

At the completion of the protocol, the dogs were euthanized with an overdose of sodium pentobarbital, the heart was weighed, and transmural LV tissue samples were harvested from the AAV-injected spots, ie, the anterolateral LV free wall, and from the remote LV region, ie, the posterolateral LV free wall, close to the left posterior descending coronary artery. They were immediately stored in liquid nitrogen or phosphate 10% formalin and coded for blinded molecular and histological analysis, or exsiccated for later counting of the microspheres. Only for comparisons of macroscopic (cardiac weight) and histological cardiac changes, we used data and tissue samples obtained from a further group of 5 healthy dogs that, after full recovery from chronic instrumentation, were euthanized because of major failures of the implanted probes. This group is indicated as "normal."

Surgical instrumentation and protocol were approved by the Institutional Animal Care and Use Committee of the New York Medical College and conform to the guiding principles for the care and use of laboratory animals published by the National Institutes of Health.

Hemodynamics, LV Regional Shortening, Echocardiographic Recordings and MVO_2

See the Online Data Supplement.

Production, Purification, and Characterization of Recombinant AAV Vectors

Mouse VEGF-B_{167} cDNA was incorporated into recombinant AAV-9 prepared by the AAV Vector Unit at ICGEB Trieste

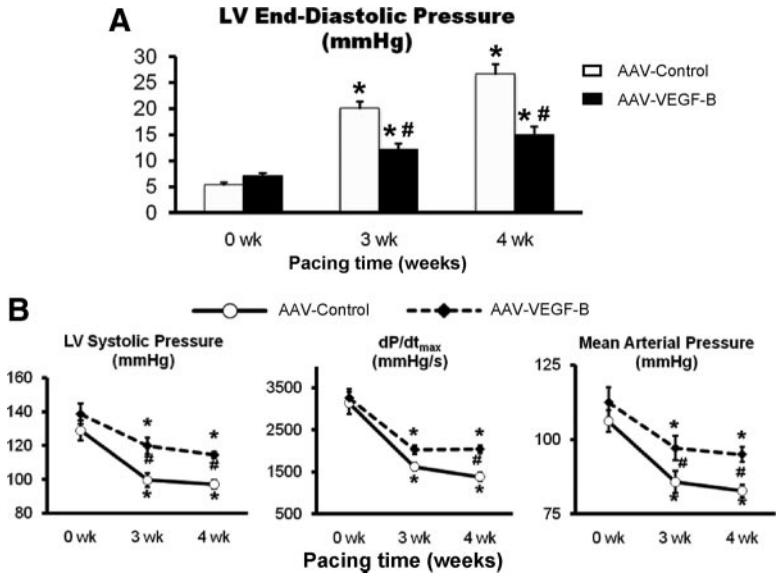

Figure 1. Changes in major hemodynamic parameters over the 4 weeks of chronic pacing. A, Changes in LV end-diastolic pressure. **B,** Changes in LV systolic pressure, dP/dtmax and mean arterial pressure. n=8 per group. Measurements were taken with the pacemaker off. *$P<0.05$ vs 0 weeks (baseline) within the group; #$P<0.05$ between groups at same time point.

(http://www.icgeb.org/avu-core-facility.html), by a cross-packaging approach whereby the AAV type 2 vector genome was packaged into AAV capsid serotype 9. Methods for production and purification were previously described.[22] AAV titers were in the range of 1×10^{12} genome copies per milliliter.

Histology and Immunofluorescence

To determine alterations in microvascular density, endothelial cells were detected using FITC-conjugated *Lycopersicum esculentum* lectin and vascular smooth muscle cells using a Cy3-conjugated anti α-SMA mouse monoclonal antibody. The microvessel number was normalized by the number of cardiac fibers. Apoptotic cells were visualized by TUNEL and cardiomyocyte cross-sectional area was measured.[9,22]

Isoprostane and Caspase-9 Activity in LV Tissue

Because the production of reactive oxygen species is increased in the failing heart,[23,24] we measured 8-isoprostane content, an index of oxidative stress, and the activity of caspase-9, which increases in response to oxidative mitochondrial damage, thus triggering the apoptotic cascade. In LV tissue homogenates, 8-isoprostane was measured by the EIA kit (Cayman Chemicals) and caspase-9 activity in LV homogenates was measured with a colorimetric activity assay kit.

PCR, ELISA, and Western Blotting

Total LV DNA was extracted to detect AAV genomic DNA and RNA was purified to quantify murine VEGF-B_{167} (AAV-carried transgene) and dog VEGF-B_{167}, VEGF-A_{165}, VEGFR-1, VEGFR-2 and Neuropilin-1 transcripts. Dog serum samples from arterial and coronary sinus blood were analyzed by ELISA for the presence of mouse VEGF-B_{167} secreted in the circulation from the transduced heart tissue. Western blot was used to quantify the activated/cleaved caspase-3, which is the final common effector of the apoptotic pathway, and to determine the activation state of Akt, a major antiapoptotic kinase,[25] and of 2 of its targets critically involved in the positive regulation of apoptosis, namely GSK-3β and FoxO3a, which are inactivated by phosphorylation in the cytosol and in the nucleus, respectively.[26–28]

Cultured Cardiac Myocytes

Potential mechanisms of cytoprotection mediated by VEGF-B_{167} were studied in neonatal rat cardiomyocytes. There are many causes of cell damage occurring in the failing heart, still partially unknown, therefore we focused on a major one, namely the upregulated angiotensin II (Ang II),[29] one of the main activators of oxidative stress.[30] Cardiomyocytes were cultured and pretreated with murine VEGF-B_{167} protein (100 ng/mL, for 24 hour) or vehicle. Then the culture medium was added with Ang II (10^{-8} mol/L, for 24 hour). After the treatment period the percent of TUNEL-positive cells, a marker of apoptosis, and caspase-3 and -9 activities were assessed in cell homogenates.

To elucidate downstream effects of Ang II, we tested Ang II–induced mitochondrial $O_2^{\cdot-}$ production and consequent damage.[31] Neonatal rat cardiomyocytes were exposed to Ang II with and without VEGF-B_{167} as described above. We then assessed Ang II–induced mitochondrial $O_{2\cdot-}$ production and total cell peroxide production. Changes in mitochondrial membrane potential were measured as they are a known downstream effect of Ang II–induced oxidative stress. We have used these methods previously.[32]

Statistical Analysis

Data are presented as means±SEM. Statistical analysis was performed by using commercially available software. Changes at different time points in the same group and differences among groups or in vitro data sets were compared by one- and two-way ANOVA followed by Tukey post hoc test. For all of the statistical analyses, significance was accepted at $P<0.05$.

Results

Hemodynamics

The hemodynamic changes found in AAV-control were very consistent with the typical evolution of this model of failure, as previously described by us.[18,19] LV end-diastolic pressure (Figure 1) reached values ≥25 mm Hg after 4 weeks of pacing, indicating a condition of end-stage, congestive heart failure. However, VEGF-B_{167} delivery markedly attenuated this increase, and, at 4 weeks, LV end-diastolic pressure was still comparable to values found at 3 weeks in AAV-control. Consistent with the development of congestive heart failure, in AAV-control arterial Po_2 decreased from 90.0±2.9 mm Hg at baseline (P=NS versus the AAV-VEGF-B group) to 67.0±4.8 mm Hg after 4 weeks of pacing ($P<0.05$ versus baseline), whereas the better preserved diastolic function in the AAV-VEGF-B group was reflected by an arterial Po_2 of 83.4±5.2 mm Hg at 4 weeks (P=NS versus baseline).

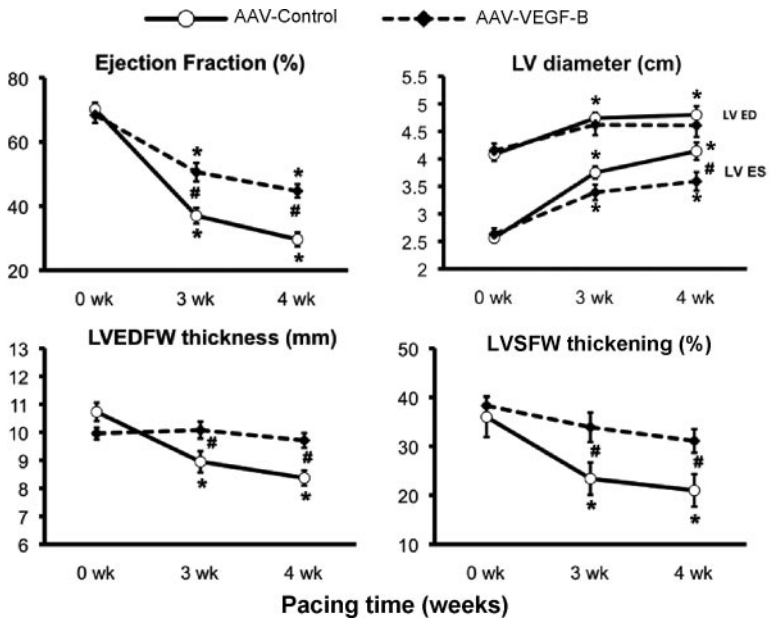

Figure 2. Changes in echocardiographic parameters over the 4 weeks of chronic pacing. LVED indicates LV end-diastolic; ED, end-diastolic; ES, end-systolic; LVEDFW, end-diastolic thickness of the LV free wall; LVSFW, LV systolic free wall. Measurements were taken with the pacemaker off. **P*<0.05 vs 0 weeks (baseline) within the group; #*P*<0.05 between groups at same time point; n=8 per group.

Figure 1 shows other major hemodynamic changes. Compared to AAV-control, VEGF-B gene delivery limited the fall in LV systolic pressure, dP/dt_{max} and mean arterial pressure during the pacing protocol. On the other hand, there were no significant hemodynamic changes from baseline during the 4-week follow up in the AAV-VEGF-B nonpaced group (data not shown).

Global and Regional Cardiac Function

Global cardiac function was evaluated by echocardiography (Figure 2). Ejection fraction decreased significantly in both groups, although it was better preserved in AAV-VEGF-B. LV end-diastolic diameter increased significantly only in AAV-control; however, the same trend was also present in AAV-VEGF-B, and therefore there was no significant difference between the 2 groups. LV end-systolic diameter increased significantly in both groups. Two parameters that did not change significantly in AAV-VEGF-B during the pacing protocol were the end-diastolic thickness and systolic thickening of the LV free wall. As expected, there were significant LV wall thinning and diminished systolic thickening in AAV-control. Thickening is an index of regional contractile performance that we measured along the selected plane of echo scanning. To further explore regional changes in contractile performance of the transduced LV areas, we measured circumferential systolic shortening with piezoelectric crystals (Figure 3), which, consistent with the echo data, decreased significantly in AAV-control, but was markedly preserved in

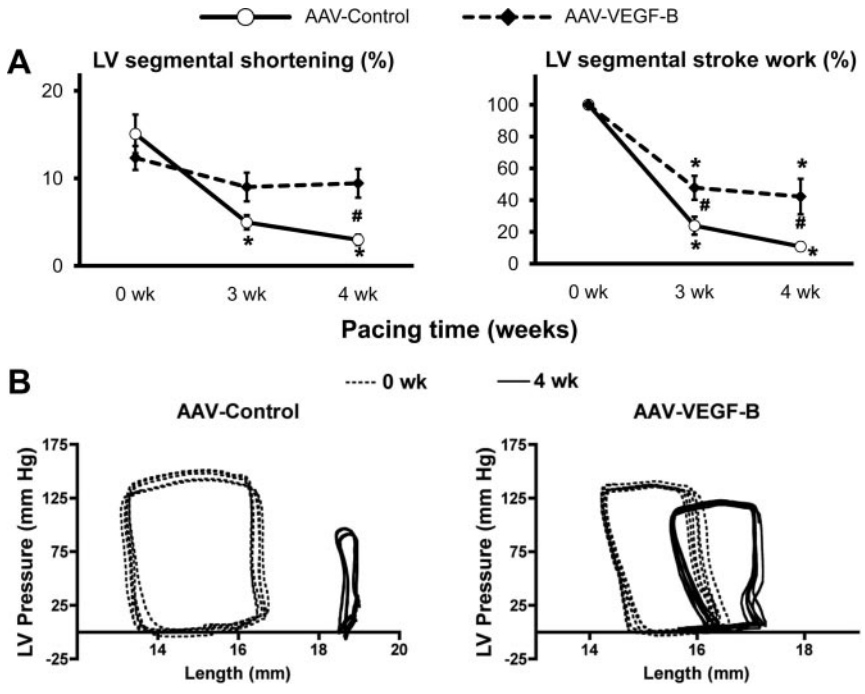

Figure 3. A, Changes in 2 indexes of regional contractile function calculated from cyclic variations of the LV distance (segmental length) between piezoelectric crystals implanted in the LV free wall. The surrogate of the regional stroke work was obtained as the area of the LV pressure–segmental length loop and normalized to baseline (n=8 per group). Measurements were taken with the pacemaker off. **P*<0.05 vs 0 weeks (baseline) within the group and #*P*<0.05 between groups at same time point. **B,** Representative pressure-length loops at 0 and 4 weeks pacing.

Table. Blood Flow in the Left Circumflex Coronary Artery in Myocardial Perfusion and in Cardiac Oxygen Consumption

	0 Weeks (Pacing Off)		0 Weeks (Acute Pacing)		4 Weeks (Pacing Off)		4 Weeks (Acute Pacing)	
	AAV-Control	AAV-VEGF-B	AAV-Control	AAV-VEGF-B	AAV-Control	AAV-VEGF-B	AAV-Control	AAV-VEGF-B
LCx CBF (mL/min)	33.14±4.03	35.63±2.91	43.64±6.37*	44.62±2.87*	34.12±4.12	31.50±2.25	41.34±5.45*	38.99±3.77*
Myocardial perfusion (mL/min/g)	1.03±0.08	1.10±0.15	1.88±0.28*	1.75±0.16*	1.23±0.06	1.15±0.20	1.76±0.20*	1.73±0.17*
MVO_2 (mL/min)	6.72±0.68	8.18±0.40	8.62±0.64*	12.06±1.24*	6.9±0.34	7.9±0.56	8.96±0.62*	9.52±1.68*

Blood flow in the left circumflex coronary artery (LCx CBF) in myocardial perfusion assessed by microsphere infusion and in cardiac oxygen consumption measured at 0 weeks and at 4 weeks pacing, both at spontaneous heart rate (pacing off) and during acute (10 minutes) pacing stress (n=6–8 per group). *$P<0.05$ of acute pacing vs pacing off.

AAV-VEGF-B. The integral of the LV pressure-segmental length loop provides a surrogate of regional stroke work, that, expressed as a percentage of the baseline (0 weeks), fell significantly by approximately 89% in AAV-control, but only by 58% in AAV-VEGF-B, after 4 weeks of pacing. Figure 3B shows 2 examples of changes in the pressure-length loops in the 2 groups, with the remarkable preservation of regional function in AAV-VEGF-B. Please note that the different baseline loops in the 2 groups was attributable to the unavoidable variability, from dog to dog, of the distance between crystals placed during surgery, and for that reason regional work in Figure 3A is expressed as percentage of baseline. On the other hand, there were no significant changes from baseline, in wall thickness and global and regional function, during the 4-week follow up in the AAV-VEGF-B nonpaced group (data not shown).

Coronary Flow and MVO_2

The beneficial effects of AAV-VEGF-B delivery could be possibly attributable to myocardial neoangiogenesis and therefore enhanced blood perfusion and oxygen consumption. We therefore measured coronary blood flow in the circumflex coronary artery, which is responsible for the perfusion of a large portion of the LV free wall, including the transduced areas. Moreover, we measured absolute myocardial perfusion in samples selectively taken from the AAV-injected spots. As shown in the Table, no significant differences were found between the 2 groups, both at spontaneous heart rate and during acute pacing stress, at baseline and after 4 weeks of pacing. MVO_2 displayed a trend toward increased baseline values in AAV-VEGF-B compared to AAV-control; however, these differences between the 2 groups were not statistical significant, not even during acute pacing stress.

Structural Changes at Macroscopic and Microscopic Level

The heart weight to body weight ratio was 10.07±0.29 g/kg in AAV-VEGF-B, 9.07±0.36 g/kg in AAV-control, 9.04±0.17 g/kg in nonpaced AAV-VEGF-B and 9.21±0.22 g/kg in normal (P=NS for all comparisons). Histology revealed an approximately 15% reduction in capillary density in AAV-control compared to normal, which was prevented in AAV-VEGF-B (Figure 4A and 4B). On the other hand, the density of microvessels with α-smooth muscle actin positive wall was not significantly different among groups (Figure 4A and 4C). Cardiomyocytes cross-sectional area was significantly increased in both paced and nonpaced AAV-VEGF-B compared to normal (Figure 4D and 4E), a local effect limited to the site of injection that was evidently insufficient to produce detectable LV hypertrophy. TUNEL-positive cardiomyocyte nuclei were increased by approximately eightfold in AAV-control and their number was halved in AAV-VEGF-B, although still higher than normal (Figure 5A and 5B). Consistently, caspase-9 activity was increased and cleaved caspase-3 was clearly detectable only in AAV-control (Figure 5C and 5D).

Oxidative Stress and Activation State of Major Regulators of Apoptosis

Total tissue isoprostane content was 37.9±5.4 pg/mg protein in normal LV, increased to 84.0±5.8 pg/mg in AAV-control group ($P<0.05$), but was normalized in paced AAV-VEGF-B (39.3±4.0 pg/mg).

Gene Expression of Murine VEGF-B_{167} and Endogenous VEGF-B_{167}, VEGF-A, VEGFR-1, VEGFR-2, and Neuropilin-1

The murine VEGF-B_{167} transgene delivered via AAV was expressed in the injection site and, to a much lesser extent, in the remote site (Online Figure II). However, murine VEGF-B_{167} protein concentration, both in arterial and coronary sinus blood samples, was below the ELISA threshold of detection.

VEGF-A_{165} gene expression was (normalized to Hprt gene values): 0.87±0.4 in AAV-VEGF-B, 0.63±0.1 in AAV-control ($P<0.05$ versus normal) and 1.05±0.1 in normal, yet VEGF-B_{167} was not significantly different among groups (data not shown). VEGFR-1 expression was reduced by approximately fourfold and neuropilin-1 by approximately 50% to 30% in both of AAV-control and AAV-VEGF-B compared to normal (Figure 6A). On the other hand, there were no significant differences of VEGFR-2 gene expression among groups.

Activation State of Akt, GSK-3β, and FoxO3a

Protein expression of Akt was not significantly different among groups; however, its phosphorylation was significantly higher in AAV-control compared to normal and even higher in AAV-VEGF-B (Figure 6B). We then examined GSK-3β and FoxO3a, 2 targets of Akt phosphorylation, one cytosolic and the other nuclear, both involved in the control of apoptosis. The levels of protein expression was not significantly different among groups, whereas, inconsistent with Akt hyperactivation, their phosphorylation was signifi-

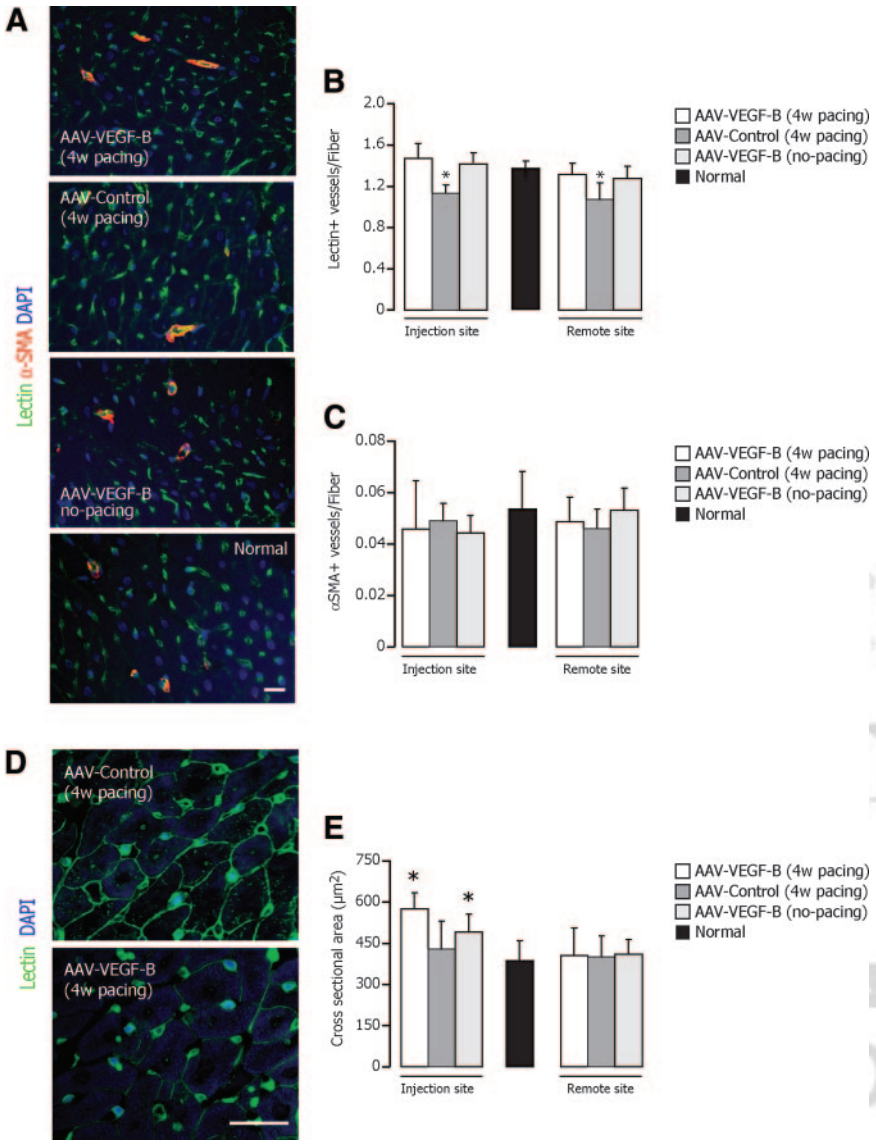

Figure 4. A, Representative photomicrographs of myocardial tissue showing double immunofluorescence staining for endothelial cells (lectin$^+$, green), vascular smooth muscle cells (α-SMA$^+$) **(red)**, whereas nuclei were stained with DAPI **(blue)**. **B and C,** Microvessel density was normalized by the number of cardiomyocyte fibers. **D and E,** ITC-conjugated lectin **(green)** was used to stain myocardium and quantify cardiomyocyte cross-sectional area. *$P<0.05$ vs normal; n=6 per group.

cantly reduced in AAV-control compared to normal. In AAV-VEGF-B; however, physiological levels of pospho-GSK-3β were reestablished, whereas phopho-FoxO3a was superphysiological (Figure 6B).

Cultured Cardiac Myocytes

Decreased mitochondrial function in cardiomyocytes is one of the earliest events of Ang II action, which leads to mitochondrial depletion and increased apoptosis. In this regard, we found that Ang II significantly increases apoptosis in cultured cardiac myocytes (Figure 7A), which was consistent with the activation of caspase-9 and -3 (Figure 7B and 7C). Moreover, treatment of cardiac myocytes with Ang II results in significant cellular (Figure 7D) and mitochondrial oxidative stress (Figure 7E through 7G), which are thought to play a role in the induction of apoptotic cell death. Importantly, VEGF-B$_{167}$ effectively protected cardiac myocytes against both Ang II–induced apoptosis (Figure 7A and 7B) and mitochondrial oxidative stress (Figure 7E through 7G). Treatment of cardiac myocytes with Ang II resulted in a loss of red fluorescence of J-aggregates and an increase in green fluorescence of JC-1 monomer (Figure 7H), indicating loss of mitochondrial membrane potential ($\Delta\psi_m$). All of these alterations were attenuated or completely prevented in the presence of VEGF-B$_{167}$, indicating a preservation of mitochondrial integrity.

Discussion

Our study shows that cardiac delivery of VEGF-B$_{167}$ transgene, obtained by no more than ten direct intramyocardial injections of AAV-9 vectors, delays the progression of pacing-induced dilated cardiomyopathy toward congestive failure. After 4 weeks of tachypacing, hearts transduced with VEGF-B$_{167}$ maintained a LV end-diastolic pressure compatible with physiological pulmonary blood oxygenation, whereas LV wall thickness and global and regional contractile function were either not significantly changed or preserved compared to baseline. On the other hand, VEGF-B$_{167}$ gene transfer did not affect myocardial blood perfusion and oxygen consumption at spontaneous heart rate or during acute

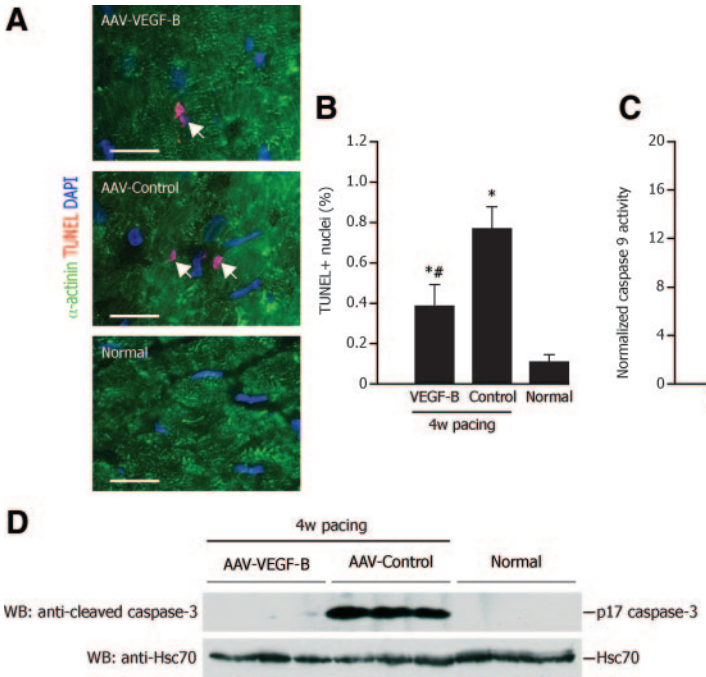

Figure 5. A and B, Cardiomyocyte apoptotic nuclei **(white arrows)** by TUNEL **(red)** analysis. Cardiomyocytes are stained with α-actinin **(green)**. **Bars:** #$P<0.05$ vs AAV-control; n=4 per group. **D,** Representative Western blotting analysis of activated/cleaved caspase-3 (17 kDa). The bands were not detectable in normal and AAV-VEGF-B, indicating virtually no cleavage.

pacing stress. Consistently, VEGF-B$_{167}$ transgene did not alter the density of LV microvessels endowed with smooth muscle wall, whereas it prevented the slight capillary rarefaction found in control paced dogs. The low rate of apoptosis and the normalized levels of active capsase-9 and -3 in myocardial tissue suggest antiapoptotic and protrophic actions of VEGF-B$_{167}$, which likely averted both of cardiomyocyte and capillary endothelial cell loss. Interestingly, the antiapoptotic kinase Akt was more active in the failing heart, as previously found in human and tachypacing-induced heart failure,[33,34] and yet the phosphorylation/inactivation of 2 major targets of this kinase in cytosolic and nuclear compartments, ie, GSK-3β and FoxO3a, known as important proapoptotic mediators,[26–28] was significantly reduced compared to normal hearts. Consistent with its antiapoptotic action, VEGF-B$_{167}$ transduction re-established normal levels of GSK-3β and FoxO3a phosphorylation.

VEGF-B$_{167}$ and Oxidative Stress

The determinants of apoptosis, in the failing heart, are notoriously numerous, and VEGF-B$_{167}$ transgene likely counteracted more than one of them. We focused on oxidative stress, a well recognized cause of myocardial cell damage in various forms of failure,[17,23,24] which is indirectly revealed by fingerprints such as 8-isoprostane and can be triggered by several factors, in particular the locally produced angiotensin II.[30] In paced dogs transduced with VEGF-B$_{167}$, tissue 8-isoprostane concentration was not significantly different from normal, suggesting a mechanism of protection against oxidative stress. Such mechanism was further tested in cultured cardiomyocytes exposed to angiotensin II: VEGF-B$_{167}$ displayed an action previously unrecognized for this factor, ie, blocked the sequence oxidative stress→mitochondrial damage→apoptosis.[30,31] This adds to cell trophic state enhancement and antiapoptotic effects of VEGF-B$_{167}$ on cultured cardiomyocytes exposed to other insults such as hypoxia/reoxygenation or the genotoxic agent epirubicin, recently shown by us.[9]

Angiogenesis-Unrelated Myocardial Protection

The capability to mitigate the pathogenesis of heart failure without inducing angiogenesis, thus via a direct cytoprotective and protrophic action, has been previously attributed to other families of growth factors, for instance the fibroblast growth factor-5.[35] However, as regards the VEGF family, this is a new paradigm. In fact, the rationale that has thus far driven experimental and clinical protocols with gene delivery of VEGF-A, the best known and most widely used VEGF, in hearts with ischemic[36] and even nonischemic injury,[37] is that the therapeutic outcome of this factor is attributable to neoangiogenesis and consequent perfusion enhancement. However, substantial evidence indicates that the expression of the VEGF receptors VEGFR-1 and -2 is not restricted to endothelial cells, but is present also in other cell types including cardiomyocytes,[9,38] and that their ligand VEGF-A exerts further fundamental functions, beyond proangiogenesis.[1] In a study on VEGF-A$_{165}$ gene transfer to infarcted dog hearts, we observed a functional improvement within 48 hours, a temporal frame not compatible with the formation of new blood vessels and suggestive of a direct protective effect on cardiomyocytes,[38] as proposed also by other authors.[39] More recently, we found that VEGF-B$_{167}$ gene transfer in infarcted rat hearts caused minimal angiogenesis and yet was as much beneficial as VEGF-A.[9] The ensuing question was whether the direct cytoprotective action of a VEGF member, per se, is sufficient to delay the progression of a form of heart failure unrelated to major coronary alterations. The ideal molecular probe to address this question was VEGF-B, a selective ligand of VEGFR-1, not mediating angiogenesis, and therefore devoid of additional, confounding outcomes of

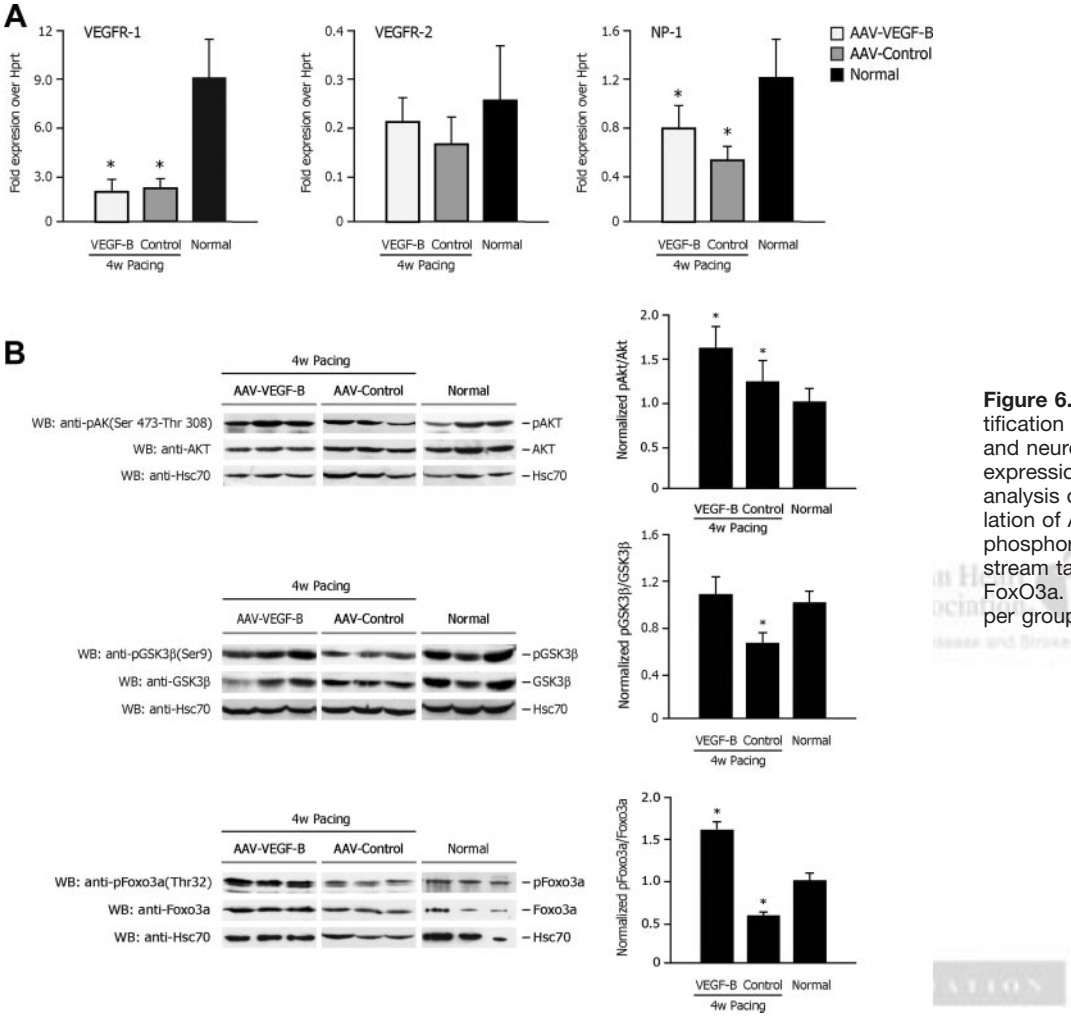

Figure 6. A, Real-time PCR quantification of VEGFR-1, VEGFR-2, and neuropilin-1 (NP-1) gene expression. **B,** Western blotting analysis of activating phosphorylation of Akt and inactivating phosphorylation of its downstream targets GSK-3β and FoxO3a. *$P<0.05$ vs normal; n=6 per group.

new vessel formation in diseased myocardium. Compared to VEGF-A, very little was known about the actions of VEGF-B in response to cell damage until seminal studies published over the past 2 years showed its marked antiapoptotic and cytoprotective effects both in vitro and in vivo.[2,3] These recent findings led us to the hypothesis that cardiac gene transfer of VEGF-B_{167} could ameliorate the evolution of a form of heart failure not caused by tissue loss from ischemic injury. Dilated cardiomyopathy was a well-suited target to test our hypothesis, because, by definition, it is characterized by ventricular chamber dilation in the absence of coronary disease and, independent of its cause that remains in many cases unrecognized, its pathogenesis involves severe cell damage leading to apoptotic death. We used pacing-induced heart failure, a long established model of dilated cardiomyopathy that, although limited as any other model, reproduces many features of the human disease, including cardiomyocyte damage and rate of apoptosis.[17] We now found a further, interesting analogy,[16] ie, decreased gene expression of VEGF-A, but not VEGF-B_{167}, associated with VEGFR-1 and neuopilin-1 downregulation, even in the AAV-VEGF-B group, whereas VEGFR-2 was not significantly altered. This suggests that supplementary, exogenous VEGF-B might have compensated for the reduced availability of its specific receptors VEGFR-1 and neuropilin-1 that, different from VEGFR-2, do not mediate angiogenesis.

Local Versus Global Effects of VEGF-B_{167} Gene Transfer

The method of gene delivery used yielded transduction that was highest in the LV site of injection, and detectable also, albeit much lower, in the remote site. It remains unclear how such nonhomogeneous distribution could affect global LV function, with repercussions on systemic hemodynamics. We could not find measurable levels of mouse VEGF-B_{167} in arterial and coronary sinus blood, ruling out a relevant cell secretion. Nonetheless VEGF-B_{167} gene transfer was sufficient to induce a local increase in the cardiomyocyte cross sectional area, but not as high to determine superphysiological or even untoward structural changes, such as neoangiogenesis and cardiac hypertrophy. Presumably, an excessive VEGF-B_{167} overexpression would have caused marked hypertrophy, as described in transgenic mice.[8] In this regard, it is interesting to note that, in infarcted rabbit and pig hearts, other authors have very recently found therapeutic angiogenesis induced by intracoronary gene delivery of the diffusible isoform VEGF-B_{186} in addition to antiapoptotic effects in cultured cardiomyocytes.[40] Perhaps such difference relative

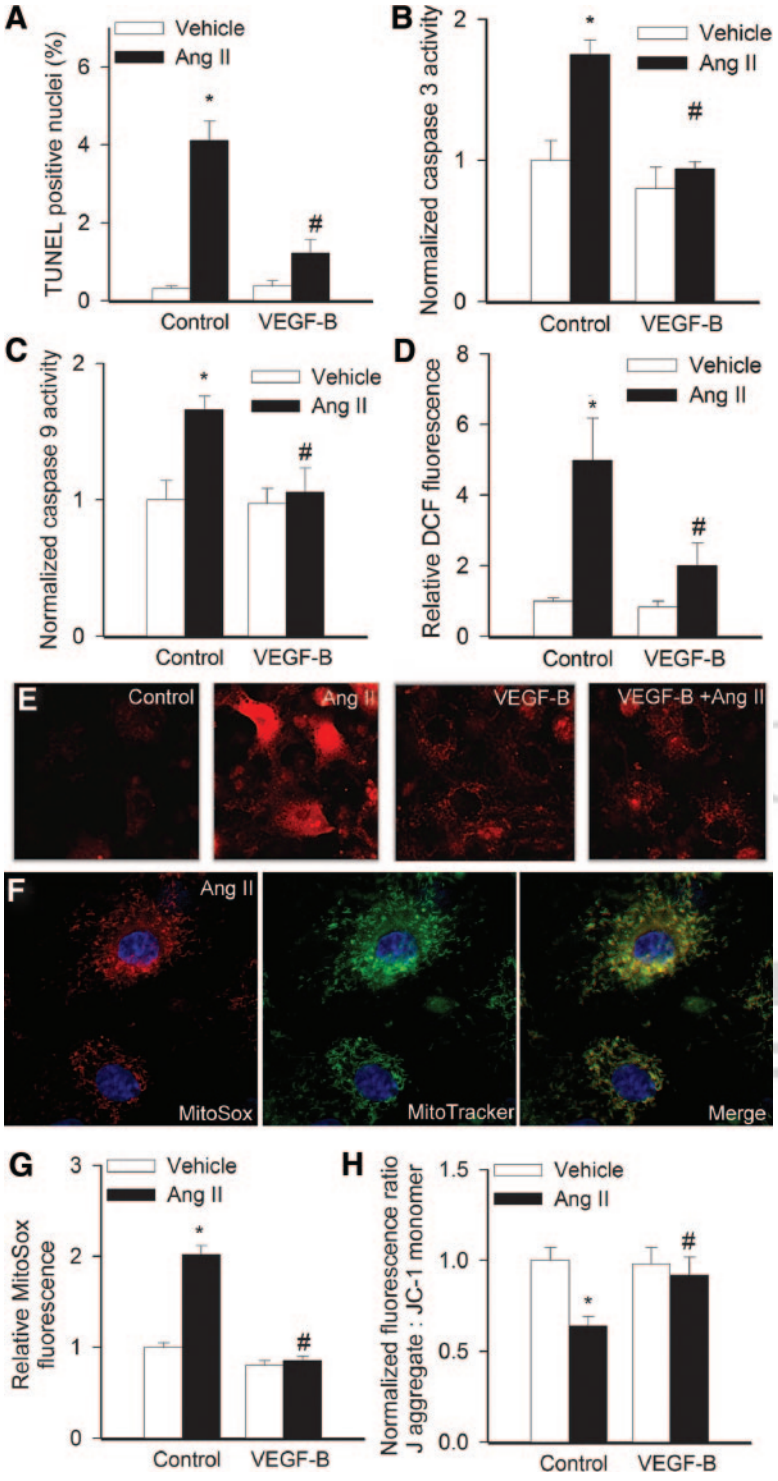

Figure 7. Percentage of TUNEL-positive nuclei (A), caspase-3 and -9 activity normalized by protein concentration **(B and C)** and cellular peroxide levels **(D)** in rat neonatal cardiac myocytes treated with Ang II (10^{-8} mol/L) with or without VEGF-B$_{167}$. **E,** Representative fluorescent images showing stronger MitoSox staining **(red fluorescence)** in Ang II–treated cardiac myocytes than in untreated controls (note also the increased number of early apoptotic cells exhibiting nuclear accumulation of MitoSox). VEGF-B$_{167}$ substantially attenuated MitoSox fluorescence in Ang II–treated cells (original magnification, ×40). **F,** Increased MitoSox staining localizes to the perinuclear mitochondria (counterstained with MitoTracker green) of nonapoptotic Ang II–treated cardiac myocytes (**blue fluorescence**: nuclear counterstaining). **G and H,** Summary of flow cytometric data showing relative MitoSox fluorescence **(E)** and J-aggregate: JC-1 monomer fluorescence ratios in rat neonatal cardiac myocytes treated with Ang II (10^{-8} mol/L) with or without pretreatment with VEGF-B. Data are means±SEM (n=6). *P<0.05 vs no Ang II; #P<0.05 vs no VEGF-B$_{167}$.

to our results is attributable to the kinetics and dynamics of the diffusible VEGF-B$_{186}$ isoform and/or to the level of its expression and/or to the presence of large areas of ischemia, a condition in which, as proposed by a recent report, this growth factor is critically required for the survival of newly formed vascular cells.[3]

Study Limitations

At least 2 limitations of our study should be pointed out. First, VEGF-B$_{167}$ gene delivery was performed during surgical instrumentation, before and not after starting the pacing protocol, and the study was only in part blinded. However, the present study was not designed as a preclinical trial, as its primary goal was to test VEGF-B$_{167}$-mediated cardioprotection in a model of progressive cardiac derangement. We needed to minimize confounding variables related to AAV delivery, therefore we chose to use multiple direct intramyocardial injections in well defined points that could be visually identified postmortem in animals that could be operated only once. Nevertheless, no significant differences between groups

were noted at baseline, before starting the pacing protocol; furthermore, we recently found VEGF-B_{167} transgene to be effective when administered after and not before inducing myocardial infarction.[9] A second limitation concerns our data on the percent of apoptosis measured by TUNEL-based analysis. Compared to other studies,[14,15,17] it seems overestimated; however, it was not meant to provide an absolute quantification, but rather an index to be interpreted together with other changes such as oxidative stress and caspase activation.

In conclusion, we provide novel evidence that VEGF-B_{167} is a cardiomyocyte protective factor capable of delaying functional derangement in a model of severe cardiomyopathy with high rate of apoptosis, without affecting myocardial blood perfusion and inducing angiogenesis. Besides expanding our knowledge on a relatively undervalued member of the VEGF family, this study has also translational implications, as it suggests a promising new candidate for gene therapy of dilated cardiomyopathy, whose cure, at present, relies on unsatisfactory pharmacological options.

Sources of Funding

This study was supported by NIH grants P01-HL-74237 (to F.A.R), P01-HL-43023 (to T.H.H.) and Fondazione CR Trieste (to M.G.). F.A.R. is an Established Investigator of the American Heart Association.

Disclosures

None.

References

1. Ferrara N, Gerber HP, LeCouter J. The biology of VEGF and its receptors. *Nat Med*. 2003;9:669–676.
2. Li Y, Zhang F, Nagai N, Tang Z, Zhang S, Scotney P, Lennartsson J, Zhu C, Qu Y, Fang C, Hua J, Matsuo O, Fong GH, Ding H, Cao Y, Becker KG, Nash A, Heldin CH, Li X. VEGF-B inhibits apoptosis via VEGFR-1-mediated suppression of the expression of BH3-only protein genes in mice and rats. *J Clin Invest*. 2008;118:913–923.
3. Zhang F, Tang Z, Hou X, Lennartsson J, Li Y, Koch AW, Scotney P, Lee C, Arjunan P, Dong L, Kumar A, Rissanen TT, Wang B, Nagai N, Fons P, Fariss R, Zhang Y, Wawrousek E, Tansey G, Raber J, Fong GH, Ding H, Greenberg DA, Becker KG, Herbert JM, Nash A, Yla-Herttuala S, Cao Y, Watts RJ, Li X. VEGF-B is dispensable for blood vessel growth but critical for their survival, and VEGF-B targeting inhibits pathological angiogenesis. *Proc Natl Acad Sci U S A*. 2009;106:6152–6157.
4. Olofsson B, Pajusola K, Kaipainen A, von Euler G, Joukov V, Saksela O, Orpana A, Pettersson RF, Alitalo K, Eriksson U. Vascular endothelial growth factor B, a novel growth factor for endothelial cells. *Proc Natl Acad Sci U S A*. 1996;93:2576–2581.
5. Li X, Aase K, Li H, von Euler G, Eriksson U. Isoform-specific expression of VEGF-B in normal tissues and tumors. *Growth Factors*. 2001;19:49–59.
6. Bellomo D, Headrick JP, Silins GU, Paterson CA, Thomas PS, Gartside M, Mould A, Cahill MM, Tonks ID, Grimmond SM, Townson S, Wells C, Little M, Cummings MC, Hayward NK, Kay GF. Mice lacking the vascular endothelial growth factor-B gene (Vegfb) have smaller hearts, dysfunctional coronary vasculature, and impaired recovery from cardiac ischemia. *Circ Res*. 2000;86:e29–e35.
7. Aase K, von Euler G, Li X, Ponten A, Thoren P, Cao R, Cao Y, Olofsson B, Gebre-Medhin S, Pekny M, Alitalo K, Betsholtz C, Eriksson U. Vascular endothelial growth factor-B-deficient mice display an atrial conduction defect. *Circulation*. 2001;104:358–364.
8. Karpanen T, Bry M, Ollila HM, Seppanen-Laakso T, Liimatta E, Leskinen H, Kivela R, Helkamaa T, Merentie M, Jeltsch M, Paavonen K, Andersson LC, Mervaala E, Hassinen IE, Yla-Herttuala S, Oresic M, Alitalo K. Overexpression of vascular endothelial growth factor-B in mouse heart alters cardiac lipid metabolism and induces myocardial hypertrophy. *Circ Res*. 2008;103:1018–1026.
9. Zentilin L, Puligadda U, Lionetti V, Zacchigna S, Collesi C, Pattarini L, Ruozi G, Camporesi S, Sinagra G, Pepe M, Recchia FA, Giacca M. Cardiomyocyte VEGFR-1 activation by VEGF-B induces compensatory hypertrophy and preserves cardiac function after myocardial infarction. *FASEB J*. In press.
10. Everly MJ. Cardiac transplantation in the United States: an analysis of the UNOS registry. *Clin Transpl*. 2008;35–43.
11. Narula J, Haider N, Virmani R, DiSalvo TG, Kolodgie FD, Hajjar RJ, Schmidt U, Semigran MJ, Dec GW, Khaw BA. Apoptosis in myocytes in end-stage heart failure. *N Engl J Med*. 1996;335:1182–1189.
12. Olivetti G, Abbi R, Quaini F, Kajstura J, Cheng W, Nitahara JA, Quaini E, Di Loreto C, Beltrami CA, Krajewski S, Reed JC, Anversa P. Apoptosis in the failing human heart. *N Engl J Med*. 1997;336:1131–1141.
13. Saraste A, Pulkki K, Kallajoki M, Heikkilä P, Laine P, Mattila S, Nieminen MS, Parvinen M, Voipio-Pulkki LM. Cardiomyocyte apoptosis and progression of heart failure to transplantation. *Eur J Clin Invest*. 1999;29:380–386.
14. Wencker D, Chandra M, Nguyen K, Miao W, Garantziotis S, Factor SM, Shirani J, Armstrong RC, Kitsis RN. A mechanistic role for cardiac myocyte apoptosis in heart failure. *J Clin Invest*. 2003;111:1497–1504.
15. Yamamoto S, Yang G, Zablocki D, Liu J, Hong C, Kim SJ, Soler S, Odashima M, Thaisz J, Yehia G, Molina CA, Yatani A, Vatner DE, Vatner SF, Sadoshima J. Activation of Mst1 causes dilated cardiomyopathy by stimulating apoptosis without compensatory ventricular myocyte hypertrophy. *J Clin Invest*. 2003;111:1463–1474.
16. Abraham D, Hofbauer R, Schäfer R, Blumer R, Paulus P, Miksovsky A, Traxler H, Kocher A, Aharinejad S. Selective downregulation of VEGF-A(165), VEGF-R(1), and decreased capillary density in patients with dilative but not ischemic cardiomyopathy. *Circ Res*. 2000;87:644–647.
17. Cesselli D, Jakoniuk I, Barlucchi L, Beltrami AP, Hintze TH, Nadal-Ginard B, Kajstura J, Leri A, Anversa P. Oxidative stress-mediated cardiac cell death is a major determinant of ventricular dysfunction and failure in dog dilated cardiomyopathy. *Circ Res*. 2001;89:279–286.
18. Pacak CA, Mah CS, Thattaliyath BD, Conlon TJ, Lewis MA, Cloutier DE, Zolotukhin I, Tarantal AF, Byrne BJ. Recombinant adeno-associated virus serotype 9 leads to preferential cardiac transduction in vivo. *Circ Res*. 2006;99:e3–e9.
19. Recchia FA, McConnell PI, Bernstein RD, Vogel TR, Xu X, Hintze TH. Reduced nitric oxide production and altered myocardial metabolism during the decompensation of pacing-induced heart failure in the conscious dog. *Circ Res*. 1998;83:969–979.
20. Qanud K, Mamdani M, Pepe M, Khairallah RJ, Gravel J, Lei B, Gupte SA, Sharov VG, Sabbah HN, Stanley WC, Recchia FA. Reverse changes in cardiac substrate oxidation in dogs recovering from heart failure. *Am J Physiol*. 2008;295:H2098–H2105.
21. Lei B, Matsuo K, Labinskyy V, Sharma N, Chandler MP, Ahn A, Hintze TH, Stanley WC, Recchia FA. Exogenous nitric oxide reduces glucose transporters translocation and lactate production in ischemic myocardium in vivo. *Proc Natl Acad Sci U S A*. 2005;102:6966–6971.
22. Zacchigna S, Pattarini L, Zentilin L, Moimas S, Carrer A, Sinigaglia M, Arsic N, Tafuro S, Sinagra G, Giacca. Bone marrow cells recruited through the Neuropilin-1 receptor promote arterial formation at the sites of adult neoangiogenesis. *J Clin Invest*. 2008;118:2062–2075.
23. Heymes C, Bendall JK, Ratajczak P, Cave AC, Samuel JL, Hasenfuss G, Shah AM. Increased myocardial NADPH oxidase activity in human heart failure. *J Am Coll Cardiol*. 2003;41:2164–2171.
24. Gupte RS, Vijay V, Marks B, Levine RJ, Sabbah HN, Wolin MS, Recchia FA, Gupte SA. Upregulation of glucose-6-phosphate dehydrogenase and NAD(P)H oxidase activity increases oxidative stress in failing human heart. *J Card Fail*. 2007;13:497–506.
25. Matsui T, Li L, del Monte F, Fukui Y, Franke TF, Hajjar RJ, Rosenzweig A. Adenoviral gene transfer of activated phosphatidylinositol 3′-kinase and Akt inhibits apoptosis of hypoxic cardiomyocytes in vitro. *Circulation*. 1999;100:2373–2379.
26. Pap M, Cooper G. Role of glycogen synthase kinase-3 in the phosphatidylinositol 3-kinase/Akt cell survival pathway. *J Biol Chem*. 1998;273:19929–19932.
27. Shiraishi I, Melendez J, Ahn Y, Skavdahl M, Murphy E, Welch S, Schaefer E, Walsh K, Rosenzweig A, Torella D, Nurzynska D, Kajstura J, Leri A, Anversa P, Sussman MA. Nuclear targeting of Akt enhances kinase activity and survival of cardiomyocytes. *Circ Res*. 2004;94:884–891.
28. Webster KA. Aktion in the nucleus. *Circ Res*. 2004;94:856–859.
29. Serneri GG, Boddi M, Cecioni I, Vanni S, Coppo M, Papa ML, Bandinelli B, Bertolozzi I, Polidori G, Toscano T, Maccherini M, Modesti PA.

Cardiac angiotensin II formation in the clinical course of heart failure and its relationship with left ventricular function. *Circ Res*. 2001;88:961–968.
30. Kajstura J, Bolli R, Sonnenblick EH, Anversa P, Leri A. Cause of death: suicide. *J Mol Cell Cardiol*. 2006;40:425–437.
31. Doughan AK, Harrison DG, Dikalov SI. Molecular mechanisms of angiotensin II-mediated mitochondrial dysfunction: linking mitochondrial oxidative damage and vascular endothelial dysfunction. *Circ Res*. 2008; 102:488–496.
32. Csiszar A, Labinskyy N, Perez V, Recchia FA, Podlutsky A, Mukhopadhyay P, Losonczy G, Pacher P, Austad SN, Bartke A, Ungvari Z. Endothelial function and vascular oxidative stress in long-lived GH/IGF-deficient Ames dwarf mice. *Am J Physiol*. 2008;295:H1882–H1894.
33. Haq S, Choukroun G, Lim H, Tymitz KM, del Monte F, Gwathmey J, Grazette L, Michael A, Hajjar R, Force T, Molkentin JD. Differential activation of signal transduction pathways in human hearts with hypertrophy versus advanced heart failure. *Circulation*. 2001;103:670–677.
34. Sasaki H, Asanuma H, Fujita M, Takahama H, Wakeno M, Ito S, Ogai A, Asakura M, Kim J, Minamino T, Takashima S, Sanada S, Sugimachi M, Komamura K, Mochizuki N, Kitakaze M. Metformin prevents progression of heart failure in dogs: role of AMP-activated protein kinase. *Circulation*. 2009;119:2568–2577.
35. Suzuki G, Lee TC, Fallavollita JA, Canty JM Jr. Adenoviral gene transfer of FGF-5 to hibernating myocardium improves function and stimulates myocytes to hypertrophy and reenter the cell cycle. *Circ Res*. 2005;96: 767–775.
36. Losordo DW, Vale PR, Hendel RC, Milliken CE, Fortuin FD, Cummings N, Schatz RA, Asahara T, Isner JM, Kuntz RE. Phase 1/2 placebo-controlled, double-blind, dose-escalating trial of myocardial vascular endothelial growth factor 2 gene transfer by catheter delivery in patients with chronic myocardial ischemia. *Circulation*. 2002;105:2012–2018.
37. Leotta E, Patejunas G, Murphy G, Szokol J, McGregor L, Carbray J, Hamawy A, Winchester D, Hackett N, Crystal R, Rosengart T. Gene therapy with adenovirus-mediated myocardial transfer of vascular endothelial growth factor 121 improves cardiac performance in a pacing model of congestive heart failure. *J Thorac Cardiovasc Surg*. 2002;123: 1101–1113.
38. Ferrarini M, Arsic N, Recchia FA, Zentilin L, Zacchigna S, Xu X, Linke A, Giacca M, Hintze TH. 1. Adeno-associated virus-mediated transduction of VEGF165 improves cardiac tissue viability and functional recovery after permanent coronary occlusion in conscious dogs. *Circ Res*. 2006;98:954–961.
39. Laguens R, Cabeza Meckert P, Vera Janavel G, Del Valle H, Lascano E, Negroni J, Werba P, Cuniberti L, Martinez V, Melo C, Papouchado M, Ojeda R, Criscuolo M, Crottogini A. Entrance in mitosis of adult cardiomyocytes in ischemic pig hearts after plasmid-mediated rhVEGF165 gene transfer. *Gene Ther*. 2002;9:1676–1681.
40. Lähteenvuo JE, Lähteenvuo MT, Kivelä A, Rosenlew C, Falkevall A, Klar J, Heikura T, Rissanen TT, Vähäkangas E, Korpisalo P, Enholm B, Carmeliet P, Alitalo K, Eriksson U, Ylä-Herttuala S. Vascular endothelial growth factor-B induces myocardium-specific angiogenesis and arteriogenesis via vascular endothelial growth factor receptor-1- and neuropilin receptor-1-dependent mechanisms. *Circulation*. 2009;119:845–856.

Novelty and Significance

What Is Known?

- Vascular endothelial growth factor (VEGF)-B, a selective ligand of the receptor VEGFR-1, is a minimally angiogenic growth factor that plays an important role in heart development and, when overexpressed, induces cardiomyocyte hypertrophy.
- The isoforms VEGF-B_{167} and VEGF-B_{186} can activate potent cytoprotective mechanisms in cells exposed to a variety of harmful conditions.
- VEGF-B exerts a marked cardioprotective effect in ischemic/infarcted hearts by binding VEGFR-1 expressed by cardiomyocytes.

What New Information Does This Article Contribute?

- VEGF-B_{167} gene delivery to the heart delays ventricular pump failure in a dog model of nonischemic dilated cardiomyopathy, while not inducing significant neoangiogenesis.
- VEGF-B_{167} attenuates oxidative stress and apoptosis, 2 interrelated, major determinants of progressive tissue loss in nonischemic dilated cardiomyopathy.
- Consistent with its cytoprotective effects in failing hearts, VEGF-B_{167} prevents oxidative stress and mitochondrial damage caused by angiotensin II in cultured cardiomyocyte.

VEGF-B is emerging as a major cytoprotective factor; however, no previous studies had tested its beneficial effects in nonischemic cardiac diseases. VEGF-B_{167} cDNA carried by adeno-associated viral vectors was delivered to the myocardium of dogs developing tachypacing-induced dilated cardiomyopathy. After 4 weeks of pacing, these dogs were still in a well-compensated state compared to control dogs. Consistently, hemodynamic and cardiac functional and morphological parameters were better preserved. Histological and molecular analysis indicated that VEGF-B_{167} markedly attenuated oxidative stress and cell apoptosis without inducing detectable neoangiogenesis. The cytoprotective effects of VEGF-B_{167} were further elucidated in cultured rat neonatal cardiomyocytes exposed to high concentrations of angiotensin II to mimic a recognized cause of oxidative stress and cell damage occurring in failing hearts. VEGF-B_{167} prevented oxidative stress, loss of mitochondrial membrane potential, and, consequently, apoptosis. We provide novel evidence that VEGF-B_{167} is a cardiomyocyte protective factor capable of delaying the onset of decompensated failure in a model of severe nonischemic cardiomyopathy, without altering myocardial vascularization. Besides expanding our knowledge of a less known member of the VEGF family, this study has also translational implications, because it suggests a promising new candidate for gene therapy of dilated cardiomyopathy, whose cure, at present, relies on unsatisfactory pharmacological options.

Supplemental Material

Intramyocardial VEGF-B_{167} gene delivery delays the progression towards congestive failure in dogs with pacing-induced dilated cardiomyopathy

First Author's surname: Pepe
Short title: VEGF-B_{167} in dilated cardiomyopathy

Martino Pepe, MD*, Mohammed Mamdani, MS*, Lorena Zentilin, PhD*, Anna Csiszar, MD, PhD, Khaled Qanud, MD, Serena Zacchigna, MD, PhD, Zoltan Ungvari, MD, PhD, Uday Puligadda, PhD, Silvia Moimas, PhD, Xiaobin Xu, MD, John G. Edwards, PhD, Thomas H. Hintze, PhD, Mauro Giacca, MD, PhD, Fabio A. Recchia, MD, PhD

Methods

Surgical instrumentation

Dogs were sedated with acepromazine maleate (1 mg/kg im), anesthetized with pentobarbital sodium (25 mg/kg iv) and ventilated with room air. A thoractotomy was performed in the fifth intercostals space. One fluid-filled Tygon catheter was inserted into the descending thoracic aorta and one in the left atrial appendage, while a silicon catheter was placed in the coronary sinus. A solid-state pressure gauge (Konigsberg Instruments, Pasadena, CA) was inserted into the LV through the apex. A Doppler flow transducer (Craig Hartley, Houston, TX) was placed around the left circumflex coronary artery, and two myocardial pacing leads were attached to the LV free wall. Two pairs of piezoelectric crystals were implanted in the mid-myocardium of the LV free wall, orthogonal to the ventricular long axis, 10-15 mm apart, to assess regional circumferential shortening. The viral vector was injected by the surgeon in a blind fashion. Wires and catheters were run subcutaneously to the intrascapular region and the chest was closed in layers. Antibiotics were given after surgery, and the dogs were allowed to fully recover for 7–10 days, then trained to lay quietly on the laboratory table.

Hemodynamics, LV regional shortening and echocardiographic recordings

Hemodynamic parameters were recorded on paper and also stored in computer memory at a sampling rate of 250 Hz. The piezoelectric crystals were connected to a sonomicrometer to measure cyclic changes in the segmental length. The best functioning pair of crystal was identified at baseline, before starting the pacing protocol, and then utilized for all the measurements from that point on. The segmental length was utilized to calculate percent segmental shortening and the area of the LV pressure-segment length loop, a surrogate of regional stroke work. These values served as indices of regional contractile function. Two-dimensional and M-mode echocardiography was performed (Sequoia C256; Acuson, Mountain View, CA) to measure ejection fraction, LV dimensions and wall thickness. Images were obtained from a right parasternal approach at the midpapillary muscle level, according to the criteria of the American Society of Echocardiography. Hemodynamics and echo were recorded and analyzed in a non blinded fashion. However, hemodynamics is

unequivocally quantifiable and objectively verifiable. On the other hand, in our Department, we have at least three experienced echocardiographists, and they customarily cross-evaluate their respective measurements.

Myocardial blood flow and oxygen consumption

Left circumflex coronary blood flow was measured with a pulsed Doppler flowmeter (Model 100, Triton Technology).

Absolute myocardial flow was measured by injecting $5x10^6$ of stable isotope-labeled 15 μm microspheres (Biopal, Worcester, MA) through the left atrial catheter, both at spontaneous heart rate and during pacing, while withdrawing blood reference samples from the aortic catheter. The neutron-activated isotopes contained in those microspheres allowed us to measure myocardial blood flow in selected regions of the ventricular wall, a method previously used by us (1)

Blood gases were measured in a blood gas analyzer (Instruments Laboratory, Bedford, MA). PO_2 was multiplied by 0.003 and added to O_2 content measured by a hemoglobin analyzer (CO-Oximeter; Instrumentation Laboratory, Bedford, MA) to obtain total oxygen content (vol/vol). Myocardial oxygen consumption (MVO_2) was calculated by multiplying the arterial-coronary sinus difference in total oxygen content by mean coronary blood flow.

Histology and immunofluorescence

To determine alterations in microvascular density, endothelial cells were detected using FITC-conjugated Lycopersicum esculentum lectin (Vector Laboratories) and vascular smooth muscle cells using a Cy3-conjugated anti α-SMA mouse monoclonal antibody (1A4, Sigma). Nuclei were counterstained with DAPI. All microvessels were normalized by the number of cardiac fibers.

Apoptotic cells were visualized by the TdT-mediated dUTP nick end labeling (TUNEL) assay on frozen sections (5 μm thick), using the in situ cell death detection kit, TMR red (Roche Diagnostics) according to the manufacturer's instructions. Anti-α-sarcomeric actinin monoclonal antibody (EA-53) 1:100 (Abcam, Cambridge MA, USA) was used to identify cardiomyocytes. The number of apoptotic cardiomyocytes was calculated as the percentage of the TUNEL positive per 1000 total cardiomyocyte nuclei. Images were analyzed using MetaView 4.6 quantitative analysis software (MDS Analytical Technologies, Toronto, Canada).

Finally, cardiomyocyte cross-sectional area was quantified from photomicrograph of FITC-conjugated Lycopersicum esculentum lectin stained paraffin histological sections, using ImageJ software (NIH). We have used these methods previously (2).

PCR, ELISA and Western blotting

Total DNA was extracted from LV tissue by proteinase-K digestion and phenol/chloroforme extraction. Real-time PCR amplification of AAV genomic DNA was performed on 100 ng of total DNA using primers and TaqMan probe designed to specifically recognize sequences on the CMV promoter present in all the AAV vectors used in this study.

Total RNA was extracted from LV tissue using TRIzol reagent (Invitrogen) according to manufacturer instructions, DNAse I digested and reverse transcribed using hexameric random primers. The cDNA was then used as template for real-time PCR amplification of the murine VEGF-B_{167} (AAV-carried transgene) and dog VEGF-B_{167}, VEGF-A_{165}, VEGFR-1, VEGFR-2 and Neuropilin-1 trancripts. Both TaqMan

technology and Syber Green incorporation were used in real time reactions. Gene expression was normalized by hypoxanthine phosphoribosyl - transferase (HPRT). The sequences of the primers used are:

CMV DNA:	Forward: 5'-TGGGCGGTAGGCGTGTA -3', Reverse: 5'-GATCTGACGGTTCACTAAACGAG-3'
Mouse VEGF-B_{167}:	Forward: 5'-TTGCACTGCTGCAGCTGGCTC-3', Reverse: 5'-GCTGGGCACTAGTTGTTTGA-3'
Canine VEGF-B_{167}:	Forward: 5'-AGAAGAAAGTGGTGCCATGG-3', Reverse: 5'-GCTGGGCACTAGTTGTTTGA-3'
Canine VEGF-A_{165}:	Forward: 5'- AACCCTGGAGCGTTCCCTGT -3', Reverse: 5'- ACCGCCTGGGCTTGTCACAT-3'
Canine VEGFR-1:	Forward: 5'- AAATCTGCCTGTGGAAGGAATG -3' Reverse: 5'- GCCTGAGCCATGTTCAAGGT -3' Probe: FAM-AACAGTTCTGCAGTA
Canine VEGFR-2:	Forward: 5'- GGAACCGGAACCTCACCAT -3' Reverse: 5'- GGCAGGTGTAGAGGCCTTCA -3' Probe: FAM- CGTAGGGTGAGGAAG
Canine neuropilin-1:	Forward: 5'- GTCAGAGATTATCCTGGAATTTGAAAG-3' Reverse: 5'- GGCAGGTGTAGAGGCCTTCA -3' Probe: FAM- CGTAGGGTGAGGAAG
Canine Hprt:	Forward: 5'- TCATTACGCTGAGGATTTGG -3' Reverse: 5'- AGAGGGCTACGATGTGATGG -3'

Dog serum samples were analyzed by ELISA for the presence of mouse VEGF-B_{167} secreted in the circulation from the transduced heart tissue. A specific commercially available polyclonal antibody (R&D) against mouse VEGFB167 was diluted at the concentration of 100 ng/ml and added to 96-well plates coated overnight at 4°C with 50 μl of undiluted or 1:50 diluted dog serum. Serial concentration, from 0,01 to 50 ng/ml, of recombinant mouse VEGFB167 was used as control standard. Plates were blocked for 2 h at RT with PBS containing 5% BSA. After overnight incubation and extensive washing with PBS containing 0.05% Tween 20 plates were incubated for 2hr at room temperature with an anti-goat HRP-labeled detection antibody. Following addition of 3, 3′,5 ,5′-Tetramethylbenzidine (TMB) substrate (Fisher Scientific), absorbance was measured at 450 nm using a fluorescence reader.

Western blot was utilized to quantify the activated/cleaved caspase-3 and to determine the activation state of Akt, and of its two targets GSK-3β and FoxO3a. The constitutive form of heat shock protein of 70 kDa (HSC70) was used for loading control. Eighty μg of proteins were resolved on SDS-PAGE minigels and transferred to nitrocellulose membranes (GE Healthcare), which were incubated with the following primary antibodies (dilution 1:1000) overnight at 4°C: rat monoclonal

HSC70 (SPA-815' StressGen Assay Designs), rabbit polyclonal anti-Akt, rabbit polyclonal anti-pAkt (Thr 308), rabbit polyclonal anti-pGSK-3β (Ser 9), rabbit polyclonal anti cleaved-caspase 3, rabbit polyclonal anti-pFoxO3a (Thr32), rabbit polyclonal anti-Foxo3a (all from Cell Signaling) and rabbit polyclonal anti-GSK-3β (Calbiochem).

Cultured cardiac myocytes

Neonatal cardiomyocytes were prepared as follows. 1-3 day neonatal rat ventricles were disaggregated by mechanical dissection followed by repeated digestions in HBSS using 0.06% Collagenase (IV) (Worthington Biochemical, Lakewood NJ) and 0.1 % trypsin. Following repeated digestion cells were centrifuged at 300 x g for 10 min and differentially plated to remove fibroblasts. Myocytes were plated at a density equivalent to 6-8 x 10^{-6} cells/100-mm plate in DMEM/F12 (10%FBS, P/S, 0.1mM 5'-bromo-2'deoxyuridine). On the day following preparation the media was removed and fresh media added DMEM/F12, (5% HS, P/S) (3-4).

Apoptosis was determined by flow cytometry (Millipore/Guava Easycyte Mini) using the Guava TUNEL Assay (Millipore) according to the manufacturer's guidelines. Acspase-3 and -9 activities were measured using a Colorimetric Activity Assay kit, according to the manufacturer's instructions (Chemicon International). Optical Density values were normalized to the sample protein concentration (5-6)

Ang II-induced mitochondrial $O_2^{\cdot -}$ production was assessed by flow cytometry using MitoSOX Red (Invitrogen, Carlsbad CA), a mitochondrion-specific hydroethidine-derivative fluorescent dye, as previously reported (5-7). Cell debris (low forward and side scatter), dead cells (Sytox Green and annexin V positive) and apoptotic cells (annexin V positive) were gated out for analysis. The data is presented as fold change in the median intensity of MitoSOX fluorescence when compared with the respective controls. To demonstrate the localization of MitoSox signal to mitochondria, the cells were counterstained with MitoTracker green and visualized by confocal microscopy. In separate experiments, the effects of VEGF-B_{167} pretreatment on cardiomyocyte peroxide production was measured fluorometrically using the C-H_2DCFDA fluorescence assay, as reported (5). Changes in mitochondrial membrane potential were detected by flow cytometry using the cationic carbocyanine dye 5,5',6,6'tetrachloro-1,1',3,3'-tetraethylbenzimidazol-carbocyanine iodide (JC-1, Invitrogen) according to the manufacturer's guidelines.

References

1. Lei B, Matsuo K, Labinskyy V, Sharma N, Chandler MP, Ahn A, Hintze TH, Stanley WC, Recchia FA. Exogenous nitric oxide reduces glucose transporters translocation and lactate production in ischemic myocardium in vivo. *Proc Natl Acad Sci USA*. 2005;102:6966-71.
2. Zacchigna S, Pattarini L, Zentilin L, Moimas S, Carrer A, Sinigaglia M, Arsic N, Tafuro S, Sinagra G, Giacca. Bone marrow cells recruited through the Neuropilin-1 receptor promote arterial formation at the sites of adult neoangiogenesis. *J Clin Invest.* 2008;118:2062-2075
3. Edwards JG, Bahl JJ, Flink I, Milavetz J, Morkin E: A repressor region in the human beta myosin heavy chain gene that has a partial position dependency. *Biochem Biophys Res Comm* 1992, 189:504-510.
4. Edwards JG, Bahl J, Flink I, Cheng S, Morkin E: Thyroid hormone influences expression of the beta myosin heavy chain gene. *Biochem Biophys Res Comm* 1994, 199:1482-1488.
5. Csiszar A, Ungvari Z, Koller A, Edwards JG, Kaley G. Proinflammatory phenotype of coronary arteries promotes endothelial apoptosis in aging. *Physiol Genomics.* 2004;17:21-30.
6. Csiszar A, Labinskyy N, Perez V, Recchia FA, Podlutsky A, Mukhopadhyay P, Losonczy G, Pacher P, Austad SN, Bartke A, Ungvari Z. Endothelial function and vascular oxidative stress in long-lived GH/IGF-deficient Ames dwarf mice. *Am J Physiol Heart Circ Physiol.* 2008;295:H1882-1894.
7. Ungvari Z, Labinskyy N, Mukhopadhyay P, Pinto JT, Bagi Z, Ballabh P, Zhang C, Pacher P, Csiszar A. Resveratrol attenuates mitochondrial oxidative stress in coronary arterial endothelial cells. *Am J Physiol.* 2009;297:H1876-1881.

Online Figures

Figure I. Predefined map for AAV intramyocardial injections.
Three injections were performed along the first diagonal of the left anterior descending (LAD) coronary artery and 7 along the second diagonal. The vector was never injected distal to the third diagonal. Two sites of injection corresponded to the space between the implanted piezoelectric crystals.

Figure II. Levels of AAV genomes and AAV-mediated transgene expression in myocardium.
Upper panel: the amount of AAV genome was not significantly different between AAV-VEGF-B and AAV-Control LV myocardium at the injection site. n= 5 per group.
Lower panel. The murine VEGF-B167 transgene transcript was clearly expressed in the injection site and detectable also in the LV remote site, although the level was approximately 85% lower. n= 5 per group.

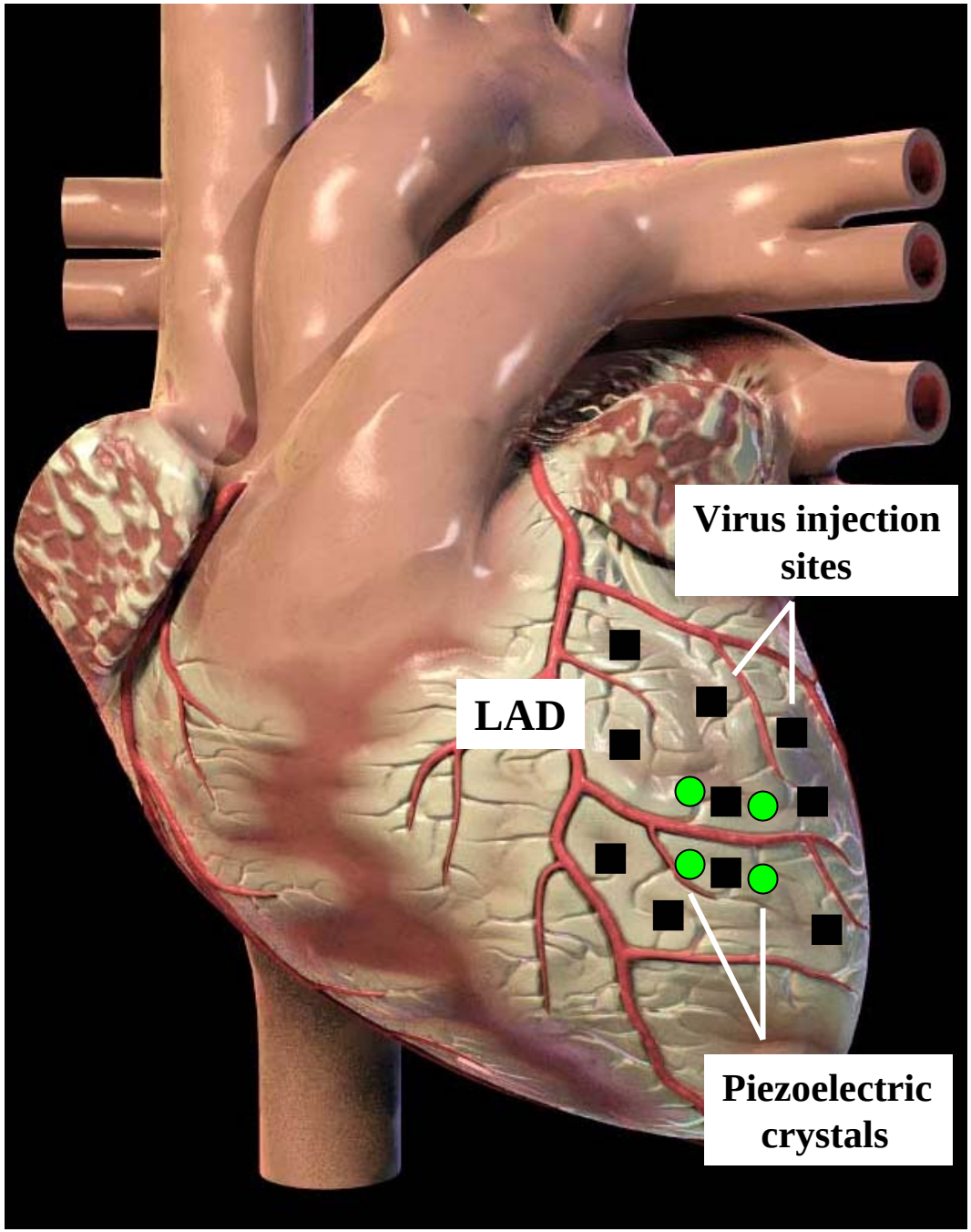

Online Figure I

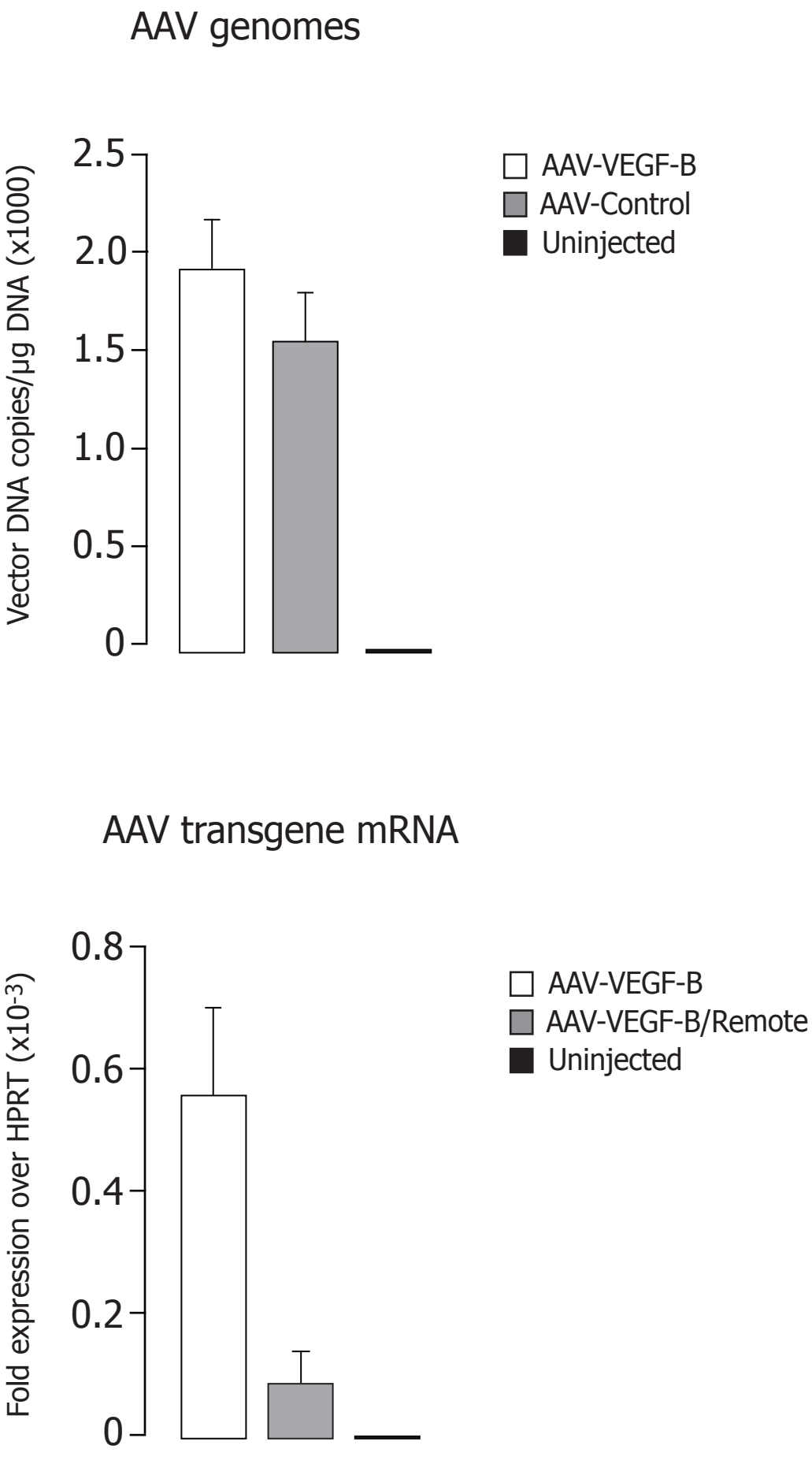

MICROSURGICAL ARTEROVENOUS LOOPS AND BIOLOGICAL TEMPLATES: A NOVEL IN VIVO CHAMBER FOR TISSUE ENGINEERING

BENEDETTO MANASSERI, M.D.,[1] GIUSEPPE CUCCIA, M.D.,[1] SILVIA MOIMAS, M.Sc.,[2] FRANCESCO STAGNO D'ALCONTRES, M.D.,[1] FRANCESCA POLITO, M.D.,[3] ALESSANDRA BITTO, M.D.,[3] DOMENICA ALTAVILLA, M.D.,[3] FRANCESCO SQUADRITO, M.D.,[3] STEFANO GEUNA, M.D.,[4] LUCIA PATTARINI, M.Sc.,[2] LORENA ZENTILIN, Ph.D.,[2] CHIARA COLLESI, Ph.D.,[2] UDAY PULIGADDA, B.Sc.,[2] MAURO GIACCA, M.D., Ph.D.,[2] and MICHELE ROSARIO COLONNA, M.D.[1]*

Background: Microsurgical tissue engineering is an emerging topic in regenerative medicine. Here we describe a new microsurgical model of bioengineering in rats based on the use of an arterovenous loop (AV) implanted into a commercially available crosslinked collagen/glycosaminoglycan template. *Methods:* The microvascular loop was created between the femoral artery and vein and covered by the template folded onto itself. The chamber was isolated from the outside tissue by an outer silicon layer to impede tissue ingrowth. *Results*: At 1-month postimplantation, the tissue chamber was found heavily vascularized, as assessed by laser Doppler perfusion analysis. Histological examination showed that the AV loop was integrated into the collagen matrix of the template and that the whole template was filled with a newly formed soft connective tissue. Most interestingly, the whole scaffold was found heavily vascularized, including the formation of a large number of α-SMA-positive arterioles. *Conclusions:* The developed microsurgical chamber provides a highly vascular, isolated tool for in vivo tissue engineering. © 2007 Wiley-Liss, Inc. Microsurgery 27:623–629, 2007.

One of the central requirements in tissue engineering is the possibility to induce neoangiogenesis or neovasculogenesis to provide adequate blood supply to the engineered tissue and to sustain viability and growth of the cells supporting regeneration.[1] This requirement appears particularly stringent for all in vivo applications of tissue engineering, including the formation of new specialized tissues (dermis, bone, cartilage, liver) or in plastic reconstructive surgery.

Over the last few years, a number of interesting surgical models for in vivo tissue reconstruction have been described.[1–5] Several studies have shown that both artificial and natural scaffolds become vascularized upon in vivo implantation, thus suggesting their potential usefulness as biological templates for tissue growth.[1,2] Yet, the search for the ideal scaffold is still open, especially considering that the vascularization of in vivo implanted scaffolds strictly depends on the invasion of the scaffold itself by a newly formed vasculature ensuing from the adjacent tissues. As a consequence, these implanted tissues are hardly removable from the sites of implantation and lose their vascular connections upon transplantation.

A more appealing alternative to scaffold implantation comes from the possibility of applying microsurgery techniques for tissue prefabrication. Previous experience with experimental prefabrication of flaps by vascular axes or microsurgical arterovenous (AV) loop implantation has proven effective in creating new vascular networks in the implanted tissues.[2–4,6,7] Moreover, the generation of microsurgical AV loops already has applications in the clinical field.[8]

Here we revisit the microsurgical AV loop model and propose the utilization of a commercially available, crosslinked collagen-glycosaminoglycan (GAG) template (INTEGRA^{TM}) for the generation of highly vascular tissue engineering chambers. We show that collagen chambers that embed an AV loop, and are completely isolated from the surrounding tissue in a month-long period, are filled with newly formed soft connective tissue and become heavily vascularized. These chambers represent excellent in vivo experimental tools for tissue engineering.

MATERIALS AND METHODS

Animals

Ten male Wistar rats (weighing 200–300 g) were used in the experiments. Animal care and treatment were conducted in conformity with institutional guidelines in compliance with national and EU laws and policies (EEC Council Directive 86/609, OJL 358, December 12, 1987). All procedures were carried out under general anesthesia using Zoletil-Virbac (tiletamine plus zolazepam), 50 mg/

[1]Department of Surgical Specialties, Plastic Surgery Division, University of Messina Medical School, Messina, Italy
[2]Molecular Medicine Laboratory, International Centre for Genetic Engineering and Biotechnology (ICGEB), Trieste, Italy
[3]Clinical and Experimental Department of Internal Medicine and Pharmacology, University of Messina Medical School, Messina, Italy
[4]Department of Clinical and Biological Sciences, University of Turin Medical School, Turin, Italy
Grant sponsor: INTEGRA^{TM}, INTEGRA LifeSciences (USA), Fondazione CRTrieste (Trieste, Italy).
*Correspondence to: Michele R. Colonna, M.D., Surgical Specialties Department, University of Messina Medical School, Messina, Italy.
E-mail: mrcolonna@unime.it
Received 16 April 2007; Accepted 10 July 2007
Published online 14 September 2007 in Wiley InterScience (www.interscience.wiley.com). DOI 10.1002/micr.20415

kg in combination with xylazine, 20 mg/kg i.m. The animals were housed in single cages and fed ad libitum.

Construction of the AV Loop and Generation of the Collagen Chamber

A microvascular loop was generated between the femoral artery and vein using a vein graft harvested from the controlateral leg. End-to-side anastomoses were performed with 11/0 nylon sutures, both on recipient artery and vein. After perfusion, the AV loop was embedded into a sandwich composed of a 2.4 cm $\times$ 1.4 cm portion of a commercially available bilayered dermal substitute template (inner layer: matrix of bovine collagen-GAG; outer layer: silicon; INTEGRA^{TM}). The template was secured on three sides by multiple 9/0 silk sutures as a sandwich. including the loop.

Laser Doppler Perfusion Imaging

A Laser Doppler (Laser Doppler Perfusion Imager, Perimed, Sweden) was used to assay the blood flow in the loop at day 0, before and after the application of the scaffold, and at day 30. The laser Doppler source was mounted onto a movable rack exactly 20 cm above the rat limbs; the animals were under anesthesia and restrained on the operation table. The laser beam (780 nm), reflected from moving RBCs in nutritional capillaries, arterioles, and venules were detected and processed to provide a computerized, color-coded image. Using image analysis software (Laser Doppler Perfusion Imager, Perimed), mean flux values representing perfusion were calculated.

Histological Analysis

On day 30, the rats were anesthetized, the chambers were exposed, the vessels ligated proximally and distally, and the specimen immediately fixed in 10% formalin and embedded in paraffin. Afterward, the animals were sacrificed by intracardiac administration of pentobarbital sodium salt (975 mg/rat). Histological sections were either stained with hematoxylin and eosin and Masson trichrom stain, or processed for immunofluorescence. Cy3-coniugated anti-α-SMA primary antibody (clone 1A4, Sigma) diluted to 1:200 in blocking buffer was used to label smooth muscle cells. DAPI (Vectashield) fluorescent staining was used to recognize cell nuclei. Sections were then analyzed by a Leica MLB upright fluorescence microscope (Leica Microsystems, Wetzler, Germany) equipped with a Coolsnap CF CCD camera (Roper Scientific, Evry, France) and MetaView 4.6 software (Molecular Devices, Downingtown, PA).

RESULTS

An AV loop was created on the femoral vascular bundle as shown in Figure 1. A vein graft was harvested from one groin, and used as a microvascular loop between the femoral artery and vein on the opposite leg (Fig. 1A, panels a–d). The vein graft was harvested as long as possible, with a mean length of 9 mm (range, 7–15 mm). Examples of AV loops in other animals are shown in Figure 1B. After perfusion of the AV loop, a bilayered collagen-GAG scaffold was folded onto itself, maintaining the outer silicon layer, and secured as a sandwich including the loop (Fig. 1A, panels e and f).

The maintenance of the silicon layer of the template ensures the complete isolation of the collagen matrix from the surrounding tissue and blocks possible vessel ingrowth from the outside. At day 30 after surgery, the chamber was exposed and femoral vessels, proximally and distally to the chamber, were assessed for patency. The loop was found patent in 8 out of 10 animals. In all animals, the chambers appeared surrounded by a dense connective capsule (Fig. 2).

Perfusion was assessed by laser Doppler imaging immediately after creation of the AV loop, after closure of the collagen chamber (day 0) and at the end of the experiment (day 30). All naked AV loops were evidently perfused before closure of the collagen chambers (shown in two representative animals in Fig. 3A). After suture of the chambers, the perfusion signal was almost completely quenched by the scaffold (Fig. 1B, upper panels). After day 30, the chambers showed intense perfusion signals with a diffuse pattern, suggestive of extensive neovascularization. The bottom part of Figure 3B reports the quantitative analysis of perfusion, showing an approximate threefold increase in blood flow.

Histological analysis of the collagen scaffold at day 30 showed an abundant new tissue, resembling a granulation tissue surrounding the AV loop, filling all the free spaces of the chamber (Fig. 4 and magnification in inset a). The collagen trabeculae of the dermal scaffold were still visible after 1 month from the implant and appeared infiltrated by several cells (Fig. 4, inset b).

The integration between the template matrix with colonizing cells is clearer in Masson's trichrom stained sections (Fig. 5), in which the collagen architecture of the dermal scaffold was still easily recognizable. Masson's staining also revealed a remarkable number of new vessels interspersed within the collagen trabeculae of the artificial tissue. This newly formed vasculature included both enlarged vessels in the closed proximity of the grafted vein wall (Figs. 5A and 5B) and smaller vessels interspersed in the granulation tissue and dermal template matrix (Figs. 5C and 5D).

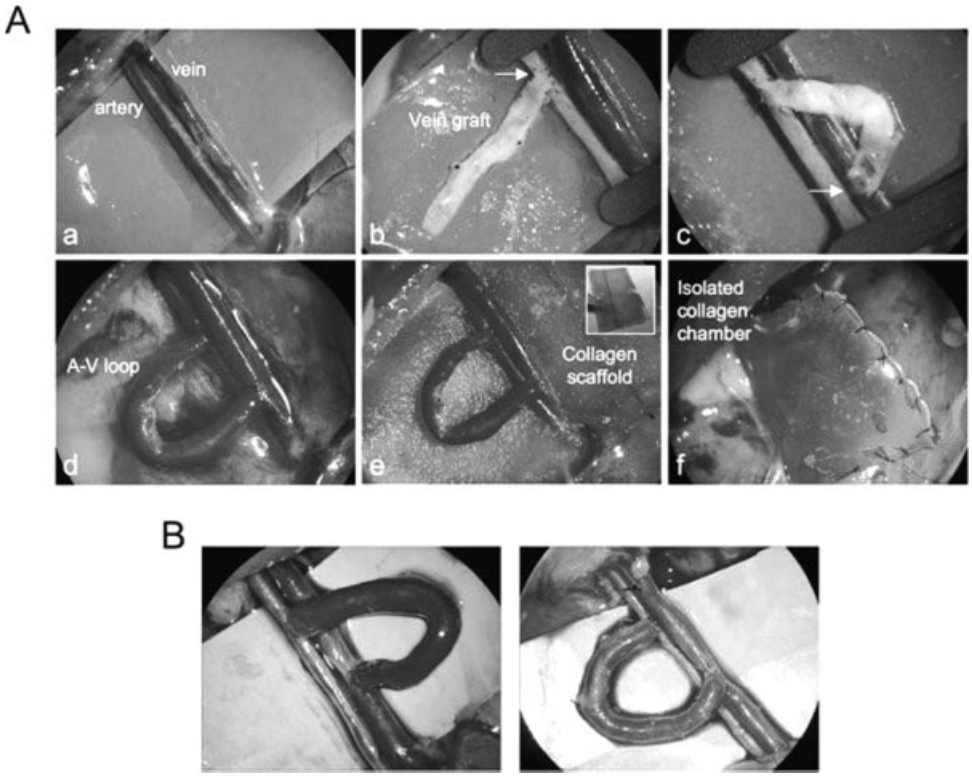

Figure 1. Microsurgical creation of an isolated collagen-GAG chamber surrounding an arterovenous loop. ***A:*** *Chamber creation. (**a**) Isolation of the femoral arterovenous (AV) bundle; (**b**) Microsurgical terminolateral (T-L) anastomosis (arrow) between the femoral artery and the distal end of a vein graft harvested from the controlateral groin; (**c**) T-L anastomosis of the proximal end of the vein graft with the femoral vein (arrow); (**d**) AV loop after surgical clamp release; (**e**) Embedding of the AV loop into the collagen-GAG scaffold. The inset shows a small scaffold island ready for implantation; (**f**) Folding and suture of the collagen-GAG scaffold on itself. The silicone outer layer of the scaffold does not allow tissue ingrowth into the chamber from the outside.* ***B:*** *Additional examples of AV loops.*

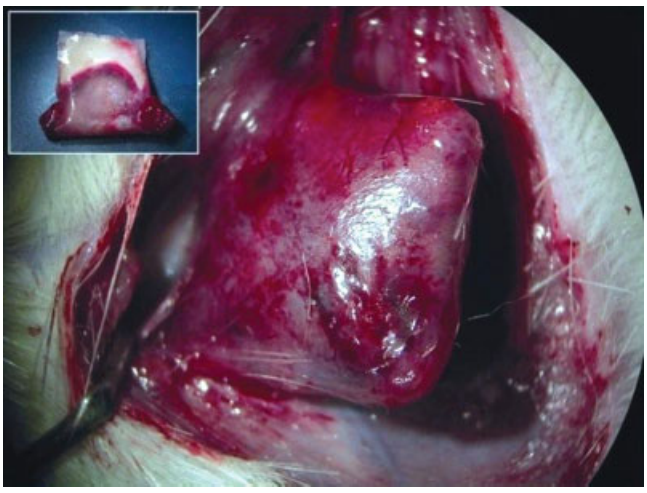

Figure 2. Chamber at 1 month after implantation. The picture shows the specimen ready to be withdrawn and after the withdrawal (inset) at day 30 post-op. A dense connective tissue envelopes the chamber. [Color figure can be viewed in the online issue, which is available at www.interscience.wiley.com.]

Further characterization performed by immunofluorescence using an antibody specific for smooth muscle α-actin confirmed that several of the observed new vessels were indeed small arterioles, which probably sprouted from the vein loop and contributed to the perfusion of the new tissue (Figs. 6A and 6B). This is in accordance with the data obtained by laser Doppler analysis. As expected, because of the increased blood flow, we observed that the vein wall underwent a process of remodeling with the presence of an increased layer of smooth muscle cells (Figs. 6C and 6D).

DISCUSSION

The claim for organ and tissue substitution has become a major requisite in modern medicine, creating a demand for alternative sources of tissues. Tissue engineering is contributing extensively to this field, with vascularization of new tissue templates being one of the most compelling, emerging topics. The vascular supply to engineered tissues can either follow an extrinsic pathway

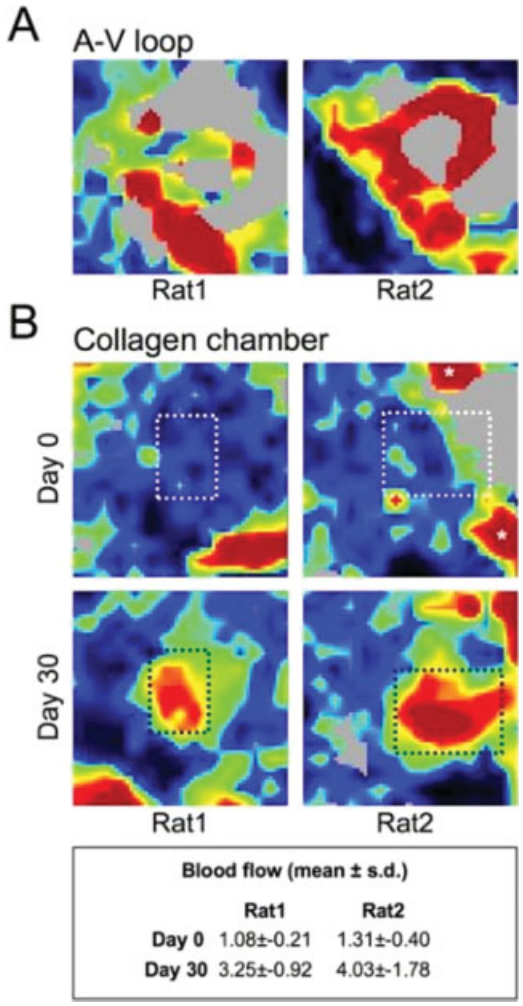

Figure 3. Quantification of blood flow by laser Doppler perfusion imaging. ***A:*** *Perfusion of the AV loop before closure of the collagen chamber in two animals.* ***B:*** *Perfusion of the collagen chamber at day 0 (top) and day 30 (bottom). The asterisks indicate the proximal and distal regions of the femoral AV bundle outside of the chambered region. The bottom part of the figure reports the quantification of the signal intensity in the boxed regions of interest (ROIs). [Color figure can be viewed in the online issue, which is available at www.interscience.wiley.com.]*

or ensue from intrinsic vascularization. In the former paradigm, new vessels coming from the recipient bed invade new tissue constructs. Important clinical examples have already been provided in this respect.[2] However, this approach is usually hampered by the relatively limited size of the implants.[9] By contrast, intrinsic vascularization occurs when new vessels develop directly from a vascular axis of the host; plastic surgeons, by proposing various models of flap prefabrication and prelamination, have paved the way to new procedures for the generation of intrinsic vascularized tissues. Over the last 30 years, several models have been described, which are mostly based on the generation of AV loops. In particular, Morrison and coworkers have recently demonstrated that this approach can be used for in vivo engineering of various newly formed tissues.[3,10–14] In fact, sandwiching an AV loop between two layers of an artificial dermis induces the formation of an internal new vascularized soft tissue that resembles a connective or adipose tissue.[3]

Here we describe a new model of tissue engineering based on the use of a commercially available crosslinked collagen/GAG template as a new type of matrix to envelop an AV loop in the rat groin. We chose the AV loop as the vascular carrier to promote neoangiogenesis of the scaffold, since we have developed long-standing, technical expertise in this surgical procedure. In the AV loop model, the occurrence of sprouting angiogenesis has been well described to depend on the development of tensional and stress forces that disturb the integrity of the endothelium and renders the vessels more susceptible to the action of angiogenic factors.[1,15,16] AV bundles have also been proposed as an alternative source for sprouting angiogenesis.[7] However, the neoangiogenetic properties of AV bundles look poorer than those of AV loops, and the bundle is at higher risk of thrombosis. Moreover, the same authors who sustained the feasibility of AV bundles also reported the lack of new tissue formation using this model.[6] On the other hand, the AV loop model is easier to establish, as it does not require vascular bundle sacrifice, and for this reason it has been successfully used even in difficult clinical conditions.[8]

In principle, the ideal template for tissue regeneration should be a biocompatible and biodegradable scaffold, capable of ensuring optimal interaction with endothelial cells to promote angiogenesis, since the architecture of the scaffold and its biochemical characteristics are known to play a role in modulating the angiogenic activities of invading cells.[17] Among the engineered artificial dermis, the collagen-GAG template we used has proven to be a standard tool in reconstructive surgery. Since its introduction in clinical practice as primary coverage for major burns after necrectomy, its clinical applications have largely widened to soft tissue deficits after scar excision, contracture release, excision of tight, painful or keloid scars, anesthetic scars, and reconstruction after large excisions (such as in giant naevi, coverage of post-traumatic defects, flap donor site coverage, resurfacing of free flaps, and deep loss of tissue after bone and joint exposure).[18]

In our model, the collagen-GAG scaffold acts as a good matrix for new tissue regeneration, allowing the growth of newly formed soft connective tissue into the chamber. Indeed, its properties to direct the ingrowth of soft-connective tissue are well known in the case of dermal regeneration, also thanks to the size and number of its pores.[18,19] Further investigations are clearly required to clarify the structure and ultrastructure of this dermal

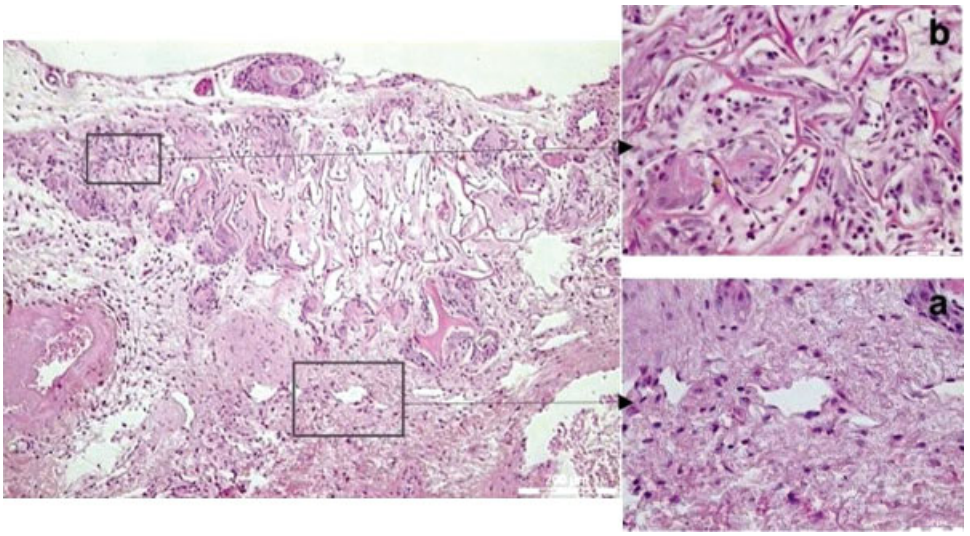

*Figure 4. Hematoxylin and eosin staining of a representative histological section of paraffin-embedded collagen implant. Inset **a:** the free space of the chamber surrounding the AV loop appears infiltrated by an abundant new tissue resembling a granulation tissue. Inset **b:** the collagen trabeculae of the collagen chamber are visible and appear infiltrated by a neoformed tissue. Magnification: ×10. [Color figure can be viewed in the online issue, which is available at www.interscience.wiley.com.]*

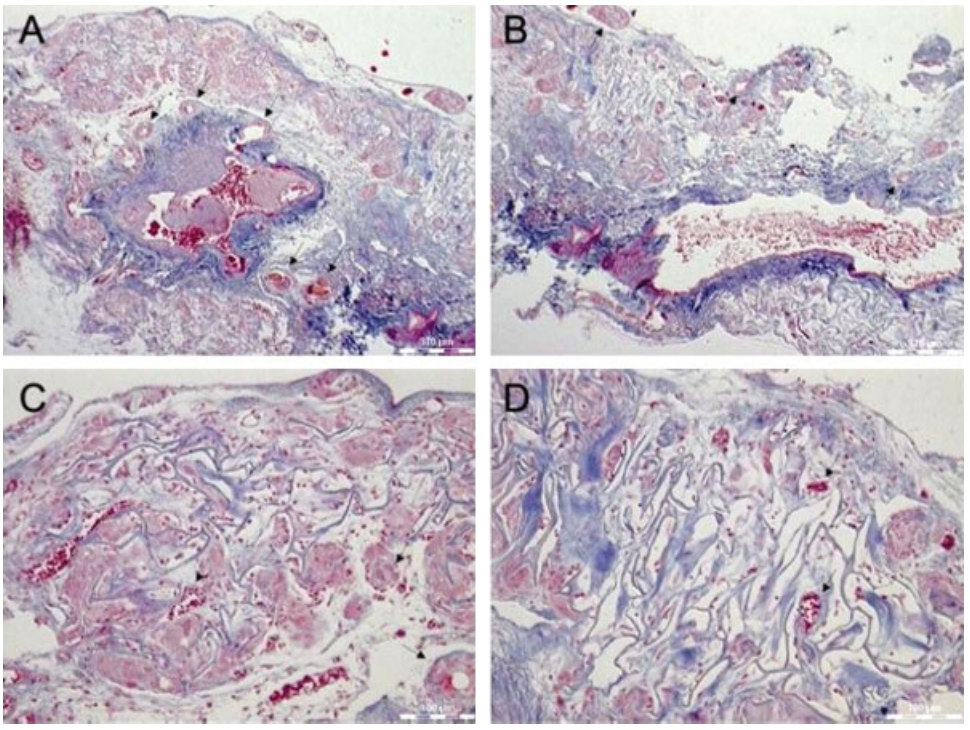

*Figure 5. Masson's trichrom staining of collagen implant. **A, B:** Histological sections showing closed integration between the collagen matrix and colonizing cells with many large vessels at the periphery and the adventitia of the grafted vein, interspersed inside the granulation tissue and the collagen matrix. Arrows indicate recognizable newly formed vessels. **C, D:** High magnification showing the architecture of the collagen scaffold and new vessels. Magnification: ×10. [Color figure can be viewed in the online issue, which is available at www.interscience.wiley.com.]*

scaffold and to understand the influence of pore size, elastic, and biochemical features on neoangiogenesis and newly formed tissue ingrowth. In this respect, it is worth mentioning that the collagen-GAG matrix is amenable to further improvements, including the creation of more capable chambers, such as boxes or 3D structures, which

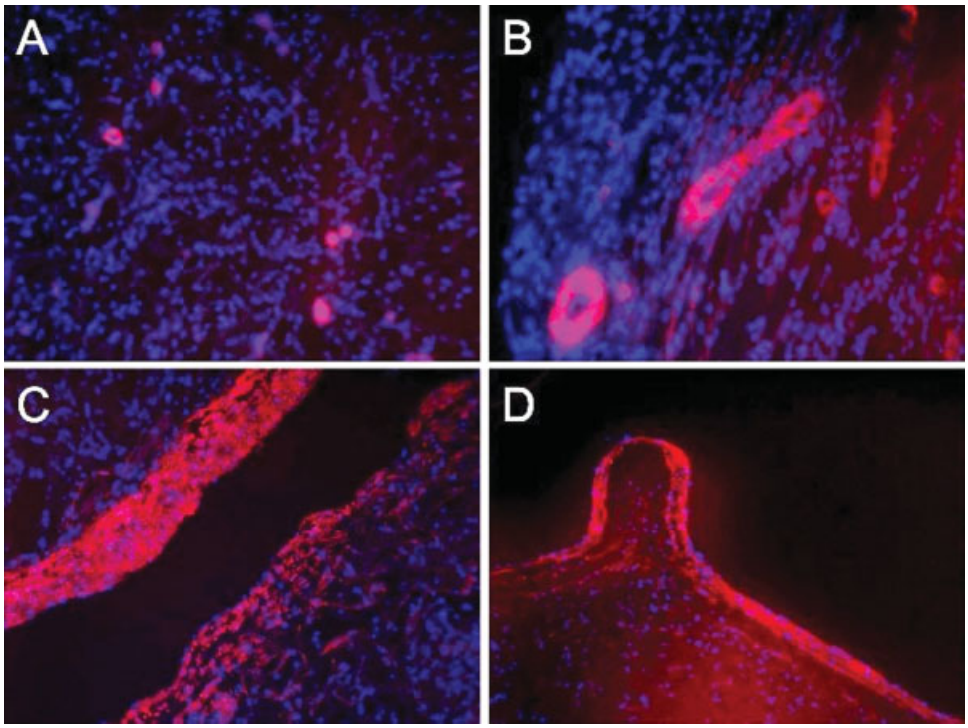

Figure 6. Immunofluorescence staining of collagen implant section. ***A, B:*** *The new vasculature formed inside the chamber was analyzed using an antibody against the α-actin isoform specific for smooth muscle cells (α-SMA). Several of the vessels present in the tissue invading the scaffold show a layer of positive smooth muscle cells in their wall, confirming to be small arteries. Magnification: ×10 (A) and ×40 (B).* ***C, D:*** *Positive staining with the α-SMA antibody was also detected in the wall of the grafted vein, indicating the occurrence of an arterialization remodeling process (panels* ***c*** *and* ***d****). Red: α-SMA positive cells. Blue: nuclei stained with DAPI. Magnification: ×10. [Color figure can be viewed in the online issue, which is available at www.interscience.wiley.com.]*

might increase tissue ingrowth and vascularization, as already suggested.[2,6]

The results of our study clearly indicate that, in addition to its dermal substitute template function, the collagen-GAG scaffold provides a novel template for the engineering of other tissues and organs, especially by exploiting the possibility to transfer the template to other tissues by using its vascular pedicle. Importantly, the observation that massive soft connective tissue formation and extensive neovascularization occurs in an isolated and transplantable chamber offers the attractive possibility that this chamber might be used as a bioreactor for the release of growth factors or drugs. More interestingly, this isolated and vascularized chamber can also be viewed as a new template for the expansion and differentiation of cell populations potentially enriched in precursor or stem cells. In this respect, further studies including viral gene transfer and bone marrow-derived cell seeding into this template are in progress.

ACKNOWLEDGMENTS

The authors thank Mauro Sturnega for his help in animal experimentation and Suzanne Kerbavcic for precious editorial assistance.

Animal care and treatment were conducted at the International Centre for Genetic Engineering and Biotechnology (ICGEB) in Trieste in conformity with institutional guidelines and in compliance with national and EU laws and policies (EEC Council Directive 86/609, OJL 358, December 12, 1987).

REFERENCES

1. Laschke MW, Harder Y, Amon M, Martin I, Farhadi J, Ring A, Torio-Padron N, Schramm R, Rucker M, Junker D, Haufel JM, Carvalho C, Heberer M, Germann G, Vollmar B, Menger MD. Angiogenesis in tissue engineering: Breathing life into constructed tissue substitutes. Tissue Eng 2006;12:2093–2104.
2. Lokmic Z, Stillaert F, Morrison WA, Thompson EW, Mitchell GM. An arteriovenous loop in a protected space generates a permanent, highly vascular, tissue-engineered construct. FASEB J 2007;21:511–522.
3. Mian R, Morrison WA, Hurley JV, Penington AJ, Romeo R, Tanaka Y, Knight KR. Formation of new tissue from an arteriovenous loop in the absence of added extracellular matrix. Tissue Eng 2000; 6:595–603.
4. Michaels JV, Levine JP, Hazen A, Ceradini DJ, Galiano RD, Soltanian H, Gurtner GC. Biologic brachytherapy: Ex vivo transduction of microvascular beds for efficient, targeted gene therapy. Plast Reconstr Surg 2006;118:54–65; discussion 66–58.
5. Tepper OM, Galiano RD, Kalka C, Gurtner GC. Endothelial progenitor cells: The promise of vascular stem cells for plastic surgery. Plast Reconstr Surg 2003;111:846–854.

6. Tanaka Y, Sung KC, Fumimoto M, Tsutsumi A, Kondo S, Hinohara Y, Morrison WA. Prefabricated engineered skin flap using an arteriovenous vascular bundle as a vascular carrier in rabbits. Plast Reconstr Surg 2006;117:1860–1875.
7. Tanaka Y, Sung KC, Tsutsumi A, Ohba S, Ueda K, Morrison WA. Tissue engineering skin flaps: Which vascular carrier, arteriovenous shunt loop or arteriovenous bundle, has more potential for angiogenesis and tissue generation? Plast Reconstr Surg 2003;112:1636–1644.
8. Bruner S, Bickert B, Sauerbier M, Germann G. Concept of arteriovenous loupes in high-risk free-tissue transfer: History and clinical experiences. Microsurgery 2004;24:104–113.
9. McIntire LV. Vascular assembly in engineered and natural tissues. Ann NY Acad Sci 2002;961:246–248.
10. Erol OO, Spira M. New capillary bed formation with a surgically constructed arteriovenous fistula. Surg Forum 1979;30:530–531.
11. Hirase Y, Valauri FA, Buncke HJ. Creation of neovascularised free flaps using vein grafts as pedicles: A preliminary report on experimental models. Br J Plast Surg 1989;42:216–222.
12. Takato T, Zuker RM, Turley CB. Prefabrication of skin flaps using vein grafts: An experimental study in rabbits. Br J Plast Surg 1991; 44:593–598.
13. Wilson YT, Kumta S, Hickey MJ, Hurley JV, Morrison WA. Use of free interpositional vein grafts as pedicles for prefabrication of skin flaps. Microsurgery 1994;15:717–721.
14. Mian RA, Knight KR, Penington AJ, Hurley JV, Messina A, Romeo R, Morrison WA. Stimulating effect of an arteriovenous shunt on the in vivo growth of isografted fibroblasts: A preliminary report. Tissue Eng 2001;7:73–80.
15. Carmeliet P. Mechanisms of angiogenesis and arteriogenesis. Nat Med 2000;6:389–395.
16. Risau W. Mechanisms of angiogenesis. Nature 1997;386:671–674.
17. Pieper JS, van Wachem PB, van Luyn MJA, Brouwer LA, Hafmans T, Veerkamp JH, van Kuppevelt TH. Attachment of glycosaminoglycans to collagenous matrices modulates the tissue response in rats. Biomaterials 2000;21:1689–1699.
18. Moiemen NS, Vlachou E, Staiano JJ, Thawy Y, Frame JD. Reconstructive surgery with Integra dermal regeneration template: Histologic study, clinical evaluation, and current practice. Plast Reconstr Surg 2006;117(7, Suppl):160S–174S.
19. Stern R, McPherson M, Longaker MT. Histologic study of artificial skin used in the treatment of full-thickness thermal injury. J Burn Care Rehabil 1990;11:7–13.